Karlsruher Institut für Technologie

Fakultät für Physik
Institut für Theorie der Kondensierten Materie

The quantum critical SYK superconductor, Lifshitz points and their holographic duals

Zur Erlangung des akademischen Grades eines
Doktors der Naturwissenschaften (Dr. rer. nat.)

von der KIT-Fakultät für Physik
des Karlsruher Instituts für Technologie
genehmigte
Dissertation

von
M.Sc. Gian Andrea Inkof
aus Genua

Tag der mündlichen Prüfung: 04.02.2022
Referent: Prof. Dr. Jörg Schmalian
Korreferent: Prof. Dr. Koenraad Schalm

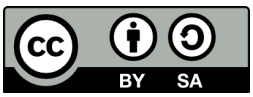

I hereby declare that I have written the present work independently, that no other than the specified sources and resources have been used and that I have indicated everything, that has been taken from the work of others, whether unchanged or with changes.

Karlsruhe, 19 January 2022

Gian Andrea Inkof

Part II of this thesis is based on the following already published article:

- Inkof, G.A., Küppers, J.M.C., Link, J.M., Goutéraux B., and Schmalian, J. Quantum critical scaling and holographic bound for transport coefficients near Lifshitz points. *J. High Energ. Phys.* **2020**, 88 (2020). https://doi.org/10.1007/JHEP11(2020)088

Part III of this thesis is based on the following already published article:

- Inkof, G.A., Schalm, K., and Schmalian, J. Quantum critical Eliashberg theory, the Sachdev-Ye-Kitaev superconductor and their holographic duals. *npj Quantum Mater.* **7**, 56 (2022). https://doi.org/10.1038/s41535-022-00460-8

The numerical analysis in Fig. 7.2 of Chap. 7 and the figure itself have been done by Dr. Davide Valentinis.

Introduction

> "*It reminds me of that old joke- you know, a guy walks into a psychiatrist's office and says, hey doc, my brother's crazy! He thinks he's a chicken. Then the doc says, why don't you turn him in? Then the guy says, I would but I need the eggs. I guess that's how I feel about quantum materials: They're totally crazy, irrational, and absurd, but we keep studying them because we need the eggs.*"
>
> *Laura Greene ∼ Woody Allen*
> *DPG Spring Meeting 2019*

I would like to begin this thesis with a quote from one of the first conferences I attended as a Ph.D. student. There was a time when even the metals we now call *conventional* appeared as *crazy, irrational*, and *absurd* to the scientific community. In fact, it took about sixty years and several attempts before reaching a complete understanding of their behavior. In 1900 Paul Drude proposed his model to describe electrical conduction in solids [1]. In the Drude model, electrons are treated as classical objects that interact with the ions through instantaneous interactions. Later, this model was made more sophisticated by incorporating quantum effects, the presence of the crystal lattice and its vibrations. Finally, in 1956 Lev Davidovič Landau introduced interactions between electrons in the well known Fermi liquid (FL) theory – see e.g. Ref. [2]. The interactions between the elementary components of a metal are the basis of this mechanism. At the same time, they are a great challenge from a theoretical point of view. In interacting many-body systems, the number of exact results is indeed minimal and numerical methods must be employed. However, analytical results are extremely important as they give us a clearer vision on which to build our intuition. One of the hallmark of FL theory is that low energy excitations of a weakly interacting Fermi gas are in one-to-one correspondence with the degrees of freedom of the free theory and therefore are commonly referred to as *quasi-particles* [2]. They have a long lifetime that satisfies:

$$\tau \gg \frac{\hbar}{k_{\mathrm{B}} T}, \tag{1}$$

where $\hbar$ and k_{B} are the Planck and Boltzmann constants respectively. Quasi-particle excitations appear as peaks in the spectral function. The width of such peaks gives the quasi-particles lifetime τ. Thermoelectric transport properties of the system are determined by the behavior of the charge carriers around the Fermi level. Among the most outstanding results of the FL theory and widely verified experimentally, we mention the quadratic-in-temperature resistivity at low T and the Wiedemann-Franz law, which gives a universal ratio between thermal and electrical conductivities. Another ubiquitous property in conventional metals is superconductivity, i.e. the disappearance of electrical resistivity and the total expulsion of the magnetic field (Meissner

effect) for sufficiently low temperature and external fields. The phenomenon was discovered in 1911 by Kamerlingh Onnes [3] by carrying out transport measurements on mercury. The first substantial step towards an understanding of the phenomenon arrived around the 1930s with the equations of the London brothers [4] and found its fulfillment in the renowned Bardeen-Cooper-Schrieffer (BCS) theory [5]. At the basis of the BCS theory is the pairing mechanism between electrons in the vicinity of the Fermi surface. See the review paper [6] for a historical overview of the theory of superconductivity.

In 1987 Bednorz and Müller received the Nobel Prize for detecting superconductivity at 35K in a Lanthanum Barium Copper Oxide compound. From that moment, the era of high-temperature superconductivity began, and nowadays, we have arrived at copper oxide compounds (the cuprates) and other families of materials such as the iron-based superconductors with increasing T_c. Other examples of systems with unconventional superconducting properties are the heavy-fermion compounds and some organic materials. Such systems have been found to exhibit *strange* metallic properties like linear-in-T electrical resistivity rather than quadratic, or violation of the Wiedemann-Franz law [7–9]. Moreover, the pairing mechanism occurring in such systems is not completely clear.

When in 2019 Greene talked about *crazy, irrational*, and *absurd* materials, she referred precisely to this type of systems.

A key question is, of course, why does this behavior occur?

A substantial difference with conventional metals lies in the lifetime of the excitations, which is extremely short. This is why Fermi-liquid theory cannot be applied to these materials. Consequently, the concept of quasi-particle excitations does not apply. The interactions in the system are so strong to significantly reduce the lifetime, usually causing it to saturate Eq.(1). Due to the strength of the interactions, any approach based on perturbations does not apply. This makes the theoretical physics of strongly correlated quantum matter one of the main intellectual challenges in modern physics. It is therefore crucial to develop alternative descriptions to model the behavior of these systems.
When a problem cannot be solved easily within a given representation, it may be crucial to adopt an alternative description of the phenomenon. This aspect underlies the concept of duality. More precisely, two theories of the same physical phenomenon are dual if they have a different distribution of the degrees of freedom, i.e. different actions.
It is not the first time that this concept has been used in physics, from the wave-particle duality at the basis of quantum mechanics to more sophisticated examples such as Montonen-Olive duality of electric and magnetic charges [10].

The main focus of this thesis lies in the application of a very particular duality which describes many-body systems without discernible quasi-particles in terms of a gravity theory in one extra dimension. This duality was conjectured by Maldacena in 1997 [11] and offers a geometric description of a strongly coupled physical system. The event horizon of a black hole behaves like a medium: it is able to dissipate energy via the area law, it can be probed and it has electromagnetic properties [12, 13]. In particular, the diffusion constant is found to scale as $1/T$, prompting that the horizon diffuses charge in the same way as a quantum liquid [14–16].
The Maldacena duality is based on the holographic principle [17], which has transformed the field

of strongly correlated quantum matter. Despite tremendous success in describing hydrodynamic response, symmetry breaking, ill-defined excitations, and quantum criticality a major drawback of the method is that it has not been possible to *derive* the gravity formulation from a given Schrödinger equation with Hamiltonian operator of electrons, lattice vibrations etc.

The principal aim of this thesis is to contribute to bridge the gap between the more conventional condensed matter description and the gravitational one.
The model of Sachdev, Ye and Kitaev (SYK) has been crucial to accomplishing this goal. As we will see, the SYK model represents an extremely successful example of a model with non-FL behavior that is solvable with conventional field theory-based methods.

Structure of the thesis

This thesis is divided into three parts, each subdivided into chapters. Each chapter ends with a summary whose purpose is to collect the main information and let the reader move through the thesis more easily. Further details and complements to the computations of the main text can be found in the appendices. Moreover, we have collected the acronyms and conventions used in the section of the same name.

In **Part I** we give the fundamentals of Maldacena duality. In **Chap.** 1 we review some core aspects of the duality that constitute (a part) of what is commonly known as *holographic dictionary*. Such a set of rules makes it possible to construct the gravity dual of a system. In **Chap.** 2 we focus on charged black holes at low temperature. The symmetries that emerge in the interior of such spacetimes are described by gravity in 2 dimensions and incredibly match to those of the 0+1 dimensional Sachdev-Ye-Kitaev model. We give an overview of the Majorana SYK model and comment on its generalization to charged fermions.

In **Part II** we analyze quantum critical transport in anisotropic systems. The resuls are based on Refs. [18, 19]. In **Chap.** 3 we introduce the condensed matter systems we focus on and develop a scaling theory for anisotropic systems near a Lifshitz point in 2+1 dimensions. We report on the violation due to rotational symmetry breaking of universal lower bounds appearing in strongly-coupled systems. Specifically, we consider the bound on shear viscosity to entropy density ratio and on charge diffusion. Key questions we address are: are these bounds affected by symmetry breaking? If yes, how can we generalize them? In **Chap.** 4 we introduce the holographic dual given by the Einstein-Maxwell-scalar model. In addition to rotational symmetry breaking, such a theory displays momentum dissipation along one of the two spatial directions. We analyze explicit solutions to the field equations. Moreover, we extend such a model beyond the two-derivatives Einstein gravity limit. In **Chap.** 5 we compute the electrical conductivity and shear viscosity tensors and confirm that the bound constructed with scaling arguments holds. We analyze momentum dissipation effects in both the regimes of high and small temperature. Finally, we determine the charge diffusion constants and butterfly velocities holographically.

Part III is devoted to a different kind of quantum criticality which involves superconductivity without quasi-particles. It is based on Ref. [20].
In **Chap.** 6 we review the extension of the microscopic 0+1 dimensional SYK model introduced in Refs. [21, 22] where a boson mediates the interaction between two fermions. This is

a solvable model with non-Fermi liquid behavior and governed by the Eliashberg equations of superconductivity. Key questions we address are: how does this system respond to an external pairing source? Does it admit a gravity dual? To test superconducting properties of the above mentioned SYK model, in **Chap.** 7 we couple it to a lattice. We then determine the superconducting phase stiffness. In **Chap.** 8 we test the response of the 0+1 dimensional model to an external pairing source. We then construct the phase diagram by analyzing the pairing susceptibility, whose behavior is mainly controlled by a quantum critical point (QCP) characterized by exponential suppression of the superconducting critical temperature. In **Chap.** 9 we develop the effective theory in the vicinity of such a QCP and explicitly derive the action of holographic superconductivity out of it. The frequency dependent response of the system is not easy to analyze with Eliashberg theory since a dynamical source generally spoils time translation invariance. In **Chap.** 10 we use our map and exploit the power of holography to determine the dynamic pairing susceptibility of the model.

Contents

Part I

Fundamentals

Chapter 1

The holographic dictionary

In this chapter, we review some fundamental aspects of the anti-de-Sitter conformal field theory correspondence (AdS/CFT) that constitutes (a part) of what is commonly known as *holographic dictionary*. These aspects are highlighted in boxes in the body of the text and summarized at the end in Sec. 1.4. The purpose of these two initial chapters is to create a foundation for developing the concepts of this thesis. A deep understanding of the correspondence would require strong prerequisites of string theory, general relativity, and conformal field theory, which is beyond the scope of this thesis. Therefore, the following chapter should be understood as a general overview of AdS/CFT without claiming to discuss in detail the arguments presented, of which precise references will be given in any case. The following analysis is based on the books [23–27] as well as on the review papers [28, 29].

In Sec. 1.1 we sketch Maldacena's argument with a focus on the conformal group and AdS spaces. In Sec. 1.2 we explore the consequences of the Gubser-Klebanov-Polyakov-Witten (GKPW) rule, giving the basics for computing retarded correlators from gravity. Finally, in Sec. 1.3 we focus on the Reissner-Nordström black hole solution and comment on the superconducting instability.

1.1 Motivation of the duality

Below we provide a non-exhaustive sketch that aims to highlight the main aspects of Maldacena's argument. For further information we refer to the books [23–25] on which the following analysis is based.

Maldacena originally considered a set of a large number of D3-branes in the context of type IIB string theory in 9 dimensions. A Dp-brane is a fundamental degree of freedom in string theory with p spatial dimensions, such that $p = 0$ corresponds to point-like object, $p = 1$ to a string, $p = 2$ to a membrane etc. A crucial parameter in Maldacena's analysis is the 't Hooft coupling

$$\lambda = 4\pi g_s N, \tag{1.1}$$

which gives a measure of the gravitational back-reaction of the D3-branes. Here g_s represents the dimensionless coupling constant, while N is the number of branes.

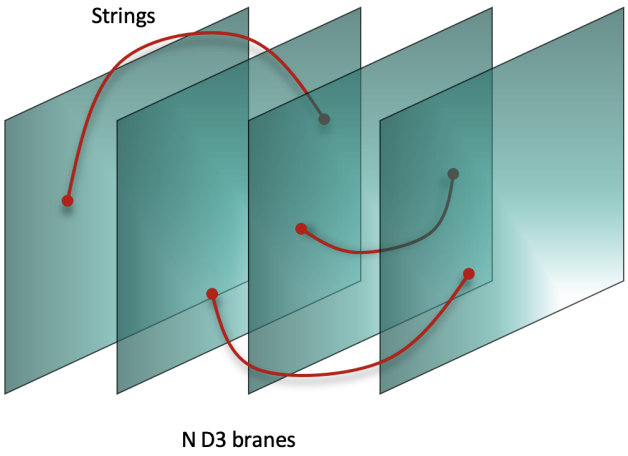

Figure 1.1: A stack of N D3 branes in the small 't Hooft coupling limit. The low energy excitations are strings that start and end on pairs of D3 branes. Figure inspired by Ref. [24].

Let us analyze what happens in two opposite cases. For $\lambda \ll 1$, the effect of the branes on the background is almost negligible, and the low-energy excitations are represented by strings that start and end on pairs of D3-branes – see the cartoon in Fig.1.1. At low energies, this system of strings turns out to be effectively described by a super-Yang-Mills (SYM) conformal field theory in $3+1$ flat spacetime dimensions [11, 24]. Its fundamental degrees of freedom are $N \times N$ matrix-valued fields, whose indexes label the D3-branes. In particular, there are $\mathcal{N} = 4$ supersymmetries, i.e. six bosonic scalars and 4 Weyl fermions described by multi-component fields Φ and Ψ respectively. The Lagrangian density is schematically given by:

$$\mathcal{L} \sim \frac{N}{\lambda} \mathrm{tr}\Big(F^2 + (\nabla\Phi)^2 + i\bar{\Psi}\not{D}\Psi + i\bar{\Psi}[\Phi,\Psi] - [\Phi,\Phi]^2\Big), \tag{1.2}$$

where F is a SU(N) field strength. The way the 't Hooft coupling enters the above expression makes the large-N limit weakly coupled and the perturbative approach well defined. In conclusion, the low energy limit of this string system is described by a conformal theory of weakly coupled $N \times N$ matrices.
In the opposite limit $\lambda \gg 1$, the gravity back-reaction of the D3-branes is no longer negligible. The resulting system is described by the well-known black hole solutions of general relativity. In the inner region of these spacetimes, close to the event horizon, the geometry factorizes in the product of anti-de-Sitter (AdS) spaces and compact manifolds, in symbols $\mathrm{AdS}_5 \times \mathbb{S}^5$. Low-energy excitations are consequently described by classical gravitational perturbations in this background. We will review AdS spaces in Sec. 1.1.2.
Maldacena conjectured that there exists an interpolation between these two limits of low and high 't Hooft coupling, such that the strong coupling regime of the large-N, $\mathcal{N} = 4$ SYM theory is given by classical gravity in $\mathrm{AdS}_5 \times \mathbb{S}^5$.

It is crucial to underline that the field theory lives in a space with one lower dimension than the gravitational dual. The interpretation of this additional dimension is non trivial and we comment on it in Sec. 1.2. It basically represents the energy scale of the dual field theory. This mismatch of dimensions is compatible with the holographic principle [17], which states that in semiclassical quantum gravity the degrees of freedom contained in a volume is encoded in its boundary area. For this reason, the correspondence is also known as *holography*. More specifically, let us consider a region of spacetime of volume V. In the absence of gravity the number of degrees of freedom is extensive and goes as $\sim V$. The maximum entropy goes like the logarithm of such a number and will then controlled by the volume. In the presence of gravity the maximum entropy is the one of the biggest black hole that fits within the region. According to the Bekenstein-Hawking formula, the entropy and hence the number of degrees of freedom scale like the area ∂V rather than the volume – see Eq.(1.22) below.

It is important to underline that Maldacena's duality is a strong-weak coupling correspondence. This aspect has made it attractive for many applications to those problems where strong interactions make any perturbative approach ill-defined. We commented on this point in the introduction of this thesis.

Rule 1 - Maldacena's duality

Strongly coupled CFT_{d+1} = Weakly coupled classical gravity on AdS_{d+2}

In its modern formulation, the AdS/CFT correspondence is defined as an identity between partition functions of a generic strongly coupled QFT_{d+1} and a classical theory of gravity in $d+2$ dimensions [30, 31] $Z_{\text{QFT}_{d+1}} = Z_{\text{grav}_{d+2}}$. We will review this argument in Sec. 1.2. Even in cases where the two sides of duality are known precisely, it is not always easy to identify exactly the elements of both the sides of the correspondence. In these cases the gravitational dual is constructed to match the symmetries of the dual field theory. This is known as *bottom-up* approach and is commonly employed in condensed matter applications.

In the following this section we analyze the two sides of the correspondence: conformal field theories in $d+1$ dimensions and AdS spacetime in $d+2$ dimensions.

1.1.1 The conformal group

In order to characterize a theory it is important to determine how a transformation of the spacetime coordinates acts on the level of the fields. This is done by means of group theory, which determines the algebra of a symmetry and the corresponding representations. In this section we extend the Poincaré group of relativistic symmetry, and briefly review the so-called *conformal transformations*. This section is based on Refs. [23, 26].

Let us consider a spacetime whose line element is given by

$$ds^2 = g_{\mu\nu}(x)dx^\mu dx^\nu. \tag{1.3}$$

	Transformation	Generators
Translation	$x'_\mu = x_\mu + a_\mu$	$P_\mu = -i\partial_\mu$
Lorentz	$x'_\mu = \Lambda_\mu{}^\nu x_\nu$	$J_{\mu\nu} = i(x_\mu\partial_\nu - x_\nu\partial_\mu)$
Dilatation	$x'_\mu = \lambda\, x_\mu$	$\underline{\Delta} = -ix^\rho\partial_\rho$
SCT	$x'_\mu = \dfrac{x_\mu - b_\mu x^2}{1 - 2b^\rho x_\rho + b^2x^2}$	$K_\mu = -i(2x_\mu x^\rho\partial_\rho - x^2\partial_\mu)$

Table 1.1: Finite conformal tranformations. Λ is a generic special Lorentz matrix, λ is a constant and a^μ, b^μ are constant vectors.

Here $g_{\mu\nu}$ is the metric tensor and $\mu, \nu = 0, ..., d$, where $d+1$ is the spacetime dimension. A conformal transformation is defined as a map that preserves angles locally. However, the interval length is not required to stay invariant. Therefore, the metric transforms as

$$g_{\mu\nu}(x) \mapsto \mathcal{C}(x) g_{\mu\nu}(x), \tag{1.4}$$

where $\mathcal{C}(x)$ is called *conformal scaling factor*.
In order to explore the implications of Eq.(1.4) we analyze the case of flat spacetime, i.e. $g_{\mu\nu} = \eta_{\mu\nu} = \text{diag}(-1, 1, ..., 1)$ and of an infinitesimal coordinate transformation $x^\mu \mapsto x^\mu + \epsilon^\mu$. Such a coordinate change is conformal if ϵ^μ fulfills the following equation

$$(\eta_{\mu\nu}\partial_\rho\partial^\rho + (d-1)\partial_\mu\partial_\nu)\partial_\rho\epsilon^\rho = 0. \tag{1.5}$$

The spacetime dimension d enters the above expression. When $d = 0$ there is no notion of angle and any smooth transformation is conformal. The $d = 1$ case should be treated separately and will not be discussed in this thesis. See e.g. Ref. [23] for details. For $d > 1$, the most general solution to Eq.(1.5) is second-order in x:

$$\epsilon^\mu = a^\mu + b^{\mu\nu}x_\nu + c^{\mu\nu\rho}x_\nu x_\rho. \tag{1.6}$$

Let us consider some limit cases. $\epsilon^\mu = a^\mu$ corresponds to spacetime translations. Considering $\epsilon^\mu = b^{\mu\nu}x_\nu$ and using Eq.(1.5), it holds that $b_{\mu\nu} = \lambda\eta_{\mu\nu} + \omega_{\mu\nu}$. The former contribution represents scale transformation, whereas ω is antisymmetric and corresponds to rigid rotations. The second-order term $c^{\mu\nu\rho}$ describes the so-called *special conformal transformations* (SCT). The finite counterparts of the infinitesimal transformations can be reconstructed by exponentiating the infinitesimal form and are given in above table. In particular, a special conformal transformations can be obtained from the composition of an inversion ($x_\mu \to x_\mu/x^2$), a translation ($x_\mu \to x_\mu - b_\mu$) and another inversion.
The set of conformal transformations forms the so-called *conformal group* which contains the

Poincaré group as subset. The symmetry generators are given in the above table and satisfy the following commutation relations

$$\begin{aligned}
&[\underline{\Delta}, P_\mu] = iP_\mu, \quad [\underline{\Delta}, K_\mu] = -iK_\mu, \\
&[K_\mu, P_\nu] = 2i(\eta_{\mu\nu}\underline{\Delta} - L_{\mu\nu}), \quad [K_\rho, J_{\mu\nu}] = i(\eta_{\rho\mu}K_\nu - \eta_{\rho\nu}K_\mu), \\
&[P_\rho, J_{\mu\nu}] = i(\eta_{\rho\mu}P_\nu - \eta_{\rho\nu}P_\mu), \\
&[J_{\mu\nu}, J_{\rho\sigma}] = i(\eta_{\nu\rho}J_{\mu\sigma} + \eta_{\mu\sigma}J_{\nu\rho} - \eta_{\mu\rho}J_{\nu\sigma} - \eta_{\nu\sigma}J_{\mu\rho}).
\end{aligned} \tag{1.7}$$

The generators can be rearranged into the following matrix

$$R_{MN} = \begin{pmatrix} J_{\mu\nu} & \frac{K_\mu - P_\mu}{2} & -\frac{K_\mu + P_\mu}{2} \\ -\frac{K_\mu - P_\mu}{2} & 0 & \underline{\Delta} \\ \frac{K_\mu + P_\mu}{2} & -\underline{\Delta} & 0 \end{pmatrix}, \tag{1.8}$$

where $M, N = 0, ..., d+2$. Notice that R is antisymmetric by construction. Analyzing the algebra it follows that

$$[R_{MN}, R_{RS}] = \mathrm{i}(\eta_{NR}J_{MS} + \eta_{MS}J_{NR} - \eta_{MR}J_{NS} - \eta_{NS}J_{MR}). \tag{1.9}$$

This is also the algebra of rotations in a $d+3$ dimensional spacetime with signature $(2, d+1)$. Therefore, there exists an isomorphism between the conformal group and SO(2,d+1). As we will see in Sec. 1.1.2, this is also the same isometry group of anti-de-Sitter space in $d+2$ dimensions.

Fields in a CFT transform under the irreducible representations of the conformal algebra. A multi-component field Ψ transforms as

$$\Psi(x) \mapsto \mathcal{C}^{\frac{\Delta}{2}}(x)\mathcal{F}_\Lambda \Psi(x), \tag{1.10}$$

where $\mathcal{C}$ is the multiplying factor of Eq.(1.4) whereas $\mathcal{F}_\Lambda$ is an appropriate representation of Lorentz symmetry. In the case of space dilatation $x \mapsto \lambda x$ and scalar field ($\mathcal{F}_\Lambda = 1$) we have

$$\Psi'(x') = \lambda^{-\Delta}\Psi(\lambda x). \tag{1.11}$$

The quantity Δ is called *scale dimension* and is fixed for the eigenstates of the dilatation operator $\underline{\Delta}$. A constraint on such a quantity is given by the unitary bound

$$\Delta > \frac{d-1}{2}. \tag{1.12}$$

Fields with scale dimension below the unitary bound would have negative norm leading to a inconsistency of the theory.

1.1.2 Anti-de-Sitter spaces

In this section we review anti-de-Sitter spaces in $d+2$ dimensions, which are fundamental building blocks of the AdS/CFT correspondence and will be ubiquitous in this thesis. AdS spaces are rigid spacetimes but these become dynamical once we consider the laws of general relativity. As we shall show below, the so-called boundary of AdS remains rigid and in that sense any spacetime with a negative cosmological constant is asymptotically AdS. The main aspects of general relativity are summarized in Sec. 10.1. Here we follow Refs. [23, 32].

anti-de-Sitter spaces belong to the class of *maximally symmetric* spacetimes, i.e. those with the highest number of isometries. For such manifolds the Riemann tensor is given by

$$\mathcal{R}_{\lambda\rho\sigma\nu} = \frac{\mathcal{R}}{d(d+2)}(g_{\nu\rho}g_{\lambda\sigma} - g_{\rho\sigma}g_{\lambda\nu}). \tag{1.13}$$

Here $\mathcal{R}$ is the Ricci scalar, $g_{\mu\nu}$ the metric, and all the indexes run over $0, ..., d-1$. Such maximally symmetric spacetimes where no point is different from any other point are intuitively "empty" spacetimes. In other words they are vacuum/ground-state solutions that should solve the Einstein equations with/without a cosmological constant for zero matter

$$\mathcal{R}_{\mu\nu} - \frac{1}{2}\mathcal{R}g_{\mu\nu} + \Lambda g_{\mu\nu} = 0. \tag{1.14}$$

$\mathcal{R}_{\mu\nu}$ is the Ricci tensor and Λ is the cosmological constant. These equations follow from the well-known Einstein-Hilbert action

$$S = \frac{1}{16\pi G_{\mathrm{N}}}\int d^{d+2}x\,\sqrt{-g}\Big(\mathcal{R} - 2\Lambda\Big), \tag{1.15}$$

where G_{N} is the Newton constant and g denotes the metric determinant. Tracing both the sides of Eq.(1.14) yields $\mathcal{R} = \frac{d+2}{d+1}\Lambda$. Maximally symmetric spaces therefore have a constant Ricci scalar whose value is controlled by the spacetime dimension and the cosmological constant. This allows for the following classification:

- $\Lambda = 0, \mathcal{R} = 0$
  Maximally symmetric solution of the Einstein equation with null curvature and cosmological constant: Minkowski space;
- $\Lambda > 0, \mathcal{R} > 0$
  Maximally symmetric solution of the Einstein equation with positive curvature and cosmological constant: de Sitter space (dS_{d+2});
- $\Lambda < 0, \mathcal{R} < 0$
  Maximally symmetric solution of the Einstein equation with negative curvature and cosmological constant: anti-de-Sitter space (AdS_{d+2}).

In conclusion, an anti-de-Sitter space is a maximally symmetric solution of the Einstein equations with negative cosmological constant. We can use its maximal symmetry to determine the metric of AdS by embedding it in a $(d+3)$-dimensional flat space with line element

$$ds^2 = -(d\xi^0)^2 + (d\xi^1)^2 + ... + (d\xi^{d+1})^2 - (d\xi^{d+2})^2 \equiv \bar{\eta}_{MN}d\xi^M d\xi^N, \tag{1.16}$$

where $M, N = 0...d+2$ and $\bar{\eta}_{MN} = \text{diag}(-,+,...,+,+,-)$. AdS_{d+2} can be viewed as an hyperboloid in such a higher dimensional space:

$$\bar{\eta}_{MN}\xi^M\xi^N = -L^2, \tag{1.17}$$

where L is usually called *AdS radius*. Notice that for large value of the coordinates ξ^M we have $\bar{\eta}_{MN}\xi^M\xi^N \approx 0$. This hypersurface defines the boundary of the space.
In order to better characterize such a geometry we consider the following parametrization

$$\begin{aligned}
\xi^0 &= \frac{L^2}{2r^2}\left(1 + \frac{r^2}{L^4}(x^i x^i - t^2 + L^2)\right),\\
\xi^i &= \frac{r x^i}{L} \quad \text{for } i \in \{1,...,d\},\\
\xi^{d+1} &= \frac{L^2}{2r}\left(1 + \frac{r^2}{L^4}(x^i x^i - t^2 - L^2)\right),\\
\xi^{d+2} &= \frac{rt}{L},
\end{aligned} \tag{1.18}$$

where $t \in \mathbb{R}$, $\xi^i = (\xi^1,...,\xi^{D-2}) \in \mathbb{R}^{D-2}$ and $r \in \mathbb{R}_+$. These are local coordinates as only one half of the space is covered due to $r > 0$. These coordinates are called *Poincaré patch*. Substituting the above expressions into Eq.(1.16) we obtain the line element

$$ds^2 = \frac{L^2}{r^2}dr^2 + \frac{r^2}{L^2}(\eta_{\mu\nu}dx^\mu dx^\nu), \tag{1.19}$$

where $\mu, \nu = 0...d+1$ and $\eta_{\mu\nu} = \text{diag}(-1,1,1,...,1)$. Notice that for fixed value of r, Eq.(1.19) is given by the Minkowski metric. Therefore, an anti-de-Sitter space in the Poincaré patch can be seen as a collection of $(d+1)$-dimensional flat spaces plus an extra emergent dimension r. In such coordinates the asymptotic boundary lies at $r = \infty$ as depicted in Fig.1.2. The Ricci scalar of Eq.(1.19) is given by $\mathcal{R} = -\frac{(d+2)(d+1)}{L^2}$ which is indeed constant and negative. In addition, this allows us to interpret the AdS radius L as the radius of curvature. By construction, the metric Eq.(1.19) has the same symmetry group as the hyperboloid in Eq.(1.17) i.e. $\text{SO}(2, d+1)$. It has $(d+2)(d+1)/2$ generators as expected for a $d+2$ dimensional maximally symmetric space. As we have seen, this is precisely also the symmetry group of a CFT in $d+1$ dimensional flat space. Therefore, we can roughly think of Eq.(1.19) as the gravity incarnation of conformal symmetry. In particular, notice that the AdS metric is invariant under the rescaling $(r, t, \mathbf{x}) \mapsto (\lambda^{-1}r, \lambda t, \lambda\mathbf{x})$. Eq.(1.19) can also be promoted to a black-hole geometry as follows. Let us consider

$$ds^2 = \frac{L^2}{f(r)r^2}dr^2 + \frac{r^2}{L^2}(-f(r)dt^2 + dx_d^2). \tag{1.20}$$

The function f is called *blackening function* and vanishes at a location r_+ which defines the event horizon of the black hole. Plugging this expression into the Einstein equations shows that

$$f(r) = 1 - \left(\frac{r_+}{r}\right)^{d+1}. \tag{1.21}$$

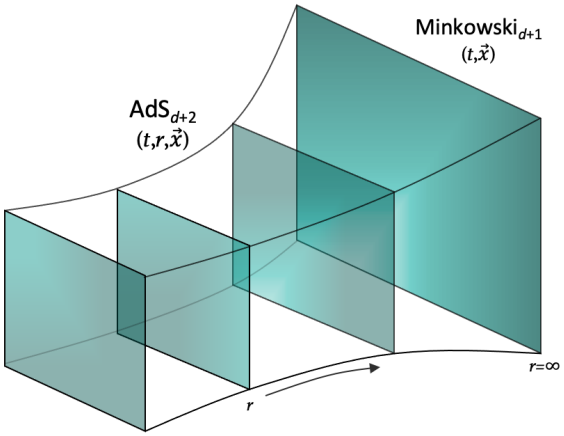

Figure 1.2: An anti-de-Sitter space in Poicaré patch coordinate can be seen as a collection of flat slices in one lower dimension. Figure re-adapted from Ref. [18].

is a solution. This is nothing but the Schwarzschild solution whose blackening function is more conventionally written as $f(r) = 1 - \frac{M}{r^{d+1}}$, where M is a parameter that can be interpreted as the mass of the black hole. Notice $f(r \approx \infty) \to 1$. Therefore, Eq.(1.20) is asymptotically anti-de-Sitter.
Hawking showed that black holes evaporate, with temperature and entropy given by [33, 34]

$$T = \frac{\hbar \kappa_s}{2\pi}, \quad S = \frac{A}{4\hbar G_N}. \tag{1.22}$$

Here A is the area of the event horizon and κ_s is the surface gravity, i.e. the force required to hold a unit mass above the horizon. In the following we will often use the relation $\kappa^2 = 8\pi G_N$. The Hawking temperature can be directly computed from the blackening function through the well known procedure of compactification of the imaginary time and yields

$$T = \frac{(d+1)r_+}{4\pi L^2}. \tag{1.23}$$

This condition ensures that after Euclidean continuation Eq.(1.20) is free of conical singularities, as required by regularity of spacetimes at the black hole horizon – see Sec. 1.2.2.

1.2 Statement of the correspondence and its implications

In the previous sections we have introduced the conformal group as well as anti-de-Sitter spaces. The implication of Maldacena's discovery for $\mathcal{N} = 4$ SYM theory and its $AdS_5 \times \mathbb{S}^5$ dual is that there is a class of quantum field theories that are also conformal (a class of conformal field theories) which have an equivalent description in terms of a general relativity theory in an anti-de-Sitter spacetime. The real of this discovery is that we know the precise relation between the two descriptions.

A central quantity of a quantum field theory are the correlation functions of operators $\mathcal{O}$. In the generating functional formalism these can be derived from the partition function

$$Z_{\rm QFT}[h(x)] = \int \mathcal{D}\mathcal{O} e^{i\int d^{d+1}x h(x)\mathcal{O}(x)} \equiv \langle e^{i\int d^{d+1}x h(x)\mathcal{O}(x)}\rangle, \tag{1.24}$$

where h is the source for the operator $\mathcal{O}$. When the theory is weakly coupled, one can compute the correlation functions through perturbative expansion of the expectation value in the right hand side of the above equation. However, we are interested in the regime where this is not the case and we need to engineer alternative tools to tackle the problem. Gubser-Klebanov-Polyakov [31] and Witten [30] gave a prescription to compute Eq.(1.24) through an alternative method. Let us consider a gravity theory which sits in an anti-de-Sitter space with one extra dimension r. As we reviewed in the introductory sections, an AdS space has a non-dynamical, flat boundary that we conventionally assume to be located at $r = \infty$ – see also Fig.1.3. This allows us to select among all the bulk fields those which asymptote the source h on the boundary. The gravity partition function can then be constructed by path-integrating over such fields:

$$Z_{\rm g}[h(x)] = \int_{\psi(r\to\infty,x)=h(x)} \mathcal{D}\psi e^{-iS[\psi(r,x)]}. \tag{1.25}$$

Here $\psi = \psi(r, x)$ is a generic bulk field and S the gravity action. The insight of GKPW is that these two partitions functions ought to be the same. Therefore:

$$Z_{\rm QFT}[h(x)] = Z_{\rm g}[h(x)]. \tag{1.26}$$

As a consequence, there is a one-to-one correspondence between physical observables and bulk fields. In this sense, the $d+1$ dimensional quantum field theory can be intuitively identified with the asymptotic boundary of AdS_{d+2} – see Fig.1.2. Moreover, if we are interested in the strongly coupled ($g \to \infty$) large-N limit, this turns out to be equivalent to a saddle-point approximation for the gravity partition function. This yields

$$Z_{\rm QFT}^{N,g\to\infty}[h(x)] = e^{-iS[\psi^\star(r\to\infty,x)=h(x)]}, \tag{1.27}$$

where $\psi^\star$ is the solution to the stationarity equations following from $\delta S = 0$. This expression makes it clear that the generating functional for the QFT is given by the gravity action evaluated on those solutions which asymptote the physical source on the boundary.

Rule 2 - GKPW

Generating functional of a strongly coupled QFT_{d+1} = d+2 dimensional bulk action evaluated on solutions which asymptote the physical sources.

In the AdS/CFT framework, the extra dimension is interpreted as the energy scale of the dual field theory [35–38]. As noted around Eq.(1.19), an AdS space in the Poincaré patch can be visualized as a collection of flat slices. Schematically, a slice at a precise value of the radial coordinate is identified as a version of the dual field theory at a given value of the energy scale,

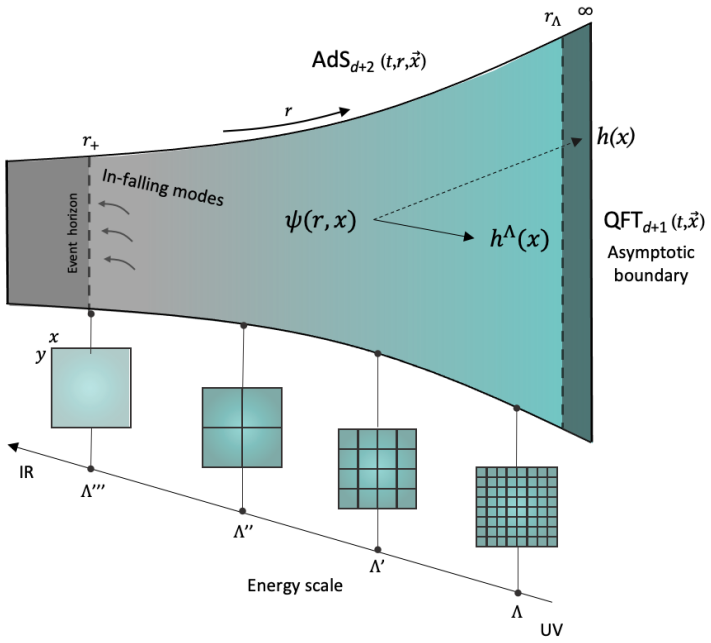

Figure 1.3: Cartoon of the AdS/CFT correspondence. A strongly coupled quantum field theory in $d+1$ dimensions sits at the boundary of an asymptotically AdS spacetime in $d+2$ dimensions. A field ψ in the bulk induces the physical source h on the boundary. Slices at constant r correspond to a version of the dual theory at a given value of the energy scale. The near-boundary region is identified with the UV while the interior one with the IR.

see Fig.1.3. In this sense, the asymptotic region near the AdS boundary corresponds to the ultraviolet regime of the field theory, while the interior of spacetime to the infrared one. Now let us suppose we want to study the universal regime of a field theory. According to the well-known Wilsonian renormalization group (RG) scheme, it is necessary to integrate-out all short distance degrees of freedom and keep only those living within a given energy cutoff Λ. By sending this cutoff to low energies, information on infrared dynamics is obtained. On the gravity side, this corresponds to considering as a reference slice not the AdS boundary but a certain cutoff surface that sits at a value of the radial coordinate, say r_Λ.
The GKPW rule can then be extended as follows

$$Z^\Lambda_{\mathrm{QFT}}[h^\Lambda(x)] = e^{-iS[\psi^\star(r\to r_\Lambda,x)=h^\Lambda(x)]}. \tag{1.28}$$

In this sense, the bulk fields induce boundary sources coupled to operators at energy scale below the cutoff. In holography, the RG flow is geometrized and the energy scale is promoted as a spacetime coordinate. The requirement that the holographic partition function is independent of the cutoff yields first-order renormalization group equations. The RG flow is mapped onto the evolution of the fields along the extra dimension. However, it is worth emphasizing that determining exactly the RG scheme of a QFT with holography, as well as the link between Λ

and r_Λ cutoffs is still an open question in general and would probably require a whole proof of correspondence. In any case, in Chap. 9 we give an explicit example of how the extra coordinate is just a measure of the energy scale.

Rule 3 - Extra dimension

RG flow of a QFT_{d+1} = Evolution of bulk fields along the holographic dimension.

In the following we test the GKPW rule by analyzing the explicit example of a real scalar field and learn how to extract correlation functions of the boundary theory from the bulk.

1.2.1 How to compute retarded Green's functions

Let us consider a real scalar field ψ in AdS_{d+2}-black hole background Eq.(1.20). The action which is lowest-order in a derivative expansion is

$$S = -\int d^{d+2}x\sqrt{-g}\left[\frac{1}{2}(\nabla\psi)^2 + \frac{1}{2}m^2\psi^2\right], \tag{1.29}$$

where g is the metric determinant, m the bare mass, and $(\nabla\psi)^2 = g^{\mu\nu}\partial_\mu\psi\partial_\nu\psi$. Our first goal is to derive the stationarity equations and to solve them. To this end we perform partial integration and get

$$S = \frac{1}{2}\int d^{d+2}x\sqrt{-g}\psi(\Box - m^2)\psi - \frac{1}{2}\int_\partial d^{d+1}x\sqrt{-\gamma}\,\psi\partial_n\psi, \tag{1.30}$$

with $\Box = \frac{1}{\sqrt{-g}}\partial_\mu\sqrt{-g}\partial^\mu$. The boundary term comes from Stokes' theorem. The normal derivative is defined as $\partial_n = n^\mu\partial_\mu$ where n^μ is an outward pointing vector normal to the boundary, while γ is the metric induced on the boundary. From the first term we can read-off the equations of motion which follow after variation of the action with respect to ψ:

$$(\Box - m^2)\psi = 0, \tag{1.31}$$

which is the Klein-Gordon equation in curved space. In the asymptotic region ($r \to \infty$) the spacetime is AdS_{d+2} and the equation is $\psi'' + \frac{d+2}{r}\psi' + \left(\frac{(\omega^2-k^2)L^4}{r^4} - \frac{m^2L^2}{r^2}\right)\psi = 0$, where we have used plane-wave decomposition $\psi(r,t,\mathbf{x}) = \psi(r)e^{-i\omega t + i\mathbf{k}\cdot\mathbf{x}}$. In the above expression, L is the AdS-radius and primes denote radial derivatives. Focusing on the asymptotic region, we solve such an equation in a series expansion as $r \to \infty$:

$$\psi = A(\omega,k)\left(\frac{r}{L}\right)^{\Delta-d-1} + B(\omega,k)\left(\frac{r}{L}\right)^{-\Delta} + ... \tag{1.32}$$

where dots denote higher orders in $1/r$. Here A and B are two integration constants to be fixed by appropriate boundary conditions, as we discuss shortly. The solution inherits the scaling behavior of the background and behaves as a power-law where Δ is the largest root of $\Delta(\Delta-d-1) = m^2L^2$:

$$\Delta = \frac{d+1}{2} + \sqrt{\frac{(d+1)^2}{4} + m^2L^2}. \tag{1.33}$$

Let us consider the rescaling $(r, t, \mathbf{x}) \mapsto (\lambda^{-1} r, \lambda t, \lambda \mathbf{x})$. In order for Eq.(1.32) to be unchanged, it must hold that $A \mapsto \lambda^{\Delta-d-1} A$ and $B \mapsto \lambda^{-\Delta} B$. From the GKPW rule Eq.(1.27), we must match the boundary value of the field with the physical source of the dual theory, i.e. $A \sim h$. The coupled operator then scales as $\mathcal{O}(x) \mapsto \lambda^{-\Delta}\mathcal{O}(\lambda x)$, and Δ can be therefore interpreted as the scale dimension of the operator dual to ψ. Notice that $\mathcal{O}$ satisfies the same scaling as the sub-leading coefficient in Eq.(1.32). In the following we make it clear that B indeed gives the expectation value of the operator $\mathcal{O}$.

Rule 4 - Mass - scale dimension

Scale dimension of a CFT_{d+1} operator = mass of the dual field.

We can also distinguish the cases where the dual operator is a marginal, relevant or irrelevant deformation of the fixed point:

$$\begin{array}{lll} \text{Irrelevant deformation} & \Delta > d+1 & m^2 > 0, \\ \text{Marginal deformation} & \Delta = d+1 & m^2 = 0, \\ \text{Relevant deformation} & \Delta < d+1 & m^2 < 0. \end{array}$$

Notice that negative values of the squared mass are allowed as long as the scale dimension Eq.(1.33) stays real, i.e.

$$m^2 L^2 \geq -\frac{(d+1)^2}{4L^2} \equiv m^2_{\mathrm{BF}}. \tag{1.34}$$

The lower value is known as *Breitenlohner-Freedman bound* (BF) and was originally introduced in Ref. [39]. Whenever the BF bound is crossed the field acquires a finite amplitudes which non trivially backreacts on the geometry. As we elaborate in Sec. 1.3.1, this mechanism is at the basis of the spontaneous symmetry breaking process in AdS/CFT.

Regularization of the scalar field action

Following the GKPW wisdom, we have to evaluate the action Eq.(1.30) on the solution. Using the equations of motion (1.31) we are left with a boundary term

$$S_{\mathrm{os}} = -\frac{1}{2}\int_{\partial} d^{d+1}x \frac{\sqrt{-\gamma}}{\sqrt{g_{rr}}}\,\psi\partial_r\psi, \tag{1.35}$$

where we have used the explicit expression for the normal vector $n_\mu = (0, \sqrt{g_{rr}}, 0, ..., 0)$. This is a boundary term and we can use the asymptotic behavior Eq.(1.32)

$$S_{\mathrm{os}} = \lim_{r\to\infty}\left(\frac{d+1-\Delta}{2L}\int_{\partial} d^{d+1}x \left(\frac{r}{L}\right)^{2\Delta-d-1} A^2 + \frac{d+1}{2L}\int_{\partial} d^{d+1}x AB + ...\right), \tag{1.36}$$

where dots denote sub-leading terms in $1/r$. If $2\Delta - d - 1 > 0$, the on-shell action diverges and must be regularized. In the holographic RG scheme, such an infinity corresponds to the usual

UV divergence of a QFT. To do this we can always consider boundary counter-terms which do not affect the equations of motion but can remove infinities. Let us consider

$$S_{\rm ct} = \frac{\Delta - d - 1}{2L} \int_\partial d^{d+1}x \sqrt{-\gamma}\psi^2. \tag{1.37}$$

If we now repeat the asymptotic, on-shell analysis we obtain the on-shell action

$$S_{\rm reg} = \frac{2\Delta - d - 1}{2L} \int_\partial d^{d+1}x A(x)B(x). \tag{1.38}$$

Since A is identified with the source, the one point function follows from Eq.(1.27) via

$$\langle \mathcal{O}(x)\rangle = \frac{\delta S_{\rm reg}}{\delta A(x)} = \frac{2\Delta - d - 1}{2L} B(x). \tag{1.39}$$

This confirms our previous intuition that the sub-leading coefficient of the expansion Eq.(1.32) gives the expectation value of the operator. The near boundary expansion of a bulk field encodes both the physical sources and expectation values of the dual theory. This is a general result of holography and applies also to higher spin fields. In this thesis we will analyze the examples of the Maxwell field A_μ, whose temporal component gives the chemical potential and the charge density, and the metric $g_{\mu\nu}$, which sources at the boundary the stress-energy tensor $T_{\mu\nu}$.
The two-point function is instead given by

$$\langle \mathcal{O}(-x)\mathcal{O}(x)\rangle = \frac{2\Delta - d - 1}{L} \frac{B(x)}{A(x)}, \tag{1.40}$$

where we have appropriately taken into account combinatorial factors. This gives us a simple tool to extract two-point functions from the bulk: it is sufficient to compare the sub-leading with the leading term of the near boundary expansion of the gravity field.
To test such a statement, let us remind that $A \propto k^{d+1-\Delta}, B \propto k^\Delta$. This gives $B/A \propto k^{2\Delta - d - 1}$ which correctly reproduces the scaling of the two-point function expected for a CFT$_{d+1}$.
Furthermore, from Eq.(1.27), the one-point function in the presence of source h can be written as $\langle \mathcal{O}(x)\rangle = \lim_{r\to\infty} \Pi(r,x)$ where $\Pi(r,x) = \delta S/\delta(\partial_r \psi)$ is the canonical momentum conjugated to the field. From this, we can rewrite Eq.(1.40) as

$$\langle \mathcal{O}(-x)\mathcal{O}(x)\rangle = -\lim_{r\to\infty} \frac{\Pi(r,x)}{\psi(r,x)}. \tag{1.41}$$

In order to fully determine the structure of the correlation function Eq.(1.40) we still have to compute the ratio B/A. So far we have just imposed one condition at the asymptotic boundary. In the next we discuss conditions in the interior of the spacetime.

1.2.2 Infalling conditions and retardation

To uniquely determine the solution we need an additional set of boundary conditions. These come from the spacetime interior and it turns out that these mostly determine the type of Green's

function one computes. Let us give an example by considering an AdS-black hole described by the metric Eq.(1.20). We will later show that this is equivalent to considering the CFT at finite temperature. There are then three natural choices of possible Green's functions, the advanced, the retarded and the (Euclidean) time-ordered. Let us focus on the near horizon limit of Eq.(1.31). The equation of motion is given by

$$\psi'' + \frac{1}{r-r_+}\psi' - \frac{\omega_n^2}{(4\pi T)^2(r-r_+)^2} = 0. \tag{1.42}$$

Here ω_n is the Euclidean-Matsubara frequency. This equation is solved by $\psi_\pm(r \approx r_+) = (r-r_+)^{\pm\omega_n/(4\pi T)}$. One solution is clearly divergent at r_+ and has to be excluded to ensure regularity of the spacetime. The singularity of the metric at $r = r_+$ is indeed just an artifact due to the Poincaré coordinates and can be removed switching to a well-behaved system of variables such as the ingoing Eddington-Finkelstein (EF) one

$$t' = t + r_\star(r). \tag{1.43}$$

Here $dr_\star = dr/\gamma(r)$ is called *tortoise coordinate* and $\gamma(r) = \sqrt{g_{tt}(r)/g_{rr}(r)}$. In such a system the spacetime turns out to be free of singularities. More generally, fields are required to be regular in Kruskal coordinates, which are an extension of Eq.(1.43). We discuss Kruskal coordinates in Sec. 5.3.2.
Turning back to Lorentzian signature and including time, the regular solution is given by

$$\psi_{\text{reg}} \sim e^{-i\omega(t+\frac{1}{4\pi T}\log(r-r_+))}. \tag{1.44}$$

This corresponds to a mode which is infalling into the interior. Therefore, this expression is often called in-going or infalling horizon condition. Remarkably, infalling conditions have been first connected to retarded Green's of the boundary theory in Ref. [40]. Therefore, solving the bulk equation with infalling conditions in the interior and matching condition at the boundary yields the retarded correlation function. At $T = 0$ the analysis is more delicate and depends explicitly on the spacetime we are working with. See e.g. Ref. [24] for details.

1.2.3 Alternative quantization(s)

In the previous section we have understood how the near-boundary expansion of a bulk field encodes both the source and expectation value of the operator in the dual theory. We re-quote it here for simplicity:

$$\psi(r) \approx A\left(\frac{r}{L}\right)^{\Delta-d-1} + B\left(\frac{r}{L}\right)^{-\Delta}. \tag{1.45}$$

In order to compute the holographic two points function we had to regularize the on-shell action Eq.(1.36). The divergence arises when $\Delta > (d+1)/2$ on the scale dimension. Another implication of this condition is on the normalizability of fields. A power-law field in AdS space with boundary at $r = \infty$ is *normalizable* if its scale dimension is below $-(d+1)/2$ [23, 41]. Operators of the dual theory have to be normalizable in order for path integrals to be well defined. The only

normalizable mode in Eq.(1.45) is the sub-leading one. The leading one has hence to be non-dynamical to ensure consistency of the theory. This is another reason why it has to represents the source of the dual theory.
The situation drastically changes in the window $\frac{d-1}{2} < \Delta < \frac{d+1}{2}$, where the left-hand-side is the unitary bound of Sec. 1.1.1. In this range both the behaviors in Eq.(1.45) are normalizable. It is then possible to choose an *alternative quantization* where the roles of the coefficients are swapped. The holographic field ψ is then dual to an operator with scale dimension $\Delta_{\rm alt} = d + 1 - \Delta$ and the Green's function is given by

$$G_{\rm alt}(x) = \frac{A(x)}{B(x)}. \tag{1.46}$$

Therefore, in the window where both the behaviors are normalizable the holographic description captures two fundamentally different CFTs duals.

Rule 5 - Green's function

Retarded two point function of an operator = ratio of the normalizable and non-normalizable falloff of the near boundary expansion of the dual field which satisfies ingoing conditions in the interior.

There is a third possibility where neither A nor B but a combination of them gives the physical source. Specifically

$$h = A - \partial_B \mathcal{W}[B], \quad \langle \mathcal{O} \rangle = B, \tag{1.47}$$

where $\mathcal{W}$ is a polynomial in B – see Refs. [42, 43]. Below we derive such an expression and give an interpretation in terms of multi-trace deformations of the field theory Lagrangian.

1.2.4 Multi-trace deformations

Let us perturb the boundary CFT with the following term $\mathcal{L}_0 \mapsto \mathcal{L}_0 + h\mathcal{O} + \mathcal{W}[\mathcal{O}]$. Here $\mathcal{L}_0$ represents the unperturbed Lagrangian and $\mathcal{W}$ is a polynomial of the operator $\mathcal{O}$ often called a *multi-trace deformation*. From a holographic point of view we need to extend the GKPW rule Eq.(1.27). Let us define

$$\langle e^{i\int d^{d+1}x\, h\mathcal{O}} \rangle_{\mathcal{W}} \equiv \exp\Big[-iS[\psi^\star(r\to\infty, x) = h(x)]\Big]. \tag{1.48}$$

Our goal is to determine the generating functional from holographic arguments. In the case of a scalar field we have seen that the regularized action assumes the form $S_{\rm reg}[A, B] = \frac{1}{2}\int_k A(k)B(-k)$ where $\int_k ... = \int \frac{d^d k d\omega}{(2\pi)^{d+1}}$. Using the linear relation Eq.(1.40) between A and B we can get a functional only of e.g. the leading coefficient: $\mathcal{I} = S_{\rm reg}[A]$. In this way, a direct computation shows that A and B are canonically conjugated variables:

$$B = \frac{\delta \mathcal{I}}{\delta A}, \quad A = -\frac{\delta \mathcal{J}}{\delta B}, \tag{1.49}$$

where $\mathcal{J}[B] = \mathcal{I} - \int d^{d+1}x A \frac{\delta \mathcal{I}}{\delta A}$. In the standard quantization the sub-leading coefficient B represents the dual operator. This suggests to identify B as variable and work with the functional $\mathcal{J}$. Therefore, the candidate generating functional is

$$S[B] = \mathcal{J}[B] + \int_k \Big(hB + \mathcal{W}[B] \Big) . \tag{1.50}$$

Stationarity of the action gives the relation $\delta_B \mathcal{J} + h + \partial_B \mathcal{W} = 0$. Using Eq.(1.49) we find $A = h + \partial_B \mathcal{W}[B]$ that is precisely our earlier Eq.(1.47). Notice that without deformations, i.e. $\mathcal{W} = 0$, we re-obtain the known result $A = h$. We conclude that setting mixed boundary conditions on the coefficients A and B of the holographic scalar field corresponds to deforming the theory via a multi-trace deformation.

1.3 Breaking scale invariance: finite temperature and density

In the previous sections, we understood that AdS spacetimes correspond to conformal field theories in one lower dimension. However, in most physical systems, scale invariance is broken. The focus of the remainder of this chapter is to understand how to break such a symmetry in the AdS/CFT framework by means of temperature and chemical potential.
In field theory, temperature can be introduced through compactification of Euclidean time. The partition function is then given by

$$Z_{\mathrm{QFT}}(T) = \int_{\mathbb{S}^1 \times \mathbb{R}^d} \mathcal{D}\mathcal{O}\, e^{-I_{\mathrm{E}}[\mathcal{O}]}, \tag{1.51}$$

where I_{E} is the euclidean action of the field theory. The GKPW rule states that the field theory lives at the boundary of an AdS space. As noted in Sec. 1.1.2, an AdS space can be promoted to a black hole by considering an appropriate blackeninging function. Black holes have a temperature given by the Hawking formula Eq.(1.22). Therefore, the natural generalization of the GKPW rule is to consider the theory at finite temperatures as placed at the boundary of the black hole provided that we identify the physical temperature with the Hawking one.

Rule 6 - Temperature

Physical temperature = Hawking temperature of the dual black hole.

In addition, black holes can also have a charge. To show this fact in the AdS/CFT context we consider the Einstein-Maxwell action. For simplicity we work in $d + 2 = 4$ bulk dimensions:

$$S_{\mathrm{EM}} = \int d^4x \sqrt{-g} \Big[\frac{1}{16\pi G_{\mathrm{N}}} \Big(\mathcal{R} - 2\Lambda \Big) - \frac{1}{4 g_F^2} F^2 \Big], \tag{1.52}$$

where $F = dA$ is the Maxwell field strength with coupling g_F, and $\Lambda = -3/L^2$.
The saddle point equations follow from stationarity of the action with respect to the fields and read:

$$\mathcal{R}_{\mu\nu} - (\mathcal{R} - 2\Lambda)\frac{g_{\mu\nu}}{2} = 16\pi G_{\mathrm{N}} T_{\mu\nu}, \quad \partial_\mu(\sqrt{-g}F^{\mu\nu}) = 0, \tag{1.53a}$$

with stress-energy tensor $T_{\mu\nu} = \frac{1}{2g_F^2}\left(\frac{1}{4}F^2 g_{\mu\nu} - F_{\mu\rho}F^{\rho}_{\nu}\right)$. Let us use the ansatz

$$ds^2 = -V(r)dt^2 + \frac{dr^2}{V(r)} + r^2 d\Omega_2^2, \quad A = A_t(r)dt, \tag{1.54}$$

where we focused on spherically symmetric solutions. The spatial coordinates indeed live on a sphere of radius r with line element $d\Omega_2^2$ and area $s_2 = 4\pi$. Plugging the above expression into the equations of motion yields the following blackening function $V(r) = 1 + \frac{r^2}{L^2} + \frac{\Theta^2}{r^2} - \frac{\mathcal{M}}{r}$. This is the well-known Reissner-Nordström solution that describes a black hole with mass $\mathcal{M}$ and charge Θ [32]. The geometry is asymptotically AdS as $r \to \infty$ and has a horizon at r_+. At the horizon V vanishes and gives the relation $\mathcal{M} = r_+\left(1 + \frac{r_+^2}{L^2} + \frac{\Theta^2}{r_+^2}\right)$. The temperature follows from the procedure of compactification of the imaginary time and gives

$$4\pi T = \sqrt{\frac{g'_{tt}(r)g'_{rr}(r)}{g_{rr}^2(r)}}\bigg|_{r_+} = \frac{1}{r_+} - \frac{4\pi G_{\mathrm{N}}\mu^2}{g_F^2 r_+} + \frac{3r_+}{L^2}. \tag{1.55}$$

To ensure regularity of both the components A_t and A^t, the gauge potential has to vanish at the event horizon. As a consequence $A_t = \mu(1 - r/r_+)$. At the boundary A_t has the characteristic leading-sub-leading behavior already found in Eq.(1.32). It is a general feature of holography that global symmetries of the QFT and local symmetries in the bulk are mapped onto each other [23–25]. The Maxwell potential A is a U(1) gauge field and has to correspond to a global U(1) on the boundary. It is then natural to interpret the subleading coefficient as the charge density, while the leading one with its source, i.e. the chemical potential μ. The former aspect will be confirmed below after a proper thermodynamic analysis. Finally, conservation of the radial current $\partial_r(\sqrt{-g}F^{rt}) = 0$ gives $g_F\Theta = \sqrt{4\pi G_{\mathrm{N}}}r_+$.

Rule 7 - Symmetries

Global symmetry of the boundary = local symmetry of the bulk.

As we also did in Sec. 1.2.1, the GKPW rule Eq.(1.27) requires the action to be regular in order to obtain the thermodynamics of the field theory dual. In particular, the grand potential density is given by $\omega = \frac{I_{\mathrm{os}}}{\beta V_2}$, where $\beta = T^{-1}$ is the inverse temperature, I_{os} is the gravitational on-shell action in Euclidean signature, and V_2 the spatial volume. In order for the on-shell action to be finite and stationary, we must consider appropriate boundary counter-terms which do not affect the bulk equations of motion. On the one hand, the pure gravity part of Eq.(1.52) is regularized by the well-known Gibbons-Hawking counter-term (see e.g. [44])

$$S_{\mathrm{GH}} = \frac{1}{16\pi G_{\mathrm{N}}}\int_{\partial} d^3x\sqrt{-\gamma}\left(2\mathcal{K} + 4 + L\mathcal{R}[\gamma]\right), \tag{1.56}$$

where $\gamma_{\mu\nu}$ is the metric induced on the boundary, $\mathcal{K}$ the trace of the extrinsic curvature and $\mathcal{R}[\gamma]$ gives the curvature of the boundary.

On the other hand, using the equations Eq.(1.53a) in the Maxwell term, it is easy to check that on-shell action vanishes as $r \to \infty$. Let us check stationarity. We have $\delta S_{\rm M}^{\rm os} \propto (\delta\mu - \delta\rho/r)$ where we used the near boundary expression for the Maxwell potential. Here we have two possibilities:

- $\delta\mu = 0 \to$ the chemical potential is fixed (grand canonical ensemble) and the on-shell action is stationary.
- $\delta\rho = 0 \to$ the charge is fixed (canonical ensemble) and the on-shell action is not stationary. To regularize the problem we have to consider the boundary counter term

$$S_{\rm M,ct} = \frac{1}{g_F^2}\int d^3x\sqrt{-\gamma}F^{\mu\nu}n_\mu A_\nu. \tag{1.57}$$

  Going on-shell, this last term is given by $S_{\rm M,ct}^{\rm o.s.} = s_2 r_+\mu^2/g_F^2 = \mathcal{Q}\mu$ with total charge $\mathcal{Q}$. As a consequence, the grand potential gets renormalized as $\Omega \mapsto \Omega + \mu\mathcal{Q}$ which is exactly the map between grand potential and free energy.

Working in the grand canonical ensemble, the grand potential density is given by

$$\omega = \frac{r_+}{2\kappa^2}\Big(1 - \frac{r_+^2}{L^2}\Big) - \frac{\mu^2 r_+}{4g_F^2}. \tag{1.58}$$

From this expression we can compute the entropy and charge density $s = r_+^2/4G_{\rm N}, \rho = \mu r_+/g_F^2$. Note how the entropy density is consistent with the Bekenstein-Hawking formula Eq.(1.22), and the charge density can also be obtained from Gauss' law evaluated at $r \to \infty$. This also confirms that the sub-leading falloff in Eq.(1.54) gives the charge density.

1.3.1 The superconducting instability

In this section we test the stability of the Reissner-Nordström solution Eq.(1.54) by perturbing it with a probe scalar field. Specifically, we consider

$$S_{\rm EM} \mapsto S_{\rm EM} - \int d^{d+2}x\sqrt{-g}\,(|D\Psi|^2 + m^2|\Psi|^2 + V(|\Psi|)). \tag{1.59}$$

The field Ψ has bare mass m and charge $q^\star$ with respect to the U(1) field strength F, and covariant derivative $D_\mu = \partial_\mu - iq^\star A_\mu$. The potential $V(|\Psi|)$ takes into account higher-order-in-$|\Psi|$ terms and may play a role in determining the backreaction onto the geometry. Here we are interested in the probe limit where the background is insensitive to the dynamics of the scalar field.

Eq.(1.59) goes under the name of *Abelian Higgs model* and was first used by Gubser to test the stability of the Reissner-Nordström solution [45]. It can be viewed as a Ginzburg-Landau action with order parameter field Ψ for U(1) symmetry breaking in curved space. However, $m^2 = 0$ does not identify a phase transition as negative squared masses not always compromises the stability of the theory in curved space. As we have seen in Eq.(1.34), m^2 needs to cross the BF bound in order to trigger an instability.

The question is whether there exists a built-in mechanism in holography that drives the mass below such a value allowing for spontaneous symmetry breaking.
The equation of motion is given by

$$\partial_r(\sqrt{-g}g^{rr}\partial_r\Psi) = \sqrt{-g}\, m_{\text{eff}}^2\, \Psi. \tag{1.60}$$

Even though we are working in the probe limit, the scalar field feels the background in a way such that its mass gets renormalized as

$$m_{\text{eff}}^2 = m^2 - |g^{tt}|q^{\star 2}A_t^2. \tag{1.61}$$

Depending on the Maxwell term, the mass may cross the BF bound. In the asymptotic region A_t vanishes and Eq.(1.61) gives the bare mass. This is an indication that the near boundary theory is stable. On the contrary, in the vicinity of the event horizon, the electromagnetic negative shift may becomes important. If $q^\star$ is big enough, the black hole electric field can excite the vacuum producing Schwinger pairs of particles and anti-particles [46]. Due to the electric-screening, one of the partner will fall into the horizon. If the temperature is low enough, the gravitational field and the electric force equilibrate the anti-partner, and a condensate with the same charge as the black hole forms.

Since the violation of the BF bound occurs in the interior, the IR scale dimension of the scalar field becomes imaginary and the correspondent Green's function acquires poles in the upper half-frequency plane [47]. Causality does not allow such poles and leads to exponentially growing perturbations. The endpoint of this process is a charge condensate localized in the near-horizon region. As a consequence, the scalar field develops a finite profile and an analysis of the coupled problem away from the probe limit must be employed. This goes under the name of *holographic superconductivity* and was first introduced in Refs. [48, 49], see also Refs. [50, 51]. The connection between holographic superconductivity and the BF bound in AdS_2 – which will be the core theme of the next chapter – was first made explicitly, with increasing precision of the statement, in Refs. [49, 52, 53].

Rule 8 - Superconductivity

Superconducting order parameter = scalar field charged under U(1) gauge symmetry.

Linear stability analysis Eq.(1.60) is valid only in the probe limit, i.e. if the back-reaction of the scalar field is small. However, it can be used to gain knowledge on the phase transition and below we give some details on the numerical determination of the critical temperature.
For this specific problem it turns out to be much easier to work with the planar RN solution:

$$\begin{aligned} ds^2 &= \frac{r^2}{L^2}\left(-f(r)dt^2 + d\mathbf{x}^2\right) + \frac{L^2dr^2}{f(r)r^2}, \\ A &= \mu\left(1 - \frac{r_+}{r}\right)dt, \quad \Psi = 0, \end{aligned} \tag{1.62}$$

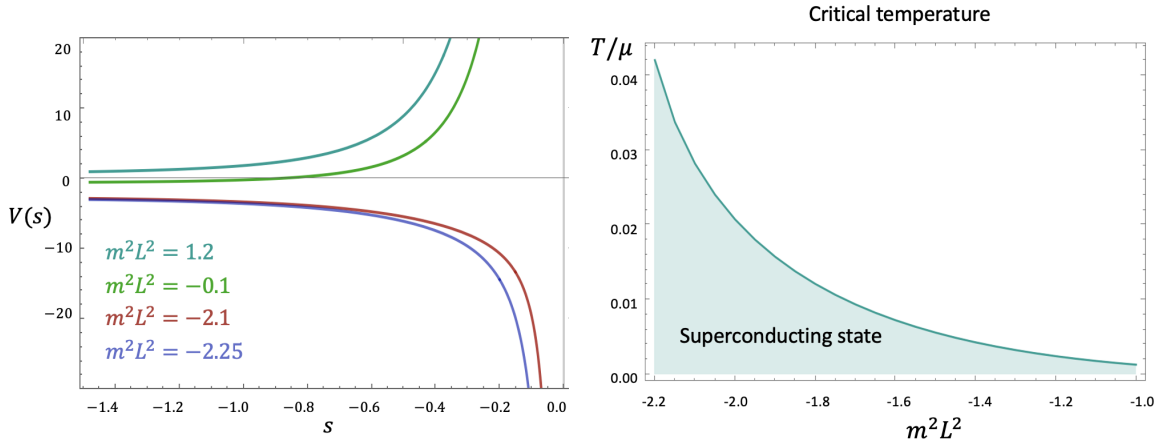

Figure 1.4: Left panel: Schroedinger potential as function of the tortoise coordinate s for different values of the squared mass m^2 and for $q^\star = 1, Q = \sqrt{3}$. The event horizon is located at $s = -\infty$, the boundary at $s = 0$. Right panel: critical temperature of the holographic superconductor as a function of m^2 for various $q^\star = 1$.

with blackening factor $f = 1 - \frac{M}{r^3} + \frac{Q^2}{r^4}$, temperature $T = \frac{3r_+}{4\pi L^2}(1 - \frac{Q^2}{3r_+^4})$, chemical potential $\mu = 2g_F Q/L^2 r_+$, and mass $M = r_+^3 + Q^2/r_+$. Here Q is the black hole charge. In the following we set $r_+ = L = 1$. We seek solutions to Eq.(1.60) able to develop a non-vanishing expectation value even in the absence of an external source. With the conventions of the asymptotic expansion Eq.(1.32), this requires $A = 0$ and $B \neq 0$. If such a solution exists, then the dual theory develops a finite order parameter and undergoes the superconducting phase transition. However, this will not be true for all choices of the parameters of the theory in Eq.(1.62). To get a sense of the right tuning, we can map Eq.(1.60) into an effective 1-dimensional Schrödinger problem, using $\Psi(s) = Z(s)\psi(s)$ with $Z = (\frac{g_{ii}g_{rr}}{-g})^{\frac{1}{4}}$ and $\frac{ds}{dr} = \sqrt{\frac{g_{rr}}{g_{ii}}}$. This yields

$$\begin{aligned} &\partial_s^2 \psi = V(s)\psi, \\ &V(s) = g_{ii} m_{\text{eff}}^2 + \left(\partial_s \log Z\right)^2 - \partial_s^2 \log Z, \end{aligned} \tag{1.63}$$

which corresponds to zero-energy modes. In the new coordinates, the horizon is mapped to $s = -\infty$ while the boundary to $s = 0$. A plot of the potential is given in Fig.1.4. The shape depends on the parameters $Q, q^\star$, and m^2. In Fig.1.4 we see that lowering m^2 deforms a barrier into a well, opening the possibility for the existence of near-boundary bound states Therefore, the instability is guaranteed by the existence of near-boundary bound states of the Schroedinger problem [38] .

In the following we solve numerically Eq.(1.60) through a shooting method. Numerics work better in the $z = 1/r$ coordinates ($z_{\text{bdy}} = 0$, $z = z_+ = 1$) as we can avoid dealing with infinities. In Ref.[54] the same method is applied for a holographic superconductor in a magnetic field. We work at fixed $q^\star$ and m^2 in the parameter region suggested by the stability analysis. To solve

the equation of motion we impose regularity at the horizon, namely $\Psi(1) = 1, \Psi'(1) = 0$, and use the function *NDSolve* in Mathematica. There will be a critical value of the charge $Q^\star$ at which $A(Q^\star) = 0, B(Q^\star) \neq 0$. To find such a value we use the fact that $A \propto \partial_z \phi$ and extract $Q^\star$ through the function *FindRoot*. Given a pair $(m, q^\star)$, for a generic value of T/μ such a solution will not exits. Scanning over T/μ one can find the critical value where the solution does exist and this denotes the critical temperature where the system becomes unstable. We show the results in Fig.1.4.

1.4 Summary

In this chapter we have reviewed the fundamental aspects of the holographic duality. In Sec. 1.1 we have given an overview of the Maldacena's conjecture which states that a very specific quantum field theory ($\mathcal{N} = 4$ SYM) with conformal symmetry and at strong coupling can alternatively be described in terms of classical gravity in anti-de-Sitter space with one additional dimension. We then have reviewed the basics of the two sides of the correspondence, highlighting that a CFT_{d+1} and an AdS_{d+2} space have the same symmetry group $\text{SO}(2, d+1)$. In Sec. 1.2 we have reviewed the more modern statement of the correspondence, provided by the GKPW rule which states that a generic strongly coupled quantum field theory in $d+1$ dimensions is dual to classical gravity in one additional dimension. More specifically, the QFT lives at the boundary of an asymptotically AdS space, and the holographic dimension represents the energy scale of the dual theory. The generating functional of the boundary theory is given by the gravity action evaluated on appropriate solutions to the gravitational equations. In Sec. 1.2.1 we have reviewed how to compute retarded two point functions from holography: the sources and operators of the physical theory are essentially encoded in the near boundary expansion of the dual bulk fields. Finally, we have considered charged black holes which correspond to a physical boundary theory at finite temperature and density. This has been the theme of Sec. 1.3 where we have also outlined the mechanism for spontaneous symmetry breaking of U(1).

1. **Maldacena's duality**
   Strongly coupled CFT_{d+1} = Weakly coupled classical gravity on AdS_{d+2}.
2. **GKPW**
   Generating functional of a strongly coupled QFT_{d+1} = $d+2$ dimensional bulk action evaluated on solutions which asymptote the physical sources.
3. **Extra dimension**
   RG flow of a QFT_{d+1} = Evolution of bulk fields along the holographic dimension.
4. **Mass - scale dimension**
   Scale dimension of a CFT_{d+1} operator = mass of the dual field.
5. **Green's function**
   Retarded two point function of an operator = ratio of the normalizable and non-normalizable falloff of the near boundary expansion of the dual field which satisfies ingoing conditions in the interior.
6. **Temperature**
   Physical temperature = Hawking temperature of the dual black hole.
7. **Symmetries**
   Global symmetry of the boundary = local symmetry of the bulk.
8. **Superconductivity** *Superconducting order parameter = scalar field charged under U(1) gauge symmetry.*

Recap Box – The holographic dictionary

Chapter 2

2 AdS_2 horizons and the SYK model

In this chapter we focus on charged black holes at zero temperature. In the first section 2.1 we show that in the interior of such geometries spatial directions decouple from the radial and temporal ones. The latter coordinates vary on an AdS_2 emergent spacetime. Many features of the full theory can be understood in terms of this lower dimensional geometry. In Sec. 2.1.1 we express the retarded correlation function of a scalar operator in terms of low-energy data. In Sec. 2.2 we derive the universal low-energy theory, described in terms of dilaton-gravity models. In Sec. 2.3 we introduce the Sachdev-Ye-Kitaev model, which is argued to be the microscopic dual to such a spacetime.

2.1 The extremal Reissner-Nordström black hole

In this chapter we focus on the spherical symmetric black holes reviewed in Sec. 1.3. The temperature Eq.(1.55) is a second order equation in the horizon location, whose largest root is $r_+(T,\mu)/L_2 = 4\pi L_2 T + \sqrt{(4\pi L_2 T)^2 - 2\kappa^2\mu^2/g_F^2}$. Here $\kappa^2 = 8\pi G_N$, $L_2 = L/\sqrt{6}$ and we will give a physical interpretation shortly. At $T = 0$ it holds that

$$\frac{r_+(T=0,\mu)}{L_2} \equiv \frac{r_\star}{L_2} = \sqrt{\frac{\kappa^2\mu^2}{g_F^2} - 2}. \tag{2.1}$$

Due to the non-vanishing chemical potential, the horizon sits at a finite value of the radial coordinate $r_\star$ known as *extremal horizon*. In such a limit, the blackening function has a double zero at the extremal horizon $V(r) \approx (r - r_\star)^2/L_2^2$ and the metric tensor is given by:

$$ds^2 = -\frac{(r-r_\star)^2}{L_2^2}dt^2 + \frac{L_2^2}{(r-r_\star)^2}dr^2 + r_\star^2 d\Omega_2^2. \tag{2.2}$$

See also Ref.[55–57]. Let us introduce a new coordinate via $r = r_\star + \frac{L_2^2}{\zeta}$. In the new reference system the extremal horizon lies at $\zeta = \infty$ and the boundary at $\zeta = 0$. The metric and the

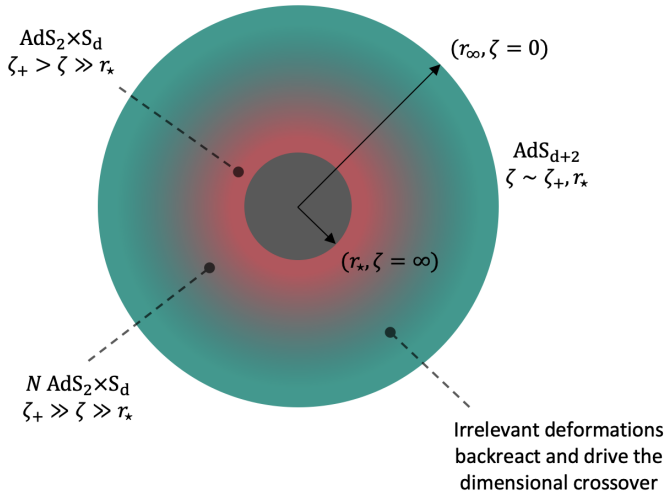

Figure 2.1: Spherical RN black hole in $d+2$ dimensions (in the figure $d=1$ and time is not displayed). At extremality an $\mathrm{AdS}_2 \times \mathbb{S}^d$ factor arises near the horizon (red area). The inner region is the energy-fluctuations dominated regime. Increasing the energy scale, irrelevant deformations back-react on the geometry, driving the spacetime to the asymptotic AdS_{d+2} region.

gauge-field Eq.(1.54) are then given by

$$ds^2 = \frac{L_2^2}{\zeta^2}(-dt^2 + d\zeta^2) + r_\star^2 d\Omega^2, \quad A = \frac{E}{\zeta}dt, \tag{2.3}$$

where E is a dimensionless electric field. We recognize that (t, ζ) together form an AdS_2 spacetime. The background crosses over from asymptotic AdS_{d+2} to a near horizon $\mathrm{AdS}_2 \times \mathbb{S}^d$ region, which signals a low energy, emergent scale invariance in time direction of the dual field theory. The length scale L_2 gives the curvature radius of the emergent AdS_2 space and it holds that $L_2 < L$. For small but finite temperature, the geometry is given by:

$$ds^2 = \frac{L_2^2}{\zeta^2}\left(-f_2(\zeta)dt^2 + \frac{d\zeta^2}{f_2(\zeta)}\right) + r_\star^2 d\Omega_2^2, \quad A = \frac{E}{\zeta}g_2(\zeta)dt. \tag{2.4}$$

This is the metric of $\mathrm{AdS}_2 \times \mathbb{S}^d$-black hole with blackening factor $f_2(\zeta) = 1-(\zeta/\zeta_+)^2, g_2(\zeta) = 1-\zeta/\zeta_+$, and temperature $2\pi T = \zeta_+^{-1}$. The phase dual to such a geometry is a very novel type of phase that was essentially unknown before its discovery in holography. Known as a *semi-local quantum liquid*, it is characterized by correlation functions of matter fields which are scale invariant with respect to time dilatation but rapidly decay in space directions [58–60].
At $T=0$ the charge density is $\rho = \mu r_\star / g_F^2$, while the entropy density is $s = 4\pi r_\star^2/2\kappa^2$. Remarkably, the entropy does not vanish at $T=0$, in contradiction with thermodynamic laws. As is well known, unless protected by a symmetry, such a state is unstable to small fluctuations to

a state of lower entropy. Importantly, the electric field in Eq.(2.4) satisfies the thermodynamic relation $2\pi E = (\partial s/\partial\rho)_T$. Finally, the specific heat is given by $\gamma = 8\pi^2 L_2^2 r_\star/\kappa^2$.

2.1.1 Near-far matching expression for holographic correlation function

Following Wilson, at low energies there should be a self-consistent way to describe the theory in terms of its low-energy degrees of freedom. This implies that the correlation functions in a full CFT at finite density dual to a charged AdS black hole at low energies should essentially be given by its dynamics near the horizon. The goal of this section is to show this relation, i.e. to relate the retarded correlators of the full theory to the Green's function of the 2-dimensional infrared sector. This section is based mainly on Refs. [25, 58–60]. To this end, we perturb the extremal RN background with a scalar field ψ charged under the Maxwell field, whose equation of motion in Fourier space is

$$\Box\psi = \sqrt{-g}\left(m^2 - g^{tt}(\omega + q^\star A_t)^2 + g^{\alpha\alpha}k_\alpha^2\right)\psi, \tag{2.5}$$

where $\Box$ denotes the Laplacian operator along the radial direction. As reviewed in Sec. 1.2.1, the two-points function of the operator dual to ψ follows from the analysis of the above equation close to the asymptotic boundary, and usually numerics is required. Below we focus on the small frequency regime where we can make some analytic computations. However, perturbation theory of Eq.(2.5) fails close to the horizon $r - r_\star \ll \omega$ (inner region). This is due to the double zero of the blackening function, that leads to a divergence of the metric element g^{tt} which always comes in with a factor of ω^2. Therefore, a full non-perturbative computation is required here. On the contrary, in the *outer region* $r - r_\star \gg \omega$, the ω-expansion is controlled.

As we will see below, the AdS_2 case is quite fortunate as it allows for exact solution of the equations. Such a behavior emerges in the interior of extremal black holes at approximately $r - r_\star \sim \mu$, as we have seen in the previous section. As depicted in Fig. 2.2, there is an overlap of the inner and outer regions when $\omega \ll \mu$. We now proceed to (i) exactly solve the equations in the inner region, (ii) perform a ω-expansion in the outer one, (iii) match the results.

Inner region: we first study the $T = 0$ case. In the inner region we use the background Eq.(2.2), and the equation of motion becomes an effective Schroedinger problem for zero energy modes

$$\partial_\zeta^2\psi_{\text{in}} = \frac{L_2^2 m^2 - (\zeta\omega + q^\star E)^2 + \frac{L_2^2}{r_\star^2}\mathbf{k}^2}{\zeta^2}\psi_{\text{in}}. \tag{2.6}$$

This equation is exactly solvable, and the solution is a combination of Whittaker's functions $\psi_{\text{in}}(\omega,\zeta) = c_1 M_{iq_\star,\nu}(-2i\omega\zeta) + c_2 W_{iq_\star,\nu}(-2i\omega\zeta)$, where c_1 and c_2 are two constants. The condition $c_1 = 0$ ensures that any out-going mode from the interior is suppressed – see Sec. 1.2.2 for details. Therefore $\psi_{\text{in}} \propto W_{iq_\star,\nu}$ and an expansion close to the AdS_2 boundary gives

$$\psi_{\text{in}}(\zeta \approx 0) = \zeta^{\frac{1}{2}-\nu_k} + \mathcal{G}_k(\omega)\zeta^{\frac{1}{2}+\nu_k}, \tag{2.7}$$

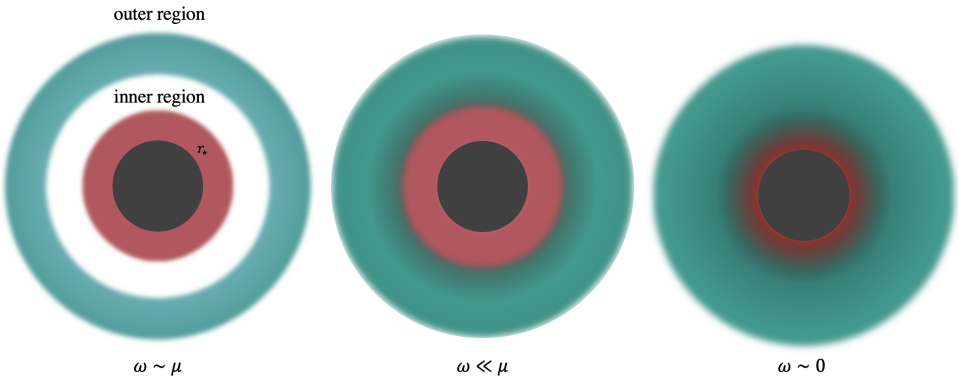

Figure 2.2: The bulk of a spherical RN black hole. In the outer region (teal area) perturbation in ω is controlled and is defined by $\omega \ll r - r_\star$. In the inner region (red area) $r - r_\star \ll \mu$ holds. In order for this regions to overlap it must hold that $\omega \ll \mu$. When $\omega = 0$, the condition defining the outer region is satisfied for all r and there is total overlap.

with $\nu_k = \sqrt{L_2^2 m^2 + \frac{L_2^2}{r_\star^2}\mathbf{k}^2 - q^{\star 2}E^2 + \frac{1}{4}}$ and

$$\mathcal{G}_k(\omega) = \frac{\Gamma(-2\nu_k)\Gamma(\frac{1}{2}+\nu_k - iq^\star E)}{\Gamma(2\nu_k)\Gamma(\frac{1}{2}-\nu_k - iq^\star E)}(-2i\omega)^{2\nu_k} \tag{2.8}$$

This corresponds to the infrared retarded correlation function of the dual field theory. This result can be extended to finite temperatures if we consider the black-hole background Eq.(2.4). The solution is in this case given by $\psi = c_+ F_+(\zeta,\omega) + c_- F_-(\zeta,\omega)$, where

$$F_\pm = e^{-\frac{1}{2}\pi\zeta_+\omega}(\zeta_+\zeta)^{\frac{1}{2}\mp\nu_k}(\zeta-\zeta_+)^{-\frac{i\zeta_+\omega}{2}}(\zeta+\zeta_+)^{-\frac{1}{2}\pm\nu_k+\frac{i\zeta_+\omega}{2}} \tag{2.9}$$

$$\times \mathcal{F}_2^{(1)}\left[\frac{1}{2}\mp\nu_k - iq^\star E, \frac{1}{2}\mp\nu_k + i(q^\star E - \zeta_+\omega), 1\mp 2\nu_k, \frac{2\zeta}{\zeta+\zeta_+}\right]. \tag{2.10}$$

Here $\mathcal{F}_2^{(1)}$ is the hypergeometric function. Expanding the solution close to the event horizon and requiring suppression of out-going modes, gives the following finite temperature correlator

$$\mathcal{G}_k^T(\omega) = (4\pi T)^{2\nu_k}\frac{\Gamma(-2\nu_k)\Gamma\left(\frac{1}{2}+\nu_k - \frac{i\omega}{2\pi T} + iq^\star E\right)\Gamma\left(\frac{1}{2}+\nu_k - iq^\star E\right)}{\Gamma(2\nu_k)\Gamma\left(\frac{1}{2}-\nu_k - \frac{i\omega}{2\pi T} + iq^\star E\right)\Gamma\left(\frac{1}{2}-\nu_k - iq^\star E\right)}. \tag{2.11}$$

Note that using the Stirling approximation $\Gamma(x+\alpha) \sim x^\alpha$ as $x \to \infty$, the above expression gives Eq.(2.8) again.

Outer region: In the outer region $r - r_\star \gg \omega$ perturbations in ω are well defined. The leading order is obtained by setting $\omega = 0$ in Eq.(2.5), which have two independent solutions $\eta_\pm$ such

that $\eta_{\pm}^{(0)}(r \to r_\star) = [(r - r_\star)/L_2^2]^{-\frac{1}{2}\pm\nu_k} + ...$ We then have

$$\psi_{\rm out}^{(0)}(\mathbf{k}, r) = \eta_{+}^{(0)}(\mathbf{k}, r) + c_k \eta_{-}^{(0)}(\mathbf{k}, r), \tag{2.12}$$

where c_k is a constant.

Overlap region and matching: at small but finite frequencies both Eq.(2.7) and Eq.(2.12) are valid and we can write

$$\psi_{\rm out}^{(0)}(\omega, \mathbf{k}, r) = \eta_{+}^{(0)}(\mathbf{k}, r) + \mathcal{G}_k(\omega)\, \eta_{-}^{(0)}(\mathbf{k}, r). \tag{2.13}$$

More generally, for higher orders in ω we have $\psi_{\rm out}(k_\mu, r) = \eta_+(k_\mu, r) + \mathcal{G}_k(\omega)\, \eta_-(k_\mu, r)$, with $\eta_\pm = \eta_\pm^{(0)} + \eta_\pm^{(1)}\omega + \eta_\pm^{(2)}\omega^2 + ...$ It is important to stress that this result holds only for not too high frequencies. Expanding the solution near the asymptotic boundary $r \to \infty$, we find

$$\psi_{\rm out}(k_\mu, r \approx \infty) = \Big(a_+ + a_- \mathcal{G}_k(\omega)\Big)\, r^{\Delta-3} + \Big(b_+ + b_- \mathcal{G}_k(\omega)\Big)\, r^{-\Delta}. \tag{2.14}$$

Thus we get for the boundary retarded Green's function

$$G_{\rm R}(\omega, k) = \frac{b_+^{(0)} + b_+^{(2)}\omega + O(\omega^2) + \mathcal{G}_k(\omega)(b_-^{(0)} + b_-^{(2)}\omega + O(\omega^2))}{a_+^{(0)} + a_+^{(2)}\omega + O(\omega^2) + \mathcal{G}_k(\omega)(a_-^{(0)} + a_-^{(2)}\omega + O(\omega^2))}. \tag{2.15}$$

The k-dependent coefficients can only be determined by solving the outer region equation numerically. However, at extremely low frequencies it holds that ${\rm Im}G_{\rm R} \propto \omega^{2\nu_k}$. Therefore, the low-energy spectral function is determined by near-horizon physics up to a frequency-independent prefactor. Moreover, matching argument in Eq.(2.15) is a key ingredient to analyze a set of holographic quantum phase transitions that are beyond the mean-field paradigm [60].

2.2 JT gravity theory

In this section we derive the low-energy universal theory living in the near-AdS_2 region of extremal black holes. We first dimensionally reduce the theory down to two dimensions and then cut off the UV at a certain energy scale ϵ lying in the near-AdS_2 region.

We start from the Einstein-Maxwell action Eq.(1.52) in Euclidean signature, which admits the Reissner-Nordström solution Eq.(1.54). Our aim is to focus on the AdS_2 sector. Therefore, we perform a dimensional reduction down to two dimensions. Assuming rotational invariance, we choose the following ansatz

$$ds^2 = \Phi^{-1}(\zeta) d\tilde{s}^2 + \Phi^2(\zeta) d\Omega_2^2, \quad A_\mu dx^\mu = \tilde{A}_a(\zeta) dx^a, \tag{2.16}$$

where $a, b = \tau, \zeta$ and the *dilaton* Φ controls the radius of the 2-sphere as we flow along the holographic direction. We denote with $\tilde{X}$ quantities in the dimensionally reduced theory. Useful

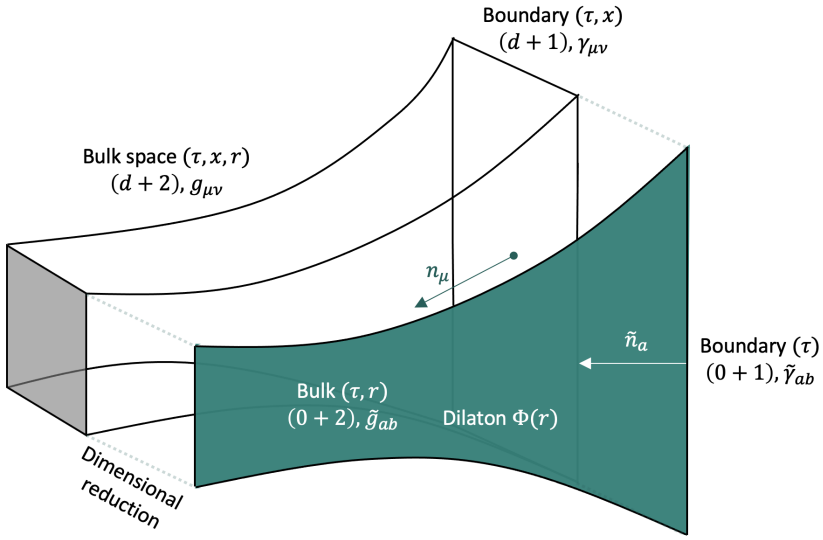

Figure 2.3: Cartoon of dimensional reduction from 3 to 2 dimensions. The spatial direction gets encoded in an additional field (the dilaton) which lives in the bulk of the reduced space.

formulae for dimensional reduction are:

$$\begin{aligned}
&\sqrt{g} = \sqrt{\tilde{g}}\sqrt{\Omega_2}\,\Phi, \quad \sqrt{\gamma} = \sqrt{\tilde{\gamma}}\sqrt{\Omega_2}\Phi^{\frac{3}{2}}, \\
&\mathcal{R} = \Phi\tilde{\mathcal{R}} + \frac{2}{\Phi^2} - \frac{3}{\Phi\sqrt{\tilde{g}}}\partial_\zeta\left(\Phi\sqrt{\tilde{g}}\partial^\zeta\Phi\right), \\
&\mathcal{K} = \sqrt{\Phi}\tilde{\mathcal{K}} + \frac{3}{2}\tilde{n}_\zeta\frac{\partial_\zeta\Phi}{\sqrt{\Phi}}, \quad F^2 = \Phi^2\tilde{F}^2.
\end{aligned} \tag{2.17}$$

Here g and γ are the bulk and boundary metric respectively, whereas $\sqrt{\Omega_2}$ is the determinant of the angular metric, and $\int d\Omega_2\sqrt{\Omega_2} = s_2 = 2\pi^{3/2}/\Gamma(\frac{3}{2}) = 4\pi$ is the area of the 2-sphere with unit radius. $\tilde{\gamma}$ is the metric induced by γ on the 1-dimensional boundary. The vector $\tilde{n}_a$ has unit norm and is normal to the boundary of the manifold described by metric $\tilde{g}$ and pointing outward ($\tilde{n}_\zeta = \sqrt{\tilde{g}_{\zeta\zeta}}$). The quantity $\tilde{\mathcal{K}}$ is the extrinsic curvature induced on the 1-dimensional boundary. Moreover, all the counterterms I_{ct} in Eq.(1.52) do not contribute as they vanish on a boundary with $d = 0$ spatial dimensions [55].
The 2-dimensional action is then given by:

$$\frac{I}{4\pi} = \int d^2x\sqrt{\tilde{g}}\left[-\frac{1}{2\kappa^2}\left(\Phi^2\tilde{\mathcal{R}} + U(\Phi)\right) + \frac{Z(\Phi)}{4}\tilde{F}^2\right] - \frac{1}{\kappa^2}\int_\partial dx\,\sqrt{\tilde{\gamma}}\,\Phi^2\tilde{\mathcal{K}}, \tag{2.18}$$

with $U(\Phi) = \frac{2}{\Phi} + \frac{6}{L^2}\Phi$, $Z(\Phi) = \frac{\Phi^3}{g_F^2}$. Two dimensional dilaton-gravity theories were originally investigated to study low energy excitations around AdS_2 solutions [61, 62]. The dilaton field

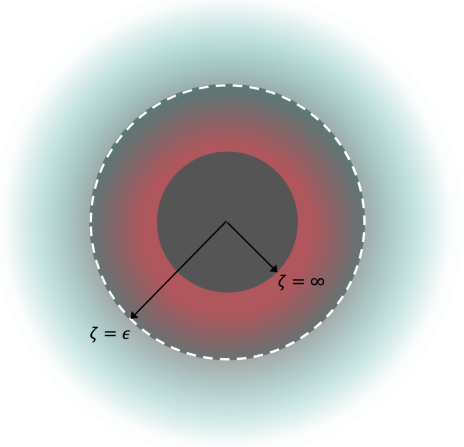

Figure 2.4: Cutoff of the asymptotic geometry. The inner region represents the universal, near-AdS_2 region.

satisfies the following equation of motion

$$2\Phi\tilde{R} + U'(\Phi) - \frac{\kappa^2}{2}Z'(\Phi)\tilde{F}^2 = 0. \tag{2.19}$$

Eq.(2.18) is just a rewriting of the Einstein-Maxwell theory. Therefore, it must have the same solution as the higher-dimensional sibling. The map between the two solutions Eqs. (1.54) and (2.16) is

$$\Phi(\zeta) = r_\star + \frac{L_2^2}{\zeta} \tag{2.20}$$

with ζ ranging in the interval $(0, \infty)$. As $\zeta \sim \infty$, the geometry become AdS_2. This behavior persists up to a certain scale ϵ below which irrelevant deformations drive the geometry back to the AdS_4 asymptotic region. In the new language of Eq.(2.20), a constant dilaton probes the low-energy region. However, AdS_2 alone does not sustain nonzero energy configurations since the stress-energy tensor vanishes [62]. A non-vanishing stress tensor is attainable by considering a non-constant dilaton. In order not to destroy the AdS_2 geometry, we consider a slowly varying dilaton by taking linear perturbation around the constant value of the form

$$\Phi^2(\zeta) = \varphi_0 + \frac{\varphi_1}{\zeta}. \tag{2.21}$$

This behavior is allowed within the window $0 \ll \epsilon < \zeta < \infty$ which probes the area in Fig.2.4. Comparing to Eq. (2.20) we can identify $\varphi_0 = r_\star^2$ and $\varphi_1 = 2r_\star L_2^2$. In the next step we Taylor-expand the action Eq. (2.18) to first order in the dilaton. Let us adopt the notation $\Phi = x_0 + \delta x$, with $x_0 = \varphi_0^{1/2}$ and $\delta x = \frac{1}{2}\varphi_0^{-1/2}\frac{\varphi_1}{\zeta}$. We have

$$I[x_0 + \delta x] = I[x_0] + I_{\mathrm{GH}}[x_0] + \left.\frac{\delta I}{\delta x}\right|_{x_0}\delta x + \left.\frac{\delta I_{\mathrm{GH}}}{\delta x}\right|_{x_0}\delta x. \tag{2.22}$$

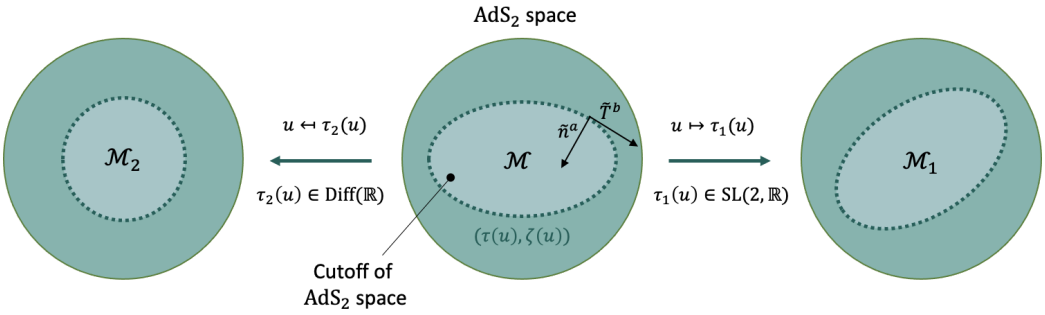

Figure 2.5: Chunk of the hyperbolic disk. The boundary is a curve embedded in AdS_2 with bulk coordinates $(\tau(u), \zeta(u))$. On the right, the chunk is rotated through a $\mathrm{SL}(2, \mathbb{R})$ transformation. On the left, the boundary of the chunk is modified through a reparametrization of the parameter u.

We get rid of the third term by using the equations of motion for x_0 Eq.(2.19). The on-shell action is then given by

$$I_{\mathrm{os}}[x_0 + \delta x] = -\frac{4\pi\varphi_0}{2\kappa^2}\left(\int_{\mathcal{M}} d^2x\sqrt{\tilde{g}}\tilde{\mathcal{R}} + 2\int_{\partial\mathcal{M}} dx\sqrt{\tilde{\gamma}}\tilde{\mathcal{K}}\right) - \frac{4\pi}{\kappa^2}\int_{\partial\mathcal{M}} dx\sqrt{\tilde{\gamma}}\frac{\varphi_1}{\epsilon}\tilde{\mathcal{K}}. \tag{2.23}$$

The domain in the above integrals has been denoted with $\mathcal{M}$, which indicates a dimension-2 manifold obtained by cutting out a chunk from AdS_2 we will shortly comment on. The first contribution can be used to compute the ground state entropy $s = \frac{2\pi\varphi_0}{\kappa^2}$ – see also Eq.(2.29) below. This term is purely topological and gives the Euler-character of the manifold according to the Gauss-Bonnet theorem. Therefore, if $\mathcal{M}$ is a simply connected chunk of the hyperbolic disk, the action is the same, independently on the shape of the boundary curve. To take energy fluctuations into account, we shall consider also the second contribution of Eq.(2.23), which we do in the following.

Goldstone modes and Schwarzian action

In this section we give a physical interpretation of the effective action Eq.(2.23) by investigating its symmetry properties. The metric in the universal region is described by the black hole solution Eq.(2.4). The 1-dimensional boundary is a curve embedded in AdS_2 with bulk coordinates $(\tau(u), \zeta(u))$ – see Fig. 2.5. Here u is a parameter that can be interpreted as the time in the boundary theory. Since the curve lives at the scale ϵ, the induced metric must solve the following relation:

$$\frac{1}{\epsilon^2} = \frac{1}{\zeta^2(u)}\left[f_2(u)\cdot[\tau'(u)]^2 + \frac{[\zeta'(u)]^2}{f_2(u)}\right], \tag{2.24}$$

where τ' and ζ' denote derivatives with respect to u. We solve the above equation for small ϵ, i.e. large energy-UV cutoffs. This also fixes the proper length of the curve imposing the Dirichlet

boundary condition $g_{uu} = 1/\epsilon^2$ – see Refs. [62, 63]. Using $\zeta(u) = \zeta_0(u) + \zeta_1(u)\epsilon + ...$ we find

$$\zeta(u) = \tau'(u)\epsilon + \left(\frac{[\tau''(u)]^2}{2\tau'(u)} - 2\pi^2 T^2[\tau'(u)]^3\right)\epsilon^3 + ... \tag{2.25}$$

We have a family of curves labeled by the function $\tau(u)$, which is just a reparametrization of the boundary time and from now on will play the role of the relevant gravitational degree of freedom. The solution is clearly not invariant under time reparametrizations (as its shape changes) and the emergent IR symmetry of the theory is spontaneously broken. The boundary curve is invariant only under rotations and translations (Fig. 2.5), therefore: the emergent IR boundary-time reparametrization invariance is spontaneously broken by the saddle point solution down to $\mathrm{SL}(2,\mathbb{R})$. The functions satisfying Eq.(2.25) represent the gravitational Goldstone modes associated to the SSB of the emergent symmetry.

We now want to make this point more precise and see this symmetry breaking pattern at the level of the effective action Eq.(2.23).
The extrinsic trace $\tilde{\mathcal{K}} = \tilde{g}^{ab}\nabla_a \tilde{n}_b$ measures the curvature of a manifold embedded in a higher dimensional environment – see e.g. Ref. [32]. The normal vector is determined by the conditions $\tilde{T}^a\tilde{n}_a = 0, \tilde{n}^a\tilde{n}_a = 1$, with tangent vector $\tilde{T}^a = (\tau', \zeta')$. For simplicity we set $T = 0$ in Eq.(2.25) and the metric is simply AdS_2. At second order in the cutoff ϵ we have $\tilde{n}_a = (\frac{\tau''}{(\tau')^2}[1 + \epsilon^2\{\tau, u\}], -\frac{1}{\epsilon\tau'}[1 - \epsilon^2(\frac{\tau''}{\tau'})^2])$. Here the operator

$$\{\tau, u\} = \frac{\tau'''}{\tau'} - \frac{3}{2}\left(\frac{\tau''}{\tau'}\right)^2, \tag{2.26}$$

is called *Schwarzian derivative* and will play a crucial role shortly. The covariant derivative is given by $\nabla_a\tilde{n}_b = \partial_a\tilde{n}_b - \Gamma^c_{ab}\tilde{n}_c$, with Christoffel symbol $2\Gamma^c_{ab} = g^{cd}(\partial_a g_{db} + \partial_b g_{da} - \partial_d g_{ab})$. For the geometry at hand, taking into account the restriction on the curve, the relations $\Gamma^\tau_{\tau\tau} = \Gamma^y_{y\tau} = -\Gamma^\tau_{yy} = -\frac{y'}{\tau'}\frac{1}{y}, \Gamma^\tau_{\tau y} = \Gamma^y_{yy} = -\Gamma^y_{\tau\tau} = -\frac{1}{y}$ hold. With these expressions at hand it is easy to show that $\tilde{\mathcal{K}} = 1 + \epsilon^2\{\tau, u\}$. Plugging this into Eq. (2.23), using that the induced metric satisfies $\sqrt{\tilde{\gamma}} = \epsilon$, and neglecting the constant divergent term [63] we finally find

$$\boxed{I_{\mathrm{os}} = I_0 - \frac{\gamma}{4\pi^2}\int_0^\beta du\,\{\tau, u\}} \tag{2.27}$$

with $\gamma = 16\pi^3\varphi_1/\kappa^2$. This is the first main result of this section. Let us emphasize how the Schwarzian structure makes the correction to the topological piece in the effective action vanishing when $\tau(u) \in \mathrm{SL}(2,\mathbb{R})$ and invariant under the $\mathrm{SL}(2,\mathbb{R})$ group. This is precisely what we predicted before at the level of the solution.

The equations of motions coming from Eq.(2.27) are $\{\tau, u\}'/\tau' = 0 \to \{\tau, u\}' = 0,\ \tau' \neq 0$. The reparametrizations which solve the model are non-constant functions with constant Schwarzian. Examples of solutions are $\tau \in \mathrm{SL}(2,\mathbb{R})$ which will not be considered since they are not dynamical. To find other options we use the composition law of the Schwarzian derivative $\{f \circ g, u\} = g'^2\{f, g\} + \{g, u\}$. This rule allows us to find the thermal solutions. Picking $f = \tan(\tau(u)/2)$ and

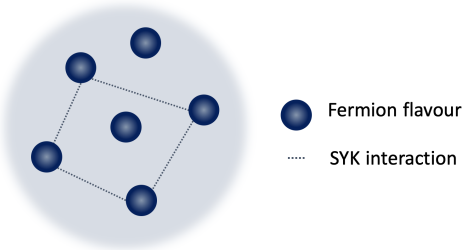

Figure 2.6: Cartoon of the Majorana SYK model. A random all-to-all interaction (dashed line) occurs among $q = 4$ fermion flavours.

$g = \tau(u)$ we have: $\{f, u\} - \{\tau, u\} = \frac{\tau'^2}{2}$. Thermal reparametrizations with constant Schwarzian are thus those with linear τ. To match the Euclidean period we choose $\tau(u) = 2\pi u/\beta$ and the thermal solution is given by

$$f(u) = \tan\Big(\frac{\pi u}{\beta}\Big), \quad \{f, u\} = \frac{2\pi^2}{\beta^2}. \tag{2.28}$$

Let us now turn to thermodynamics. From the GKPW identity Eq. (1.27), we can extract the partition function of the boundary theory from the gravity dual. This allows us to identify the free energy with the gravitational Euclidean action restricted to the thermal solutions Eq.(2.28), namely $\beta F = I^{\text{os}}_{\text{grav}}$. This yields the entropy

$$s = s_0 + \gamma T. \tag{2.29}$$

The coefficient γ in the Schwarzian action can therefore be interpreted as the specific heat. Moreover, after employing the value of the dilaton right below Eq.(2.21) we find exactly the heat capacity derived for the extremal solution. The approach *à la Schwarzian* is therefore able to capture the low energy behavior of systems at finite charge densities.

2.3 The SYK model: an overview

What we shall show now is that this Schwarzian effective action also emerges as the IR effective theory from a special condensed matter model. The Sachdev-Ye model was originally introduced in Ref. [64] in the context of spin liquids and later complemented by Kitaev [65, 66]. In this section we make an overview of the key points of such a model. An extensive review of the topic can be found in Refs. [67, 68], on which this section is mainly based. Let us consider the Sachdev-Ye-Kitaev (SYK) model for a random all-to-all interaction between q components of a fermionic Majorana vector field. The (0+1)-dimensional Hamiltonian is given by

$$H = \frac{(i)^{q/2}}{q!} \sum_{\{i_k\}} j_{i_1 i_2 \ldots i_q}\ \chi_{i_1}\chi_{i_2}\cdots\chi_{i_q}, \tag{2.30}$$

where the factor of i is necessary to ensure hermiticity of the Hamiltonian. Here the flavor index i_k labels the N components of the field, which satisfy the usual anti-commutation relations $\{\chi_{i_k}, \chi_{i_{k'}}\} = \delta_{i_k i_{k'}}, k, k' = 1, ..., q$.
The SYK model encodes disorder in the coupling constants, which are real random variables drawn from a Gaussian distribution.

$$\overline{j^m_{i_1...i_q}} = \int dj_{i_1...i_q}\, \varrho(j_{i_1...i_q})\, j^m_{i_1...i_q}, \tag{2.31a}$$

$$\overline{j_{i_1...i_q}} = 0, \quad \overline{j^2_{i_1...i_q}} = \frac{j^2(q-1)!}{N^{q-1}}, \tag{2.31b}$$

$$\varrho(j_{i_1...i_q}) = \sqrt{\frac{a_q}{\pi}} e^{-a_q j^2_{i_1...i_q}}. \tag{2.31c}$$

Here a_q follows from the normalization of the distribution, and Eq.(2.31b) gives its variance. It is characterized by the parameter j, which we take to be the same for all coefficients. From the Majorana algebra follows that $[\chi] = 0$, in units of energy. Therefore, $[H] = [j] = 1$, and the js are *relevant couplings*. This means that the SYK model is strongly coupled in the IR, while captures the physics of free Majorana fermions in the UV. Last but not least, from the Majorana algebra follows that $j_{i_1...i_j i_k...i_q} = -j_{i_1...i_k i_j...i_q}$ for any pair in the set, meaning that the js are completely antisymmetric couplings.

2.3.1 Large-N analysis

To prepare the Feynman diagram analysis, we derive the SYK Lagrangian from Eq.(2.30) via a Legendre transformation. For simplicity we work in the $q = 4$ case where $\mathcal{L} = -\frac{1}{2}\chi_j \frac{d}{d\tau}\chi_j - \frac{j_{ijkl}}{q!}\chi_i\chi_j\chi_k\chi_l$. Here we work with imaginary time τ as it allows for finite temperatures. The action S follows from the τ-integration of the Lagrangian over the thermal circle, i.e. $S = \int_0^\beta d\tau \mathcal{L} \equiv S_0 + S_{\text{int}}$. The full propagator is given by

$$G_{ij}(\tau_{12}) = \int \mathcal{D}\chi\, e^{-S}\chi_i(\tau_1)\chi_j(\tau_2) = \int \mathcal{D}\chi e^{-S_0}\Big(1 - S_{\text{int}} + \frac{(S_{\text{int}})^2}{2!} + ...\Big)\chi_i(\tau_1)\chi_j(\tau_2),$$

with $\tau_{12} = \tau_1 - \tau_2$. Here it is important to distinguish the quantum averages over the fields configurations ($\langle ... \rangle$) from the disorder averages ($\overline{...}$).
The zeroth-order contribution yields the propagator of free Majoranas

$$\int \mathcal{D}\chi\, e^{-S_0}\, \chi_i(\tau_1)\chi_j(\tau_2) = \frac{1}{2}\text{sgn}(\tau_{12})\delta_{ij} \equiv G_0(\tau_{12})\delta_{ij}. \tag{2.32}$$

The first-order term looks like $\overline{j_{k_1k_2k_3k_4}} \int d\tau \langle \chi_{k_1}(\tau)\chi_{k_2}(\tau)\chi_{k_3}(\tau)\chi_{k_4}(\tau)\, \chi_i(\tau_1)\chi_j(\tau_2)\rangle_0$. Due to Wick's contractions, at least two indices of the j-matrix will be contracted, yielding zero contribution due to the antisymmetry property. In addition, the disorder average $\overline{j_{k_1k_2k_3k_4}}$ yields zero due to Eq.(2.31b). At second-order the only connected diagram is represented in Fig. 2.7. Notice that from Eq.(2.31), the second momentum $\overline{j_{k_1...k_q} j_{k_1...k_q}}$ contributes only if the former set of indices is an even permutation of the latter. Therefore the disorder average forces pair of

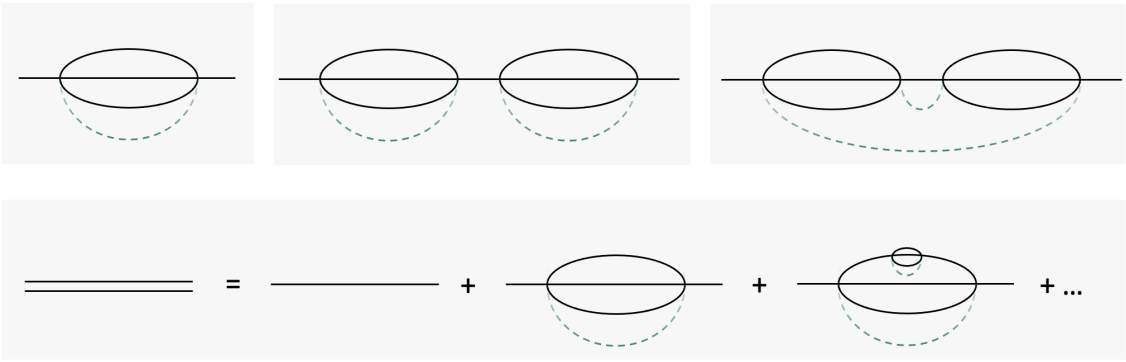

Figure 2.7: Upper panel: second and fourth order contribution to the full propagator. The dashed line represent disorder averages. Lower panel: Dyson series of the large N-SYK model. Figure inspired by Ref. [68].

indices belonging to distinct sets to be equal. The disorder average hence makes the indices of the first vertex equal to the ones of the second, and the Wick's contraction yields

$$G_0(\tau_1-\tau)G_0^3(\tau-\tau')G_0(\tau'-\tau_2)\times\delta_{ik}(\delta_{k_1k_1})^3\delta_{kj}\times\overline{j_{k_1k_2k_3k_4}j_{k_1k_2k_3k_4}}. \tag{2.33}$$

Each delta-trace contributes linearly in N, while the disorder average factor follows from (2.31b). The second order therefore contributes in the same way at any N with self-energy

$$\Sigma(\tau)=j^2G^3(\tau). \tag{2.34}$$

The next non trivial order is the fourth. It is easy to check that the first fourth-order diagram Fig.2.7 contributes with j^4, while the second as j^4/N^2. This basically follows from the fact that the disorder averages couple the vertex in way such that in the latter diagram there are lower number of δ-traces. As N grows, the latter is strongly suppressed, and the Dyson series reduces to the lower panel of Fig. 2.7. The full propagator then satisfies the Schwinger-Dyson equation

$$G(\tau_{12})=G_0(\tau_{12})+\int d\tau\; G_0(\tau_1-\tau)\int d\tau'\Sigma(\tau-\tau')G(\tau'-\tau_2), \tag{2.35}$$

with self energy given only by Eq. (2.34). This can alternatively be expressed in the frequency domain as

$$G^{-1}(\epsilon_n)=i\epsilon_n-\Sigma(\epsilon_n), \tag{2.36}$$

with $\epsilon_n=2\pi(n+\frac{1}{2})$ being the fermionic Matsubara frequencies. The above equations are well defined in any regime, even beyond the perturbative one $|\beta j|\ll 1$, as they are the *exact* summation of the Dyson series. In the low-energy limit, i.e. dropping the explicit $i\epsilon$ in Eq.(2.36), the equations further simplify:

$$\int d\tau'\,\Sigma(\tau-\tau')G(\tau'-\tau_2)=-\delta(\tau-\tau_2),\quad G(\epsilon_n)\Sigma(\epsilon_n)=-1. \tag{2.37}$$

At low energies these equations have an emergent time reparametrization invariance $\tau \mapsto g(\tau)$ which leads to the following transformation laws

$$\begin{aligned} G(\tau_1 - \tau_2) &\mapsto \Big[g'(\tau_1)g'(\tau_2)\Big]^{\Delta} G(g(\tau_1) - g(\tau_2)), \\ \Sigma(\tau_1 - \tau_2) &\mapsto \Big[g'(\tau_1)g'(\tau_2)\Big]^{(q-1)\Delta} \Sigma(g(\tau_1) - g(\tau_2)), \end{aligned} \tag{2.38}$$

with $\Delta = 1/q$. At low energies it is also easy to find an explicit solution to these equations. It is given by the conformal propagator

$$G_{\rm c}(\tau) = \frac{b}{|\tau|^{2\Delta}} \mathrm{sgn}(\tau), \tag{2.39}$$

with b fixed to $j^2 b^q \pi = (\frac{1}{2} - \Delta) \tan \pi\Delta$. The parameter Δ therefore defines the scale dimension of the low energy propagator. This power-law form signals an emergent non-Fermi liquid behavior. This makes the SYK model appealing as it represents a solvable toy model with strange-metallic features. We underline that $G_{\rm c}$ is not invariant under time-reparametrizations, as it transforms according to Eq.(2.38). Only maps with unitary Jacobian leave the saddle point invariant, therefore the emergent conformal invariance is spontaneously broken down to $\mathrm{SL}(2, \mathbb{R})$ by the saddle $G_{\rm c}$.

Eq.(2.38) maps solutions onto solutions, and can be therefore employed to get the finite-temperature answer from Eq.(2.39). Both $f(\tau) = e^{2\pi\tau/\beta}$ or $f(\tau) = \tan \frac{\tau\pi}{\beta}$ map the circle into a line, yielding

$$G^T(\tau) = b \left[\frac{\pi}{\beta \sin \frac{\pi\tau}{\beta}}\right]^{2\Delta} \mathrm{sgn}(\tau), \tag{2.40}$$

where G^T denotes the thermal propagator.

2.3.2 Large-N effective action

In this section we derive the disorder averaged effective action which provides an alternative description of the model. This approach yields a clearer physical interpretation of the spontaneous breaking of the conformal symmetry, and constitutes a strong connection to the gravitational dual. We first perform disorder average and then integrate out the fermions using standard Lagrange-multiplier techniques and Gaussian integration. This will yield a theory of bi-local fields. We perform the computation for the $q = 4$-body interaction.

Replica trick and disorder average: thermodynamics is generated by the logarithm of the partition function. Disorder averages of such terms are technically hard, and it is necessary to find another way to handle them. The core idea lies in the following identity

$$\overline{\log Z} = \lim_{m \to 0} \frac{\overline{Z}^m - 1}{m}. \tag{2.41}$$

It is indeed possible to avoid log-average by introducing m-replicas of the system. To label such copies we endow the fields in Eq.(2.30) with a further index $a = 1, ..., m$, and obtain

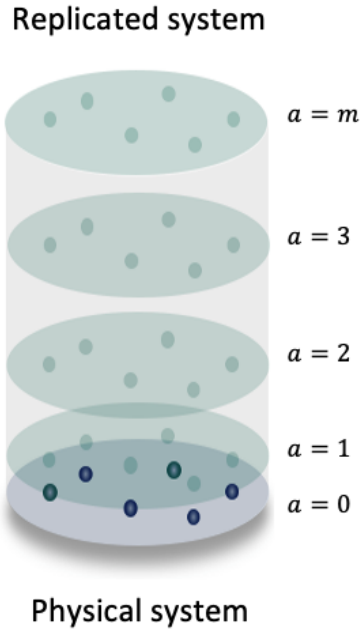

Figure 2.8: Cartoon of replica trick. Certain number of copies of the system is produced. The index a labels the different replicas.

$$\overline{Z^m} = \sqrt{\frac{a_4}{\pi}} \int dj_{ijkl} \mathcal{D}\chi_i^a \, e^{-S_0} \, e^{\sum_{ijkl} \left[-a_4 j_{ijkl}^2 + \int d\tau \sum_a \frac{j_{ijkl}}{4!} \chi_i^a \chi_j^a \chi_k^a \chi_l^a \right]}, \tag{2.42}$$

where $\mathcal{D}\chi^a = \prod_{a=1}^m \mathcal{D}\chi^a$, and a_4 follows from Eq.(2.31). The above expression is quadratic in the coupling constants and we perform Gaussian integration. This gives the following disorder-averaged partition function:

$$\overline{Z^m} = \int \mathcal{D}\chi_i^a \exp\Big[-\frac{1}{2} \sum_{a,i} \int d\tau \, \chi_i^a \partial_\tau \chi_i^a + \frac{j^2 N}{8} \sum_{ab} \int d^2\tau \Big(\sum_i \frac{1}{N} \chi_i^a(\tau_1) \chi_i^b(\tau_2) \Big)^4 \Big], \tag{2.43}$$

where we have ignored numerical pre-factors coming from Gaussian integration.

Bi-local fields: the Majorana fermions enter the above expression quadratically. This naturally suggests to rephrase the theory in terms of the following bi-local in time composite operators

$$G_{ab}(\tau_1, \tau_2) = \frac{1}{N} \sum_{i=1}^{N} \chi_i^a(\tau_1) \chi_i^b(\tau_2). \tag{2.44}$$

However, the price to pay will be the non-locality of the resulting effective theory. We insert G in the path integral Eq.(2.43) as follows

$$\overline{Z^m} = \int \mathcal{D}\chi_i^a \mathcal{D}G_{ab} e^{-\frac{1}{2}\sum_{a,i} \int d\tau \chi_i^a \partial_\tau \chi_i^a + \frac{j^2 N}{8} \sum_{ab} \int d\tau_1 d\tau_2 G_{ab}^4(\tau_1,\tau_2)} \delta\Big(G_{ab}(\tau_1,\tau_2) - \sum_i \frac{1}{N} \chi_i^a(\tau_1) \chi_i^b(\tau_2) \Big).$$

Lagrange-multipliers: it is useful to give a path-integral representation of the δ-function $\delta(G-G') \propto \int \mathcal{D}\Sigma\, e^{-\frac{N}{2}\Sigma(G-G')}$, where Σ is a Lagrange multiplier. This gives

$$\overline{Z^m} = \int \mathcal{D}\chi_i^a\, \mathcal{D}G_{ab}\, \mathcal{D}\Sigma_{ab} \exp\Big[-\frac{1}{2}\sum_{a,i}\int d\tau \chi_i^a \partial_\tau \chi_i^a + \frac{j^2 N}{8}\sum_{ab}\int d^2\tau G_{ab}^4(\tau_1,\tau_2) \\ - \frac{N}{2}\int d^2\tau \Sigma_{ab}(\tau_1,\tau_2)G_{ab}(\tau_1,\tau_2) - \frac{1}{2}\int d^2\tau \Sigma_{ab}(\tau_1,\tau_2)\sum_i \chi_i^a(\tau_1)\chi_i^b(\tau_2)\Big].$$

The above expression is quadratic in the fermions χ and can be simplified through Grassmann integration. In the following we consider a replica-diagonal ansatz $G_{ab} = \delta_{ab}G, \Sigma_{ab} = \delta_{ab}\Sigma$ [69]. As a consequence, a further overall factor of m arises and we obtain $\overline{Z^m} = \int \mathcal{D}G\mathcal{D}\Sigma\, e^{-mS_{\text{eff}}}$ with effective action

$$\frac{S_{\text{eff}}}{N} = -\frac{1}{2}\log\det(\partial_\tau - \Sigma) + \frac{1}{2}\int d\tau_1 d\tau_2 \Big[\Sigma(\tau_1,\tau_2)\; G(\tau_1,\tau_2) - \frac{j^2}{q}G(\tau_1,\tau_2)^q\Big]. \tag{2.45}$$

Let us stress that the determinant of the above formula involves just the time matrix structure. The derivative operator implicitly contains a δ-function while the Lagrange multiplier is bi-local in time.
In the above expression bi-local fields are written as matrices in the τ-space, namely $(\Sigma)_{\tau_1,\tau_2} \equiv \Sigma(\tau_1,\tau_2)$ and $(\partial_\tau)_{\tau_1,\tau_2} \equiv \delta(\tau_1-\tau_2)\partial_\tau$. Note that Eq.(2.45) is stationary exactly on the Schwinger-Dyson equations Eq.(2.36). The saddle points are hence given by the results of the preceding section. In addition, also the effective action exhibits an emergent conformal invariance in the IR, when we neglect the time derivative in the log term. We conclude that SYK can equivalently be investigated both with the canonical diagrammatic expansion and non-perturbative variational methods. This latter approach will straightforwardly lead to an effective theory of energy fluctuations of SYK as we will see in the following.

2.3.3 The Schwartzian action for the reparametrization

Expanding Eq.(2.45) around its saddle points $G_{\text{s}}, \Sigma_{\text{s}}$ yields a quadratic action for the fluctuations:

$$\frac{S_{\text{eff}}^{(2)}[\delta g]}{N} = \frac{j^2(q-1)}{4}\int d^4\tau \delta g(\tau_1,\tau_2)(\tilde{K}_{\text{s}}^{-1}(\tau_1,\tau_2,\tau_3,\tau_4) - 1)\delta g(\tau_3,\tau_4). \tag{2.46}$$

All the technical details can be found in Appendix A. Here δg measures the deviation of the G-field from the saddle G_{s} and the four points function is given by $\tilde{K}(\tau_1,\tau_2,\tau_3,\tau_4) = -j^2(q-1)|G(\tau_{12})|^{\frac{q-2}{2}}G(\tau_{13})G(\tau_{24})|G(\tau_{34})|^{\frac{q-2}{2}}$. In Eq.(2.46) $\tilde{K}$ has been evaluated on the saddle G_{s}.

Spontaneous symmetry breaking (SSB): as already mentioned, the effective action Eq.(2.45) enjoys conformal invariance in the infrared limit, and the saddle point is given by the conformal propagator $G_{\text{s}} = G_{\text{c}}$ in Eq.(2.39). As observed in Sec. 2.3.1, the saddle spontaneously breaks the reparametrization symmetry. The action Eq.(2.46) indeed vanishes on fluctuations induced by reparametrizations of the conformal correlator $S_{\text{eff}}[\delta g = \delta G_{\text{c}}] = 0$ – see Appendix A. In other words, δG_{c} are eigenvectors of $\tilde{K}$ with eigenvalue 1. Such zero modes can be identified

with the Goldstones that arise from the spontaneous breaking of the conformal symmetry [68]. Therefore, reparametrizations of the conformal correlator are Goldstone modes of the conformal SSB. Contrary to the diagrammatic technique, the variational approach offers a prescription to identify the Goldstone modes associated to the breaking of the conformal symmetry.

Explicit symmetry breaking (ESB): if we want to investigate e.g. chaotic properties of the SYK model, we shall compute the four-point functions [70]. From Eq. (2.46), the four-point function contains a term proportional to $(\tilde{K}_{\rm s}-\mathbb{1})^{-1}$, and hence diverges in the IR limit. This is a direct consequence of the vanishing of the action along the reparametrization of the conformal correlator. To fix this we shall include non-conformal UV corrections, which will ultimately yield a finite four-points function. An expansion of the eigenvalues of $\tilde{K}_{\rm s}$ in $(\beta\mathcal{J})^{-1}$ encodes the desired corrections. Here $\mathcal{J}\equiv j\sqrt{q}/2^{\frac{q-1}{2}}$, with j scaled in a way such that $\mathcal{J}$ is fixed in $q\to\infty$ limit [68].
In appendix A we derive the correction due to an infinitesimal reparametrization $\tau\mapsto\tau+\epsilon(\tau)$, whose action turns out to be given by:

$$\frac{S^{(2)}_{\rm eff}[\epsilon]}{N}=\frac{\alpha_{\rm S}}{\mathcal{J}}\int d\tau\frac{1}{2}\Big[|\epsilon''|^2-\Big(\frac{2\pi}{\beta}\Big)^2|\epsilon'|^2\Big], \tag{2.47}$$

with $\alpha_{\rm S}=\frac{\alpha_\epsilon}{6\alpha_0 q^2}$, $\alpha_0^{-1}\equiv b^q j^2(q-1)=\frac{(q-1)(q-2)}{2q\pi}\tan\frac{\pi}{q}$, and α_ϵ measures the eigenvalue shift from 1 in the $(\beta\mathcal{J})^{-1}$ expansion – see Eq.(A.18) of the appendix. This result can be easily generalized to finite reparametrizations $\tau\mapsto g(\tau)$. Up to a translation of $g(0)$ and a rescaling of $g'(0)$, that have no effect on the $T=0$ correlator, this is given by $g(\tau)=\tau+\frac{1}{2}\frac{g''(0)}{g'(0)}\tau^2+\ldots$ This can be brought into the infinitesimal form provided that $\epsilon(0)=\epsilon'(0)=0$ and $\epsilon''(0)=g''(0)/g'(0)$. This suggests to map the action (2.47) into $\frac{S^{(2)}_{\rm eff}[g]}{N}=\frac{\alpha_{\rm S}}{\mathcal{J}}\int d\tau\frac{1}{2}\Big(\frac{g''}{g'}\Big)^2$. Up a total derivative this can be furthermore expressed as

$$\boxed{\frac{S^{(2)}_{\rm eff}[g]}{N}=-\frac{\alpha_{\rm S}}{\mathcal{J}}\int d\tau\,\{g,\tau\}\,,} \tag{2.48}$$

with $\{g,\tau\}$ is the Schwarzian derivative in Eq.(2.26). Note how this expression is the simplest combination in derivatives that vanishes for $g\in{\rm SL}(2,\mathbb{R})$, and is invariant after a global ${\rm SL}(2,\mathbb{R})$ transformation, namely $\{h,\tau\}=\{g,\tau\}$ with $g\xmapsto{{\rm SL}(2,\mathbb{R})}\frac{ag+b}{cg+d}$. The former property follows from the fact that the saddle point $G_{\rm c}$ is invariant under ${\rm SL}(2,\mathbb{R})$. The action Eq.(2.46) vanishes not due to the eigenvalue 1, but because $\delta_{{\rm SL}(2,\mathbb{R})}G_{\rm c}=0$. Such reparametrizations are hence not zero-modes, they simply do not contribute to the path-integral. Moreover, subjecting a reparametrization to an ${\rm SL}(2,\mathbb{R})$ transformation does not change the saddle as, again, $\delta_{{\rm SL}(2,\mathbb{R})}G_{\rm c}=0$.
To switch temperature on, we use $g(\tau)=\tan\frac{\tau\pi}{\beta}$:

$$S^{(2)}_{\rm eff}[\tan(\pi\tau/\beta)]=-2\pi^2\alpha_{\rm S}\frac{N}{\beta\mathcal{J}}=\beta F, \tag{2.49}$$

where F is the free energy. This expression represents the small temperature correction to the free energy. The coefficient $\alpha_{\rm S}$ can then be related to the specific heat ($\gamma=-\partial^2F/\partial T^2$) via $\alpha_{\rm S}=\frac{\mathcal{J}}{N}\frac{\gamma}{4\pi^2}$.

To summarize, the effective theory has an IR emergent conformal symmetry, which is both spontaneously and explicitly broken. The relevant physics is captured by the dynamics of pseudo-Nambu-Goldstone modes in Eq.(2.48). As we have seen, the same pattern of breaking of conformal symmetry happens in the dilaton-gravity model introduced in the previous section. Even the low-energy effective actions Eq.(2.48) and Eq.(2.27) have identical structure and encode the same physics.

2.3.4 Finite density complex SYK

We end this section by mentioning that the above Majorana SYK model can be generalized to the complex fermionic case. This has been done e.g. in Ref. [71]. The Hamiltonian of the model now reads

$$H = \sum_{\{i_1 \dots i_q\}=1}^{N} j_{i_1,\dots,i_q} c^\dagger_{i_1} \dots c^\dagger_{i_{\frac{q}{2}}} c_{i_{\frac{q}{2}+1}} \dots c_{i_q}, \tag{2.50}$$

where q is an even integer number. The fermionic operators satisfy the usual algebra $\{c_i, c^\dagger_{j'}\} = \delta_{ij}\delta_{\sigma\sigma'}$ and $\{c_i, c_j\} = 0$. Moreover, the couplings are complex random numbers satisfying $j_{i_1\dots i_{q/2}, i_{q/2+1}\dots i_q} = j^\star_{i_{q/2+1}\dots i_q, i_1\dots i_{q/2}}$, $\overline{j^2_{i_1\dots i_q}} = j^2 (q/2)!^2/N^{q-1}$. Contrary to the Majorana case, we can define the fermion number via $\mathcal{Q} = \frac{1}{N}\sum_i \langle c^\dagger_i c_i\rangle - 1/2$. The analysis of the model parallels those of the previous section. The Schwinger-Dyson equations are given by

$$\Sigma(\tau) = -(-1)^{q/2} q j^2 [G(\tau)]^{q/2} [G(-\tau)]^{q/2-1}, \tag{2.51a}$$

$$G^{-1}(\epsilon_n) = \epsilon_n + \mu - \Sigma(\epsilon_n). \tag{2.51b}$$

At low energy, such equations are solved by the power-law ansatz

$$G_{\rm s}(\tau) \sim \begin{cases} -|\tau|^{-2\Delta}, & \tau > 0 \\ e^{-2\pi\mathcal{E}} |\tau|^{-2\Delta}, & \tau < 0 \end{cases} \tag{2.52}$$

The spectral asymmetry parameter is defined through the thermodynamic relation $\lim_{T\to 0}(\partial\mu/\partial T)_{\mathcal{Q}} = -2\pi\mathcal{E}$, μ being the chemical potential – see Ref. [71]. In the IR limit Eqs.(2.51) enjoy invariance under both reparametrizations and U(1):

$$\begin{aligned} &G(\tau_1,\tau_2) = [g'(\tau_1) g'(\tau_2)]^{\Delta} e^{i(\varphi(\tau_1)-\varphi(\tau_2))} G(g(\tau_1), g(\tau_2)), \\ &\Sigma(\tau_1,\tau_2) = [g'(\tau_1) g'(\tau_2)]^{(1-\Delta)} e^{i(\varphi(\tau_2)-\varphi(\tau_1))} \Sigma(g(\tau_1), g(\tau_2)). \end{aligned} \tag{2.53}$$

As in the Majorana case, we can alternatively perform the disorder average and introduce bi-local fields. This yields an effective action for the model Eq.(2.50) given by

$$\begin{aligned} S[G,\Sigma] = &- \operatorname{Tr}\ln\Big[\delta(\tau-\tau')(-\partial_\tau + \mu) - \Sigma(\tau,\tau')\Big] + \frac{\mu}{2T} \\ &- \int_0^\beta d\tau d\tau' [\Sigma(\tau,\tau') G(\tau',\tau) + (-1)^{q/2} J^2 [G(\tau,\tau')]^{q/2} [G(\tau',\tau)]^{q/2}]. \end{aligned} \tag{2.54}$$

Fluctuations around the saddle provide information on the energy and $\mathcal{Q}$-fluctuations of the quantum theory. Expanding to the quadratic order Eq.(2.54) yields, for infinitesimal time reparametrizations,

$$\frac{S}{N} = \frac{\chi_\rho}{2}\int_0^\beta d\tau[\partial_\tau\varphi + i(2\pi\mathcal{E}T)\partial_\tau\epsilon]^2 - \frac{\gamma}{4\pi^2}\int_0^\beta d\tau\left\{\tan\Big(\pi T[\tau+\epsilon(\tau)]\Big),\tau\right\}. \tag{2.55}$$

In addition to the specific heat γ, here the coefficient $\chi_\rho = (\frac{\partial\rho}{\partial\mu})_T$ gives the charge compressibility – see Ref. [71] for details. Remarkably, also this type of action can be derived from holography. See Refs. [55–57].

2.4 Summary

In the latter half of this chapter we have introduced a (0+1)-dimensional quantum mechanical model that enjoys conformal invariance at low energies. Away from the infrared, such a symmetry is both spontaneously and explicitly broken and the action for the Goldstone modes has a Schwarzian form given in Eq.(2.48). The same pattern of conformal symmetry breaking occurs in dilaton-gravity geometries, typical for the low-energy limit of extremal black holes. We have reviewed this in the earlier half of this chapter in in Sec. 2.2 where we also commented on the matching argument for UV and IR correlation functions. The SYK model and gravity in 2 dimensions share many features and it is believed that those systems are dual-pairs. To make this statement even stronger, in the final part we have extended the SYK model considering deviations from half filling. Charge fluctuations are captured by a low-energy effective action which couples to the one for reparametrization modes. In Refs. [55–57] the same type of action has been derived from holography, by considering fluctuations of a gauge field in the gravitational background.

Electric $\mathbf{AdS}_2 \times \mathbb{S}^d$ black hole

$$ds^2 = \frac{L_2^2}{\zeta^2}\left(-\left(1-(2\pi T\zeta)^2\right)dt^2 + \frac{d\zeta^2}{1-(2\pi T\zeta)^2}\right) + r_\star^2 d\Omega_2^2$$
$$A = \frac{E}{\zeta}\left(1-2\pi T\zeta\right)dt$$

Matching formula

$$G_{\rm R}(\omega,k) = \frac{b_+(\omega)+\mathcal{G}_k(\omega)b_-(\omega)}{a_+(\omega)+\mathcal{G}_k(\omega)a_-(\omega)}$$

Effective action for Near-$\mathbf{AdS}_2$

$$I_{\rm os} = I_0 - \frac{\gamma}{4\pi^2}\int_0^\beta du\,\{\tau,u\}$$

Schwarzian derivative $\{\tau,u\} = \frac{\tau'''}{\tau'} - \frac{3}{2}\left(\frac{\tau''}{\tau'}\right)^2$

Recap Box – Near extremal black holes

Majorana SYK Hamiltonian

$$H = \frac{(i)^{q/2}}{q!} \sum_{\{i_k\}} j_{i_1 i_2 \ldots i_q}\ \chi_{i_1}\chi_{i_2}\cdots\chi_{i_q}$$

Conformal solution

$$G_{\mathrm{c}}(\tau) = \frac{b}{|\tau|^{2\Delta}}\mathrm{sgn}(\tau)$$

Action for energy fluctuations

$$S^{(2)}_{\mathrm{eff}}[g] = -\frac{\gamma}{4\pi^2}\int d\tau\,\{g,\tau\}$$

Complex SYK Hamiltonian

$$H = \sum_{\{i_1 \ldots i_q\}=1}^{N} j_{i_1,\ldots,i_q} c^{\dagger}_{i_1}\ldots c^{\dagger}_{i_{\frac{q}{2}}} c_{i_{\frac{q}{2}+1}}\ldots c_{i_q}$$

Conformal solution

$$G_{\mathrm{s}}(\tau) \sim \begin{cases} -|\tau|^{-2\Delta}, & \tau > 0 \\ e^{-2\pi\mathcal{E}}|\tau|^{-2\Delta}, & \tau < 0 \end{cases}$$

Spectral asymmetry

$$\lim_{T\to 0}\left(\frac{\partial\mu}{\partial T}\right)_{\mathcal{Q}} = -2\pi\mathcal{E}$$

Action for energy and charge fluctuations

$$\frac{S}{N} = \frac{\mathcal{K}}{2}\int_0^\beta d\tau[\partial_\tau\varphi + i(2\pi\mathcal{E}T)\partial_\tau\epsilon]^2 - \frac{\gamma}{4\pi^2}\int_0^\beta d\tau\left\{\tan\Big(\pi T[\tau+\epsilon(\tau)]\Big),\tau\right\}$$

Recap Box – The SYK model

Part II

Using holography for transport bounds in anisotropic systems

Chapter 3
Scaling theory close to a Lifshitz point

Bounds on transport coefficients are an important tool to quantify the strength of correlations in quantum many-body systems. In Sec. 3.1 we give an overview of bounds on the shear viscosity to entropy density ratio and on charge diffusion obeyed by isotropic theories. In Sec. 3.2 we analyze the behavior of such quantities in the vicinity of a low-energy fixed point where rotational symmetry is broken. Contrary to the isotropic case, the scale dimensions of shear viscosity and entropy density do not match contrary to the isotropic case. We develop a scaling theory which identifies expressions well defined in the anisotropic case. This chapter is based on Ref. [18].

3.1 Introduction and description of the condensed matter system

If one can identify a theoretical value for a minimal electrical conductivity or viscosity, then one can judge how strongly-interacting a system is. A highly influential bound for momentum-conserving scattering of quantum fluids was proposed by Kovtun, Son, and Starinets [72] (KSS) for the ratio of the shear viscosity and entropy density

$$\eta/s \geq \frac{\hbar}{4\pi k_{\mathrm{B}}}. \tag{3.1}$$

It is obeyed in systems like the quark gluon plasma [73] or cold atoms in the unitary scattering limit [74]. Graphene at charge neutrality is another example that is expected to be close to this bound [75]. Within the Boltzmann transport theory one finds that a bound for η/s can be related to the ratio $\ell_{\mathrm{mfp}}/\lambda$ of the mean-free path ℓ_{mfp} and the mean distance λ between carriers. However, Eq.(3.1) is valid even for systems that cannot be described in terms of the quasi-classical Boltzmann theory. Indeed, the bound is saturated for quantum field theories in the strong coupling limit as was shown in Ref. [72] using the holographic duality of conformal field theory and gravity in anti-de-Sitter spacetime [11, 30, 31].
Limiting bounds for the charge transport like the electrical conductivity are somewhat more subtle. A much discussed example is the Mott-Ioffe-Regel limit [76–78] that corresponds to a threshold value of the electrical resistivity when $\ell_{\mathrm{mfp}}/\lambda \sim \mathcal{O}(1)$. While some systems clearly show a saturation of the resistivity once $\lambda/\ell_{\mathrm{mfp}}$ reaches unity, materials like the cuprates or iron-based

superconductors violate this limit [79]. For a detailed discussion of correlated materials that obey or systematically violate the Mott-Ioffe-Regel bound, see Ref. [80]. Transport properties in quantum critical systems were argued under certain circumstances to be governed by a Planckian relaxation rate $\hbar\tau^{-1} \approx k_{\mathrm{B}}T$ [81, 82], which would also limit the electrical conductivity at quantum critical points. A bound on charge transport that is less restrictive and theoretically better justified than the Mott-Ioffe-Regel limit was proposed in Ref. [14]. It constrains the value of the charge diffusivity:

$$D_c \geq C_D \frac{\hbar v^2}{k_{\mathrm{B}}T}, \tag{3.2}$$

with C_D a numerical coefficient of order unity. Here v is the characteristic velocity of the problem. At charge neutrality the heat and electric currents are decoupled, and the charge diffusivity is determined by the Einstein relation $D_c = \sigma/\chi_\rho$. Here σ is the electrical conductivity, and $\chi_\rho = \partial\rho/\partial\mu$ the charge susceptibility with particle density ρ and chemical potential μ. The latter is related to the charge compressibility since $\chi_\rho = -\frac{\rho^2}{V}\frac{\partial V}{\partial p}$. If $v^2\chi_\rho$ stays constant as $T \to 0$, the electrical resistivity cannot vanish slower than linearly in T [14]. Refs. [15, 16] proposed the butterfly velocity $v = v_{\mathrm{B}}$ as the characteristic velocity. The quantity v_{B} follows from the analysis of out-of-time-order (OTOC) correlations $C(\mathbf{x},t) = -\langle[A(\mathbf{x},t), B(\mathbf{0},0)]^2\rangle$ that are discussed in the context of chaos and information scrambling [70, 83–86]. Here A and B are two generic operators of the field theory under consideration whose form is unimportant for the subsequent discussion. It can be obtained from the long-distance behavior, e.g. via

$$C(\mathbf{x},t) \sim e^{2\lambda_{\mathrm{L}}\left(t-\frac{|\mathbf{x}|}{v_{\mathrm{B}}}\right)}. \tag{3.3}$$

The scrambling rate λ_{L} that enters the OTOC is also subject to the bound $\lambda_{\mathrm{L}} \leq 2\pi k_{\mathrm{B}}T/\hbar$ [70]. While the interpretation of λ_{L} and its relation to transport and thermalization rates is not always correct [87–92], the butterfly velocity seems to yield a natural scale for the characteristic velocity of a system, even if no clear quasi-particle description is available. A caveat applies when a symmetry of the system is weakly broken and triggers a sound-to-diffusion crossover: in this case, the resulting diffusivity is more naturally expressed in terms of the sound velocity and the gap [89, 93, 94].

The focus of this part of the thesis is the investigation of anisotropic systems, where the conductivity tensor $\sigma_{\alpha\beta}$ and the viscosity tensor $\eta_{\alpha\beta\gamma\delta}$ exhibit a more complex structure with potentially different temperature dependencies for distinct tensor elements [19, 95]. The anisotropy that we consider is most naturally expressed in terms of the relation between characteristic energies and momenta along different directions. For a system with two space dimensions, it holds then that:

$$\omega \sim |k_x|^{z/\phi}, \quad \omega \sim |k_y|^z, \tag{3.4}$$

with dynamical exponent z. We characterize the anisotropy in terms of the exponent ϕ that relates typical momenta along the two directions according to

$$|k_x| \sim |k_y|^\phi. \tag{3.5}$$

A single-particle dispersion that is consistent with such scaling would be $\varepsilon(\mathbf{k}) \sim |k_x|^{z/\phi} + a|k_y|^z$ that corresponds to a system at a Lifshitz point [96–103]. However, our conclusions do not require the existence of well defined quasi-particles with this dispersion relation.

Anisotropic systems, that obey scaling behavior of a Lifshitz transition were recently shown to violate the viscosity bound [19, 104–111]. In Ref. [19] a model of anisotropic Dirac fermions that emerged from two ordinary Dirac cones was analyzed as an explicit condensed matter realization [112]. Within a quasi-particle description of the transport processes and a Boltzmann equation approach, the conductivity anisotropy was found to diverge: one direction is metallic and another one insulating. Based on the quasi-particle transport theory, a modified bound was conjectured, that involves not just the viscosity tensor elements $\eta_{\alpha\beta\alpha\beta}$ and the entropy density $s(T)$, but also the conductivities [19]:

$$\frac{\eta_{\alpha\beta\alpha\beta}}{s}\frac{\sigma_{\beta\beta}}{\sigma_{\alpha\alpha}} \geq \frac{\hbar}{4\pi k_{\mathrm{B}}}. \tag{3.6}$$

Here, no summation over repeated indices is implied. Other tensor elements like $\eta_{\alpha\beta\beta\alpha}$ continue to obey Eq.(3.1). The combination $\frac{\eta_{\alpha\beta\alpha\beta}}{s}\frac{\sigma_{\beta\beta}}{\sigma_{\alpha\alpha}}$ serves as an indicator of strong coupling behavior in anisotropic systems. In Fig. 3.1 we show typical temperature dependencies for these transport coefficients for a specific value of the crossover exponent ϕ that characterizes the anisotropy. When translations are broken along the β-direction, $\eta_{\alpha\beta\gamma\beta}$ loses its hydrodynamic meaning and just gives the stress-tensor correlation function. The tensor element satisfies a holographic relation which we analyze in both the limits of high and low temperature. The origin for this combined viscosity-conductivity bound is the different scaling behavior of the typical velocities v_α for different directions. Candidate materials with Lifshitz transitions are the organic conductor $\alpha - (\mathrm{BEDT\text{-}TTF_2})\mathrm{I_3}$ under pressure [113], and the heterostructure of the $5/3\mathrm{TiO_2}/\mathrm{VO_2}$ supercell [114, 115]. Moreover, the surface modes of topological crystalline insulators with unpinned surface Dirac cones [116] and quadratic double Weyl fermions [117] are expected to exhibit such a behavior.

The analysis of Ref. [19] was based on the Boltzmann equation and did not allow to explicitly analyze a model that satisfies this bound or determine the precise numerical coefficient in Eq.(3.6), i.e. the factor $1/4\pi$. This can only be done within a formalism that addresses transport in strongly-coupled non-quasi-particle many-body systems. In the same context it is of interest to address the related question of whether the diffusivity bound, Eq.(3.2), is also modified for anisotropic systems.

Before we present the theories that yield these results, we give some general scaling arguments, assuming charge and momentum conservation.

3.2 Scaling arguments

We consider the scaling behavior of transport coefficients in anisotropic systems near a quantum critical Lifshitz point. As we will see, scaling arguments can be efficiently used to make statements about transport bounds. Once a combination of physical observables has scaling dimension zero, it naturally approaches a universal value in the limit $T, \mu, \omega \cdots \to 0$, that corresponds to an underlying quantum critical state. If one can argue, usually based on an analysis of conservation

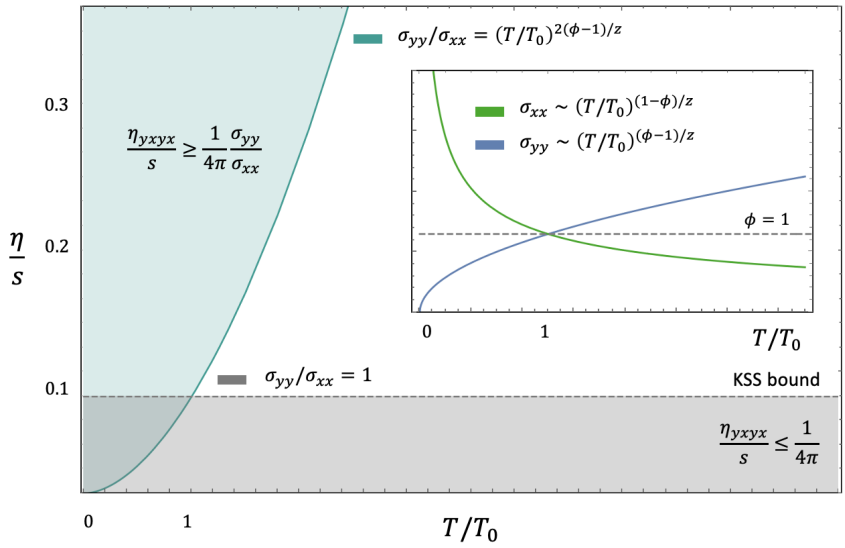

Figure 3.1: Main panel: temperature dependence of the η/s tensor. In the anisotropic case the KSS bound can be parametrically violated. Here, T_0 is a temperature scale below which the anisotropy effects are dominant. The conductivity ratio might constitute a new lower bound when rotations are broken. Inset: temperature dependence of the conductivity tensor elements σ_{xx} and σ_{yy}. ϕ is the crossover exponent that characterizes the anisotropy between the different spatial directions $k_x \sim k_y^{1/\phi}$. Once $\phi \neq 0$ one element of the conductivity of a two-dimensional system must be insulating and the other must be metallic. Figure re-adapted from Ref. [18].

laws, that this value is neither zero nor infinity, it should be some dimensionless number times the natural unit of the observable. In other words, this combination should be insensitive to irrelevant deformations of the quantum critical point. As an example we consider the electrical conductivity at zero density. For isotropic systems its scaling dimension is $d-2$, a result that follows from single-parameter scaling and charge conservation. Thus the conductivity of a zero density two-dimensional system is expected to reach a universal value in units of the natural scale e^2/h. Under the same conditions, both the viscosity and the entropy density have scale dimension d such that their ratio has scaling dimension zero. Then η/s should approach a universal value times $\hbar/k_B$ which yields the correct physical unit. This observation helps to rationalize a result like Eq.(3.1). As an aside, these scaling considerations also offer a natural explanation why the bound Eq.(3.1), while applicable, is not very relevant for Fermi liquids.

The conclusions of this section require that scaling relations are valid, i.e that the system under consideration behaves critical and is below its upper critical dimension. In the remainder of this section we assume that this is the case. To be specific, we analyze a d-dimensional system and allow for one direction to be governed by a characteristic length scale with a different scaling dimension $\phi \neq 1$ than the other spatial directions, see Eqs.(3.4,3.5) above. In addition, the

temporal direction is characterized by a dynamic scaling exponent z. Let us then consider a physical observable $O(\mathbf{k}, \omega)$. By assumption the observable obeys the scaling relation

$$O\left(k_\perp, \mathbf{k}_\parallel, \omega\right) = b^{-\Delta_O} O\left(b^\phi k_\perp, b\mathbf{k}_\parallel, b^z \omega\right). \tag{3.7}$$

Here Δ_O is the scaling dimension of the observable. The d-dimensional momentum vector $\mathbf{k} = (k_\perp, \mathbf{k}_\parallel)$ consists of one component $k_\perp$ that is governed by the exponent ϕ and a $d-1$ dimensional component $\mathbf{k}_\parallel$. In the subsequent holographic analysis we focus on a system with two spatial coordinates and use the notation $k_\perp = k_x$ and $k_\parallel = k_y$. While the scaling analysis presented here cannot determine the values of the exponents, it allows for rather general conclusions once those exponents are known. For an explicit model with nontrivial exponents z and ϕ, see Ref. [19].

3.2.1 Scaling of thermodynamic quantities

We begin our discussion of scaling laws with thermodynamic quantities. For the free-energy density of the system the following scaling law holds:

$$f(T, \mu) = b^{-d_{\text{eff}} - z} f\left(b^z T, b^z \mu\right), \tag{3.8}$$

with effective dimension

$$d_{\text{eff}} = d - 1 + \phi. \tag{3.9}$$

As an energy density, f should scale as unit energy per unit volume. To obtain its scaling dimension it is then easiest to start from the usual result $d + z$ for isotropic systems [82] and replace d by d_{eff}. This takes into account the different weight of the directions $\mathbf{k}_\parallel$ and $k_\perp$. With $s = -\partial f / \partial T$ and $\rho = \partial f / \partial \mu$ we obtain immediately the scaling dimensions $\Delta_s = \Delta_\rho = d_{\text{eff}}$ for the entropy density s and particle density ρ, respectively. Away from zero density, the relation $\Delta_\rho = d_{\text{eff}}$ generally does not hold and one should take into account the anomalous scaling dimension of the charge density operator, which distinguishes between the density of charged critical fluctuations from those contributing to the entropy [89, 118, 119]. The second derivative of the free energy with respect to the chemical potential yields charge susceptibility

$$\chi_\rho(T, \mu) = b^{-\Delta_\chi} \chi_\rho(b^z T, b^z \mu), \tag{3.10}$$

with $\Delta_\chi = d_{\text{eff}} - z$. We can now use these thermodynamic relations to determine the scaling behavior of the conductivity and viscosity. This is possible because of the restrictions that follow from charge and momentum conservation.

3.2.2 Scaling of transport coefficients

Electric conductivity: the conductivity is determined via a Kubo formula from the current-current correlation function, e.g.

$$\operatorname{Re} \sigma_{\alpha\beta}(\omega) = \frac{\operatorname{Im} \Pi_{\alpha\beta}(\omega)}{\omega}. \tag{3.11}$$

At zero density, the system has a finite d.c. conductivity. The function $\Pi_{\alpha\beta}(\omega)$ is the Fourier transform of the retarded current-current correlation function $\Pi_{\alpha\beta}(t) = -i\theta(t)\langle[j_\alpha(t), j_\beta]\rangle$. In order to exploit the implications of charge conservation we use the continuity equation

$$\partial_t \rho + \partial_\alpha j_\alpha = 0, \tag{3.12}$$

and obtain the well known relation between the longitudinal conductivity $\sigma_{\alpha\alpha}(\omega)$ and the density-density correlation $\bar{\chi}_\rho(\mathbf{k},\omega)$

$$\sigma_{\alpha\alpha}(\omega) = \lim_{\mathbf{k}\to 0} \frac{\omega}{k_\alpha^2} \bar{\chi}_\rho(\mathbf{k},\omega). \tag{3.13}$$

Here $\bar{\chi}_\rho(\mathbf{k},\omega)$ is the temporal Fourier transform of $\bar{\chi}_\rho(\mathbf{k},t) = -i\theta(t)\langle[\rho(\mathbf{k},t), \rho(-\mathbf{k},0)]\rangle$, where $\rho(\mathbf{k},t)$ is the spatial Fourier transform of the density $\rho(\mathbf{x},t)$. Since $\chi_\rho = \lim_{\mathbf{k}\to 0} \bar{\chi}_\rho(\mathbf{k},\omega=0)$, the scaling dimension of χ_ρ is also Δ_χ, given below Eq.(3.10). Thus we find

$$\begin{aligned} \Delta_{\sigma,\parallel} &= \Delta_\chi + z - 2 = d_{\text{eff}} - 2, \\ \Delta_{\sigma,\perp} &= \Delta_\chi + z - 2\phi = d_{\text{eff}} - 2\phi, \end{aligned} \tag{3.14}$$

for the conductivities along the two directions. This yields the conductivities:

$$\begin{aligned} \sigma_\parallel(T,\omega) &= b^{3-\phi-d}\sigma_\parallel(b^z T, b^z\omega), \\ \sigma_\perp(T,\omega) &= b^{\phi+1-d}\sigma_\perp(b^z T, b^z\omega). \end{aligned} \tag{3.15}$$

If we return to the isotropic limit, where $\phi = 1$, both components of the conductivity behave the same with the usual conductivity scaling dimension $d-2$. Interestingly, in the anisotropic case, this continues to be the dimension of the geometric mean $\sqrt{\sigma_\parallel \sigma_\perp}$. Distinct scaling exponents for the tensor elements imply a different temperature dependency of the conductivity for different directions. Thus, a more insulating behavior along one direction will force the other direction to be more metallic. For a two-dimensional system, one direction will have to be insulating and the other then has to be metallic as long as $\phi \neq 1$. Finally, the ratio $\sigma_\parallel/\sigma_\perp$ of the conductivity is governed by $\Delta_{\sigma,\parallel} - \Delta_{\sigma,\perp} = 2(\phi-1)$, i.e.

$$\frac{\sigma_\parallel(T)}{\sigma_\perp(T)} = b^{-2(\phi-1)} \frac{\sigma_\parallel(b^z T)}{\sigma_\perp(b^z T)}. \tag{3.16}$$

Viscosity: let us consider a bi-dimensional fluid trapped between two plates as sketched in Fig. 3.2; the upper one is movable while the lower is fixed. If we apply a force to the upper one the fluid will start to move non-uniformly due to the relative friction between two narrow layers. As a result, the velocity field $\vec{u}$ varies along the vertical direction depending on the details of the setup and on the force applied. At linear order this can be expressed as $T_{xy} = \eta\,\partial_y u_x$, where $T_{\alpha\beta}$ is the stress tensor of the fluid while η is the shear viscosity coefficient. We can generalize the above formula for arbitrary anisotropic fluids as follows

$$T_{\alpha\beta} = \sum_{\gamma\delta} \eta_{\alpha\beta\gamma\delta}\,\partial_\gamma u_\delta. \tag{3.17}$$

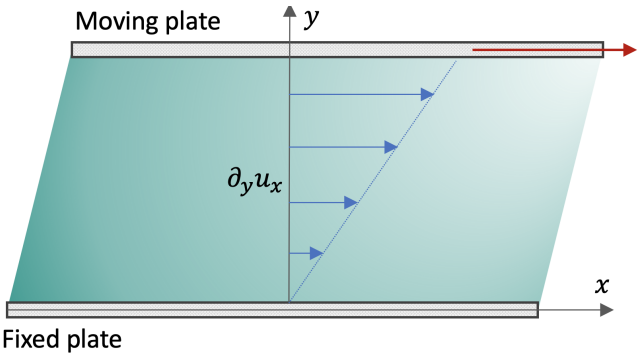

Figure 3.2: Flow of a viscous fluid through a pipe. The upper boundary moves at constant velocity inducing a flow due to the friction between narrow layers of fluid.

It follows that the viscosity is a four-rank tensor whose components characterize the flow of the fluid along the various directions.
The viscosity can be more generally computed in the Kubo formalism from the stress tensor correlation function via

$$\operatorname{Re}\eta_{\alpha\beta\gamma\delta}(\omega)=\frac{\operatorname{Im}\Pi_{\alpha\beta\gamma\delta}(\omega)}{\omega}, \tag{3.18}$$

with $\Pi_{\alpha\beta\gamma\delta}(\omega)$ the Fourier transform of the retarded stress-tensor correlation function $\Pi_{\alpha\beta\gamma\delta}(t)=-i\theta(t)\langle[T_{\alpha\beta}(t),T_{\gamma\delta}]\rangle$. Momentum conservation gives rise to the continuity equation for the momentum density $g_\alpha\equiv T^0_\alpha$:

$$\partial_t g_\beta+\partial_\alpha T_{\alpha\beta}=0. \tag{3.19}$$

We are considering a system without rotation invariance. In this case it is important to keep track of the order of the tensor indices as $T_{\alpha\beta}$ cannot be brought into a symmetric form [120]. From the continuity equation for the momentum it follows for the viscosity

$$\eta_{\alpha\beta\gamma\delta}(\omega)=\lim_{\mathbf{k}\to 0}\frac{\omega}{k_\alpha k_\gamma}\chi^{(g)}_{\beta\delta}(\mathbf{k},\omega), \tag{3.20}$$

with momentum-density correlation function $\chi^{(g)}_{\beta\delta}(\mathbf{k},\omega)$, i.e. the Fourier transform of $\chi^{(g)}_{\beta\delta}(\mathbf{k},t)=-i\theta(t)\langle[g_\beta(\mathbf{k},t),g_\delta(-\mathbf{k},0)]\rangle$. Thus, we only need to know the scaling dimension of $\chi^{(g)}_{\beta\delta}$ to determine the behavior of the viscosity. The easiest way to obtain this scaling dimension is to realize that under a boost operation, a velocity field is thermodynamically conjugate to the momentum density. A velocity has scaling dimension $z-1$ for the directions along $\mathbf{k}_\parallel$ and $z-\phi$ for $k_\perp$. To capture all the options we write this as $z-\varphi_\alpha$ where $\varphi_\alpha=1$ for all directions but along $k_\perp$ where we have $\varphi_\alpha=\phi$. Thus, it holds

$$\chi^{(g)}_{\beta\delta}(k_\perp,\mathbf{k}_\parallel,\omega)=b^{-\Delta_{g,\beta\delta}}\chi^{(g)}_{\beta\delta}(b^\phi k_\perp,b\mathbf{k}_\parallel,b^z\omega), \tag{3.21}$$

with $\Delta_{g,\beta\delta}=d_{\text{eff}}-z+\varphi_\beta+\varphi_\delta$. Using $\Delta_{g,\beta\delta}$ allows us to determine the scaling behavior of the viscosity tensor

$$\eta_{\alpha\beta\gamma\delta}(T)=b^{-\Delta_{\eta,\alpha\beta\gamma\delta}}\eta_{\alpha\beta\gamma\delta}(b^z T), \tag{3.22}$$

with

$$\begin{aligned}\Delta_{\eta,\alpha\beta\gamma\delta} &= \Delta_{g,\beta\delta} + z - \varphi_\alpha - \varphi_\gamma \\ &= d_{\text{eff}} - \varphi_\alpha + \varphi_\beta - \varphi_\gamma + \varphi_\delta. \end{aligned} \tag{3.23}$$

For isotropic systems, this gives the well known result that the scaling dimension of the viscosity is d, i.e. the same as for the entropy or particle density. For an anisotropic system the scaling dimensions of the viscosity and the entropy density can still be the same. This is the case whenever $\varphi_\alpha + \varphi_\gamma = \varphi_\beta + \varphi_\delta$. Examples are $\eta_{\perp\perp\perp\perp}$, $\eta_{\perp\perp cd}$, $\eta_{ab\perp\perp}$,$\eta_{a\perp\perp d}$, or $\eta_{\perp bc\perp}$, where a,b etc. stand for components of $\mathbf{k}_\parallel$.

However, the scaling dimension of the viscosity can also be different from the one of the entropy density. This is the case for

$$\begin{aligned}\eta_{a\perp c\perp}(T) &= b^{-(d-3+3\phi)}\eta_{a\perp c\perp}(b^z T), \\ \eta_{\perp b\perp d}(T) &= b^{-(d+1-\phi)}\eta_{\perp b\perp d}(b^z T). \end{aligned} \tag{3.24}$$

If we now take the ratio of the viscosity to entropy density, we find

$$\begin{aligned}\frac{\eta_{a\perp c\perp}(T)}{s(T)} &= b^{-2(\phi-1)}\frac{\eta_{a\perp c\perp}(b^z T)}{s(b^z T)}, \\ \frac{\eta_{\perp b\perp d}(T)}{s(T)} &= b^{2(\phi-1)}\frac{\eta_{\perp b\perp d}(b^z T)}{s(b^z T)}. \end{aligned} \tag{3.25}$$

Thus, for $\phi \neq 1$ there is always one tensor element of the viscosity, where $\eta_{\alpha\beta\gamma\delta}/s$ diverges as $T \to 0$ and another one that vanishes. The latter will then obviously violate any bound for the ratio of a viscosity to entropy density. In Ref. [19] it was shown that precisely these tensor elements turn out to be important for the hydrodynamic Poiseuille flow of anisotropic fluids.

The origin of unconventional scaling of both the conductivities and the viscosities is geometric, i.e. rooted in the anisotropic scaling of spatial coordinates at the Lifshitz point. If one combines Eqs.(3.16) and (3.25), it is straightforward to see that the combinations that enter Eq.(3.6) always have scaling dimension zero. While it certainly does not offer a proof of Eq.(3.6) this is necessary for such quantity to approach a universal, constant low-temperature value.

Diffusivity: finally we comment on the scaling behavior of the diffusivity bound, Eq.(5.51). To check whether this bound even makes sense for an anisotropic system, we consider the quantity

$$X_\alpha = k_{\text{B}} T D_{\rho,\alpha}/\hbar v_\alpha^2, \tag{3.26}$$

where v_α is the characteristic velocity along the α-th direction and $D_{\rho,\alpha} = \sigma_{\alpha\alpha}/\chi_\rho$ the diffusivity along this direction. It obviously holds that

$$\Delta_{X_\alpha} = z + \Delta_{\sigma,\alpha} - \Delta_\chi - 2(z - \varphi_\alpha) \tag{3.27}$$

where we used again that a velocity scales as $z - \varphi_\alpha$. If we now insert our above results, it follows that

$$\Delta_{X_\parallel} = \Delta_{X_\perp} = 0. \tag{3.28}$$

This implies that X_α should approach a universal constant times $\hbar/k_{\text{B}}$. Thus, we expect Eq.(3.2) to be valid even for anisotropic systems, which yields Eq.(5.51). In this sense, this bound is even more general than the original viscosity bound of Eq.(3.1).

3.3 Summary

In this chapter we have reported on the violation of universal lower bounds appearing in strongly-coupled systems due to rotational symmetry breaking . We have analyzed the shear viscosity over entropy density ratio and the charge diffusion bounds. In particular, we have focused on their behavior close to a Lifshitz point which is characterized by a different scaling of the spatial directions. We have emphasized how the violation may occur when the combination of transport coefficients considered has a nonzero scaling dimension. This is the case of some elements of the viscosity tensor which scale differently from the entropy density. As a consequence, in order obtain a dimensionless quantity and to correctly generalize the KSS bound to the anisotropic case we have to take into account of the ratio of the electric conductivities. This is the theme of Sec. 3.2.

Isotropic bounds

$$\eta/s \geq \frac{\hbar}{4\pi k_{\mathrm{B}}}, \quad D_c \geq C_D \frac{\hbar v^2}{k_{\mathrm{B}} T}$$

OTOC and butterfly effect

$$C\left(\mathbf{x},t\right) = -\left\langle \left[A\left(\mathbf{x},t\right), B\left(\mathbf{0},0\right)\right]^2 \right\rangle \sim e^{2\lambda_{\mathrm{L}}\left(t-\frac{|\mathbf{x}|}{v_{\mathrm{B}}}\right)}$$

Lifshitz scaling

$$\omega \sim |k_x|^{z/\phi}, \quad \omega \sim |k_y|^z$$

Critical exponents

z	dynamical exponent
ϕ	anisotropy exponent
θ	hyperscaling violating exponent

Anisotropic bounds

$$\frac{\eta_{\alpha\beta\alpha\beta}}{s} \geq \frac{\hbar}{4\pi k_{\mathrm{B}}} \frac{\sigma_{\alpha\alpha}}{\sigma_{\beta\beta}}, \quad D_{\rho,\alpha} \geq \frac{d_{\mathrm{eff}} - \theta}{\Delta_\chi} \frac{\hbar v_{B,\alpha}^2}{2\pi k_{\mathrm{B}} T}$$

Recap Box – Scaling analysis

Chapter 4
4 The holographic model

In this chapter we perform a holographic analysis of anisotropic transport, exploiting the duality between strongly coupled quantum field theories in $d+1$ dimensions and gravity theories in one additional dimension [11]. In Sec. 4.1 we introduce an Einstein-Maxwell-dilaton (EMD) holographic action, where the anisotropy is generated by massless scalar fields. In Chap. 5 we apply our findings and discuss how symmetry breaking impacts the universal bounds introduced in the previous chapter. The following analysis is mainly based on Ref. [18]

4.1 The Einstein-Maxwell-dilaton-axion(s) model

Our goal is to analyze transport in a 2+1 dimensional compressible phase with anisotropy in the spatial directions. Pure gravity alone is isotropic (and homogeneous) and needs to be coupled to other fields to break symmetries. We introduce an extension of the scalar model discussed in Sec.1.2.1 and consider a (2+2)-dimensional Einstein-Maxwell-dilaton (EMD) axions model with action

$$S = \int dx^{2+2}\sqrt{-g}(\mathcal{L}_0 + \mathcal{L}_{\rm g} + \mathcal{L}_{\rm M}) \tag{4.1}$$

and Lagrangian

$$\mathcal{L}_0 = \frac{1}{2\kappa^2}\mathcal{R}, \quad \mathcal{L}_{\rm g} = -\frac{1}{4g_F^2}Z(\Phi)F^2, \tag{4.2a}$$

$$\mathcal{L}_{\rm M} = -\frac{1}{2\kappa^2}\Big(\frac{1}{2}(\partial\Phi)^2 + V(\Phi) + \frac{1}{2}\sum_{I=1}^{p} Y^I(\Phi)(\partial\psi_I)^2\Big). \tag{4.2b}$$

Here $Z(\Phi), Y^I(\Phi)$ are couplings we discuss shortly. In the following we work in units such that $2\kappa^2 = g_F = 1$. Moreover, $\mathcal{R}$ and F are the Ricci scalar and Maxwell field respectively. See Chap. 1 for details. The field Φ is the *dilaton*, a real scalar field which enters in the action modifying all the couplings involved and $V(\Phi)$ is its potential. In a top-down sense, the dilaton arises from consistent truncation of the gravitational string action, see e.g. Refs. [24, 121]. In the bottom-up perspective, Φ is an essential ingredient of the theory to engineer non-trivial RG flows. As we

will discuss in Sec. 4.2.1, without the dilaton $\Phi = 0$ the model reduces to the usual AdS_4 system. The fields ψ_I are massless scalar fields useful to break symmetries in the dual theory called *axions*. I is an internal index that labels different fields. We will discuss the cases where we have one or two axions. These holographic systems have been previously studied in Refs. [104–107, 109–111, 122–128].

The evolution of each field in the model Eq.(4.1) is governed by appropriate equations of motion that can be derived from the action through standard variational techniques

$$\frac{1}{\sqrt{-g}}\frac{\delta\mathcal{S}}{\delta\Psi} = 0, \tag{4.3}$$

for any involved field Ψ. In the following we discuss each possible case.

Einstein equations: $\Psi = g_{\mu u}$ and

$$\mathcal{R}_{\mu\nu} - \frac{1}{2}\mathcal{R}g_{\mu\nu} = T^{\rm EM}_{\mu\nu} + T^{\Phi}_{\mu\nu} + T^{\psi}_{\mu\nu}, \tag{4.4}$$

where

$$T^{\rm EM}_{\mu\nu} = \frac{1}{2}Z(\Phi)\Big[F_{\nu\sigma}F^{\sigma}_{\mu} - \frac{1}{4}F^2 g_{\mu\nu}\Big], \tag{4.5a}$$

$$T^{\Phi}_{\mu\nu} = \frac{1}{2}\partial_\mu\Phi\,\partial_\nu\Phi - \frac{1}{4}\Big[(\partial\Phi)^2 + 2V(\Phi)\Big]g_{\mu\nu}, \tag{4.5b}$$

$$T^{\psi}_{\mu\nu} = \frac{1}{2}\sum_I Y^I(\Phi)\Big[\partial_\mu\psi_I\,\partial_\nu\psi_I - \frac{1}{2}(\partial\psi_I)^2 g_{\mu\nu}\Big], \tag{4.5c}$$

are the holographic stress-energy tensors of the gauge and matter fields. For later purposes we introduce the tensor

$$\mathcal{E}_{\mu\nu} \equiv R_{\mu\nu} - \frac{1}{2}Rg_{\mu\nu} - T^{\rm EM}_{\mu\nu} - T^{\Phi}_{\mu\nu} - T^{\psi}_{\mu\nu}, \tag{4.6}$$

so that Einstein equations become $\mathcal{E}_{\mu\nu} = 0$.

Gauge equations: $\Psi = A_\mu$ and

$$\partial_\mu(\sqrt{-g}Z(\Phi)F^{\mu\nu}) = 0, \tag{4.7}$$

The dilaton and axion are neutral fields such that we do not obtain bulk currents as sources on the right hand side. In our theory charge currents are formally only present at the boundary and enter the system via appropriate boundary conditions.

Scalar equations: $\Psi = \psi_I, \Phi$ and

$$\partial_\mu(\sqrt{-g}\,Y^I(\Phi)\partial^\mu\psi_I) = 0, \tag{4.8}$$

$$\partial_\mu(\sqrt{-g}\,\partial^\mu\Phi) = \partial_\Phi V_{\rm eff}, \tag{4.9}$$

where

$$\frac{V_{\rm eff}}{\sqrt{-g}} = V(\Phi) + \sum_I \frac{Y^I(\Phi)}{2}(\partial\psi_I)^2 + \frac{Z(\Phi)}{4}F^2. \tag{4.10}$$

4.2 The anisotropic ansatz

Looking at the equations of motion we note that the axions back-react on the other fields through spatial gradients. Choosing axions that are linear in the boundary coordinates consistently with Eq.(4.8) preserves homogeneity of the background. We thus work within the following ansatz

$$\begin{aligned} &ds^2 = -g_{tt}(r)dt^2 + g_{rr}(r)dr^2 + g_{xx}(r)dx^2 + g_{yy}(r)dy^2, \\ &\Phi = \Phi(r), \quad A = A_t(r)dt, \\ &\psi_I = a_I \delta_{I\alpha} x_\alpha, \;\; I, J = 1...p, \;\; \alpha = x, y, \end{aligned} \tag{4.11}$$

where p is the number of axion fields. This is a simple mechanism to break rotational symmetry without dealing with PDE in the bulk of the AdS space. In Refs. [108, 129] isotropy is broken by means of an axial field. We assume $g_{xx} \neq g_{yy}$. In the double axion case ($p = 2$), isotropy can be restored by setting $a_x^2 Y_x(\Phi) = a_y^2 Y_y(\Phi)$, while in the single axion one ($p = 1$) it is enough to require $a^2 Y(\Phi) = 0$. However, the boundary sources induced by the axions are coordinate-dependent. As a consequence, the scalars also break translation invariance and momentum is not conserved. A holographic renormalization analysis [130] yields the following Ward-identity for the boundary stress tensor

$$\partial_\beta \langle T_{\alpha\beta} \rangle \propto a_\alpha. \tag{4.12}$$

Momentum is dissipated along the α-direction of the dual field theory at a rate proportional to a_α. If the symmetry breaking occurs explicitly, the viscosity cannot be interpreted as a hydrodynamic coefficient. It is well known that in such holographic frameworks the KSS bound is violated [104–111, 131–137]. However, even if the viscosity cannot be interpreted as the transverse momentum conductivity, the η/s tensor can be used to quantify the increase of the entropy production due to a slowly varying strain with a weaker formulation of the KSS bound [131].

We will also investigate the case where translations are broken spontaneously through the use of a so-called Q-lattice homogeneous ansatz [138–140], in which case momentum is still conserved and the shear viscosity remains well-defined at all temperatures.

Once we have built the ansatz following symmetry arguments, we plug it into the field equations obtaining coupled II-ODEs for which we have to set appropriate conditions at both the asymptotic boundary and the horizon.

4.2.1 Asymptotic region: UV conditions

Working in a coordinate system where the conformal boundary is located at $r \to \infty$, we require the following UV conditions:

$$\begin{aligned} &ds^2 = -r^2 dt^2 + \frac{dr^2}{r^2} + r^2 d\vec{x}^2, \\ &A = 0, \quad \Phi = \Phi_0 r^{\Delta_\Phi - 3} + \Phi_1 r^{-\Delta_\Phi}. \end{aligned} \tag{4.13}$$

Here Δ_Φ is the scaling dimension of the dilaton given by largest solution of $m^2 = \Delta_\Phi(\Delta_\Phi - 3)$, m being the mass of the field – see also Eq.(1.33). Notice that $\Delta_\Phi < 3$ and the dilaton vanishes at

the asymptotic boundary. In standard quantization, the leading falloff Φ_0 is the source dual to the dilaton while the sub-leading one Φ_1 is the vacuum expectation value (VEV) of the correspondent operator. In order for the action Eq.(4.1) to approach an Einstein-Maxwell-scalar model in the UV, the couplings must obey

$$V_{\rm UV} = V(0) = -6 + \frac{1}{2}m^2\Phi^2, \quad Z_{\rm UV} = Z(0) = 1. \tag{4.14}$$

The condition on the axion couplings is more delicate. If $Y^I_{\rm UV} = \Phi^2$ we can reorganize all the scalar fields into $p-1$ complex degrees of freedom ψ_I via

$$(\Phi, \psi_I) \mapsto \tilde{\Phi}_I = \frac{\Phi}{\sqrt{2}} e^{i\sqrt{2}\psi_I}. \tag{4.15}$$

The new masses and scaling dimensions coincide with the dilaton parameters. Tuning m such that $\Delta_\Phi < 3$ we have a holographic Q-Lattice which describes a system periodically deformed by means of complex relevant operators [126, 141, 142]. If instead $Y^I_{\rm UV} \neq \Phi^2$, the dynamics of the axion and of the dilaton are independent, and the former will be dual to a source of explicit symmetry breaking. Finally, also the gauge field exhibits a similar behavior $A_t \to \mu - \rho r^{-1}$, with μ the chemical potential and ρ the charge density However, we will be mainly interested in the charge neutral case, hence we directly set $A = 0$.

4.2.2 Inner region: IR scaling conditions

In order to describe quantum critical phases of the dual system, we look for a power-law behavior of the geometry in the IR region ($\Phi \to \infty$, $r \to 0$). We work with a hyperscaling violating (or Lifshitz) geometry of the form:

$$\begin{aligned} ds^2 &= r^\theta \Big(-\frac{dt^2}{r^{2z}} + \tilde{L}^2 \frac{dr^2}{r^2} + \frac{dx^2}{r^{2\phi}} + \frac{dy^2}{r^2} \Big), \\ A &= 0, \quad \Phi = 2\kappa \log(r/r_0). \end{aligned} \tag{4.16}$$

This power-law behavior is dual to a quantum critical point with dynamical critical exponent z that parametrizes the different scaling between space and time. The quantity ϕ is a measure of rotational symmetry breaking of spatial coordinates. Note that under a rescaling $(t, \mathbf{x}, r) \mapsto (\lambda^z t, \lambda \mathbf{x}, \lambda r)$ the metric transforms as $ds^2 \mapsto \lambda^{\theta/2} ds^2$. Since the metric is dual to the boundary stress-tensor, the exponent θ signals the dual energy operator acquire an anomalous dimension. θ is known as hyperscaling violating exponent. $\tilde{L}$ is a length scale that can be varied over a range of values by changing the critical exponents, as explicitly shown in appendix B. Each value allows to describe a specific quantum critical point [90]. The running dilaton follows from the solution to Eq.(4.9) and the scale r_0 is related to the cross-over to the IR region – in the following we set $r_0 = 1$. The remaining fields are solution to the equations of motion if the couplings are given by

$$V_{\rm IR} = V(\infty) = -|V_0| e^{\delta\,\Phi}, \quad Y^I_{\rm IR} = Y^I(\infty) = e^{\lambda_I \Phi}, \quad Z_{\rm IR} = Z(\infty) = e^{\xi\Phi}. \tag{4.17}$$

Here the parameters δ, λ_I, ξ are all real numbers. Notice that with the logarithmic behavior of the dilation, such couplings also have power-law behavior. This is consistent with some supergravity truncations where couplings are found to be combination of exponentials – see e.g. [24, 143, 144]. We discuss explicit solution to the equations of motion in appendix B.

4.2.3 Finite temperature

In order to turn on a small temperature, we consider a blackening factor f with the requirement that it does not change the EOMs; more precisely

$$g_{tt}(r) \mapsto g_{tt}(r) f(r), \quad f(r_+) = 0, \tag{4.18}$$

where r_+ is the location of the event horizon. The dilaton field equation is not affected if

$$f(r) = 1 - (r/r_+)^{\delta_0}. \tag{4.19}$$

The exponent δ_0 depends on the particular model we choose and will be fixed by the equations of motion below. The Hawking temperature following from the holographic formula Eq.(1.22) $4\pi T = \frac{|\delta_0|}{\tilde{L}} r_+^{-z}$. Notice that $T \to b^z T$, consistently with the scaling analysis. The entropy density follows from the area law Eq.(1.22) and the heat capacity are given by

$$s = 4\pi r_+^{\theta-\phi-1} \sim T^{\frac{d_\theta}{z}}, \quad \gamma = T\frac{\partial s}{\partial T} = \frac{d_\theta}{z} s, \tag{4.20}$$

where $d_\theta = d_{\text{eff}} - \theta$ is the effective dimension of the fixed point – see also Eq.(3.9).

4.3 Thermodynamic stability

In the previous sections we have introduced a holographic model for quantum critical anisotropic phases with momentum dissipation. However, in order to make the description more realistic we have to focus on thermodynamically stable solutions that minimize the free energy. In this section we derive a stability condition for spatially modulated phases with period ℓ_α where translations are broken spontaneously in the IR.

The free energy-density is given by the Euclidean on-shell action via

$$f = \frac{1}{\beta V_{(d)}} I_{\text{os}}(\gamma_{\mu\nu}, \alpha_\mu; \beta, \ell_\alpha), \tag{4.21}$$

where β is the euclidean time-period and $V_{(d)} = \ell_1 \cdot \ell_2 ...$ is the spatial volume. Here $\gamma_{\mu\nu}$ and α_μ are the induced metric and gauge field on the boundary. The optimal phase minimizes the above expression. Therefore our goal is to find the variation of f with respect to all parameters, i.e. the periods. Fluctuations lead to

$$\delta I_{\text{os}} = -\int d^{d+1}x \sqrt{\gamma}\Big(\frac{1}{2}\langle T^{\mu\nu}\rangle \delta\gamma_{\mu\nu} + \langle J^\mu\rangle \delta\alpha_\mu\Big), \tag{4.22}$$

where $\langle T^{\mu\nu}\rangle$ and $\langle J^{\mu}\rangle$ are the VEV of the boundary stress-tensor and current, and integrals run from 0 to the periods. We rescale the coordiantes according to $\tau \mapsto \tau/\beta$ and $x^{\alpha} \mapsto x^{\alpha}/\ell_{\alpha}$. Using the transformation laws for rank-2 tensors and 1-forms it follows that

$$\begin{aligned}\delta f &= -\frac{1}{V_{(d)}}\int d^dx\sqrt{\gamma}\left(\frac{1}{2}\langle T^{\mu\nu}\rangle\delta\gamma_{\mu\nu}+\langle J^{\mu}\rangle\delta\alpha_{\mu}\right)-s\delta T \\ &- \sum_{ij}\frac{\delta\ell_{\alpha}}{\ell_{\alpha}}\left[w+\frac{1}{V_{(d)}}\int d^dx\sqrt{\gamma}\left(T^{t\alpha}\gamma_{t\alpha}+T^{\alpha\beta}\gamma_{\alpha\beta}+J^{\alpha}a_{\alpha}\right)\right],\end{aligned} \tag{4.23}$$

where s is the entropy-density – see Ref. [145] for details on the computations. The condition $\delta f/\delta\ell_{\alpha}=0$ yields

$$f=-\frac{1}{V_{(d)}}\int d^dx\sqrt{\gamma}\left(T^{t\alpha}\gamma_{t\alpha}+\sum_{\beta}T^{\alpha\beta}\gamma_{\alpha\beta}+J^{\alpha}a_{\alpha}\right), \tag{4.24}$$

for each α.

Our next goal is to apply these results to the charge-neutral EMD model with axion $\psi = ay$. The spatial modulation is confined in the y-direction, therefore $\ell_x = \infty, \ell_y = 2V_{(d)}/a$. The boundary is flat ($\gamma_{\mu\nu}=\eta_{\mu\nu}$) and the stability conditions Eq.(4.24) become

$$\boxed{f=-\bar{T}^{xx}=-\bar{T}^{yy},} \tag{4.25}$$

where quantities are averaged over a period. As a consequence, thermodynamic stability sets a constraint on the free energy and equalizes the averaged pressures in the various directions.

In the following we compute the free energy density and the boundary stress-tensor explicitly through the holographic renormalization procedure, and analyze the implications of Eq.(4.25).

4.3.1 Holographic renormalization

In this section we perform the holographic renormalization of the action Eq.(4.1). From the GKPW rule, this will lead the free energy and stress-tensor of the dual theory.

The first step is to manipulate the action Eq.(4.1) by using the equations of motions. The Ricci scalar term can be removed by using a constraint that follows from the trace of both the sides of Einstein equations Eq.(4.6). Furthermore, summing the radial and temporal components of Einstein equations leads to the following on-shell action

$$S_{\rm os}=-\int d^4x\left[\sqrt{-g}\,\frac{a^2Y(\Phi)}{2g_{yy}}+\partial_r\left(\frac{\sqrt{-g}}{g_{rr}}\partial_r\log\sqrt{g_{xx}g_{yy}}\right)\right]. \tag{4.26}$$

Applying Stokes theorem, it is easy to show that this expression is singular and must be regularized. We consider the following counter-term introduced in Ref. [138]

$$S_{\rm ct}=\int_{r=\Lambda}d^3x\sqrt{-\gamma}\left[2\mathcal{K}+4+\mathcal{R}[\gamma]+\frac{1}{2}\Phi^2-\frac{1}{2}Y(\Phi)(\psi-ay)^2\right]. \tag{4.27}$$

Here Λ is a UV regulator, γ is the metric induced on the $r=\Lambda$ manifold, and $\mathcal{K}$ is the trace of the extrinsic curvature. Focusing on the spontaneous case where $Y_{\rm UV}\sim\Phi^2$, the above expression essentially follows from the asymptotic map Eq.(4.15) to a theory of a single complex scalar field $\tilde{\Phi}$. Then the standard counterterm is $\sim\tilde{\Phi}^\star\tilde{\Phi}$. Taking variations yields scalar counterterms that agree with the last one in Eq.(4.27) order by order.

The quantity $\mathcal{R}[\gamma]$ is vanishing as the boundary is flat, and the axion part do not contribute at the background level. The extrinsic trace $\mathcal{K}$ has been calculated with Mathematica leading to the renormalized action

$$S_{\rm ren}=\lim_{\Lambda\to\infty}\int d^3x\Big[-\frac{1}{2}a^2I_Y+\frac{1}{2}\sqrt{-\gamma}\phi^2+\frac{\sqrt{-\gamma}}{\sqrt{g_{rr}}}\left(4\sqrt{g_{rr}}+\partial_r\log\left(g_{tt}\sqrt{g_{xx}g_{yy}}\right)\right)\Big]_{r=\Lambda}, \tag{4.28}$$

with $I_Y(r)=\int_r^{r_+}\sqrt{-g}\frac{Y(r)}{g_{yy}}$. Since the above expression is purely asymptotic, it is convenient to use a near boundary expansion of the fields. We adopt the Fefferman-Graham gauge, which is basically the asymptotic expansion of the spacetime in the radial gauge $g_{r\mu}=0$ [36]. Solving the field equations close to the asymptotic boundary yields:

$$\begin{aligned}
&r^{-2}g_{tt}(r)\approx 1+\frac{d_t}{r^3}+\frac{3\rho^2-2\Phi_1^2}{16}\frac{1}{r^4}-\frac{1}{72}\left[a^2\Phi_1^2-9(3{d_t}^2-d_td_x-{d_x}^2)\right]\frac{1}{r^6},\\
&r^{-2}g_{zz}(r)=1,\\
&r^{-2}g_{xx}(r)\approx 1+\frac{d_x}{r^3}-\frac{\rho^2+2\Phi_1^2}{16}\frac{1}{r^4}-\frac{1}{72}\left[a^2\Phi_1^2+9({d_t}^2+d_td_x-3{d_x}^2)\right]\frac{1}{r^6},\\
&r^{-2}g_{yy}(r)\approx 1-\frac{d_t+d_x}{r^3}-\frac{\rho^2+2\Phi_1^2}{16}\frac{1}{r^4}-\frac{1}{72}\left[5a^2\Phi_1^2-27({d_t}^2+\frac{7}{3}d_td_x+{d_x}^2)\right]\frac{1}{r^6},\\
&\Phi(r)\approx\frac{\Phi_1}{r^2}+\frac{a^2\Phi_1}{6}\frac{1}{r^4}+\frac{\Phi_1\left(2a^4+18\Phi_1^2-3\rho^2\right)}{240}\frac{1}{r^6},\\
&\psi=ay,\\
&A_t(r)\approx\mu-\frac{\rho}{r}-\frac{\rho d_t}{4}\frac{1}{r^4}-\frac{\rho}{160}\left(5\rho^2+2\Phi_1^2\right)\frac{1}{r^5}.
\end{aligned} \tag{4.29}$$

Here we have considered $m_\Phi^2=-2$ ($\Delta_\Phi=2$) and spontaneous symmetry breaking of translations (no linear-in-r^{-1} in the expansion of the dilatons). The remaining free parameters d_t,d_x,Φ_1 will be related to physical quantities below by renormalization. Notice how no log-terms enter the above expression as the boundary spacetime dimension is odd ($d=3$) – see Ref. [36]. Plugging the above expansion into Eq.(4.28) and Wick-rotating to imaginary time leads to

$$I_{\rm ren}=\beta V_{(2)}\Big(-\frac{a^2}{2}I_Y(0)+\frac{3}{2}d_t\Big). \tag{4.30}$$

The free energy density is then given by

$$\boxed{f=\frac{I_{\rm ren}}{\beta V_{(2)}}=\frac{3}{2}d_t-\frac{a^2}{2}I_Y(0),} \tag{4.31}$$

where $V_{(2)}$ is the spatial volume of the boundary.

We next evaluate the boundary stress-energy tensor. Let us introduce fluctuations around the background value of the fields. In particular we consider $g_{\mu\nu} \mapsto g_{\mu\nu} + h_{\mu\nu}$ with asymptotic expansions $r^{-2}h_{\mu\nu} = \sum_{n=0} h^{(n)}_{\mu\nu} r^{-n}$. The leading correction to the action was computed in Ref. [146] and is given by

$$S^{(1)}_{\text{ren}} = \int_{r=\infty} d^d x \left(\frac{3d_t}{2} h^{(0)}_{tt} - \frac{3d_x}{2} h^{(0)}_{xx} + \frac{3(d_t + d_x)}{2} h^{(0)}_{yy} \right), \tag{4.32}$$

where we give only the metric-dependent part. From this expression we can read off the expectation value of the boundary stress-tensor. Using Eq.(4.29) we obtain

$$\langle T^{tt} \rangle = \epsilon = -3d_t, \quad \langle T^{xx} \rangle = 3d_x, \quad \langle T^{yy} \rangle = -3(d_t + d_x). \tag{4.33}$$

In the isotropic limit $\langle T^{xx} \rangle = \langle T^{yy} \rangle$ and our finding is consistent with Ref. [138]. Note that these VEVs are proportional to the sub-leading falloffs of Eq.(4.29). This is indeed the power of the Fefferman-Graham gauge where the identification of the sub-leading part of the metric with the boundary expectation value of the boundary stress-energy tensor is direct.
Now we are able to comment on the thermodynamically stable phases. From the stability conditions Eq.(4.25) it follows that $\langle \bar{T} \rangle_{xx} = \langle \bar{T} \rangle_{yy} \to 2d_x = -d_t$. Using $f = -T^{yy}$ and the free energy Eq.(4.31), we have

$$a^2 I_Y(0) = 0. \tag{4.34}$$

Minimizing the free energy then corresponds to setting $a = 0$. In such a limit the effects of the symmetry breaking field ψ are negligible, and the stable phase is then homogeneous and isotropic. In order to get anisotropic stable phases dissipating momentum at a finite a, we need to consider higher derivatives corrections, going beyond the Einstein gravity model. This will be the focus of the next section.

4.3.2 Beyond Einstein gravity: a higher derivative model

In this section we follow Ref. [138] and analyze an extension of Eq.(4.1) given by

$$\mathcal{L} = \mathcal{R} - \frac{1}{2}(\partial\Phi)^2 - V(\Phi) - \frac{1}{2}\Big[Y(\Phi) + \lambda_2 Y_2(\Phi)(\partial\psi)^2\Big](\partial\psi)^2 - \frac{1}{4}\Big[Z(\Phi) + \lambda_1 Z_2(\Phi)(\partial\psi)^2\Big]F^2. \tag{4.35}$$

Here we have included higher-derivatives corrections to the gauge and axion couplings, with $Y_2, Z_2 \sim \Phi^2$ in the UV. This can again be motivated by considering the asymptotic map Eq.(4.15) to a theory of single complex scalar field $\tilde{\Phi}$. The higher derivative terms follows from expansion of terms like $(\partial\tilde{\Phi}\partial\tilde{\Phi}^\star)F^2$ and $(\partial\tilde{\Phi}\partial\tilde{\Phi}^\star)^2$. The stress energy tensors are given by

$$T^{\rm EM}_{\mu\nu} = \frac{1}{2}\Big[Z(\Phi) + \lambda_1 Z_2(\Phi)(\partial\psi)^2\Big]\Big[F_{\nu\sigma}F^{\sigma}_{\mu} - \frac{1}{4}F^2 g_{\mu\nu}\Big], \tag{4.36}$$

$$T^{\Phi}_{\mu\nu} = \frac{1}{2}\partial_\mu\Phi\,\partial_\nu\Phi - \frac{1}{4}\Big[(\partial\Phi)^2 + 2V(\Phi)\Big]g_{\mu\nu}, \tag{4.37}$$

$$T^{\psi}_{\mu\nu} = -\frac{1}{4}\Big[(\partial\psi)^2\left(Y(\Phi) + \lambda_2 Y_2(\Phi)(\partial\psi)^2\right)\Big]g_{\mu\nu} \tag{4.38}$$
$$+ \frac{1}{2}\sum_I \Big[Y(\Phi) + 2\lambda_2 Y_2(\Phi)(\partial\psi)^2 + \frac{\lambda_1}{2}Z_2(\Phi)F^2\Big]\partial_\mu\psi\partial_\nu\psi.$$

Repeating the same renormalization procedure as in the previous section we find

$$S_{\rm ren} = \lim_{\Lambda\to\infty}\int d^3x\left[\frac{1}{2}\sqrt{-\gamma}\Phi^2 + \frac{\sqrt{-\gamma}}{\sqrt{g_{rr}}}\left(4\sqrt{g_{rr}} + \partial_r\log\left(g_{tt}\sqrt{g_{xx}g_{yy}}\right)\right) - \frac{a^2}{2}I_Y - \lambda_2 a^4 I_{Y_2} - \frac{\lambda_1 a^2}{4}I_{Z_2}\right]_{r=\Lambda},$$

with $I_Y(r) = \int_r^{r_+}\sqrt{-g}\,Y(r)g^{yy}(r)$, $I_{Y_2}(r) = \int_r^{r_+}\sqrt{-g}\,Y_2(r)g^{yy}(r)^2$, $I_{Z_2}(r) = \int_r^{r_+}\sqrt{-g}\,Z_2(r)g^{yy}(r)F^2$. Using the Fefferman-Graham ansatz analogue to Eq.(4.29) and Wick-rotating to imaginary times yields the free energy

$$\boxed{f = \frac{3}{2}d_t - \frac{a^2}{2}I_Y(0) - \lambda_2 a^4 I_{Y_2}(0) - \frac{\lambda_1 a^2}{4}I_{Z_2}(0).} \tag{4.39}$$

On the other hand the stress-energy tensor is still given by Eqs.(4.33), and the stability condition $w = -\bar{T}^{ii}$ yields

$$\boxed{I_Y(0) + 2a^2\lambda_2 I_{Y_2}(0) + \frac{\lambda_1}{2}I_{Z_2}(0) = 0.} \tag{4.40}$$

Contrary to the two-derivatives result Eq.(4.34), finite a are consistent with Eq.(4.40), opening the possibility of the existence of anisotropic stable phases breaking translations spontaneously. This can only happen if the higher-derivative couplings are not all of the same sign. Working out exactly what the stability range is is generally a complicated quest. This is best known for the case of Gauss-Bonnet, where it was demonstrated that both signs are allowed [147]. For the type of higher derivative terms considered in this section, things are less clear. Some preliminary analysis was made in Ref. [148] for purely ESB cases.

4.4 Summary

In this chapter we have introduced a holographic model for the anisotropic phases analyzed in Chap. 3. Essentially, this is achieved by considering the conventional Einstein-Maxwell action coupled to a matter sector whose purpose is to break symmetries and to lead to anisotropic phases in the infrared. In Sec. 4.2 we have introduced the background ansatz, characterized by a metric tensor whose spatial elements are different from each other. This is the way the gravitational background encodes the anisotropy of the boundary theory. Isotropy is broken by

means of the axion, a massless scalar field linear in the boundary coordinates. This assumption simplifies the bulk field equations but also leads to breaking of translation symmetry of the boundary. Finally, in Sec. 4.3 we have commented on thermodynamically stable phases. In the model considered, the stable phase is the one where anisotropy is absent. In order to get a stable state with rotational symmetry breaking, one has to consider holographic actions with higher derivative corrections.

EMD-axion Lagrangian

$$\mathcal{L}_{\text{EMD}} = \mathcal{R} - \frac{1}{4}Z(\Phi)F^2 - \frac{1}{2\kappa^2}\left(\frac{1}{2}(\partial\Phi)^2 + V(\Phi) + \frac{1}{2}\sum_{I=1}^{p} Y^I(\Phi)(\partial\psi_I)^2\right)$$

IR background

$$ds^2 = r^\theta\left(-\frac{dt^2}{r^{2z}} + \tilde{L}^2\frac{dr^2}{r^2} + \frac{dx^2}{r^{2\phi}} + \frac{dy^2}{r^2}\right),$$
$$A = 0, \quad \Phi = 2\kappa\log(r/r_0)$$

Higher derivative model

$$\mathcal{L} = \mathcal{R} - \frac{1}{2}(\partial\Phi)^2 - V(\Phi) - \frac{1}{2}\Big[Y(\Phi) + \lambda_2 Y_2(\Phi)(\partial\psi)^2\Big](\partial\psi)^2$$
$$- \frac{1}{4}\Big[Z(\Phi) + \lambda_1 Z_2(\Phi)(\partial\psi)^2\Big]F^2$$

Thermodynamic stability condition $f = -\bar{T}^{xx} = -\bar{T}^{yy}$

Two derivatives model

$$a^2\int_0^{r_+}\sqrt{-g}\frac{Y(r)}{g_{yy}} = 0$$

Higher derivatives model

$$\int_0^{r_+}\sqrt{-g}\frac{Y(r)}{g_{yy}} + 2a^2\lambda_2\int_0^{r_+}\sqrt{-g}\frac{Y_2(r)}{g_{yy}} + \frac{\lambda_1}{2}\int_0^{r_+}\sqrt{-g}\frac{Y_2(r)}{g_{yy}} = 0$$

Recap Box – Einstein-Maxwell-dilaton-axion model

Chapter 5
Holographic bounds on transport coefficients

As our focus in this work is on the anisotropy of the system, we will choose a geometry where momentum is conserved along one of the spatial directions, say the β-direction. Thus, the stress tensor elements $T_{\alpha\beta}$ serve as currents of the conserved momentum density along the direction β. Consequently, the viscosity elements $\eta_{\alpha\beta\gamma\beta}$ maintain their meaning as hydrodynamic coefficients, for all α and γ. Therefore we consider the single axion geometry with $\psi = ay$ – see appendix B.1 for details.
In Sec. 5.1 and 5.2 we compute the electric conductivity and viscosity tensor and analyze the KSS bound. We then investigate how translational symmetry breaking impacts such a bound. In Sec. 5.3 we compute the charge diffusivity and butterfly velocity, and show that the bound on charge diffusion is not affected by rotational symmetry breaking.

5.1 The electric conductivity

The goal of this section is to extract the response to an external electric field of the holographic model Eq.(4.7). To compute the electrical conductivity defined in the Kubo formula Eq.(3.11), we consider a gauge field of the form:

$$A \mapsto A_t(r,t)dt + A_\alpha(r,t)dx_\alpha. \tag{5.1}$$

Near the boundary $r = \infty$, the gauge field admits the following expansions

$$A_t(r \approx \infty) = \mu + \frac{\rho}{r} + ..., \tag{5.2a}$$

$$A_\alpha(r \approx \infty) = -E_\alpha t + \frac{j_\alpha}{r} + ..., \tag{5.2b}$$

where dots denote higher order in $1/r$ terms. Here μ and E_α are sources (chemical potential and electric field) while ρ and j_α the correspondent responses. To extract the conductivity we use

Eq.(1.41). Therefore, we rewrite the Maxwell equations Eq.(4.7) in the Hamiltonian formalism:

$$j^\mu = \sqrt{-g} Z(\Phi) F^{\mu r}, \tag{5.3}$$
$$\partial_r j^\mu = 0. \tag{5.4}$$

Here $j^\mu = \delta S/\delta(\partial_r A_\mu)$ is the canonical momentum conjugate to the gauge field A_μ, whose boundary value gives the density current. This allows us to rewrite the electrical conductivity in terms of holographic quantities:

$$\sigma_{\alpha\alpha} = \lim_{\omega\to 0} \frac{j^\alpha(\omega)}{E_\alpha} = \lim_{\substack{\omega\to 0 \\ r\to\infty}} \mathrm{Im} \frac{j^\alpha(r,\omega)}{\omega A_\alpha(r,\omega)}. \tag{5.5}$$

Note that Eq.(5.4) represents the radial conservation j^μ. This means that we can alternatively calculate the boundary current by evaluating the canonical momentum at any value of the radial direction. In particular

$$j^\mu\left(r=\infty, \mathbf{x}, t\right) = \lim_{r\to r_+} j^\mu\left(r, \mathbf{x}, t\right). \tag{5.6}$$

As we will shortly see, this yields simple expressions for electric conductivities in terms of the horizon as extensively reviewed in Ref. [141]
Let us discuss the case $\alpha = y$ first. The electric field in Eq.(5.2b) polarizes the system, inducing small fluctuations of the other fields

$$\begin{aligned} &A_y = -E_y t + \delta A(r), \\ &g_{ty} = \delta g_{ty}(r), \quad g_{ry} = g_{yy}(r)\delta\bar{g}_{ry}(r), \\ &\psi = ay + \delta\psi(r). \end{aligned} \tag{5.7}$$

All the terms are assumed to be first order in the electric field. Inserting these expressions into the canonical momentum, at lowest order we find

$$j^y(r) = -\frac{\sqrt{-g}Z(\Phi)}{g_{rr}g_{yy}}\partial_r(\delta A) - \frac{\rho}{g_{yy}}\delta g_{ty}. \tag{5.8}$$

In order to evaluate this quantity at the horizon, we need to specify appropriate IR conditions for the perturbations. Let us denote with $\mathcal{E}^{(n)}_{\mu\nu}$ the nth-order perturbatios of the Einstein tensor Eq.(4.6). If we consider the combination $\mathcal{E}^{(1)}_{ry} - \delta\bar{g}_{ry}\mathcal{E}^{(0)}_{yy} = 0$ we find an algebraic equation for $\delta\bar{g}_{ry}$ given by

$$\delta\bar{g}_{ry} = -\frac{g_{rr}E_y\rho}{\sqrt{-g}aY(\Phi)} + \frac{\partial_r(\delta\psi)}{a}. \tag{5.9}$$

Notice that $\delta\bar{g}_{ry}$ diverges in the interior as it is proportional to $g_{rr} \propto (r-r_+)^{-1}$. However, fields must be regular in the Eddington-Finkelstein coordinates, where time is changed according to $t' = t + r_\star(r)$, with tortoise coordinate $dr_\star = dr/\gamma(r)$ and $\gamma = \sqrt{g_{tt}/g_{rr}}$ – see also Sec. 1.2.2. In particular, in the new coordinate system (r', t', x', y') it holds that $g_{r'y'} = -\delta g_{ty}/\gamma + g_{yy}\delta\bar{g}_{ry}$. Due

to our finding Eq.(5.9), the only way to obtain a (r', y')-component, that is regular at the horizon, is to require analyticity of the axion field at r_+ and to suppress the divergence by choosing

$$\delta g_{ty}|_{r_+} = -\sqrt{\frac{g_{yy}}{g_{xx}}}\frac{E_y \rho}{aY(\Phi)}\bigg|_{r_+}. \tag{5.10}$$

The only missing information to evaluate Eq.(5.8) is the horizon value of the gauge field fluctuation δA. In the EF coordinates it holds that $A_y = -E_y t' + E_y r_\star(r) + \delta A(r)$. Therefore, regularity implies that

$$\delta A = -E_y r_\star(r). \tag{5.11}$$

As anticipated above, the fluctuations Eq.(5.10) and (5.11) are caused by the electric fields E_y. Plugging the above results into the current and using Eq.(5.5) yields the conductivity

$$\sigma_{yy} = \lim_{r\to r_+}\frac{j^y}{E_y} = \sqrt{\frac{g_{xx}}{g_{yy}}}Z(\Phi) + \frac{\rho^2}{\sqrt{g_{yy}g_{xx}}\,aY(\Phi)}\bigg|_{r_+}. \tag{5.12}$$

In a completely analogous way we can get the conductivity along the x direction $\sigma_{xx} = \lim_{r\to r_+} j^x/E_x = (g_{yy}/g_{xx})^{1/2}Z(\Phi)$. We notice that at charge neutrality $\rho = 0$, the conductivity ratio is determined by the metric at the horizon

$$\boxed{\frac{\sigma_{\alpha\alpha}}{\sigma_{\beta\beta}} = \frac{g_{\beta\beta}}{g_{\alpha\alpha}}\bigg|_{r+}}. \tag{5.13}$$

5.2 The viscosity

In order to compute the retarded correlation function Eq.(3.18) in the holographic formalism, we act on the bulk-metric field which is dual to the boundary stress tensor. In particular, to get the shear viscosity components, we switch on small off-diagonal fluctuations of the spatial metric tensor

$$ds^2 \mapsto ds^2 + e^{-i\omega t}\delta h_{xy}(r)dxdy. \tag{5.14}$$

In the following we adopt the one-index-up parametrization and linearize the Einstein equations to extract the radial momentum and the viscosity. However, since we are working with an anisotropic bulk, we will have two fluctuations satisfying different equations of motion.

Let us begin with the simpler case to review the standard derivation of the viscosity, and consider $\delta h_{xy} = g_{xx}(r)h^x_y(r)$. The combination $h^x_y\mathcal{E}^{(0)}_{xx} - \mathcal{E}^{(1)}_{xy} = 0$ yields

$$\partial_\mu\left(\frac{\sqrt{-g}}{\mathcal{N}}\partial^\mu h^x_y\right) = 0, \tag{5.15}$$

where $\mathcal{N} = g_{yy}g^{xx}$. This can be viewed as the equation of motion for a massless scalar field with radial dependent coupling $\mathcal{N}^{-1}$. In the Hamiltonian formalism the above equation reads

$$\Pi^y_x = \frac{\sqrt{-g}}{\mathcal{N}(r)}\partial^r h^x_y, \;\; \partial_r\Pi^y_x = -\omega^2 g^{tt}\frac{\sqrt{-g}}{\mathcal{N}(r)}h^x_y. \tag{5.16}$$

The viscosity is then given by

$$\eta_{yxyx} \equiv \eta^{yy}_{xx} = \lim_{\substack{\omega\to 0\\ r\to\infty}} \frac{1}{\omega}\,\mathrm{Im}\frac{\Pi^y_x(r,\omega)}{h^x_y(r,\omega)}. \tag{5.17}$$

The low frequency limit of the Hamilton system (i.e. $\omega \to 0$ keeping ωh and Π fixed [13]) is $\partial_r \Pi^y_x = 0 + \mathcal{O}(\omega^2 h), \partial_r(\omega h^x_y) = 0 + \mathcal{O}(\omega\Pi)$, which expresses the radial conservation of both the fluctuation and the momentum. This allows us to switch to the near horizon limit in Eq.(5.17) where the fluctuation satisfies the in-falling conditions $h^y_x(r,\omega) \to h_0(r)\, e^{-i\omega r_\star(r)}$. See again Sec. 1.2.2 for details. Here h_0 is the real solution to the frequency independent wave equation, which asymptotes constant values both at the boundary and at the horizon. Due to the radial conservation, $h_0(r) = \text{const} \equiv 1$. Plugging this expression into Eq.(5.17) we find

$$\eta_{yxyx} = \frac{s}{4\pi}\frac{g_{xx}}{g_{yy}}\bigg|_{r_+} = \frac{s}{4\pi}\frac{\sigma_{yy}}{\sigma_{xx}}, \tag{5.18}$$

where we used Eq.(5.13). The viscosity-conductivity bound Eq.(3.6) is saturated.

Let us now consider the y-index-up parametrization and analyze the combination $h^y_x \mathcal{E}^{(0)}_{yy} - \mathcal{E}^{(1)}_{xy} = 0$. In this case we obtain

$$\partial_\mu\left(\sqrt{-g}\mathcal{N}(r)\,\partial^\mu h^y_x\right) = \sqrt{-g}\mathcal{N}(r)\, m^2(r) h^y_x, \tag{5.19}$$

where the mass term $m^2 = a^2 Y g^{yy}$ arises due to the momentum dissipation along the y-direction. This corresponds again to an action for a scalar field with radial coupling $\mathcal{N}$ and mass m. As before, we define the conjugate momentum via

$$\Pi^x_y = \sqrt{-g}\mathcal{N}(r)\,\partial^r h^y_x, \;\; \partial_r \Pi^x_y = \sqrt{-g}\mathcal{N}(r)(m^2 - \omega^2 g^{tt}) h^y_x, \tag{5.20}$$

and the viscosity is given by

$$\eta_{xyxy} = \eta^{xx}_{yy} = \lim_{\substack{\omega\to 0\\ r\to\infty}} \frac{1}{\omega}\,\mathrm{Im}\frac{\Pi^x_y(r,\omega)}{h^y_x(r,\omega)}. \tag{5.21}$$

Due to the non-vanishing mass term, we cannot switch to the horizon limit as in the previous case. To determine the correlation function, we manipulate the above expression with a trick similar to those of Ref. [149]. For an alternative AdS/CFT computation see e.g. Ref. [150]. Even if the canonical momentum is not radially conserved, we can obtain an r-independent quantity by multiplying and dividing the holographic viscosity formula by the complex conjugate fluctuation

$$\eta_{xyxy} = \lim_{\substack{\omega\to 0\\ r\to\infty}} \frac{\mathrm{Im}[\Pi^x_y\, h^{y\star}_x]}{\omega |h^{y\star}_x|^2}, \tag{5.22}$$

where we took out the real denominator from the imaginary-part. The radial derivative of the numerator is given by $\partial_r \mathrm{Im}[\Pi^x_y\, h^{y\star}_x] \propto \mathrm{Im}\left[(m^2 - \omega^2 g^{tt})|h^y_x|^2 + g^{rr}|\partial_r h^y_x|^2\right]$, where we have used

Eq.(5.20). Since the quantity in brackets is real, $\mathrm{Im}[\Pi^x_y\, h^\star]$ is radially constant and can be hence evaluated at any r. In particular we can switch to the near horizon limit in the numerator of Eq.(5.22). Using the in-falling conditions in the numerator we obtain:

$$\frac{\eta_{xyxy}}{s} = \frac{1}{4\pi}\frac{g_{yy}}{g_{xx}}\bigg|_{r_+} h_0^2(r_+) = \frac{1}{4\pi}\frac{\sigma_{xx}}{\sigma_{yy}} h_0^2(r_+), \tag{5.23}$$

where $h_0(r_+)$ denotes the horizon value assumed by $h^y_x(r)$. This result is consistent with Refs. [131, 151, 152]. See also Ref. [153] for another study of shear response in momentum dissipating backgrounds. Here h_0 is again the zero frequency solution to the wave equation. In this case the fluctuation is not radially conserved, hence the boundary value will be in general different from the horizon one, $h_0(r_+) \neq h_0(\infty) \equiv 1$. This is due to the translational symmetry breaking, which gives mass to the graviton in Eq.(5.19). However, there is no way to send $a \to 0$ without restoring rotational symmetry within a single axion model as anticipated in Sec. 4.2.2. In Tab. 5.2 we have summarized the results for single axion with x dependence and double axions along x and y.

In the following we review the argument of Ref. [131] on the $m^2 > 0$ case. It is helpful to rewrite Eq.(5.19) as:

$$g^{rr}\partial_r^2 h^y_x + \frac{\partial_r\left(\sqrt{-g}\mathcal{N}g^{rr}\right)}{\sqrt{-g}\mathcal{N}}\partial_r h^y_x = m^2 h^y_x \tag{5.24}$$

Near the horizon both $\sqrt{-g}$ and $\mathcal{N}$ are regular, while g^{rr} vanishes at r_+ and increases away from the IR. Therefore $\sqrt{-g}\mathcal{N}g^{rr}$ increases as well, and the coefficient of the first derivative term in Eq.(5.24) is then positive. Assuming $h^y_x(r_+) > 0$, we see that if $m^2 > 0$ then $\partial_r h^y_x$ is positive near the horizon, so the h^y_x is an increasing function of r. Let us assume the fluctuation stops increasing at some point. Then $\partial_r h^y_x = 0$. From Eq.(5.24) it follows that the second derivative is positive, denoting a local minimum, which is in contrast with the increasing behavior. A fluctuation with positive mass squared monotonically decreases from the boundary to the horizon with a tunneling rate $\Gamma \propto h^y_x(r_+) < 1$.

	$\psi_x = 0$	$\psi_x = a_x x$
$\psi_y = 0$	$m_x^2 = 0, m_y^2 = 0$ $4\pi\frac{\eta_{xyxy}}{s} = \frac{\sigma_{xx}}{\sigma_{yy}}$ $4\pi\frac{\eta_{yxyx}}{s} = \frac{\sigma_{yy}}{\sigma_{xx}}$	$m_x^2 = a_x^2 Y_x g^{xx}, m_y^2 = 0$ $4\pi\frac{\eta_{xyxy}}{s} = \frac{\sigma_{xx}}{\sigma_{yy}}$ $4\pi\frac{\eta_{yxyx}}{s} = \frac{\sigma_{yy}}{\sigma_{xx}}(h_y^x(r_+))^2$
$\psi_y = a_y y$	$m_x^2 = 0, m_y^2 = a_y Y_y g^{yy}$ $4\pi\frac{\eta_{xyxy}}{s} = \frac{\sigma_{xx}}{\sigma_{yy}}(h_x^y(r_+))^2$ $4\pi\frac{\eta_{yxyx}}{s} = \frac{\sigma_{yy}}{\sigma_{xx}}$	$m_x^2 = a_x^2 Y_x g^{xx}, \quad m_y^2 = a_y Y_y g^{yy}$ $4\pi\frac{\eta_{xyxy}}{s} = \frac{\sigma_{xx}}{\sigma_{yy}}(h_x^y(r_+))^2$ $4\pi\frac{\eta_{yxyx}}{s} = \frac{\sigma_{yy}}{\sigma_{xx}}(h_y^x(r_+))^2$

Table 5.1: Single and double axion cases. When momentum dissipation is turned on along one axis, the graviton aquires mass causing violation of the viscosity-conductivity bound.

5.2.1 High temperature analysis

As we have seen in the previous section, momentum dissipation leads to a violation of the viscosity-conductivity bound Eq.(3.6). On the holographic side, the metric fluctuation h_x^y acquires a mass, and enters explicitly the shear viscosity tensor as in Eq.(5.23). The focus of the following section is the analysis of this expression in both the low and high temperature regimes.

In this section we comment on the high temperature behavior of the conductivity-viscosity bound Eq.(5.23). As depicted in Fig. 5.1, we can think of the spacetime as subdivided into three regions. The UV is described by AdS_4 deformed by matter fields, while the IR by the Lifshitz geometry Eq.(4.16). Moreover, an intermediate region interpolates between the UV and the IR, whose size is larger the smaller the temperature is. Since the scales in our problem are the momentum dissipation parameter a and the temperature T, high temperature coincides with the regime where $a \ll T$.
The scalar backreaction depends quadratically on the axion, and the first nonzero corrections will therefore be proportional to a^2. This motivates us to consider the following ansatz:

$$\begin{aligned} ds^2 &= -(D(r) + D_2(r)a^2)dt^2 + (B(r) + B_2(r)a^2)dr^2 \\ &\quad + (C(r) + C_{2x}(r)a^2)dx^2 + (C(r) + C_{y2}(r)a^2)dy^2, \qquad (5.25a) \\ h_x^y(r) &= h_0(r) + h_2(r)a^2 + h_4(r)a^4. \qquad (5.25b) \end{aligned}$$

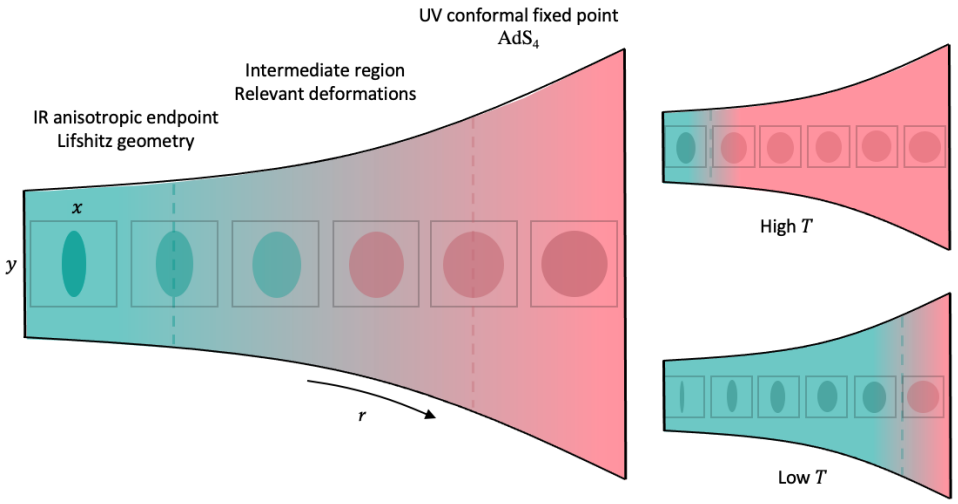

Figure 5.1: The RG flow starts from the UV conformal fixed point at the boundary of the AdS_4, and is driven by relevant deformation to an IR anisotropic fixed point described by the Lifshitz geometry Eq.(4.16). We have depicted how a circle gets deformed into an ellipse as one flows to the IR. For high temperatures, the black hole becomes big ($r_+ \to \infty$) and we can approximate the entire geometry with the AdS_4 metric deformed by the matter fields. On the other hand, the scaling region dominates for low T.

Plugging this expressions into the field equations and solving order by order we find

$$h_0(r) = 1, \tag{5.26a}$$

$$h_2(r) = -\int_r^\infty \sqrt{\frac{B}{D}}\frac{1}{C}\left(\int_{r_+}^{r_2}\sqrt{BD}\,Y(\Phi)dr_1\right)dr_2. \tag{5.26b}$$

Our result coincides with the isotropic analysis of Ref. [140]. This is due to the fact that anisotropic effects appear at second order in a in Eq.(5.25a). Note how both in the ESB ($Y(\Phi) = 1$) and in the SSB ($Y(\Phi) = \Phi^2$) case the correction is negative. This is consistent with the prediction that the fluctuation decreases from the boundary towards the horizon. The conductivity ratio here becomes an upper bound for the η/s tensor element affected by momentum dissipation:

$$4\pi\frac{\eta_{xyxy}}{s} < \frac{\sigma_{xx}}{\sigma_{yy}}. \tag{5.27}$$

In the following we calculate the viscosity correction up to $O(a^2)$ both in the ESB and SSB cases.

ESB case: as explained in Sec. 4.2.1, when $Y(\Phi) = 1$, the axion induces a coordinate-dependent source and translations are broken explicitly. We use an AdS-Schwarzschild background and perform the integral in Eq.(5.26b). This gives $h_x^y(z_+) = 1 - \frac{c_{\rm esb}}{2}(\frac{a}{T})^2$ with

$c_{\rm esb} = (9\log 3 - \sqrt{3}\pi)/16\pi^2 \approx 0.0281553$ and leads to

$$4\pi \frac{\sigma_{yy}}{\sigma_{xx}} \frac{\eta_{xyxy}}{s} \approx 1 - c_{\rm esb} \left(\frac{a}{T}\right)^2 . \tag{5.28}$$

SSB case: this case is more delicate as the dilaton enters Eq.(5.26b) explicitly, and we need the expression of Φ. We work in the probe limit where the back-reaction is negligible. Moreover, due to the asymptotic map Eq.(4.15) the effects of the axion are small as well. Hence we take $\psi = 0$. At charge neutrality $F = 0$ and we choose as dilaton potential $V(\Phi) = -6 - \Phi^2$, which corresponds to the mass $m_\Phi^2 = -2$. The full solution to Eq.(4.9) is

$$\Phi(r) = c_{1\,(2)}F_1\left(\frac{1}{3}, \frac{2}{3}; 1; \frac{r^3}{r_+^3}\right) + c_{2\,(2)}F_1\left(\frac{1}{3}, \frac{2}{3}; 1; 1 - \frac{r^3}{r_+^3}\right), \tag{5.29}$$

where the ${}_{(2)}F_1$ is the hypergeometric function and $c_{1,2}$ are two constants. Close to the boundary it behaves as $\Phi(r \approx \infty) = \frac{1}{r}(\Phi_0 + \frac{\Phi_1}{r})$ where we have introduced $\Gamma^2(2/3)\Phi_0 = (c_2 - (-1)^{2/3}c_1)\Gamma(1/3)r_+, \Gamma^2(1/3)\Phi_1 = (c_2 - \sqrt[3]{-1}c_1)\Gamma(-1/3)r_+^2$. Moreover, the near horizon expansion exhibits log-divergent terms which have to be removed to ensure regularity. This is the case if the following condition is fulfilled

$$\Phi_1 = \frac{\sqrt{\pi} r_+ \Gamma(-1/6)}{\Gamma^2(1/6)} \Phi_0 \equiv \alpha \Phi_0 . \tag{5.30}$$

Note how SSB conditions in standard quantization ($J_\Phi = 0, \langle O_\Phi \rangle \neq 0$) would force both Φ_0 and Φ_1 to vanish. Moreover, a Taylor-expansion of Eq.(5.29) reveals that the coefficients Φ_0 and Φ_1 appears at any order in r. Therefore, SSB would make the dilaton vanish not only asymptotically but everywhere in the bulk. We cannot realize the SSB in the standard way. The dilaton mass is such that both the falloffs are normalizable, meaning that we can fix not only or Φ_0 or Φ_1 but also a combination of them, imposing the so-called *mixed boundary conditions*. As we have seen in Sec. 1.2.4, the combination $J = \Phi_1 + \partial_{\Phi_0}\mathcal{W}(\Phi_0)$ sources an operator with expectation value given by $\langle O_\Phi \rangle = \Phi_0$ [154]. Here $\mathcal{W}(\Phi_0)$ is a polynomial whose degree must be chosen within the interval $[2, 3]$. Spontaneous boundary conditions on the new source $J = 0$ set the form of the polynomial:

$$\partial_{\Phi_0}\mathcal{W}(\Phi_0) = \alpha \Phi_0 , \tag{5.31}$$

where we used the regularity condition Eq.(5.30). Therefore, $\mathcal{W}(\Phi_0) = \beta + \frac{\alpha}{2}\Phi_0^2$ that is a double trace deformation, involving two powers of the VEV $\langle O_\Phi \rangle$.
Now it is time to compute the integral Eq.(5.26b). Since temperature is high, we can approximate the integrand using the UV expression for the dilaton. We find: $h_x^y(z_+) = 1 - \frac{c_{\rm ssb}}{2}\left(\frac{\Phi_0}{T}\right)^2\left(\frac{a}{T}\right)^2$, with $c_{\rm ssb} \approx 0.000435607$. This leads to

$$4\pi \frac{\sigma_{yy}}{\sigma_{xx}} \frac{\eta_{xyxy}}{s} \approx 1 - c_{\rm ssb}\left(\frac{\Phi_0}{T}\right)^2 \left(\frac{a}{T}\right)^2 . \tag{5.32}$$

Compared to the ESB case Eq.(5.28), deviations from the bound are further suppressed by extra powers of T and will generally become more important for lower temperatures than in the explicit case.

5.2.2 Low temperature analysis

In order to determine the temperature scaling of Eq.(5.23), we need the IR scaling dimension of the fluctuation h_0. This can be extracted from the asymptotic behavior near the boundary $r_\partial^{\rm ir}$ of the IR region, namely that portion of spacetime which is fully described by the Lifshiz metric Eq.(4.16). Plugging a power law ansatz $h_x^y \sim r^\alpha$ into Eq.(5.19), we find for $r_+ \ll r \ll \infty$ and marginal axions (in the irrelevant case the mass decays faster then the kinetic term) the following behavior:

$$h_x^y(r) \approx A\left(\frac{r}{r_+}\right)^{\alpha_-} + B\left(\frac{r}{r_+}\right)^{\alpha_+}, \tag{5.33}$$

where $2\alpha_\pm = \delta_T(1 \pm \sqrt{1+(2La/\delta_T)^2})$, A and B are constants, and $\delta_T = 3\phi - 1 + z - \theta$. For low temperatures, the scaling is controlled by the falloff with the lower exponent. This yields:

$$\frac{\sigma^{xx}}{\sigma^{yy}}\frac{\eta_{xx}^{yy}}{s} \sim T^{-\frac{2\alpha_-}{z}}, \tag{5.34}$$

with $2\alpha_- = z(3\phi-\theta)(-1+\sqrt{1+(2(\phi-1)[(\theta-2)\theta-2(\phi-1)\phi]V_0)/(\theta-2)(\theta-3\phi)^2})$ when $p=1$ and $2\alpha_- = (3\phi-\theta-1+z)(-1+\sqrt{1+2(\phi-z)[(\theta-2z)\theta^2-2(\phi-z)-2(1-z)]V_0/(\theta-2z)(\theta-z-3\phi+1)^2})$ when $p=2$. The isotropic limit of the $p=2$ case result coincides with the computations of Ref. [152]. For $p=1$, $\phi=1$ implies also a suppression of momentum dissipation.
Alternatively, the action ψ can source an irrelevant deformation. We studied in detail such a case in appendix B.1. Equation (5.26b) still applies and we obtain

$$4\pi\frac{\sigma_{yy}}{\sigma_{xx}}\frac{\eta_{xyxy}}{s} \approx 1 - c_{\rm esb}^{ir}\left(\frac{a}{T^{\Delta_a}}\right)^2, \tag{5.35}$$

where $\Delta_a < 0$ is the IR scale dimension of a.

5.2.3 Viscosity-conductivity bound beyond Einstein gravity

In this section we briefly comment on the viscosity-conductivity bound in the higher derivative model of Sec. 4.3.2.
Repeating the analysis of the previous section we end up again with Eq.(5.19) for the shear perturbation but with graviton mass given by

$$m^2 = a^2 g^{yy} Y(\Phi) + \frac{a^2 g^{yy}}{2}\lambda_1 Z_2(\Phi) F^2 + 2(a^2 g^{yy})^2 \lambda_2 Y_2(\Phi). \tag{5.36}$$

Notice that the stability condition Eq.(4.40) can be rewritten as $\int_{r+}^0 \sqrt{-g}\, m^2 = 0$. The electric conductivity again follows from the fluctuations of Eq.(5.7). Repeating the same analysis we obtain

$$\sigma_{yy} = \sqrt{\frac{g_{xx}}{g_{yy}}}\left(Z(\Phi) + \frac{a^2\lambda_1 Z_2(\Phi)}{g_{yy}}\right) + \frac{4\pi}{s}\frac{\rho^2}{g_{yy}m^2}\Bigg|_{r_+}. \tag{5.37}$$

while σ_{xx} diverges as momentum is not dissipated along x. For zero densities $\sigma_{xx} = \sqrt{\frac{g_{yy}}{g_{xx}}}\Big[Z(\Phi) + \frac{a^2\lambda_1 Z_2(\Phi)}{g_{yy}}\Big]_{r_+}$, and the viscosity can be expressed again in terms of the conductivity ratio as in Eq.(5.22).

5.3 Charge diffusion bound

In this section we perform a holographic analysis of the bound Eq.(3.2) on charge diffusion. In strongly coupled systems the natural velocity scale is provided by the butterfly velocity introduced in Eq.(3.3) – see also Refs. [15, 16]. In the following we compute both the charge diffusion constant and the butterfly velocity in the holographic model Eq.(4.1). See Refs. [87, 108, 111, 122, 155–158] for previous studies. Without loss of generality we set $\xi = 0$ in the IR conditions Eq.(4.17), as in the charge neutral case the exponent of $Z_{\rm IR} = e^{\xi\Phi}$ plays no role– see Sec. 4.2.2.

5.3.1 Charge diffusion constant

Charge diffusion occurs when a small gradient in the charge density ρ is introduced; charge will move to suppress this imbalance, restoring the thermodynamic equilibrium. This effect is governed by an equation of the form $\partial_t\rho - D_\rho\nabla^2\rho = 0$, where D_ρ is the diffusivity. Diffusion and transport of charge are related phenomena. We can indeed extract the diffusion constant from the electrical conductivity using the Einstein relation $D_\rho = \sigma/\chi_\rho$. Here $\chi_\rho = (\partial\rho/\partial\mu)_T$ is the charge compressibility. The holographic electric conductivities are given in Eq.(5.12). It useful to recast Maxwell equations Eq.(4.7) as

$$\partial_r\rho = 0, \quad \partial_r A_t = \frac{\rho}{\sqrt{-g}Z(\Phi)g^{rr}g^{tt}}. \tag{5.38}$$

The solution to the latter equation is given by $A_t(r) = A_t(r_+) + \rho\int_{r_+}^{r} dr\, i(r)$, with $i(r) = (\sqrt{-g}Z(\Phi)g^{rr}g^{tt})^{-1}$. Here we dropped the constant ρ. Since A_t vanishes at the horizon and gives the chemical potential near the boundary, we have

$$\mu = \lim_{r\to\infty} A_t(r) = \rho\int_{r_+}^{\infty} dr\, i(r). \tag{5.39}$$

The compressibility is then given by

$$\chi_\rho^{-1} = \int_{r_+}^{\infty} dr\, i(r). \tag{5.40}$$

The above results can be easily generalized to the anisotropic case where the diffusion depends on the direction $D_{{\rm c},\alpha} = \chi_\rho^{-1}\sigma_{\alpha\alpha}$. In the following we offer two methods to compute the integral Eq.(5.40) analytically.
Keeping in mind that $r_+ \propto T^{-1/z}$, we observe that the near horizon geometry contribution scales as $T^{-\Delta_\chi/z}$, with $\Delta_\chi = d_{\rm eff} - z$. Within a low temperature analysis, this is the dominant term if $\Delta_\chi/z > 0$ and the charge diffusion is uniquely controlled by the IR physics, in accord with the isotropic analysis of Refs. [15, 16]. In this case we obtain

$$\chi_\rho^{-1} = -\frac{L}{\Delta_\chi}\frac{r^{\Delta_\chi}}{Z(\Phi)}\bigg|_{r_+}. \tag{5.41}$$

Alternatively, we can perform a Taylor expansion near the horizon of the integrand in Eq.(5.40): $i(r) = \sum_{n=0}^{\infty}(r-r_+)^n(i_+^{(n)}/n!)$, where $i_+^{(n)} = \partial_r^n i|_{r_+}$. As $r \to r_+$, the derivatives satisfy the recursion rule $i^{(n)}(r) = \frac{(-1)^n}{r^n}\left[\prod_{k=1}^{n}(k-\Delta_\chi)\right] i(r)$, which can be proven by mathematical induction. Plugging the above expression into the Taylor expansion and performing the resulting geometric series finally gives $i(r) = i(r_+)(r/r_+)^{\Delta_\chi - 1}$, which yields Eq.(5.41) after integration.
The susceptibility together with the holographic conductivities yields the diffusion constants

$$D_{c,\alpha} = -\frac{L}{\Delta_\chi}\frac{r^{\theta-z}}{g_{\alpha\alpha}(r)}\bigg|_{r_+}. \tag{5.42}$$

5.3.2 The butterfly velocity

The butterfly velocity gives the scale with which the out-of-time-order correlation functions (OTOC) of local operators grows – see Eq.(3.3). In this section we compute it holographically by means of a shock-wave analysis. We analyze the back-reaction of the metric due to a massless particle falling towards the black hole horizon, whose velocity of growth is identified as the butterfly velocity. We perform the computation in the accelerating Kruskal reference frame, where a translation of the physical time t corresponds to a boost in the new coordinates [84], hence this is the natural environment to probe the butterfly effect. Kruskal coordinates are defined as

$$uv = -e^{\gamma'(r_+)r_\star(r)}, \tag{5.43a}$$

$$u/v = -e^{-\gamma'(r_+)t}, \tag{5.43b}$$

where $\gamma(r) = \sqrt{g_{tt}(r)/g_{rr}(r)}$, $\gamma'(r) = \partial_r\gamma$ and $dr_\star = dr/\gamma(r)$ is the tortoise coordinate. Our first goal is to translate the unperturbed ansatz Eq.(4.11) into these new coordinates. We observe that the former relation expresses the equivalence between the r and $u\cdot v$ dependencies, so we will simply replace the radial dependence of fields with the product of Kruskal coordinates.

$$\begin{aligned} ds^2 &= -g_{uv}(uv)\,dudv + \sum_\alpha g_{\alpha\alpha}(uv)\,dx_\alpha^2, \\ \Phi &= \Phi(uv), \quad \psi = ay, \\ A &= -\frac{A_t(uv)}{\gamma'(r_+)}\frac{du}{u} + \frac{A_t(uv)}{\gamma'(r_+)}\frac{dv}{v}. \end{aligned} \tag{5.44}$$

Now we perturb this background by adding a small amount of energy E_0 at $\mathbf{x} = 0$ on the boundary. Then, this perturbation will freely evolve following a light-like geodesics, which in Kruskal coordinates is a 45-degrees line. After a time $\Delta t > T^{-1}$ the amount of energy will be localized near the $u = 0$ horizon and exponentially increased, as it is moving in the accelerating Kruskal frame. If Δt is big enough, we have to take into account its back-reaction $\delta\mathcal{T}_{uu} \propto E_0 e^{2\pi T\Delta t}\delta(u)\delta^{(d)}(\mathbf{x})$. This stress tensor sources a (u,u)-component of the metric tensor in the vicinity of the $u = 0$ horizon

$$ds^2 = -g_{uv}(uv)\,dudv + \sum_\alpha g_{\alpha\alpha}(uv)\,dx_\alpha^2 + g_{uv}(uv)\,h(x,y)du^2. \tag{5.45}$$

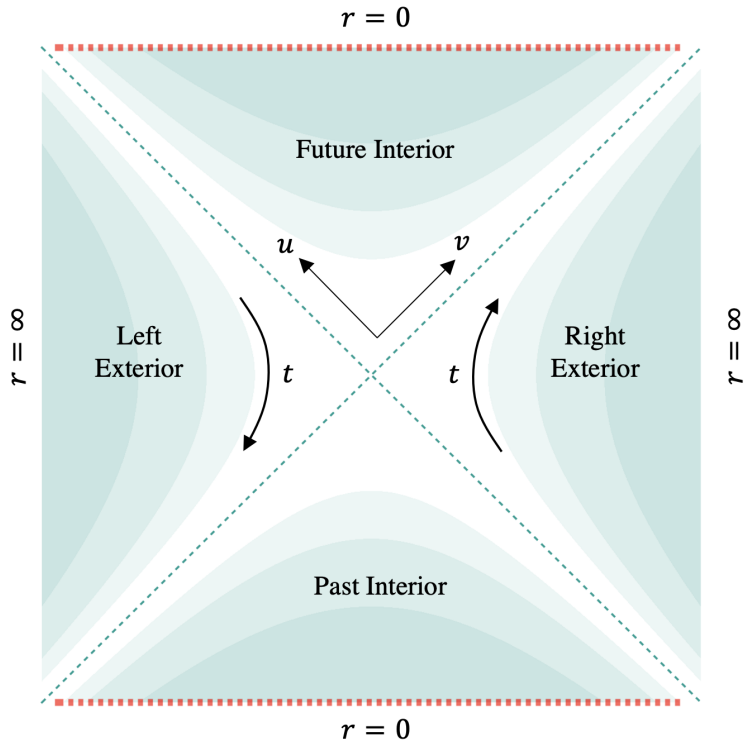

Figure 5.2: AdS spacetime in Kruskal coordinates. Figure re-adapted from Ref. [18].

This is called *shock wave geometry*. The (u,u)-component of Einstein equation evaluated at the horizon yields:

$$\left(\sum_{\alpha}\frac{\partial_{\alpha}^{2}}{c_{\alpha}^{2}}-m_{h}^{2}\right)h(x,y)=b\delta(x)\delta(y), \tag{5.46}$$

with $c_\alpha=\sqrt{g_{\alpha\alpha}(0)}$, $b\propto Ee^{2\pi T\Delta t}/g_{uv}(0)$ and mass $m_h^2=\frac{1}{g_{uv}}\frac{\partial\log\left(g_{xx}g_{yy}\right)}{\partial(uv)}|_{u=0}$. The above equation reproduces the isotropic case studied in Refs. [15, 16].
Through the coordinate change $\hat{x}_\alpha\mapsto c_\alpha x_\alpha$ we obtain a Green's functions problem

$$\left[\frac{\partial^{2}}{\partial\hat{x}^{2}}+\frac{\partial^{2}}{\partial\hat{y}^{2}}-m_{h}^{2}\right]f(\hat{x},\hat{y})=\delta(\hat{\mathbf{x}}), \tag{5.47}$$

where $f(\hat{x},\hat{y})=\frac{h(x,y)}{b\,c_x c_y}$. The solution is hence given by $h(x,y)\propto-\frac{b\,c_x c_y}{2\pi}\mathcal{K}_0(m_h\varrho)$, where $\mathcal{K}_0$ is the 0th modified Bessel function of the second kind and $\varrho^2=c_x^2x^2+c_y^2y^2$. At large values of ϱ, i.e. at large spatial distances, this gives

$$h(x,y)\propto\frac{1}{\sqrt{\varrho}}\exp\left[2\pi T\left(\Delta t-\frac{m_h}{2\pi T}\varrho\right)\right]. \tag{5.48}$$

The above exponential dependency coincides with the behavior of the OTOC [15] provided that $\Delta t-\frac{m_h\varrho}{2\pi T}=\Delta t-\frac{\varrho}{\bar{v}_{\mathrm{B}}}$. This identifies the direction averaged scale for the velocity as $\bar{v}_{\mathrm{B}}=2\pi T/m_h$.

Now we switch to the original system of coordinates where $g_{uv} = (\frac{2}{\gamma'(r_+)})^2 \frac{g_{tt}}{uv} = (\frac{2}{\gamma'(r_+)})^2 \frac{g_{rr}}{uv}\gamma^2(r)$, and obtain

$$\bar{v}_{\mathrm{B}}^2 = -\frac{2\pi T L}{d_{\mathrm{eff}} - \theta} r_+^{\theta - z}, \tag{5.49}$$

where in the last step we used the power law scaling behavior of the metric Eq.(4.16). To determine the butterfly velocity along x, we consider the case where $y = 0$ and we move in the x-direction. This gives $\frac{\varrho}{\bar{v}_{\mathrm{B}}} = \frac{c_x |x|}{\bar{v}_{\mathrm{B}}} \equiv \frac{|x|}{v_{\mathrm{B},x}}$. It then follows for the velocity along the α-direction $v_{\mathrm{B},\alpha} = \bar{v}_{\mathrm{B}}/\sqrt{g_{\alpha\alpha}(r_+)}$. Explicitly, this gives

$$v_{\mathrm{B},x}^2 = \frac{|1 + 2\phi - \theta|}{2(\theta - \phi - 1)}, \quad v_{\mathrm{B},y} = \frac{|1 + 2\phi - \theta|}{2(\theta - \phi - 1)} r_+^{2(1-\phi)}. \tag{5.50}$$

In the isotropic case, the butterfly velocity is bounded from above. For (2+1) dimensional boundary such a bound is given by $v_{\mathrm{B}}^2 \leq 3/4$ – see Ref. [159] for details. As in the KSS case, this bound is violated when rotations are broken. This aspect was first pointed out in Ref. [157]. Moreover, for asymptotically AdS geometries, v_{B} was shown to be bounded by the speed of light [158]. In the parameter space shown in Fig. B.1 of appendix B it holds that $\frac{1}{2} \leq v_{\mathrm{B},x}^2 \leq 1$, violating the upper bound as expected, but still remaining smaller than the speed of light. In the y-direction the upper bound can be parametrically violated. However, at low temperature it holds that $v_{\mathrm{B},y}^2 < 1$.

Combining the diffusivities Eq.(5.42) and the butterfly velocities Eq.(5.50), we obtain

$$D_{\rho,\alpha} = \frac{d_{\mathrm{eff}} - \theta}{\Delta_\chi} \frac{\hbar v_{B,\alpha}^2}{2\pi k_{\mathrm{B}} T}, \tag{5.51}$$

where we have restored the units. Here d_{eff} is the effective spatial dimensionality Eq.(3.9). We conclude that the bound of Eq.(3.2) also applies to anisotropic systems. In distinction to the viscosity bound, anisotropy only changes the universal coefficient that now depends on the exponents ϕ, z, and θ. Furthermore, Eq.(5.51) recovers the limit of isotropic charge neutral theories [15]. In Ref. [122], the thermal diffusivity was computed in an anisotropic setups and also found to obey a relation similar to (5.51). See Ref. [108] for an alternative proposal to Eq. (5.51) at an anisotropic QCP.

5.4 Summary

In this chapter we have computed response functions using the holographic dictionary. Specifically in Sec. 5.1 we have considered perturbations around the background and computed the electrical conductivities, which are expressed in terms of horizon data in a simple fashion. In Sec. 5.2 we have computed in a similar manner the holographic viscosity tensor and verified that one element satisfies the bound proposed with scaling arguments in Chap. 3. The other tensor element violates such a bound due to momentum dissipation induced by the coordinate dependent axion field of Chap. 4. We have then analyzed such a violation in the cases where

the translational symmetry is broken explicitly and spontaneously. In Sec. 5.3 we have analyzed the bound on charge diffusion. Differently from the other quantities, the diffusivity is not solely given by data on the horizon and is expressed through an integral over the holographic direction. Although we do not have the full expression of bulk fields, we have derived a near horizon formula for the compressibility, and could relate the diffusion constant to the horizon data in a simple fashion. We then have extracted the butterfly velocity in Sec. 5.3.2 by means of a shock wave technique, and confirmed that the bound on charge diffusion proposed in Chap. 3 holds.

Holographic conductivity ratio

$$\frac{\sigma_{\alpha\alpha}}{\sigma_{\beta\beta}} = \frac{g_{\beta\beta}}{g_{\alpha\alpha}}\bigg|_{r+}$$

Viscosity-conductivity bound

$$\eta_{yxyx} = \frac{s}{4\pi}\frac{g_{xx}}{g_{yy}}\bigg|_{r_+} = \frac{s}{4\pi}\frac{\sigma_{yy}}{\sigma_{xx}}$$

Viscosity-conductivity bound with momentum dissipation

$$\frac{\eta_{xyxy}}{s} = \frac{1}{4\pi}\frac{g_{yy}}{g_{xx}}\bigg|_{r_+} h_0^2(r_+) = \frac{1}{4\pi}\frac{\sigma_{xx}}{\sigma_{yy}}h_0^2(r_+)$$

Charge diffusion constant

$$D_{\mathrm{c},\alpha} = -\frac{L}{\Delta_\chi}\frac{r^{\theta-z}}{g_{\alpha\alpha}(r)}\bigg|_{r_+}$$

Butterfly velocity

$$v_{\mathrm{B},\alpha} = \frac{\bar{v}_{\mathrm{B}}}{\sqrt{g_{\alpha\alpha}(r_+)}}, \quad \bar{v}_{\mathrm{B}}^2 = -\frac{2\pi T L}{d_{\mathrm{eff}}-\theta}r_+^{\theta-z}$$

Charge diffusion bound

$$D_{\rho,\alpha} = \frac{d_{\mathrm{eff}}-\theta}{\Delta_\chi}\frac{\hbar v_{B,\alpha}^2}{2\pi k_{\mathrm{B}}T}$$

Recap Box – Holographic bounds on quantum critical transport coefficients

Part III

Deriving holography from the SYK superconductor

Chapter 6
The Yukawa-SYK model

As we reviewed in Chap. 2, the SYK model is solvable when the number of flavors is large, and exhibits a non-Fermi liquid behavior at low energies. At the same time, we look for an analogous model accounting for superconductivity in non-quasi-particle states. The SYK model can been extended in this direction in a variety of ways. Superconductivity in lattice fermionic SYK models can be triggered by instantaneous interactions, leading to a large superconducting gap in the incoherent regime [160], or by additional correlations among the interaction matrix-elements between spinful fermions [161]. See also Ref. [162] for the case of Majorana-SYK dots. In the (0+1) dimensional case, a negative Hubbard interaction [163] or an intra-dot coupling through charge conserving two-body interactions is able to generate superconductivity.

In this chapter we review the model introduced originally in Ref. [21] and extended in Ref. [22] based on pairing via boson exchange – see also Refs. [164, 165]. We are interested in the analysis of the phase transition in the incoherent, quantum critical phase found in such a model. Therefore, we focus low-T, normal state solution only. Details on the superconducting state can be found in Refs. [21, 22]. We introduce the effective action and demonstrate that the saddle point is governed by the Eliashberg equations of phonon-mediated superconductivity. Such a formalism includes retardation that is crucial in critical systems [166–169] where pairing is caused by magnetic [166, 167, 170] or Ising nematic [171, 172] quantum critical fluctuations, color magnetic interaction in high-density quark matter [168, 173], or where it occurs in U(1) and Z_2 spin-liquid states [171].

In Sec. 6.2 we qualitatively discuss the phase diagram and in Sec. 6.3 we discuss the low-temperature, quantum critical solution.

6.1 Phonon-fermion dot

Let us consider the following (0+1) dimensional Hamiltonian:

$$H = -\mu \sum_{\sigma,i=1}^{N} c_{i\sigma}^{\dagger} c_{i\sigma} + \frac{1}{2} \sum_{k=1}^{M} \left(\pi_k^2 + \omega_0^2 \phi_k^2 \right) + \sum_{\sigma;ijk} (g_{ij,k} + g_{ji,k}^{\star}) c_{i\sigma}^{\dagger} c_{j\sigma} \phi_k. \tag{6.1}$$

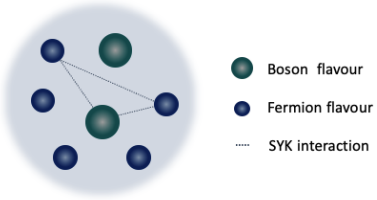

Figure 6.1: Cartoon of the Yukawa SYK model Eq.(6.1). A large number of fermion and boson flavors interact through a random SYK-like interaction.

This model describes the interaction between N fermion and M boson flavors. The former are described by the operators $c_{i\sigma}$ and $c^\dagger_{i\sigma}$ that satisfy the fermionic algebra $\{c_{i\sigma}, c^\dagger_{j\sigma'}\} = \delta_{ij}\delta_{\sigma\sigma'}$ and $\{c_{i\sigma}, c_{j\sigma}\} = 0$ with spin index $\sigma = \uparrow, \downarrow$. The latter are represented by scalar fields ϕ_k, with conjugated momentum π_k satisfying $[\phi_k, \pi_{k'}] = i\delta_{kk'}$. Here ω_0 is the bare boson frequency, while the flavor indexes run over the following intervals $i, j = 1 \cdots N$ and $k = 1 \cdots M$. We will refer to the above model as the *Yukawa-SYK model*.

At a purely technical level, we need a model able to generate composite objects involving products as e.g. $c_\sigma c_{\sigma'}$ in addition to the normal ones $c^\dagger_\sigma c_{\sigma'}$ – see e.g. Eq. (2.44) of the introductory chapters. This might lead to finite expectation values for the superconducting order parameter. To this end, the choice of the coupling constants in Eq.(6.1) is crucial. They can be either complex $g_{ijk} = g'_{ijk} + ig''_{ijk}$ or real. In the first case, $g_{ij,k} = (g_k)_{ij}$ are sampled from the Gaussian unitary ensemble (GUE) for a given k, while in the second they are chosen from the orthogonal one (GOE). Details on the probability distribution function (PDF) are summarized in the table below.

In both cases, the probability distribution has zero mean, and the second moment is expressed in terms of $\bar{g}$ with dimensions of (energy)$^{3/2}$. The other natural energy scale in the problem is the boson frequency ω_0. Therefore, it is convenient to introduce a dimensionless coupling constant $g^2 = \bar{g}^2/\omega_0^3$. As we will see below, for complex coupling constants no superconductivity occurs, due to the complete breaking of time-reversal symmetry. On the other hand, when $g \in \mathbb{R}$ anomalous terms can be generated.

As outlined in Sec. 2.3.2, the SYK model can be equivalently described in terms of a disorder averaged effective action. In the case of Eq.(6.1) this is given by

$$\begin{aligned}\frac{S^{\text{eff}}}{N} &= -\text{Tr}\log\left(\hat{G}_0^{-1} - \hat{\Sigma}\right) + \frac{M}{2N}\text{Tr}\log\left(D_0^{-1} - \Pi\right) \\ &\quad - 2\int d^2\tau G(\tau', \tau)\Sigma(\tau, \tau') \\ &\quad + \frac{M}{2N}\int d^2\tau D(\tau', \tau)\Pi(\tau, \tau') \\ &\quad - \int d^2\tau \left(F(\tau'\tau)\Phi^\dagger(\tau, \tau') + F^\dagger(\tau'\tau)\Phi(\tau, \tau')\right) \\ &\quad + \bar{g}^2\frac{M}{N}\int d^2\tau \left(G(\tau, \tau')G(\tau', \tau) - F^\dagger(\tau, \tau')F(\tau', \tau)\right) D(\tau, \tau').\end{aligned} \tag{6.2}$$

	GOE	GUE
$\overline{g'_{ijk}g'_{i'j'k'}}$	$\frac{\bar{g}^2}{2N^2}\delta_{kk'}\left(\delta_{ii'}\delta_{jj'}+\delta_{ij'}\delta_{ji'}\right)$	$\frac{\bar{g}^2}{4N^2}\delta_{kk'}\left(\delta_{ii'}\delta_{jj'}+\delta_{ij'}\delta_{ji'}\right)$
$\overline{g''_{ijk}g''_{i'j'k'}}$	0	$\frac{\bar{g}^2}{4N^2}\delta_{kk'}\left(\delta_{ii'}\delta_{jj'}-\delta_{ij'}\delta_{ji'}\right)$

Table 6.1: Probability distribution function of the SYK interaction coupling constant. The first column represents real coupling constants, extracted from the Gaussian orthogonal ensamble (GOE). The second describes the complex case, where the ensamble is the Gaussian unitary (GUE) one [174].

A detailed derivation of such an expression can be found in Appendix C.1 . $\hat{G}^{-1}(\epsilon_n) = i\epsilon_n\hat{\sigma}_0+\mu\hat{\sigma}_3$ and $D_0^{-1}(\nu_n) = \nu_n^2+\omega_0^2$ are the fermion and boson free propagators, whereas

$$G(\tau,\tau') = \frac{1}{N}\sum_i c^\dagger_{i\sigma'}(\tau')c_{i\sigma}(\tau), \quad F(\tau,\tau') = \frac{1}{N}\sum_i c_{i\downarrow}(\tau')c_{i\uparrow}(\tau),$$
$$D(\tau,\tau') = \frac{1}{M}\sum_k \phi_k(\tau')\phi_k(\tau). \tag{6.3}$$

are the bi-local fields of the disorder averaged theory. Moreover, we have made use of the Nambu formalism for the self-energy degrees of freedom $\hat{\Sigma}(\tau,\tau') = \begin{pmatrix}\Sigma(\tau,\tau') & \Phi(\tau,\tau')\\ \Phi^\dagger(\tau,\tau') & -\Sigma(\tau',\tau)\end{pmatrix}$.

6.1.1 Saddle-point equations

The action Eq.(6.2) has an overall factor of N, which allows us to perform a saddle-point approximation when N is large – here we are assuming finite M/N.
Let us first focus on the variation with respect to the self energies. The relevant part of the action can be organized as

$$\frac{S_{\hat{\Sigma}}}{N} = -\operatorname{Tr}\left[\log\left(\hat{G}_0^{-1}-\hat{\Sigma}\right)+\hat{G}\cdot\hat{\Sigma}\right]. \tag{6.4}$$

Varying w.r.t. $\hat{\Sigma}$ gives the Dyson equation $\hat{G}(\tau,\tau') = \left(\hat{G}_0^{-1}-\hat{\Sigma}\right)^{-1}_{\tau,\tau'}$, with

$$\hat{G}(\tau,\tau') = \begin{pmatrix}G(\tau,\tau') & F(\tau,\tau')\\ F^\dagger(\tau,\tau') & -G(\tau',\tau)\end{pmatrix}. \tag{6.5}$$

The other equations follow straightforwardly from Eq.(6.2) and are given by

$$D(\tau,\tau') = \left(D_0^{-1} - \Pi\right)^{-1}_{\tau,\tau'}, \tag{6.6a}$$
$$\Sigma(\tau,\tau') = \bar{g}^2 \frac{M}{N} G(\tau,\tau') D(\tau',\tau), \tag{6.6b}$$
$$\Phi^{(\dagger)}(\tau,\tau') = -\bar{g}^2 \frac{M}{N} F^{(\dagger)}(\tau,\tau') D(\tau',\tau), \tag{6.6c}$$
$$\Pi(\tau,\tau') = -2\bar{g}^2 \left(G(\tau,\tau')G(\tau',\tau) - F^{\dagger}(\tau,\tau')F(\tau',\tau)\right). \tag{6.6d}$$

On this large-N saddle point, it is reasonable to assume time translation invariance. As a consequence, we can write the above system in Matsubara space, where the equations are fully algebraic. We have

$$\hat{G}^{-1}(\epsilon_n) = i\epsilon_n \hat{\sigma}_0 + \mu\hat{\sigma}_3 - \hat{\Sigma}(\epsilon_n), \tag{6.7a}$$
$$D^{-1}(\nu_n) = \nu_n^2 + \omega_0^2 - \Pi(\nu_n), \tag{6.7b}$$
$$\Sigma(\epsilon_n) = \bar{g}^2 \frac{M}{N} T \sum_{n'} G(\epsilon_{n'}) D(\epsilon_n - \epsilon_{n'}), \tag{6.7c}$$
$$\Phi^{(\dagger)}(\epsilon_n) = -\bar{g}^2 \frac{M}{N} T \sum_{n'} F^{(\dagger)}(\epsilon_{n'}) D(\epsilon_n - \epsilon_{n'}), \tag{6.7d}$$
$$\Pi(\nu_n) = -2\bar{g}^2 T \sum_{n'} \left(G(\epsilon_{n'} + \nu_n) G(\epsilon_{n'}) - F(\epsilon_{n'} + \nu_n) F^{\dagger}(\epsilon_{n'})\right), \tag{6.7e}$$

where ω_n and ν_n are the fermionic and bosonic Matsubara frequencies respectively.

6.2 Phase diagram

In this section we give an overview of the phases described by the Hamiltonian Eq.(6.1) and depicted in the phase diagram Fig. 6.2. For details see Ref. [21]. The phase diagram of the model is richer than the pure fermionic one. The additional coupling constant g, given by the SYK interaction and the bare phonon mass, indeed allows us to distinguish between a weakly coupled region $g < 1$ and a strongly coupled one $g > 1$.

6.2.1 Normal state solution at criticality and low temperature

At the lowest temperatures, the solution is very similar to the purely electronic SYK model:

$$G_{\mathrm{n}}^{-1}(\epsilon_n) = i\epsilon_n \left(1 + c_1 \left|\frac{g^2}{\epsilon_n}\right|^{2\Delta}\right), \tag{6.8a}$$
$$D_{\mathrm{n}}^{-1}(\nu_n) = \nu_n^2 + \omega_r^2 + c_3 \left|\frac{\nu_n}{g^2}\right|^{4\Delta-1}. \tag{6.8b}$$

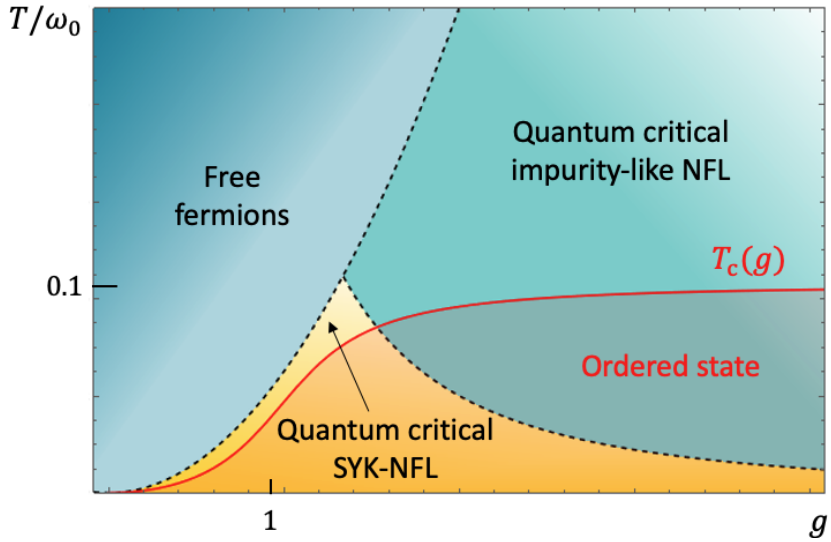

Figure 6.2: Reproduction of the phase diagram in Ref. [21] Fig.1. At weak values of the dimensionless coupling constant $g = \bar{g}/\omega_0^{3/2}$ and low temperature the system enters a quantum critical phase characterized by Landau damping of bosons. In the strong coupling region and at higher temperature, quantum critical fermions interact with almost quasi-classical bosons.

.

At low energies, these are power-law propagators and Landau damping dominates the bosons giving singular behavior to $D_{\rm n}(\nu_n)$. The exponent Δ is the anomalous dimension and can be tuned in the interval $\frac{1}{4} < \Delta < \frac{1}{2}$ by acting either on the ratio M/N or on the charge of the system – see Eq.(6.25) below. The parameters $c_{1,2,3}$ are numerical coefficients of order unity while $\omega_r^2 = c_2(T/g^2)^{4\Delta-1}$ is the renormalized phonon frequency [21]. The spectral function $A(\epsilon) = -\frac{1}{\pi}\mathrm{Im}G_{\rm n}(\epsilon)$ is sharply peaked around $\epsilon = 0$. However, such a peak has a power law structure, signaling a non-Fermi liquid behavior.

6.2.2 Normal state solution at criticality and high temperature

As depicted in the phase diagram Fig. 6.2, the quantum critical regime of the previous section is valid only below an upper cutoff that depends on the dimensionless coupling g. Indeed, in the temperature interval $g^{-2} < T/\omega_0 < g^2$ the solution reads

$$G_{\rm n}(\epsilon_n) = \frac{-2i\mathrm{sign}(\epsilon_n)}{\sqrt{\epsilon_n^2 + \Omega_0^2} + |\epsilon_n|}, \tag{6.9a}$$

$$D_{\rm n}(\nu_n) = \frac{1}{\nu_n^2 + \omega_r^2}, \tag{6.9b}$$

with a large fermionic energy scale $\Omega_0 = \frac{16}{3\pi}g^2$ and small phonon energy $\omega_r^2 = (3\pi/8)^2 T/g^2$. In this case, the fermionic spectral function is almost structureless [21], and the electrons are completely

incoherent. The reason is that the natural boson frequency Ω_0 gets so low that they look like classical impurities. Even though this quantum critical phase is made up by almost classical degrees of freedom, the system is still non-trivial because it actually becomes superconducting [21].

6.2.3 Superconducting properties

To learn more about the superconducting state, we focus on the $\mu = 0$ case and invert Eq.(6.7a). We obtain

$$\hat{G}(\epsilon_n) = -\frac{1}{\epsilon_n^2 Z^2(\epsilon_n) + |\Phi(\epsilon_n)|^2} \begin{pmatrix} i\epsilon_n Z(\epsilon_n) & \Phi(\epsilon_n) \\ \Phi^\dagger(\epsilon_n) & i\epsilon_n Z(\epsilon_n) \end{pmatrix}, \tag{6.10}$$

where we have introduced the quasi-particle weight Z defined via $\Sigma(\epsilon_n) = i\epsilon_n(1-Z(\epsilon_n))$. Inserting this expression into the self-energy equations Eq.(6.7), we end up with

$$\begin{aligned} i\epsilon_n \left(1 - Z\left(\epsilon_n\right)\right) &= -\bar{g}^2 \frac{M}{N} T \sum_{n'} \frac{D\left(\epsilon_n - \epsilon_{n'}\right) i\epsilon_{n'} Z\left(\epsilon_{n'}\right)}{\epsilon_n^2 Z^2(\epsilon_n) + |\Phi(\epsilon_n)|^2}, \qquad (6.11a) \\ \Phi\left(\epsilon_n\right) &= \bar{g}^2 \frac{N}{M} T \sum_{n'} \frac{D\left(\epsilon_n - \epsilon_{n'}\right) \Phi\left(\epsilon_{n'}\right)}{\epsilon_n^2 Z^2(\epsilon_n) + |\Phi(\epsilon_n)|^2}, \\ \Pi\left(\nu_n\right) &= -2\bar{g}^2 T \sum_{n'} \left(G\left(\epsilon_{n'} + \nu_n\right) G\left(\epsilon_n\right) - F\left(\epsilon_{n'} + \nu_n\right) F^\dagger\left(\epsilon_{n'}\right)\right). \end{aligned}$$

These are precisely the Eliashberg equations of phonon-mediated superconductivity [175–180]. The complete knowledge of the ordered state requires numerical solution of these coupled equations, extensively carried out in Ref. [21]. To get insights into the transition temperature, the above equations can be linearized around $\Phi = 0$. The anomalous self energy is indeed very small close to the phase transition. The gap equation then becomes:

$$\Phi\left(\epsilon_n\right) = \bar{g}^2 \frac{N}{M} T \sum_{n'} \frac{D\left(\epsilon_n - \epsilon_{n'}\right)}{\epsilon_n^2 Z^2(\epsilon_n)} \Phi\left(\epsilon_{n'}\right). \tag{6.12}$$

The problem of determining the critical temperature therefore translates to an eigenvalue equation in Matsubara sub-space $\bar{\bar{M}}\Phi = \Phi$. Here T_c can then be numerically extracted by determining the eigenvalue 1 fo the matrix $\bar{\bar{M}}$. The result is schematically depicted in Fig. 6.2, where superconductivity takes place everywhere in the phase diagram, i.e. at any coupling g.
At weak couplings, the transition temperature decays quadratically $T_c(g \ll 1) \approx 0.16 g^2 \omega_0$. In this regime, superconductivity sets in instead of the critical behavior, preventing the system from being so critical. For strong couplings, the transition temperature saturates $T_c(g \to \infty) \approx 0.11188\omega_0$ [21]. The incoherent soup of completely ill-defined carriers is able to undergo a transition to the superconducting state. This is analogous to Anderson's theorem for which impurities do not destroy superconductivity in disordered systems and the leftover quantum fluctuations can still trigger the phase transition [181].

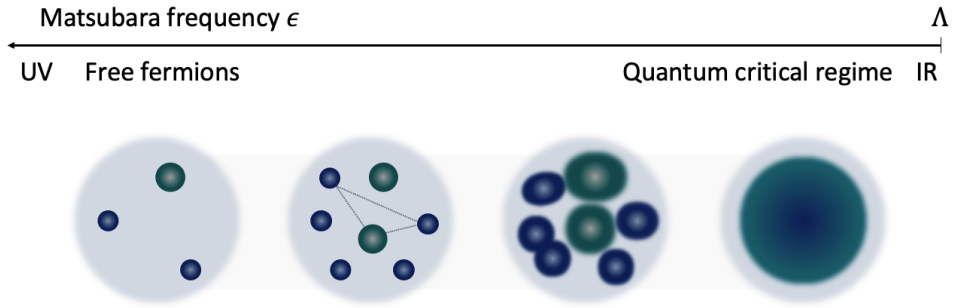

Figure 6.3: Cartoon of the RG flow towards quantum critical phases of the Yukawa-SYK model, sketched in terms of the fermionic Matsubara frequency ϵ. Both fermions and bosons lose their quasi-particle identities and end up into a *quantum-soup* phase. Here the energy scale Λ represents the crossover between the free phase and the non-Fermi liquid one.

6.3 Quantum critical, normal state solution

In this section we provide a step-by-step solution to the $T = 0$ saddle point equations as it will constitute the building block for the mapping to holography of Chap. 9.
At low energies, the action Eq.(6.2) has emergent U(1) and re-parametrization invariance as in the conventional SYK case. As a consequence the normal state propagators and self-energies transform according to the following law

$$G_{\rm n}(\tau,\tau') \;=\; e^{i\varphi(\tau_1)}g'(\tau)^{\frac{1-2\Delta}{2}}\,G_{\rm n}(g(\tau)-g(\tau'))g'(\tau')^{\frac{1-2\Delta}{2}}e^{-i\varphi(\tau_2)}, \tag{6.13}$$

where $\tau \mapsto g(\tau)$ expresses the time reparametrization and φ is a phase mode. This relation can e.g. be used to generate the finite temperature solution starting from the $T = 0$ one. In this section we review the derivation of the latter. We set $F = \Phi = 0$ and take the $T \to 0$ limit, where the spacing between the discrete Matsubara frequencies gets infinitesimal and we are allowed to replace Masubara sums with integrals $T\sum_{\epsilon_n}(...) \mapsto \int \frac{d\epsilon}{2\pi}(...)$. Moreover, we work at finite chemical potential μ – details on the $\mu = 0$ solution at $M = N$ can be found in Appendix B of Ref.[21]. Using the generalization of Luttinger's theorem [182] to include the anomalies of the power-law spectrum [164, 183, 184] yields the following parametrization of the electron density:

$$\varrho_n = \frac{1}{N}\sum_{i=1}^{N}\langle c^\dagger_{i\sigma}c_{i\sigma}\rangle = \frac{1}{2} - \frac{\theta}{\pi} - \left(\frac{1}{2}-\Delta_g\right)\frac{\sin(2\theta)}{\sin(2\pi\Delta_g)}. \tag{6.14}$$

Here Δ_g is the anomalous exponent of the fermionic spectrum and θ is a measure of the deviation from half filling. Both enter the single particle propagator as

$$G_{\rm n}(\tau) \;=\; b_g\frac{\Theta+\mathrm{sign}(\tau)}{|\tau|^{2\Delta_g}}, \tag{6.15}$$

where b_f is a numerical coefficient, Δ_g the scaling dimension, and

$$\Theta = \frac{\tan\theta}{\tan(\pi\Delta_g)} = \tanh(\pi q\mathcal{E}). \tag{6.16}$$

The spectral asymmetry parameter $\mathcal{E}$ can be related to the particle density Eq.(6.14) as reviewed in Sec. 2.3.4. Furthermore, it holds that $\mathcal{E}(\varrho_n = 1/2) = 0$. It is also related to the density dependence of the zero-point entropy [185] $2\pi\mathcal{E} = \partial_{\varrho_n} S_0$. In addition, we make the following power-law ansatz for the bosonic one:

$$D_{\rm n}(\tau) = \frac{b_b}{|\tau|^{2\Delta_b}}, \tag{6.17}$$

where again, b_b is a numerical constant and Δ_b the scale dimension. The fermion and boson self energies follow from Eqs.(6.6b) (6.6d) and are given by

$$\Sigma_{\rm n}(\tau) = \frac{M}{N}\bar{g}^2 b_b b_g \frac{\Theta + \mathrm{sign}(\tau)}{|\tau|^{2(\Delta_b+\Delta_g)}}, \quad \Pi_{\rm n}(\tau) = 2\bar{g}^2 b_g^2 \frac{1-\Theta^2}{|\tau|^{4\Delta_g}}. \tag{6.18}$$

Our next goal is to reduce the number of free constants by using the saddle point equations. This is easiest in Fourier space where the propagators assume the form

$$G_{\rm n}(\epsilon) = b_g a_g(\Delta_g)\left[\tan\theta + i\mathrm{sign}(\epsilon)\right]|\epsilon|^{-1+2\Delta_g}, \tag{6.19}$$

$$D_{\rm n}(\epsilon) = b_b a_b(\Delta_b)\,|\epsilon|^{-1+2\Delta_b}, \tag{6.20}$$

with

$$\begin{aligned} a_g(x) &= 2\cos(\pi x)\Gamma(1-2x) = 2\int_0^\infty dt \frac{\sin t}{|t|^{2x}}, \\ a_b(x) &= 2\sin(\pi x)\Gamma(1-2x) = 2\int_0^\infty dt \frac{\cos t}{|t|^{2x}}, \end{aligned} \tag{6.21}$$

which are convergent for $0 < \Delta_{f,b} < \frac{1}{2}$ only. Moreover, the Fourier transforms of Eq.(6.18) are UV divergent. Indeed, if $\Delta_g > \frac{1}{4}$, the zeroth mode $\int d\tau \Pi_{\rm n}(\tau) \propto \Lambda^{4\Delta_g-1}$ with upper cut-off Λ and similarly for the fermionic self-energy. To avoid these infinities, we analyze the dynamical parts $\delta\Sigma_{\rm n}(\epsilon) = \Sigma_{\rm n}(\epsilon) - \Sigma_{\rm n}(0)$, $\delta\Pi_{\rm n}(\epsilon) = \Pi_{\rm n}(\epsilon) - \Pi_{\rm n}(0)$ which are non-divergent and contain universal low-energy information – see Ref.[21] for details. Performing the Fourier transformation yields

$$\begin{aligned} \delta\Sigma_{\rm n}(\epsilon) &= \frac{M}{N}\bar{g}^2 b_b b_g a_g(\Delta_g+\Delta_b)[i\mathrm{sign}(\epsilon) + \Theta\tan(\pi(\Delta_b+\Delta_g))]|\epsilon|^{-1+2(\Delta_g+\Delta_b)}, \\ \delta\Pi_{\rm n}(\epsilon) &= 2\bar{g}^2 b_g^2 a_b(2\Delta_g)(1-\Theta^2)|\epsilon|^{-1+4\Delta_g}. \end{aligned} \tag{6.22}$$

Let us manipulate the boson Dyson equation $D_{\rm n}^{-1}(\epsilon) = \epsilon^2 + \omega_0^2 - \Pi_{\rm n}(0) - \delta\Pi_{\rm n}(\epsilon)$. We can neglect the quadratic ϵ^2 term against the singular frequency dependence of $\delta\Pi_{\rm n}$ due to the Landau damping. Moreover, a power-law solution is possible only when $\omega_0^2 - \Pi_{\rm n}(0) = 0$. Under these conditions,

we can consider the following version of Dyson equations: $\delta\Sigma_{\rm n}(\epsilon)G_{\rm n}(\epsilon) = -1,\ \delta\Pi_{\rm n}(\epsilon)D_{\rm n}(\epsilon) = -1$. Using our findings we obtain

$$\begin{aligned}\frac{M}{N}\bar{g}^2 b_b b_g^2 a_g(\Delta_g+\Delta_b)a_g(\Delta_g)[i\mathrm{sign}(\epsilon)+\Theta\tan(\pi(\Delta_b+\Delta_g))]& \\ \times[i\mathrm{sign}(\epsilon)+\Theta\tan(\pi\Delta_g)]|\epsilon|^{-2+4\Delta_g+2\Delta_b} &= -1, \\ 2\bar{g}^2 b_b b_g^2 a_b(2\Delta_g)a_b(\Delta_b)(1-\Theta^2)|\nu|^{-2+4\Delta_g+2\Delta_b} &= -1.\end{aligned}$$

To simplify the above equations we focus on the class of solutions satisfying the constraint $\tan(\pi(\Delta_b+\Delta_g)) = -\tan(\pi\Delta_g)$. This induces the following relation between the boson and fermion anomalous dimensions $\Delta_b = 1-2\Delta_g$, and we will simply use $\Delta_g = \Delta$. The two conditions then become $\frac{M}{N}\bar{g}^2 b_b b_g a_g(1-\Delta)a_g(\Delta)(1+\tan^2\theta) = 1$ and $2\bar{g}^2 b_b b_g^2 a_b(2\Delta)a_b(1-2\Delta)\left(1-\frac{\tan^2\theta}{\tan^2(\pi\Delta)}\right) = -1$. From Eq.(6.21) it follows that $a_g(\Delta)a_g(1-\Delta) = \frac{2\pi\cos(\pi\Delta)}{(1-2\Delta)\sin(\pi\Delta)}$, and $a_b(2\Delta)a_b(1-2\Delta) = -\frac{2\pi\sin(2\pi\Delta)}{(1-4\Delta)\cos(2\pi\Delta)}$. It then follows

$$\bar{g}^2 b_b b_g^2 = \frac{(1-2\Delta)\sin(\pi\Delta)}{2\pi\frac{M}{N}\cos(\pi\Delta)(1+\tan^2\theta)} = \frac{(1-4\Delta)\cos(2\pi\Delta)}{4\pi\sin(2\pi\Delta)\left(1-\frac{\tan^2\theta}{\tan^2(\pi\Delta)}\right)}, \tag{6.23}$$

and

$$\bar{g}^2 b_b a_b(1-2\Delta)b_g^2 a_g^2(\Delta) = \frac{\cosh^2(\pi q\mathcal{E})}{C_\Delta}, \tag{6.24}$$

with $C_\Delta = -8\cos(\pi\Delta)\sin^3(\pi\Delta)\Gamma^2(2\Delta)\Gamma(1-4\Delta)/\pi^2$.
The constants b_b and b_g depend on non-universal details of the SYK model and can only be determined from the numerical solution of the full equations. However, the above combinations are dimensionless and universal. Putting everything together we obtain

$$\frac{(1-2\Delta)\sin(\pi\Delta)}{2\pi\frac{M}{N}\cos(\pi\Delta)(1+\tan^2\theta)} = \frac{(1-4\Delta)\cos(2\pi\Delta)}{4\pi\sin(2\pi\Delta)\left(1-\frac{\tan^2\theta}{\tan^2(\pi\Delta)}\right)}. \tag{6.25}$$

This is a relation between Δ and θ that, together with the generalized Luttinger theorem Eq.(6.14), allows us to determine the parameters Δ and θ for given ϱ_n and M/N.
In conclusion, the normal state of the Hamiltonian (6.1) is a strongly coupled, quantum-critical fluid composed of interacting and incoherent bosons and fermions, as depicted in Fig.6.3.

6.4 Summary

In this chapter we have introduced the Yukawa-SYK model. Contrary to the model reviewed in Sec. 2.3, the interaction occurs among two fermion and one boson flavors. In Sec. 6.1 we have introduced the Hamiltonian and the disorder-averaged effective action. All the details of the derivation can be found in appendix C.1. In Sec. 6.2 we have described the phase diagram of the model, which exhibits a low temperature, quantum critical phase which will be fundamental for the following chapters of this thesis. The details of its derivation are contained in Sec. 6.3. Importantly, this model is unstable towards superconductivity and constitutes a solvable toy-model for quantum critical superconductivity.

Yukawa-SYK Hamiltonian

$$H = -\mu \sum_{\sigma,i} c^\dagger_{i\sigma} c_{i\sigma} + \frac{1}{2} \sum_k \left(\pi_k^2 + \omega_0^2 \phi_k^2 \right) + \sum_{\sigma;ijk} (g_{ij,k} + g^\star_{ji,k}) c^\dagger_{i\sigma} c_{j\sigma} \phi_k$$

Effective action

$$\begin{aligned} \frac{S^{\text{eff}}}{N} &= -\text{Tr}\log\left(\hat{G}_0^{-1} - \hat{\Sigma}\right) + \frac{M}{2N}\text{Tr}\log\left(D_0^{-1} - \Pi\right) \\ &\quad - 2\int d^2\tau G(\tau',\tau)\Sigma(\tau,\tau') + \frac{M}{2N}\int d^2\tau D(\tau',\tau)\Pi(\tau,\tau') \\ &\quad - \int d^2\tau \left(F(\tau'\tau)\Phi^\dagger(\tau,\tau') + F^\dagger(\tau'\tau)\Phi(\tau,\tau') \right) \\ &\quad + \bar{g}^2 \frac{M}{N} \int d^2\tau \left(G(\tau,\tau')G(\tau',\tau) - F^\dagger(\tau,\tau')F(\tau',\tau) \right) D(\tau,\tau') \end{aligned}$$

$$\hat{G}_0^{-1}(\tau,\tau') = -(\partial_\tau - \mu)\delta(\tau-\tau')\,\hat{\sigma}_0$$

$$\hat{\Sigma}(\tau,\tau') = \begin{pmatrix} \Sigma(\tau,\tau') & \Phi(\tau,\tau') \\ \Phi^\dagger(\tau,\tau') & -\Sigma(\tau',\tau) \end{pmatrix}, \quad \hat{G}(\tau,\tau') = \begin{pmatrix} G(\tau,\tau') & F(\tau,\tau') \\ F^\dagger(\tau,\tau') & -G(\tau',\tau) \end{pmatrix}$$

Normal state, quantum critical solution

$$G_{\text{n}}(\epsilon) = c_g \left(\tan\theta + i\,\text{sign}(\epsilon) \right) |\epsilon|^{2\Delta-1}, \quad D_{\text{n}}(\epsilon) = c_b\,|\epsilon|^{1-4\Delta}$$

Recap Box – The Yukawa-SYK model

Chapter 7

Electrodynamics of the Yukawa-SYK model

The goal of this chapter is to investigate the superconducting and electrodynamic properties of the Yukawa-SYK model Eq.(6.1). To do so, we need to embed the boson-fermion dot in an environment with finite spatial extent. This can be done e.g. by coupling several dots through either a SYK_4 [71, 186, 187] or SYK_2 [188, 189] interaction. In Ref. [190] it has been shown that a band structure arises when the hopping matrix is not random. Moreover, superconductivity in extended SYK systems has been investigated in e.g. Refs. [160, 161]. All of these cases lead to non-Fermi liquid behavior.
This chapter is organized as follows. In Sec. 7.1 we follow Ref. [188] and choose a random hopping matrix, with the simplifying assumption that the inter-dot couplings $g_{ij,k}$ do not depend on the site – see also [191]. This way, translation invariance is preserved. Finally, in Sec. 7.2 we investigate electrodynamics of the condensed state, and derive both the superconducting stiffness and the optical conductivity at low energies.

7.1 Higher dimensional embedding

In this section we embed the Yukawa-SYK dot Eq.(6.1) into a lattice – see Fig.7.1. We consider the following higher-dimensional Hamiltonian

$$H = -\mu \sum_{\sigma,i,x} c^\dagger_{i\sigma x} c_{i\sigma x} + \frac{1}{2}\sum_{k,x}\left(\pi^2_{kx} + \omega_0^2 \phi^2_{kx}\right) + \sum_{\sigma;ijk,x} (g_{ij,k} + g^\star_{ji,k}) c^\dagger_{i\sigma x} c_{j\sigma x}\phi_{kx} + \sum_{\substack{\langle x,x'\rangle \\ ij\sigma}} t_{ij,xx'} c^\dagger_{j\sigma x'} c_{i\sigma x}. \tag{7.1}$$

Here x, x' label the sites of a d-dimensional lattice, and $\sigma, \sigma' = \uparrow, \downarrow$ are again spin indexes. The indices ij, k are fermion and boson flavours, which in this chapter are assumed to be equal in number, i.e. $M = N$. The operators $c_{i\sigma x}$, $c^\dagger_{i\sigma x}$ and ϕ_{kx} are the associated operators satisfying $\{c_{i\sigma x}, c^\dagger_{j\sigma' x'}\} = \delta_{ij}\delta_{\sigma\sigma'}\delta^{(d)}(x - x')$, $\{c_{i\sigma x}, c_{j\sigma x}\} = 0$, and $[\phi_{kx}, \pi_{k'x'}] = i\delta_{kk'}\delta^{(d)}(x - x')$.

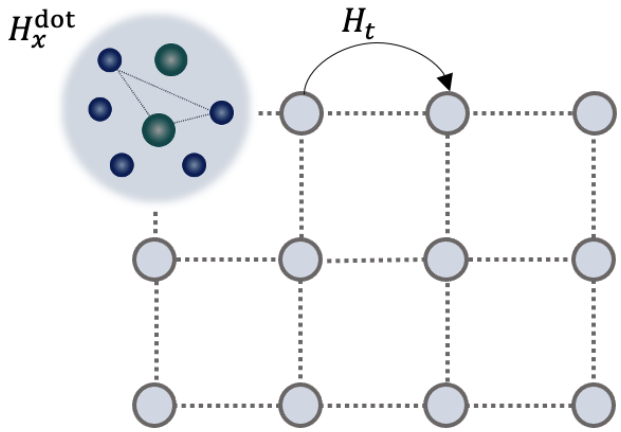

Figure 7.1: The finite dimensional embedding of the phonon-fermion SYK dot. The sites of the lattice are coupled by a random hopping term H_t.

The embedding is realized through the hopping matrix $t_{ijxx'} = t'_{ijxx'} + it''_{ijxx'}$, which couples each dot by creation and annihilation of a fermion flavour. We focus on real hopping couplings, i.e. we extract them from the Gaussian orthogonal ensemble. To ensure hermiticity of the Hamiltonian it must hold that $t_{ij,xx'} = t_{ji,x'x}$. Specifically, we consider the following zero mean $\overline{t_{ijxx'}} = 0$ probability distribution function (PDF)

$$\begin{aligned}\overline{t'_{ijxx'}t'_{i'j'yy'}} &= \frac{t_0^2}{2N}\left(\delta_{ii'}\delta_{jj'}\delta_{xy}\delta_{x'y'} + \delta_{ij'}\delta_{ji'}\delta_{xy'}\delta_{x'y}\right), \\ \overline{t''_{ijxx'}t''_{i'j'yy'}} &= 0.\end{aligned} \tag{7.2}$$

The model is controlled by the following disorder averaged effective action

$$\begin{aligned}\frac{S}{N} =& -\sum_x \operatorname{Tr}\log\left(\hat{G}_0^{-1} - \hat{\Sigma}_x\right) + \frac{1}{2}\sum_x \operatorname{Tr}\log\left(D_0^{-1} - \Pi_x\right) \\ &- 2\sum_x \int d\tau d\tau' G_x(\tau',\tau)\Sigma_x(\tau,\tau') + \frac{1}{2}\sum_x \int d\tau d\tau' D_x(\tau',\tau)\Pi_x(\tau,\tau') \\ &- \sum_x \int d\tau d\tau' \left(F_x(\tau'\tau)\Phi_x^\dagger(\tau,\tau') + F_x^\dagger(\tau'\tau)\Phi_x(\tau,\tau')\right) \\ &+ \bar{g}^2 \sum_x \int d\tau d\tau' \left(G_x(\tau,\tau')G_x(\tau',\tau) - F_x^\dagger(\tau,\tau')F_x(\tau',\tau)\right) D_x(\tau,\tau') \\ &+ \frac{t_0^2}{2}\sum_{\langle x,x'\rangle} \int d\tau d\tau' \left(G_x(\tau,\tau')G_{x'}(\tau',\tau) - F_x^\dagger(\tau,\tau')F_{x'}(\tau',\tau)\right).\end{aligned} \tag{7.3}$$

Here the bi-local fields Eq.(6.3) have been promoted to lattice variables by including a site index x. Details can be found in appendix C.3.

7.1.1 Saddle point equations

The saddle point equations of the action Eq.(7.3) are

$$\begin{aligned}
&\hat{G}_x(\tau,\tau') = \left(\hat{G}_0^{-1} - \hat{\Sigma}_x\right)^{-1}_{\tau,\tau'}, \quad D_x(\tau,\tau') = \left(D_0^{-1} - \Pi_x\right)^{-1}_{\tau,\tau'}, \\
&\Sigma_x(\tau,\tau') = \bar{g}^2 G_x(\tau,\tau') D_x(\tau',\tau) + \frac{t_0^2}{2} \sum_{x' \,\mathrm{nn}\, x} G_{x'}(\tau,\tau'), \\
&\Phi_x(\tau,\tau') = -\bar{g}^2 F_x(\tau,\tau') D_x(\tau',\tau) - \frac{t_0^2}{2} \sum_{x' \,\mathrm{nn}\, x} F_{x'}(\tau,\tau'), \\
&\Pi_x(\tau,\tau') = -2\bar{g}^2 \left(G_x(\tau,\tau') G_x(\tau',\tau) - F_x^\dagger(\tau,\tau') F_x(\tau',\tau)\right),
\end{aligned} \tag{7.4}$$

where in $\sum_{x' \,\mathrm{nn}\, x}(...)$ only those sites next neighbor to x are considered.
From now on we focus on translation invariant solutions both in time and space [188]. This is consistent with the mean-field approach, where inhomogeneities are usually assumed to be energetically disadvantageous. Physically, translation invariance is restored in the same way as e.g. averages over impurities in crystals which lead to averaged quantities which are homogeneous by definition. We have

$$\hat{G}(\tau) = \left(\hat{G}_0^{-1}(\tau) - \hat{\Sigma}(\tau)\right)^{-1}, \tag{7.5a}$$

$$D(\tau) = \left(D_0^{-1}(\tau) - \Pi(\tau)\right)^{-1}, \tag{7.5b}$$

$$\Sigma(\tau) = \bar{g}^2 G(\tau) D(\tau) + \frac{z t_0^2}{2} G(\tau), \tag{7.5c}$$

$$\Phi(\tau) = -\bar{g}^2 F(\tau) D(\tau) - \frac{z t_0^2}{2} F(\tau), \tag{7.5d}$$

$$\Pi(\tau) = -2\bar{g}^2 \left(G(\tau) G(-\tau) - F^\dagger(\tau) F(-\tau)\right), \tag{7.5e}$$

where z is the coordination number of the SYK dots lattice.
Let us discuss the $\bar{g} \to 0$ limit to see if the above system of equations is consistent with our expectations. It is easiest to work in frequency space. We have the following solutions:

1. $\phi^{(\dagger)}, F^{(\dagger)} \neq 0$, $\Sigma(\epsilon_n) = \alpha^2 G(\epsilon_n)$,

$$G(\epsilon_n) = \frac{i\epsilon_n - \mu}{\alpha^2}, \tag{7.6}$$

2. $\phi^{(\dagger)}, F^{(\dagger)} = 0$, $\Sigma(\epsilon_n) = \alpha^2 G(\epsilon_n)$,

$$G(\epsilon_n) = \frac{\mu + i\epsilon_n}{2\alpha^2} \left(1 \pm \sqrt{1 - \frac{4\alpha^2}{(\mu + i\epsilon_n)^2}}\right) \overset{\epsilon_n \gg \mu}{\approx} \frac{1}{i\epsilon_n}, \tag{7.7}$$

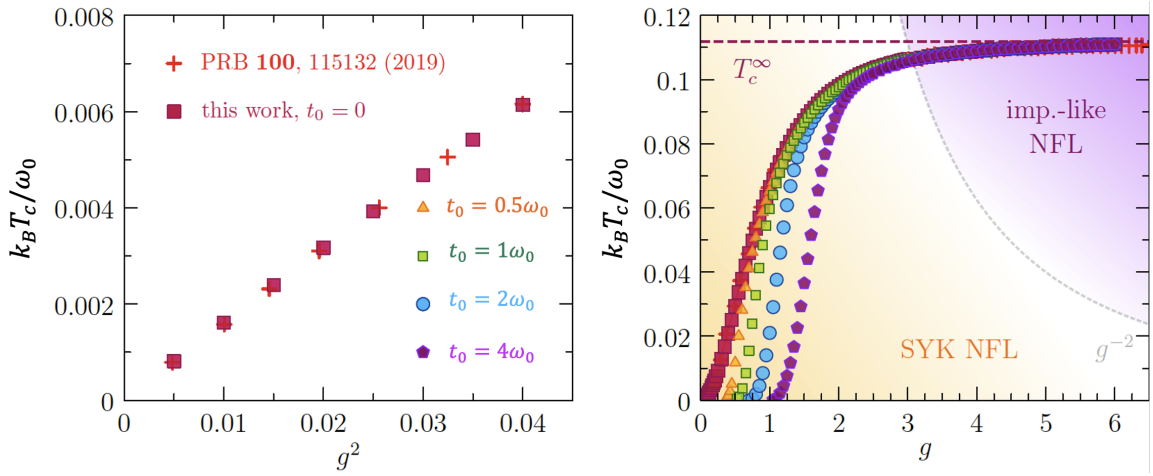

Figure 7.2: Superconducting critical temperature as function of the SYK coupling g for different values of the hopping parameter t_0 for coordination number $z = 1$. Left panel: in the small coupling regime T_c vanishes quadratically as a function of g. Right panel: for larger couplings the critical temperature saturates at the value $T_c^\infty \sim 0.111897\omega_0$ that marks the infinite-coupling limit. Finite values of t_0 have the effect of decreasing T_c. For large enough g the system crosses over from the SYK-NFL fixed point to the impurity-like NFL one.

where we defined $2\alpha^2 = t_0^2 z$. The first solution has a non-physical high frequency behavior, since it would have to decay as $1/\epsilon$. Therefore, we simply discard this case. The second solutions have the correct high-frequency behavior. Propagators have indeed to be causal. The Kramers-Kronig relations between real and imaginary parts put a constraint on the large frequency behavior, namely that the function itself must decay at least linearly in frequency at large frequency.
In Fig. 7.2 we show the superconducting critical temperature as function of the SYK coupling g for different values of the hopping parameter t_0. The numerical analysis follows from the strategy outlined around Eq.(6.12). It has been carried out by Dr. Davide Valentinis and will be reported upon elsewhere in more detail [192]. As in the case of the 0+1 dimensional model, T_c saturates at strong coupling and vanishes quadratically when $g \to 0$. At a given value of g, T_c decreases for increasing t_0, hence hopping acts against superconductivity. However, such a suppression does not lead to any quantum critical point as T_c is finite for any values of g. In any case, this is still a good model to describe pairing of incoherent fermions, since for low temperature and coupling the system approaches a quantum critical, non-FL (SYK NFL) fixed point which is unstable towards superconductivity.

7.2 Electrodynamics of SYK

In this section we analyze electrodynamics of the extended SYK model. As we reviewed in appendix D, the current response to an external vector potential is given by

$$\delta j_\alpha(\mathbf{q},\epsilon) = \mathcal{K}_{\alpha\beta}(\mathbf{q},\epsilon)A_\beta(\mathbf{q},\epsilon), \tag{7.8}$$

where $\delta\mathbf{j}$ is the current induced by an external field. Notice that this is different from the total current which involves also external contributions. The electrodynamic kernel $\mathcal{K}$ encodes both the longitudinal electric conductivity and the superconducting stiffness

$$\sigma_l(\mathbf{q},\epsilon) = c\frac{\mathcal{K}_l(\mathbf{q},\epsilon)}{i\epsilon}, \quad \rho_s = -\frac{c}{4\pi}\lim_{\mathbf{q}\to 0}\mathcal{K}_t'(\mathbf{q},\epsilon=0), \tag{7.9}$$

see appendix D for the derivation. Below we set $c=1$.
In the following we derive $\mathcal{K}$ by analyzing the low energy charge fluctuations around the saddle point of the action Eq.(7.3).

7.2.1 Charge fluctuations: the phase mode action

We follow the strategy outlined in Ref. [188] and derive the low energy effective theory for the phase mode $\varphi(x,\tau)$ associated to charge fluctuations.
Let us consider the IR limit of the effective action Eq.(7.3). In the pure IR limit, the action is invariant under the following U(1) transformations:

$$\hat{G}_x\left(\tau_1,\tau_2\right) \;=\; e^{i\varphi_x(\tau_1)\hat{\sigma}_z}\hat{G}\left(\tau_1-\tau_2\right)e^{-i\varphi_x(\tau_2)\hat{\sigma}_z}, \tag{7.10}$$

and similarly for the self-energy matrix $\hat{\Sigma}_x$. This parallels the single dot case Eq.(6.13) in the SYK section 2.3.
These identities tell us that the generic solution on the left hand side can be generated from the translations-invariant one by applying a U(1) transformation. Notice that we do not let the boson fluctuate as it is not charged under this specific U(1).
This symmetry is spontaneously broken by the saddle point solution. Away from the IR, such a symmetry is also broken explicitly, and our next goal is to derive the effective action of the associated pseudo-Nambu-Goldstone modes. We make an expansion to second order in φ. Importantly, we neglect linear contributions as they vanish in the vicinity of a saddle point where:

$$S[X] = S[X_{\text{s.p.}}] + \cancel{\frac{\delta S}{\delta X}\Big|_{\text{s.p.}}}\delta X + \frac{\delta^2 S}{\delta X^2}\Big|_{\text{s.p.}}\delta X^2 + \ldots \tag{7.11}$$

The deviation from the saddle point δX can be due to different factors. In the case of Eq.(7.10) they come from the fluctuating phase field. Other examples are the reparametrization symmetry which generates energy fluctuations, or small external fields as we will see in Sec. 7.2.
All the terms in the effective action Eq.(7.3) are invariant under the U(1) transformations Eq.(7.10) except for the trace-log term, and the last one involving the hopping physics. The

first line is local-in-space and hence contributes to the time dynamics only, while the last plays a role in the space dynamics. Specifically, we will be considering the following expression

$$S' = -\sum_x \mathrm{Tr}\log\left(\hat{G}_0^{-1} - \hat{\Sigma}_x\right) + \frac{t_0^2}{2}\sum_{\langle x,x'\rangle}\int d^2\tau\left(G_x(\tau_1,\tau_2)G_{x'}(\tau_1,\tau_2) - F_x^\dagger(\tau_1,\tau_2)F_{x'}(\tau_2,\tau_1)\right). \tag{7.12}$$

In Appendix C.4 we perform the fluctuation analysis around the saddle point of the above action that leads to

$$\frac{S[\varphi]}{N} = -T\sum_{p,\epsilon_n}\varphi(-p,\epsilon_n)\left(\epsilon_n^2\Pi_-(i\epsilon_n) + \epsilon(p)L(i\epsilon_n)\right)\varphi(p,-\epsilon_n), \tag{7.13}$$

where ϵ_n are the Matsubara fermionic frequencies with $\varphi(\tau,x) = T\sum_{p,\epsilon_n}\varphi_{p\epsilon_n}e^{i(px-\epsilon_n\tau)}$. Here we have defined $\Pi_G(\tau) = G(\tau)G(-\tau)$, $\Pi_F(\tau) = F^\dagger(\tau)F(-\tau)$, and $\Pi_\pm(\tau) = \Pi_G(\tau) \pm \Pi_F(\tau)$. Moreover, $L(i\epsilon_n) = \frac{t_0^2}{2}(\Pi_G(0) - \Pi_G(i\epsilon_n) - \Pi_F(0) - \Pi_F(i\epsilon_n))$. In the above expression we have defined $\epsilon(p) = \frac{1}{2}\sum_{x'\text{near }x}(\vec{p}\cdot\vec{a})^2$,which in the case of isotropic Bravais lattices with unit spacing, is simply given by $\epsilon(p) = |\mathbf{p}|^2$.

7.2.2 Computation of the kernel $\mathcal{K}$

To compute the kernel $\mathcal{K}$ in Eq.(7.8) we induce a vector-potential dependence by using the so-called *Peierls substitution* [193]

$$c_{xi\sigma}(\tau) \mapsto c_{xi\sigma}(\tau)e^{-i\theta_x(\tau)}, \quad \theta_x(\tau) = e\int_{x_0}^{x} d\vec{y}\cdot\vec{A}(y,\tau), \tag{7.14a}$$

where x_0 is some reference site. This is basically a gauge transformation which allows to switch-on a small external vector potential. Notice that only the non-local-in-x part of Eq.(7.1) is affected by the transformation Eq.(7.14). We have

$$G_x(\tau_2,\tau_1)G_{x'}(\tau_1,\tau_2) \mapsto e^{i(\theta_x(\tau_1)-\theta_{x'}(\tau_1))}e^{-i(\theta_x(\tau_2)-\theta_{x'}(\tau_2))}G_x(\tau_2,\tau_1)G_{x'}(\tau_1,\tau_2), \tag{7.15a}$$

$$F_x^\dagger(\tau_2,\tau_1)F_{x'}(\tau_1,\tau_2) \mapsto e^{i(\theta_x(\tau_1)-\theta_{x'}(\tau_1))}e^{i(\theta_x(\tau_2)-\theta_{x'}(\tau_2))}F_x^\dagger(\tau_2,\tau_1)F_{x'}(\tau_1,\tau_2), \tag{7.15b}$$

where we have kept the replica and spin indexes implicit. For simplicity we introduce $\theta_x(\tau) - \theta_{x'}(\tau) \equiv \Delta_\theta(\tau)$. With the replica-diagonal and spin-singlet ansatz we find

$$\frac{2}{t_0^2}\frac{S^{\mathrm{hop}}}{N} = \sum_{\langle xx'\rangle}\int d^2\tau\left(A_+\,G_x(\tau_1,\tau_2)G_{x'}(\tau_2,\tau_1) - A_-\,F_x^\dagger(\tau_1,\tau_2)F_{x'}(\tau_2,\tau_1)\right), \tag{7.16}$$

with $A_\pm = e^{i(\Delta_\theta(\tau_2)\mp\Delta_\theta(\tau_1))}$. Now we repeat the procedure of Sec. 7.2.1 to find the effective action for the phase mode. The coefficients in (7.16) then map onto

$$A_\pm \mapsto e^{\pm i\left([\mathbf{a}\cdot\vec{\nabla}_x\varphi(\tau_1)-\Delta_\theta(\tau_1)]\mp[\mathbf{a}\cdot\vec{\nabla}_x\varphi(\tau_2)-\Delta_\theta(\tau_2)]\right)}. \tag{7.17}$$

If the vector field in Eq.(7.14a) is slowly varying we can approximate $\Delta_\theta(\tau) = e\int_{x'}^{x} d\mathbf{y}\cdot\mathbf{A}(y,\tau) \sim e\,\mathbf{a}\cdot\mathbf{A}(x,\tau)$. From this and Eq.(7.17) we realize that an small external vector field can be introduced with the minimal substitution

$$ip_\alpha\varphi(\mathbf{p},\tau) \mapsto ip_\alpha\varphi(\mathbf{p},\tau) - eA_\alpha(\mathbf{p},\tau), \tag{7.18}$$

where we switched to momentum space. The recipe is clear now: applying the above map to the effective phase mode action Eq.(7.13) introduces a finite vector potential. Focusing on isotropic Bravais lattices yields for which $\epsilon(p) = |\mathbf{p}|^2$, we find

$$S[\varphi, A] = S[\varphi] - \int_p j_\alpha(p)A_\alpha(-p) + \frac{1}{2}\int_p A_\alpha(p)m_{\alpha\beta}(\epsilon_n)A_\beta(-p), \tag{7.19}$$

with mass term $m_{\alpha\beta}(i\epsilon_n) = -2Ne^2L(i\epsilon_n)\delta_{\alpha\beta}$ and source term $j_\alpha(p) = -iNe\,[L(i\epsilon_n) + L(-i\epsilon_n)]\varphi(p)p_\alpha$. Moreover we used the conventions $p = (-\epsilon_n, \mathbf{p})$, $\int_p(...) = T\sum_{\epsilon_n,p}(...)$.
The partition function is defined as $Z = \int \mathcal{D}\,\varphi e^{-S[\varphi]+jA-\frac{1}{2}AmA}$. The total current therefore is

$$J_\alpha(q) = \frac{\delta \log Z}{\delta A_\alpha(-q)} = \langle j_\alpha(q)\rangle_A - m_{\alpha\beta}A_\alpha(q). \tag{7.20}$$

The kernel in Eq.(7.8) ($J = \mathcal{K}A$) then follows after a further differentiation with respect to the gauge field

$$\mathcal{K}_{\alpha\beta}(\mathbf{q}, i\epsilon_n) = \frac{\delta J_\alpha(q)}{\delta A_\beta(q)}\bigg|_{A=0} = \frac{\delta^2 \log Z}{\delta A_\beta(q)\delta A_\alpha(-q)}\bigg|_{A=0}. \tag{7.21}$$

We start with $\frac{\delta\langle j_\alpha(q)\rangle_A}{\delta A_\beta(q)} = \langle j_\alpha(-q)\rangle_A\langle j_\beta(q)\rangle_A - \langle j_\alpha(q)j_\beta(-q)\rangle_A$. The first terms evaluated at $A = 0$ is the one-point-function $\langle j(p)\rangle$ which is vanishing at zero field as we are working in the linear response regime. The second term is

$$\langle j_\alpha(q)j_\beta(-q)\rangle = N^2e^2[L(i\epsilon_n) + L(-i\epsilon_n)]^2q_\alpha q_\beta\langle\varphi(-q)\varphi(q)\rangle. \tag{7.22}$$

Putting all together, the kernel Eq.(7.21) is then given by

$$\frac{\mathcal{K}_{\alpha\beta}(\mathbf{q}, i\epsilon_n)}{2Ne^2L(i\epsilon_n)} = \delta_{\alpha\beta} + \frac{2L(i\epsilon_n)q_\alpha q_\beta}{\epsilon_n^2\Pi_-(i\epsilon_n) + \epsilon(q)L(i\epsilon_n)}, \tag{7.23}$$

where we used the evenness property $L(-i\epsilon_n) = L(i\epsilon_n)$. Splitting in longitudinal and transverse components w.r.t. the momentum of the probe photon, we have

$$\mathcal{K}_l(\mathbf{q}, i\epsilon_n) = 2Ne^2L(i\epsilon_n)\left(1 + \frac{2L(i\epsilon_n)\,\mathbf{q}^2}{\epsilon_n^2\Pi_-(i\epsilon_n) + \epsilon(q)L(i\epsilon_n)}\right), \quad \mathcal{K}_t(\mathbf{q}, i\epsilon_n) = 2Ne^2L(i\epsilon_n). \tag{7.24}$$

7.2.3 Testing superconductivity: the superconducting phase stiffness

In the previous section we have derived the kernel $\mathcal{K}$ and now we are able to test superconductivity. Let us first rewrite the components Eq.(7.24) on the real axis by performing the analytic continuation $i\epsilon_n \mapsto \epsilon$. We have

$$\mathcal{K}_l(\mathbf{q},\epsilon) = 2Ne^2L(\epsilon)\left(1 - 2NL(\epsilon)\left\langle\varphi(-q)\varphi(q)\right\rangle\mathbf{q}^2\right), \tag{7.25a}$$

$$\mathcal{K}_t(\mathbf{q},\epsilon) = 2e^2NL(\epsilon). \tag{7.25b}$$

We have focused on isotropic Bravais lattices for which $\epsilon(q) = \mathbf{q}^2$. Using Eq.(7.9), the superconducting stiffness is given by

$$\rho_s = -\frac{2Ne^2}{4\pi}L'(0) = \frac{Ne^2t_0^2}{2\pi}\int d\tau F^\dagger(\tau)F(-\tau). \tag{7.26}$$

A numerical solution of the saddle-point equations Eq.(7.5) is required in order to extrapolate e.g. the temperature dependence of the superconducting stiffness.

7.2.4 Normal state: IR optical conductivity

In this section we compute the optical conductivity in the IR regime. It is defined as

$$\sigma(\epsilon) = \sigma_l'(\mathbf{q}=0,\epsilon>0) = \frac{\mathcal{K}_l''(\mathbf{q}=0,\epsilon>0)}{\epsilon} = 2Ne^2\frac{L''(\epsilon)}{\epsilon}, \tag{7.27}$$

where we have used Eq.(7.9). The analysis of Sec. 7.2.1 gave the function L on the imaginary frequency axis. To derive $\sigma(\epsilon)$ we have to perform an analytic continuation to the real frequency axis. For simplicity we work at $T = 0$, where the spacing between Matsubara frequencies gets infinitesimal and sums become integrals. We therefore have

$$L(i\epsilon) = \frac{t_0^2}{2}(\Pi_G(0) - \Pi_G(i\epsilon)) = \frac{t_0^2}{2}\int_{-\infty}^{\infty} d\tau\Pi_G(\tau)\left(1 - e^{-i\epsilon\tau}\right). \tag{7.28}$$

Notice that, since $\Pi_G(-\tau) = \Pi_G(\tau)$, L is an even function of ϵ. In the IR the $G_{\rm n}(\tau) = b_g\,\mathrm{sign}(\tau)/|\tau|^{2\Delta}$ and the above integral becomes

$$L(i\epsilon) = -b_g^2\frac{t_0^2}{2}\int_{-\infty}^{\infty} d\tau|\tau|^{-4\Delta}(1 - e^{-i\epsilon\tau}). \tag{7.29}$$

Using $\Gamma(z) = \int_0^\infty |x|^{z-1}e^{-x}dx$, the above integral converges to

$$L(i\epsilon) = \frac{t_0^2}{2}b_g^2c_b(2\Delta)|\epsilon|^{4\Delta-1}, \tag{7.30}$$

provided that $1/4 < \Delta < 3/4$. Here $c_b(x) = 2\sin(\pi x)\Gamma(1-2x)$ and is negative in the convergence interval – see also Eq.(6.21). Therefore, $L(i\epsilon)$ is negative and the Gaussian theory of phase mode is consequently well defined.

To perform the analytic continuation we use the Kramers-Kronig transformation

$$L(i\epsilon) = -\int_{-\infty}^{\infty} \frac{d\epsilon}{\pi} \frac{L''(\epsilon)}{i\epsilon - \epsilon} = \int_{-\infty}^{\infty} \frac{d\epsilon}{\pi} \frac{\epsilon + i\epsilon}{\epsilon^2 + \epsilon^2} L''(\epsilon). \tag{7.31}$$

The only way to satisfy $L(-i\epsilon) = L(i\epsilon)$, is that $L''(-\epsilon) = -L''(\epsilon)$. This gives $L(i\epsilon) = \frac{2}{\pi}\int_0^\infty d\epsilon \frac{\epsilon}{\epsilon^2+\epsilon^2} L''(\epsilon)$. In general $L(0)$ should vanish in the normal state. However, the above expression satisfies $L(0) \neq 0$. Therefore we subtract by hand the zero-frequency contribution and consider

$$L(i\epsilon) = \frac{2}{\pi}\int_0^\infty d\epsilon \left(\frac{\epsilon}{\epsilon^2+\epsilon^2} - \frac{1}{\epsilon}\right) L''(\epsilon) = -\frac{2}{\pi}\int_0^\infty d\epsilon \frac{\epsilon^2}{\epsilon(\epsilon^2+\epsilon^2)} L''(\epsilon). \tag{7.32}$$

From this we can also anticipate the sign of L'': since $L(i\epsilon)$ is negative, L'' must be positive. In order for this expression to be consistent with Eq.(7.30) it must hold that $L''(\epsilon) = \frac{t_0^2}{2} A \,\mathrm{sign}(\epsilon)|\epsilon|^{4\Delta-1}$, with $A = -2b^2\Gamma(1-4\Delta)\sin^2(2\pi\Delta)$. The sign function ensures the oddness of L'' with respect of argument inversion. Here L'' is positive only in the regime $[\frac{1}{4}, \frac{1}{2}]$. Plugging this into Eq.(7.27) we get

$$\sigma_{\mathrm{ir}}(\epsilon) = N e^2 t_0^2 A\, \epsilon^{4\Delta-2}. \tag{7.33}$$

If we do the same analysis at finite T, we expect for the resistivity $\rho \sim T^{2-4\Delta}$. For the usual SYK model with $\Delta = 1/4$ it follows that the resulting resistivity is linear $\rho \propto T$ while for the electron phonon problem with $\Delta \approx 0.42037$ it follows that the resistivity exponent is $2 - 4\Delta = 0.3185$. Near the strong coupling fixed point we expect $\Delta \to 1/2$ yielding a constant resistivity.

7.3 Summary

In this chapter we have embedded the 0+1 dimensional model of Chap. 6 into a higher dimensional lattice. The model Hamiltonian and the disorder averaged effective action can be found in Sec. 7.1, whereas the details on derivations are contained in appendix C.3. In Sec. 7.2 we have analyzed the response of this system to an external electromagnetic field. In particular we have determined the analytic expression for the low-energy electric conductivity and for the superconducting phase stiffness. In order to determine the behavior of such a thermodynamic quantity, a numerical analysis of the saddle point equations has to be employed.

Effective action

$$\frac{S[\varphi]}{N} = -\sum_p \int d^2\tau\ \varphi_p(\tau_1)\Big[\Pi_-(\tau_1-\tau_2) + \epsilon(p)L(\tau_1-\tau_2)\Big]\varphi_{-p}(\tau_2)$$

$$L(\tau) = t_0^2\left(\delta(\tau)\int_{-\beta}^{\beta} d\bar{\tau}\Pi_-(\bar{\tau}) - \Pi_+(\tau)\right)$$

$$\Pi_G(\tau) = G(\tau)G(-\tau)$$

$$\Pi_F(\tau) = F^\dagger(\tau)F(-\tau)$$

$$\Pi_\pm(\tau) = \Pi_G(\tau) \pm \Pi_F(\tau)$$

Matsubara frequencies

$$\varphi(\tau,x) = T\sum_{p,\epsilon_n} \varphi_{p\epsilon_n} e^{i(px-\epsilon_n\tau)}, \quad \varphi_{p\epsilon_n} = \frac{1}{2}\int d\tau e^{i\epsilon_n\tau}\varphi_p(\tau)$$

$$\frac{S[\varphi]}{N} = T\sum_{p,\epsilon_n} D^{-1}_{p,\epsilon_n}\varphi_{-p,\epsilon_n}\varphi_{p,-\epsilon_n}, \quad D^{-1}_{p,\epsilon_n} = -\epsilon_n^2\Pi_-\epsilon_n - \epsilon(p)L_{\epsilon_n}$$

$$\epsilon(p) = p^2, \quad \text{for isotropic Bravais lattices}$$

$$L(i\epsilon_n) = \frac{t_0^2}{2}(\Pi_G(0) - \Pi_G(i\epsilon_n) - \Pi_F(0) - \Pi_F(i\epsilon_n))$$

$$\approx -\frac{t_0^2}{2}\left(2\int d\tau\Pi_F(\tau) + i\epsilon_n\int d\tau\Pi_+(\tau)\right) + O(\epsilon_n^2)$$

Recap Box – charge fluctuations

Peierls substitution

$$c_{xi\sigma}(\tau) \mapsto c_{xi\sigma}(\tau)e^{-i\theta_x(\tau)}, \quad \theta_x(\tau) = e\int_{x_0}^{x} d\mathbf{y}\cdot\mathbf{A}(y,\tau),$$
$$\nabla_x\varphi(\tau) \mapsto \nabla\varphi_x(\tau) - e\mathbf{A}(x,\tau)$$

$$\frac{S[\varphi,A]}{N} = \frac{S[\varphi]}{N} - \int_p j_\alpha(p)A_\alpha(-p) + \frac{1}{2}\int_p A_\alpha(p)m_{\alpha\beta}(\epsilon_n)A_\beta(-p)$$
$$m_{\alpha\beta}(i\epsilon_n) = -2Ne^2L(i\epsilon_n)\delta_{\alpha\beta} \quad j_\alpha(p) = -2iNe\,L(i\epsilon_n)\varphi(p)p_\alpha$$

The superconducting Kernel

$$J_\alpha(\mathbf{p},\epsilon) = \mathcal{K}_{\alpha\beta}(\mathbf{p},\epsilon)A_\beta(\mathbf{p},\epsilon),$$
$$\sigma(\mathbf{p},\epsilon) = -i\frac{\mathcal{K}(\mathbf{p},\epsilon)}{\epsilon+i0^+}$$
$$\mu^{-1}(\mathbf{p},0) = 1 - \frac{4\pi}{c}\frac{\mathcal{K}_t(\mathbf{p},0)}{|\mathbf{p}^2|} \quad \lambda^{-2} = \frac{4\pi}{c}\rho_s = -\lim_{\mathbf{p}\to 0}\mathcal{K}_t'(\mathbf{p},\epsilon=0)$$
$$\frac{\mathcal{K}_{\alpha\beta}(\mathbf{p},i\epsilon_n)}{2Ne^2L(i\epsilon_n)} = \delta_{\alpha\beta} - \frac{2L(i\epsilon_n)q_\alpha q_\beta}{\epsilon_n^2\Lambda(i\epsilon_n) - \epsilon(q)L(i\epsilon_n)}$$
$$\mathcal{K}_l(\mathbf{p},i\epsilon_n) = 2Ne^2L(i\epsilon_n)\left(1 - \frac{2L(i\epsilon_n)\,\mathbf{p}^2}{\epsilon_n^2\Lambda(i\epsilon_n) - \epsilon(q)L(i\epsilon_n)}\right)$$
$$\mathcal{K}_t(\mathbf{p},i\epsilon_n) = 2Ne^2L(i\epsilon_n)$$

Recap Box – SYK Electrodynamics

Chapter 8

The pairing response of the quantum critical Yukawa-SYK model

In the previous chapters we have analyzed the SYK superconductor based on the Hamiltonian Eq.(6.1). This is a good, solvable toy-model for critical superconductivity, that acquires a finite stiffness against magnetic field penetration when coupled to a higher dimensional lattice – see Eq.(7.26).
In this chapter we tackle further questions: what is such a superconductor most susceptible to, how can we destroy it, and how does it behave when we do so. To this end, we employ the probability distribution of Ref. [22] for the coupling constants $g_{ij,k} = g'_{ijk} + ig''_{ijk}$:

$$\begin{aligned} \overline{g'_{ijk}g'_{i'j'k'}} &= \left(1-\frac{\alpha}{2}\right)\frac{\bar{g}^2}{2N^2}\delta_{kk'}\left(\delta_{ii'}\delta_{jj'}+\delta_{ij'}\delta_{ji'}\right), \\ \overline{g''_{ijk}g''_{i'j'k'}} &= \frac{\alpha}{2}\frac{\bar{g}^2}{2N^2}\delta_{kk'}\left(\delta_{ii'}\delta_{jj'}-\delta_{ij'}\delta_{ji'}\right). \end{aligned} \tag{8.1}$$

When $\alpha = 0$, each configuration enjoys time reversal symmetry (TRS) and couplings are drawn from the GOE, whereas $\alpha = 1$ corresponds to the opposite scenario (GUE). See also table 6.1. In the intermediate case $0 < \alpha < 1$, TRS is partially broken, and the parameter α serves as a knob to interpolate between the two ensembles. As we will see, the superconducting critical temperature T_c vanishes at some critical value of α, which corresponds to a quantum phase transition. This allows us to interpret α as a pair breaking parameter.

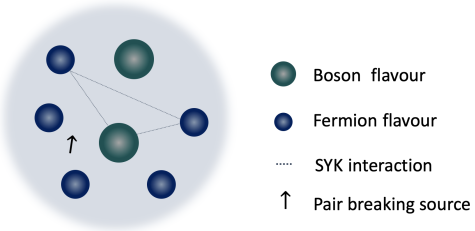

Figure 8.1: Cartoon of the Yukawa SYK with pair-breaking sources represented by arrows.

8.1 Pairing source and effective theory

$$\begin{aligned}\frac{S^{\text{eff}}}{N} &= -\text{Tr}\log\left(\hat{G}_0^{-1}-\hat{\Sigma}\right)+\frac{M}{2N}\text{Tr}\log\left(D_0^{-1}-\Pi\right)\\ &-2\int d\tau d\tau' G(\tau',\tau)\Sigma(\tau,\tau')+\frac{M}{2N}\int d\tau d\tau' D(\tau',\tau)\Pi(\tau,\tau')\\ &-\int d\tau d\tau'\left(F(\tau'\tau)\Phi^\dagger(\tau,\tau')+F^\dagger(\tau'\tau)\Phi(\tau,\tau')\right)\\ &+\bar{g}^2\frac{M}{N}\int d\tau d\tau'\left(G(\tau,\tau')G(\tau',\tau)-(1-\alpha)F^\dagger(\tau,\tau')F(\tau',\tau)\right)D(\tau,\tau')\\ &-\int d\tau J_0(\tau)\left(F(\tau,\tau)+F^\dagger(\tau,\tau)\right).\end{aligned} \tag{8.2}$$

The saddle point equations are again of the form of Eliashberg equations (6.11) with the addition of the source term J_0 and pair-breaking parameter. In particular, the anomalous self-energy equation Eq.(6.11b) is mapped into

$$\Phi\left(\epsilon_n\right) \;=\; (1-\alpha)\,\bar{g}^2\frac{N}{M}T\sum_{n'}\frac{D\left(\epsilon_n-\epsilon_{n'}\right)\Phi\left(\epsilon_{n'}\right)}{\left(\epsilon_{n'}Z\left(\epsilon_{n'}\right)\right)^2+\Phi\left(\epsilon_{n'}\right)^2}+J_0. \tag{8.3}$$

The pairing response of the system is encoded in the susceptibility

$$\chi(\tau)=\left.\frac{d\mathcal{O}(\tau)}{dJ_0}\right|_{J_0=0}=T\sum_{\epsilon_n}\left.\frac{d\langle F(\epsilon_n,\tau)\rangle}{dJ_0}\right|_{J_0=0}. \tag{8.4}$$

In the second equality we have Matsubara-transformed with respect to the relative time $\tau-\tau'$, while keeping the dependence on the absolute one $(\tau+\tau')/2$ explicit. Note that we Fourier transformed w.r.t. $\tau-\tau'$ and then evaluated the correlation at $\tau=\tau'$. The pairing susceptibility can be measured by exploiting proximity effects in a Josephson junction between two different superconductors – see e.g. Ref. [194]. In the following we focus on the static limit $\tau\to 0$ and use the notation $\chi(\tau=0)=\chi$. Dynamical processes will be considered in the next two chapters. Close to the phase transition, F is small, and is linearly related to the anomalous self-energy through Eq.(6.10) $F(\epsilon_n)=G_{\text{n}}(\epsilon_n)G_{\text{n}}(-\epsilon_n)\Phi(\epsilon_n)$. Here we have used normal state results (G_{n}

etc.) for the fermion and boson propagators since we are assuming to approach the phase transition from the normal side.
At low temperature, the susceptibility is therefore given by

$$\chi = \int_{\epsilon} G_{\mathrm{n}}(\epsilon) G_{\mathrm{n}}(-\epsilon) \frac{d\Phi(\epsilon)}{dJ_0}\Big|_{J_0=0}. \tag{8.5}$$

In order to determine the vertex function $d\Phi(\epsilon)/dJ_0$, we now focus on Eq.(8.3).

8.1.1 The linearized gap-equation

The linearized version of Eq.(8.3) reads

$$\Phi(\epsilon) = \lambda_p \bar{g}^2 \int_{\epsilon'} \frac{D_{\mathrm{n}}(\epsilon-\epsilon')}{(\epsilon' Z_{\mathrm{n}}(\epsilon'))^2} \Phi(\epsilon') + J_0, \tag{8.6}$$

with quasi-particle weight $\Sigma_{\mathrm{n}}(\epsilon) = i\epsilon(1 - Z_{\mathrm{n}}(\epsilon))$ and $\lambda_p = (1-\alpha)\frac{M}{N}$. Since we are working at low temperature, we use the quantum critical expressions reviewed in Sec. 6.3, which we re-quote here for completeness:

$$G_{\mathrm{n}}(\epsilon) = c_g \left(\tan\theta + i\,\mathrm{sign}(\epsilon)\right) |\epsilon|^{-\frac{1-\gamma}{2}}, \quad D_{\mathrm{n}}(\epsilon) = c_b |\epsilon|^{-\gamma}. \tag{8.7}$$

Here we have parametrized the anomalous dimension through a new exponent $\gamma = 4\Delta - 1$, which can be tuned within the window $0 < \gamma < 1$ either by driving the system away from neutrality $\theta \neq 0$ or by acting on the population of the fermionic and bosonic modes M/N according to Eq.(6.25).
The gap equation Eq.(8.6) then becomes

$$\Phi(\epsilon) = p_\gamma \int_{\epsilon'} \frac{\Phi(\epsilon')}{|\epsilon-\epsilon'|^{\gamma} |\epsilon'|^{1-\gamma}} + J_0. \tag{8.8}$$

Even though the combination $p_\gamma = \lambda_p \bar{g}^2 c_g^2 c_b$ involves UV parameters, this specific product is universal and dimensionless. Using the results of Sec. 6.3, we indeed have $p_\gamma = \frac{M}{N}(1-\alpha)\cosh^2(\pi q \mathcal{E})/C_\gamma$, with $C_\gamma = -\Gamma(-\gamma)\Gamma^2((\gamma+1)/2)(\sin(\pi\gamma) + 2\cos\left(\frac{\pi\gamma}{2}\right))/\pi^2$ and $\mathcal{E}$ the spectral asymmetry.

Notice that Eq.(8.8) is the same gap equation that occurs in theories with pairing due to critical gauge-field, nematic fluctuations, and massless gluons in high-density quark matter [168, 170, 172, 173, 195]. Thus, we argue our analysis goes beyond the specifics of the SYK model and is directly relevant to a much broader class of physical systems.

Let us momentarily set $J_0 = 0$. To solve such an equation we make a power-law ansatz of the form $\Phi(\epsilon) \propto |\epsilon|^{-b}$, with b a complex number. We get:

$$1 = \frac{p_\gamma}{2\pi} \int_{-\infty}^{\infty} dx \frac{1}{|1-x|^\gamma |x|^{1+b-\gamma}}. \tag{8.9}$$

As shown in Ref. [166], it must hold that $b = -\frac{\gamma}{2} \pm \nu$ with ν imaginary number, and the full solution is a combination of two independent behaviors $\Phi(\epsilon) \sim |\epsilon|^{-\frac{\gamma}{2}\pm\nu}$. The parameter ν can be determined by the condition

$$1 = \frac{p_\gamma}{2\pi} \mathcal{J}_\gamma(\nu) = \frac{p_\gamma}{2\pi} \int_{-\infty}^{\infty} dx \frac{1}{|1-x|^\gamma |x|^{1-\frac{\gamma}{2}+\nu}}. \tag{8.10}$$

Note that the integral can be performed explicitly, but its expression is unimportant for the subsequent analysis. Clearly, the constraint $\mathrm{Re}(b) = \gamma/2$ is no longer true if ν becomes real. Consequently, at $\nu = 0$ we no longer have a solution. This corresponds to the following critical value of the pair breaking parameter $\alpha_c = 1 - \frac{N}{M} \frac{2\pi}{\mathcal{J}_\gamma(0)\bar{g}^2 c_g^2 c_b}$. In Ref. [22] it has been found that $\alpha_c \approx 0.626531$ for the charge neutral case and for $M = N$. As we will confirm shortly, the transition temperature T_c is exponentially suppressed here, and α_c (and $\nu = 0$) therefore defines a quantum critical point.

8.1.2 From the integral gap equation to a solvable differential problem

In the following we convert the Eliashberg gap equation (8.8) into a second order differential equation. Although this approach is valid for small γ only, it will let us determine quite easily the superconducting transition temperature. Moreover, after a suitable coordinate change, we will also be able to make the first connection to holography.
We start by splitting the integrand in Eq.(8.8)

$$\int_{-\infty}^{+\infty} \frac{d\epsilon'}{2\pi} \frac{\Phi(\epsilon')}{|\epsilon-\epsilon'|^\gamma |\epsilon'|^{1-\gamma}} = \int_0^{+\infty} \frac{d\epsilon'}{2\pi} \left(\frac{1}{|\epsilon-\epsilon'|^\gamma} + \frac{1}{|\epsilon+\epsilon'|^\gamma} \right) \frac{\Phi(\epsilon')}{\epsilon'^{1-\gamma}}, \tag{8.11}$$

where we have assumed $\Phi(-\epsilon) = \Phi(\epsilon)$. The power law behavior Eq.(8.7) holds within a certain range of frequencies $T < \epsilon < \Lambda$, with upper cutoff Λ. T sets the lower cutoff as it represents the lowest energy scale.
Let us consider $\epsilon > 0$ and split the integration into the regimes $\epsilon' < \epsilon$ and $\epsilon' > \epsilon$ which we approximate as $\epsilon' \gg \epsilon$ and $\epsilon' \ll \epsilon$ respectively. Then it follows:

$$\Phi(\epsilon) \approx \frac{2p_\gamma}{\epsilon^\gamma} \int_T^\epsilon \frac{d\epsilon'}{2\pi} \frac{\Phi(\epsilon')}{\epsilon'^{1-\gamma}} + 2p_\gamma \int_\epsilon^\Lambda \frac{d\epsilon'}{2\pi} \frac{\Phi(\epsilon')}{\epsilon'} + J_0. \tag{8.12}$$

This approximation is exact when $(1-(\epsilon/\epsilon')^\pm)^\gamma \approx 1$, i.e. when $\gamma \to 0$. The problem can be recast in terms of a differential equation

$$\partial_\epsilon \left(\epsilon^{1-\gamma} \partial_\epsilon \epsilon^\gamma \Phi(\epsilon) \right) = -\frac{\gamma p_\gamma}{\pi} \frac{\Phi(\epsilon)}{\epsilon}. \tag{8.13}$$

The boundary conditions come from Eq.(8.12) and are given by

$$\partial_\epsilon(\epsilon^\gamma\Phi(\epsilon))_{\epsilon=T} = \gamma T^{\gamma-1}\Phi(T), \tag{8.14a}$$
$$\partial_\epsilon(\epsilon^\gamma\Phi(\epsilon))_{\epsilon=\Lambda} = \gamma\Lambda^{\gamma-1}J_0. \tag{8.14b}$$

If we furthermore use the logarithmic variables $x = \log(\Lambda/\epsilon)$ and $x_T = \log(\Lambda/T)$ and introduce $\Phi(\epsilon) \equiv \epsilon^{-\gamma} f\Big(\log\frac{\Lambda}{\epsilon}\Big)$, the above differential equation becomes a damped harmonic oscillator

$$f''(x) + \gamma f'(x) + \frac{\gamma p_\gamma}{\pi} f(x) = 0, \tag{8.15a}$$
$$f'(0) = -\gamma\Lambda^\gamma J_0, \tag{8.15b}$$
$$f'(x_T) = -\gamma f(x_T). \tag{8.15c}$$

8.1.3 Analysis without source field: the transition temperature

The question we tackle first is whether the system is able to develop an order parameter $\Phi \neq 0$ spontaneously, i.e. when the external source is switched off ($J_0 = 0$). This approach will yield the superconducting critical temperature.
The generic solution to Eq.(8.13) is given by

$$\Phi(\epsilon) = A|\epsilon|^{-\frac{\gamma}{2}+\nu} + A^\star|\epsilon|^{-\frac{\gamma}{2}-\nu}, \tag{8.16}$$

which mirrors our previous result for the analysis of the integral equation. However, in this case $\nu = \sqrt{\gamma(\frac{\gamma}{4} - \frac{p_\gamma}{\pi})}$, which indeed coincides with the small γ-expansion of the condition Eq.(8.10). If $p_\gamma < \pi\gamma/4$, ν is real ($\nu^2 > 0$) and the solution is a linear combination of power-law behaviors with real exponents. Using the boundary conditions Eq.(8.14) yields a homogeneous linear system for the coefficients A and $A^\star$, which is thus solved by $A^{(\star)} = 0$. Consequently, the gap function is zero $\Phi = 0$ and no superconductivity occurs. This is consistent with the analysis of the integral equation where we also found that ν has to be imaginary in order to get a solution.
We now focus on $p_\gamma > \gamma/4$ ($\nu^2 < 0$) and use logarithmic variables. We have

$$f(x) = f_0 e^{-\frac{\gamma x}{2}} \sin\Big(|\nu|x + \varphi_0\Big). \tag{8.17}$$

The UV boundary condition Eq.(8.15b) without source reads $f'(0) = 0$ and fixes the phase $\tan\varphi_0 = 2|\nu|/\gamma$. The IR boundary condition Eq.(8.15c) gives $\tan\Big(|\nu|x_T + \varphi_0\Big) = -2|\nu|/\gamma = -\tan(\varphi_0)$. Combining these conditions we get

$$|\nu|x_T + 2\arctan\frac{2|\nu|}{\gamma} = n\pi. \tag{8.18}$$

This relation expresses the quantization of the parameter $|\nu|$, and reveals a tower of modes also found in Refs. [196–201] and in holographic works Refs. [59, 60]. Each of such modes is excited

at a temperature scale given by

$$T^{(n)}(\nu) = \Lambda \exp\left(\frac{2\,\mathrm{atan}\frac{2|\nu|}{\gamma} - n\pi}{|\nu|}\right). \tag{8.19}$$

When $\nu \to 0$ and $n > 0$, such temperature scale goes to 0, and $\nu = 0$ defines a quantum critical point. The mode with the smallest temperature corresponds to $n = 1$. Therefore, the critical temperature is $T_c = T^{n=1}(\nu \approx 0)$ and get

$$T_c = \Lambda e^{-\frac{\pi}{\sqrt{p_\gamma/\pi - \gamma/4}}}. \tag{8.20}$$

Such an exponential suppression of the critical temperature is typical for the BKT scaling [202–204]. In the RG language, such a behavior is due to the collision of two fixed points (see e.g. Ref. [205]), and has also been observed in holographic works e.g. Refs. [60, 206].
Finally, close to this critical point, the leading mode behaves as $f_{n=1}(x) \approx f_0(2|\nu|/\gamma)e^{-\frac{\gamma x}{2}}(1 + \gamma x/2)$. The gap function is therefore given by $\Phi_{n=1}(\epsilon) \propto |\nu||\epsilon|^{-\frac{\gamma}{2}}(1+\frac{\gamma}{2}\log(\Lambda/|\epsilon|))$, which vanishes as expected.

8.1.4 Analysis with source field

We now solve the system Eq.(8.15) with non-vanishing source. We start with $p_\gamma > \frac{\pi\gamma}{4}$, where the solution is again given by Eq.(8.17) but with a different phase φ. Using the boundary conditions we obtain

$$\sin(\varphi - \varphi_0) = \frac{2\Lambda^\gamma J_0 \cos\varphi_0}{f_0}, \quad \sin\Big(|\nu| x_T + \varphi + \varphi_0\Big) = 0, \tag{8.21}$$

where φ_0 is the phase of the source-less analysis. From the second relation we obviously have $\varphi = -\varphi_0 - |\nu| x_T + n\pi$. As a consequence we obtain the amplitude $f_0 = -2\Lambda^\gamma J_0 \cos\varphi_0 / \sin\Big(2\varphi_0 + |\nu| x_T - n\pi\Big)$. Differently from the previous case, the amplitude is fixed. Plugging this into the solution and switching to the original variables, we find

$$\Phi(\epsilon) = 2\left(\frac{\Lambda}{\epsilon}\right)^{\frac{\gamma}{2}} \cos\varphi_0 \frac{\sin\left(|\nu| \log\frac{|\epsilon|}{T} + \varphi_0\right)}{\sin\left(|\nu| \log\frac{\Lambda}{T} + 2\varphi_0\right)} J_0. \tag{8.22}$$

We conclude by considering the opposite case $p_\gamma < \frac{\pi\gamma}{4}$. Here the solution is a linear combination of real exponentials $f(x) = e^{-\frac{\gamma x}{2}}(f_1 e^{-\nu x} + f_2 e^{\nu x})$. The amplitudes are fixed by the boundary conditions as $f_2 = \frac{2\gamma(\gamma-2\nu)\Lambda^\gamma J_0}{(\gamma-2\nu)^2 - (\gamma+2\nu)^2(\Lambda/T)^{2\nu}}$, $f_1 = \left(\frac{\Lambda}{T}\right)^{2\nu} f_2$. Using the original variables and $\gamma + 2\nu = \sqrt{\gamma^2 - 4\nu^2}e^{\vartheta_0}$ with angle $\vartheta_0 = \mathrm{arctanh}(2\nu/\gamma)$, we finally find

$$\Phi(\epsilon) = \left(\frac{\Lambda}{\epsilon}\right)^{\frac{\gamma}{2}} \cosh\vartheta_0 \frac{\sinh\left(\nu \log\frac{\epsilon}{T} + \vartheta_0\right)}{\sinh\left(\nu \log\frac{\Lambda}{T} + 2\vartheta_0\right)} J_0. \tag{8.23}$$

This form can be also recovered from Eq.(8.22) after analytic continuation $|\nu| \mapsto i\nu$.

8.2 The static susceptibility

Equations (8.22) and (8.23) determine the anomalous self-energy valid in the small γ limit. However, such expressions hold also for general γ, if ν is chosen such that the integral relation Eq.(8.10) is satisfied. We now have all the ingredients to determine the pairing susceptibility Eq.(8.5).
Let us start with $\nu^2 < 0$. Using the fermionic propagator Eq.(8.7) and the solution Eq.(8.22), we find

$$\chi(\nu, T) = \chi_c \cos\varphi_0 \frac{\sin\left(|\nu| \log \frac{\Lambda}{T}\right)}{\sin\left(|\nu| \log \frac{\Lambda}{T} + 2\varphi_0\right)}, \tag{8.24}$$

where $\chi_c = 2c_{g,\theta}^2 \Lambda^\gamma / \pi\gamma$ and $c_{g,\theta}^2 = c_g^2(1 + \tan^2\theta)$. There is a divergence for $|\nu| \log \frac{\Lambda}{T_c} = -2\varphi_0 + n\pi$ which is precisely the condition on the critical temperature previously found in Eq.(8.18). Approaching T_c at finite ν we indeed find the typical mean-field behavior that signals a second-order phase transition

$$\chi(\nu, T \to T_c) = -\chi_c \cos\varphi_0 \frac{\sin\left(|\nu| \log \frac{\Lambda}{T}\right)}{|\nu|} \frac{T_c}{T - T_c}. \tag{8.25}$$

If we instead keep the temperature finite but send $\nu \to 0$ we find

$$\chi(\nu \to 0, T) = \frac{\gamma\chi_c}{4} \frac{\log \frac{\Lambda}{T}}{1 + \frac{\gamma}{4} \log \frac{\Lambda}{T}}. \tag{8.26}$$

If we further take the low-T limit we find that

$$\chi(\nu \to 0, T \to 0) = \chi_c. \tag{8.27}$$

Therefore χ_c is the value of the static susceptibility at the BKT quantum critical point. Contrary to the predictions of the Ginzburg-Landau paradigm, the susceptibility stays finite at the phase transition. This is consistent with new types of quantum critical points introduced e.g. in Refs. [60, 207–210]. The quantum phase transition is however signaled by the derivatives of the susceptibility, which are the objects that actually encode quantum critical fluctuations. At low T, differentiation with respect to the tuning parameter gives

$$\partial_{\nu^2}\chi = -\chi_c \frac{2}{\nu\gamma(1 + 2\nu/\gamma)^3}, \tag{8.28}$$

which is indeed infinite at $\nu = 0$. We can alternatively determine the thermal-derivative. At $\nu = 0$ and finite T we get

$$\partial_T\chi = -4\gamma\chi_c \frac{1}{T(\gamma \log\left(\frac{\Lambda}{T}\right) + 4)^2}, \tag{8.29}$$

which also diverges as $T \to 0$.

Finally, we give the expression for the susceptibility at $\nu^2 > 0$. From Eq.(8.23) it follows that

$$\begin{aligned}\chi &= \gamma^2 \chi_c \frac{\Lambda^{2\nu} - T^{2\nu}}{(\gamma+2\nu)^2\Lambda^{2\nu} - (\gamma-2\nu)^2 T^{2\nu}} \\ &= \chi_c \cos\vartheta_0 \frac{\sinh\left(\nu \log\frac{\Lambda}{T}\right)}{\sinh\left(\nu\log\frac{\Lambda}{T} + 2\vartheta_0\right)},\end{aligned} \tag{8.30}$$

where again $\vartheta_0 = \operatorname{arctanh}(2\nu/\gamma)$. The denominator vanishes at a temperature given by $T^\star = \Lambda \exp\left(\frac{1}{\nu}\log\left(\frac{\gamma+2\nu}{\gamma-2\nu}\right)\right)$, which lies outside the regime of validity since it is much bigger than the upper cutoff Λ. We conclude that there is no phase transition at low temperatures in the $\nu^2 > 0$ side.

8.2.1 Phase diagram

In this section we utilize our findings to construct the phase diagram of the model. It is useful to consider a dimensionless susceptibility $\bar{\chi} = \chi/\chi_c$. As we found above, if $\nu^2 < 0$ there exists a critical temperature given in Eq.(8.20) that follows a BKT-type of scaling close to $\nu = 0$, whose full expression is

$$\frac{T_c}{\Lambda} = \exp\left(\frac{-\pi + 2\,\mathrm{atan}\left(2|\nu|/\gamma\right)}{|\nu|}\right). \tag{8.31}$$

The green area in Fig. 8.2 represents the condensed phase. As shown in Eq.(8.25), close to T_c the susceptibility follows a Curie-Weiss law $\bar{\chi}^{-1}_{\mathrm{CW}} \propto T - T_c$. Here we estimate the regime of validity of the Curie-Weiss formula using the criterion $|\bar{\chi}^{-1}_{\mathrm{CW},2} - \bar{\chi}^{-1}| < 10^{-1}$. Our result is marked red in Fig. 8.2.

Next we consider the side where $T_c = 0$ i.e. $\nu^2 > 0$. As stated in the previous section, the right object that capture the quantum critical behavior is not the susceptibility but its derivatives. For example, the thermal derivative is given by

$$\partial_T \bar{\chi} = -\frac{4\gamma\nu^2}{(\gamma^2-4\nu^2)^2} \frac{1}{T\sinh^2\left[\nu\log\frac{\Lambda}{T} + 2\mathrm{arctanh}\left(\frac{2\nu}{\gamma}\right)\right]}, \tag{8.32}$$

which can be exploited to estimate the crossover between the quantum-critical and the so-called quantum disordered behavior. Close to $\nu = 0$ $\partial_T\bar{\chi} \sim 1/T\log^2 T$. Such a quantum critical behavior persists as long as

$$\nu\log\frac{\Lambda}{T} + 2\mathrm{arctanh}\left(\frac{2\nu}{\gamma}\right) \ll 1. \tag{8.33}$$

For temperatures outside such a regime the system is no longer quantum-critical and crosses over to a quantum-disordered regime. This happens when $\frac{T^\star}{\Lambda} \sim \exp\left(\frac{-\pi+2\mathrm{atanh}(2\nu/\gamma)}{\nu}\right)$. Here we have added the factor π in order to parallel the scaling in Eq.(8.31). Close to the quantum critical point $\nu \to 0$ this gives rise again to a BKT-type of scaling. The quantum-disordered to quantum-critical crossover is represented by the dashed line in the phase diagram Fig. 8.2.

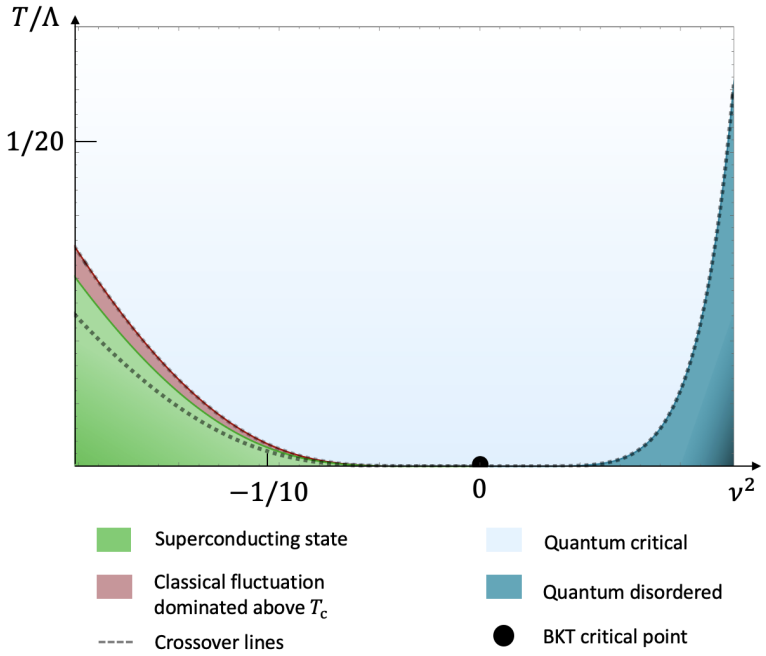

Figure 8.2: Phase diagram of the Yukawa-SYK model spanned by temperature T and distance from the critical point ν. The parameter ν can be tuned by acting on the pair-breaking parameter α. For $\nu^2 < 0$ the theory becomes superconducting as temperature is lowered. The green area represents the symmetry-broken state. In the red one, the pairing susceptibility diverges following a Curie-Weiss law and the system is governed by classical fluctuations. The dashed line in the superconducting phase denotes the same behavior. However, a quantitative estimation would require knowledge of the ordered state. At $\nu = 0$ the critical temperature vanishes following a BKT scaling. The point $\nu = 0$ is a quantum critical point where the pairing susceptibility does not diverge contrary to the MF paradigm. The milder transition is signaled by its derivatives, which we have used to estimate the crossover from the quantum critical to quantum disordered regime on the $\nu^2 > 0$ side. Figure re-adapted from Ref. [20].

8.3 Contact to holography

We conclude this chapter by highlighting two analogies between our findings and the holographic methods outlined at the beginning of this thesis. Specifically, we show that the differential gap-equation Eq.(8.13) coincides with those of a massive order parameter field in AdS_2, and that the static susceptibility of the SYK model takes the form of the matching expression discussed in Chap. 2. These two facts hint at an intimate connection between the quantum critical physics explained in these chapters and holographic superconductivity. The two methods should indeed describe the same physics. These arguments will be the base of the next two chapters where we will prove the equivalence of such theories.

8.3.1 Mapping to holography on the level of the equations

The differential Eliashberg equation Eq.(8.13) can be manipulated and re-expressed as

$$\partial_\epsilon \left(\epsilon^{1+\gamma}\partial_\epsilon \Phi(\epsilon)\right) = -\gamma \frac{p_\gamma}{\pi}\frac{\Phi(\epsilon)}{\epsilon^{1-\gamma}}, \tag{8.34}$$

with boundary conditions $\partial_\epsilon\Phi|_{\epsilon=\Lambda} = -\frac{\gamma}{\Lambda}(\Phi(\Lambda) - J_0)$, and $\partial_\epsilon\Phi|_{\epsilon=T} = 0$. Let us apply the following map

$$\tilde{\psi}(\epsilon) = c_\Phi \epsilon^{-y}\Phi(\epsilon), \quad z = \frac{c_z}{\bar{\epsilon}}\left(\frac{\bar{\epsilon}}{\epsilon}\right)^{2y+\gamma}, \tag{8.35}$$

where c_Φ and c_z are constants and $\bar{\epsilon}$ is a frequency scale that fixes the dimensions of the coordinate change. We obtain the following equation:

$$-\partial_z^2\tilde{\psi} - \frac{\nu^2 - 1/4}{z^2}\tilde{\psi} = 0, \tag{8.36}$$

where $\nu^2 = \frac{(p_\gamma/\pi + y)\gamma + y^2}{(2y+\gamma)^2} + \frac{1}{4}$. The solution is given by

$$\tilde{\psi}(z) = \tilde{A} z^{\frac{1}{2}-\nu} + \tilde{B} z^{\frac{1}{2}+\nu}. \tag{8.37}$$

The integration constants are fixed by the boundary conditions, which become

$$-(2y+\gamma) z_\Lambda^{\frac{y+\gamma}{2y+\gamma}}\partial_z\tilde{\psi}(z_\Lambda) + (y+\gamma) z_\Lambda^{-\frac{y}{2y+\gamma}}\tilde{\psi}(z_\Lambda) = \frac{c_\Phi \gamma J_0}{\bar{\epsilon}^{\frac{(2y+\gamma-1)y}{2y+\gamma}} c_z^{\frac{y}{2y+\gamma}}}, \quad \frac{\partial_z\tilde{\psi}(z_T)}{\tilde{\psi}(z_T)} = \frac{y}{2y+\gamma}\frac{1}{z_T},$$

with $z_T = z(T)$ and $z_\Lambda = z(\Lambda)$.
We have therefore identified a family of maps, parametrized by the exponent y, that leads to a Schroedinger problem for zero modes. Notice that the potential in Eq.(8.36) scales as $1/z^2$, a behavior typical of massive scalar fields in AdS_2 background, already encountered in Eq.(2.6) of Chap. 2. Eq.(8.36) holographically encodes the same physics of the Eliashberg gap-equation (8.34).

8.3.2 Near-far matching expression of the susceptibility

The static susceptibility Eq.(8.30) can be cast into the following form

$$\chi = \chi_c \frac{b_+ + b_- \mathcal{G}(T)\Lambda^{-2\nu}}{a_+ + a_- \mathcal{G}(T)\Lambda^{-2\nu}}, \tag{8.38}$$

with $\mathcal{G}(T) = \frac{2\nu-\gamma}{2\nu+\gamma} T^{2\nu}$, and $b_\pm = 1 \mp 2\nu/\gamma, a_\pm = (1 \mp 2\nu/\gamma)(1 \pm 2\nu/\gamma)^2$. This is precisely the form of the susceptibility as it occurs from the matching of AdS_4 to AdS_2 – see Eq.(2.15) of Chap.2. To make the contact to holography even stronger, we introduce the following quantities

$$\begin{aligned} b_\pm &= 1 \mp 2\nu/\gamma \equiv \beta \pm \widetilde{\beta}\nu, \\ a_\pm &= 1 \pm 2\nu/\gamma \equiv \alpha \pm \widetilde{\alpha}\nu, \\ 2\nu_U &= \frac{1}{\beta\widetilde{\alpha} - \widetilde{\beta}\alpha}. \end{aligned} \tag{8.39}$$

By construction we have $\beta = 1, \widetilde{\beta} = -2/\gamma, \alpha = 1, \widetilde{\alpha} = 2/\gamma$, and $2\nu_U = \gamma/4$.
With these notations Eq.(8.28) becomes $\partial_{\nu^2}\chi = -\chi_c \frac{1}{4\nu_U \alpha\beta} \frac{1}{\nu}$, which coincides exactly with Eqs.(7.7-7.8) of Ref. [60]. See also Ref. [169] for a broad study of the pairing response in different regimes.

8.4 Summary

In this chapter we have considered an extension of the Yukawa-SYK model of Chap. 6 which takes into account pair breaking effects. To test the pairing response of this model, in Sec. 8.1 we have considered and external pairing source and commented on the disorder-averaged effective action. This allowed us to compute the static pairing susceptibility analytically from the linearized gap-equation, and to extract the critical temperature for the superconducting phase transition. Remarkably, T_c is exponentially suppressed close to a critical value of the pair breaking parameter, which defines a quantum critical point of the BKT variety. In Sec. 8.2.1 we have constructed the phase diagram of the model which, in addition to the above mentioned superconducting phase transition, is characterized by a quantum-critical to quantum-disordered crossover. Finally, in Sec. 8.3 we have commented on the similarities that this analysis shares with holography. In particular, we have shown that (i) the linearized gap-equation can be mapped onto the equation of motion for a holographic order parameter field in AdS_2 space, and (ii) the static pairing susceptibility of SYK assumes the matching form typical of holography as reviewed in Chap. 2. The findings of this section are indications that quantum critical Eliashberg theory and holography might be equivalent in the description of superconducting order parameter condensation and the response to an external pairing field. In the next chapter we show the equivalence of these two theories on the level of the action.

Couplings probability distribution function with pair-breaking

$$\begin{aligned}\overline{g'_{ijk}g'_{i'j'k'}} &= \left(1-\frac{\alpha}{2}\right)\frac{\bar{g}^2}{2N^2}\delta_{kk'}\left(\delta_{ii'}\delta_{jj'}+\delta_{ij'}\delta_{ji'}\right)\\ \overline{g''_{ijk}g''_{i'j'k'}} &= \frac{\alpha}{2}\frac{\bar{g}^2}{2N^2}\delta_{kk'}\left(\delta_{ii'}\delta_{jj'}-\delta_{ij'}\delta_{ji'}\right)\end{aligned}$$

Effective action

$$\begin{aligned}\frac{S^{\text{eff}}}{N} &= -\mathrm{Tr}\log\left(\hat{G}_0^{-1}-\hat{\Sigma}\right)+\frac{M}{2N}\mathrm{Tr}\log\left(D_0^{-1}-\Pi\right)\\ &\quad -2\int d\tau d\tau' G(\tau',\tau)\Sigma(\tau,\tau')+\frac{M}{2N}\int d\tau d\tau' D(\tau',\tau)\Pi(\tau,\tau')\\ &\quad -\int d\tau d\tau'\left(F(\tau'\tau)\Phi^\dagger(\tau,\tau')+F^\dagger(\tau'\tau)\Phi(\tau,\tau')\right)\\ &\quad +\bar{g}^2\frac{M}{2N}\int d\tau d\tau'\left(G(\tau,\tau')G(\tau',\tau)-(1-\alpha)F^\dagger(\tau,\tau')F(\tau',\tau)\right)D(\tau,\tau')\\ &\quad -\int d\tau J_0(\tau)\left(F(\tau,\tau)+F^\dagger(\tau,\tau)\right)\end{aligned}$$

Static pairing susceptibility

$$\chi=\gamma^2\chi_{\mathrm{c}}\frac{\Lambda^{2\nu}-T^{2\nu}}{(\gamma+2\nu)^2\Lambda^{2\nu}-(\gamma-2\nu)^2T^{2\nu}}$$

$\chi_{\mathrm{c}}=2c_g^2(1+\tan^2\theta)\Lambda^\gamma/\pi\gamma$

Critical temperature

$$\frac{T_{\mathrm{c}}}{\Lambda}=\exp\left(\frac{-\pi+2\mathrm{atan}(2|\nu|/\gamma)}{|\nu|}\right) \tag{8.40}$$

Recap Box – Pairing response of the Yukawa-SYK model

Chapter 9

Gravitational dual of the superconducting state

In this chapter we analyze superconducting fluctuations of the Yukawa-SYK model in the low-energy, quantum critical regime. Starting from the effective action Eq.(8.2), we focus on the superconducting degrees of freedom and perform an expansion with respect to bi-local pairing fields F and Φ to quadratic order. The subsequent analysis is based on Ref. [20].

9.1 From SYK to holography

From the action Eq.(8.2) we have

$$\begin{aligned}\frac{S_{\rm sc}}{N} &= -\mathrm{Tr}\log\left(\hat{G}_0^{-1}-\hat{\Sigma}\right)-\frac{\bar{g}^2\lambda_p}{2}\int d\tau^2\, F^\dagger(\tau,\tau')F(\tau',\tau)D(\tau,\tau') \\ &- \int d\tau^2\,\left(F(\tau'\tau)\Phi^\dagger(\tau,\tau')+F^\dagger(\tau'\tau)\Phi(\tau,\tau')\right). \end{aligned} \tag{9.1}$$

Let us focus on the the trace-log term. To set up the expansion, we separate the superconducting degrees of freedom from the normal ones by introducing the following quantities

$$\hat{\mathcal{G}}^{-1} \equiv \hat{G}_0^{-1}-\begin{pmatrix}\Sigma_{\rm n} & 0\\ 0 & \widetilde{\Sigma}_{\rm n}\end{pmatrix}\equiv\begin{pmatrix}G_{\rm n}^{-1} & 0\\ 0 & \widetilde{G}_{\rm n}\end{pmatrix}, \tag{9.2}$$

$$\hat{\mathcal{S}} \equiv \begin{pmatrix}0 & \Phi\\ \Phi^\dagger & 0\end{pmatrix}=\begin{pmatrix}0 & \Phi(\tau,\tau')\\ \Phi^\star(\tau',\tau) & 0\end{pmatrix}, \tag{9.3}$$

where the normal state propagator depends on times difference, i.e. $G_{\rm n}(\tau,\tau')=G_{\rm n}(\tau-\tau')$, and $\widetilde{G}_{\rm n}(\tau_1,\tau_2)=-G_{\rm n}(\tau_2,\tau_1)$. Close to the superconducting phase transition, Φ is small and we can perform an expansion. This gives

$$\mathrm{Tr}\log\left(\hat{G}_0^{-1}-\hat{\Sigma}\right)\approx \mathrm{Tr}\hat{\mathcal{G}}^{-1}-\mathrm{Tr}\,\hat{\mathcal{G}}\hat{\mathcal{S}}-\frac{1}{2}\mathrm{Tr}\,\hat{\mathcal{G}}\hat{\mathcal{S}}\hat{\mathcal{G}}\hat{\mathcal{S}}. \tag{9.4}$$

It is easy to show that the linear term yields no contribution, i.e. $\mathrm{Tr}\,\hat{\mathcal{G}}\hat{\mathcal{S}} = 0$. The quadratic term is instead given by $\mathrm{Tr}\hat{\mathcal{G}}\hat{\mathcal{S}}\hat{\mathcal{G}}\hat{\mathcal{S}}{=}2\widetilde{G}_{\mathrm{n}} \otimes \Phi^{\dagger} \otimes G_{\mathrm{n}} \otimes \Phi$, where we used the cyclic property of the trace. The action up to second order in Φ is then given by:

$$S^{(\mathrm{sc})} \approx \widetilde{G}_{\mathrm{n}} \otimes \Phi^{\dagger} \otimes G_{\mathrm{n}} \otimes \Phi - \frac{\bar{g}^2\lambda_p}{2}(F^{\dagger}F) \otimes D_{\mathrm{n}} - F^{\dagger} \otimes \Phi - F \otimes \Phi^{\dagger}, \tag{9.5}$$

where we have used the following notation for the trace in time sub-space: $M \otimes N = \int d^2\tau M(\tau,\tau')N(\tau',\tau)$. Since the above action is quadratic in Φ, we can perform Gaussian integration. To this end, it is easiest to move to frequencies space via Fourier transformation. However, the composite field Φ depends on two time variables τ and τ', out of which we can construct the physical absolute and relative times $\frac{\tau+\tau'}{2}$ and $\tau - \tau'$ respectively. The former describes the evolution of the entire system, the latter is connected to the internal dynamics. The resulting action reads

$$\boxed{\frac{S^{(\mathrm{sc})}}{N} = \int_{\omega,\epsilon} \frac{F^{\star}(\omega,\epsilon)\,F(\omega,\epsilon)}{\Pi(\omega,\epsilon)} - \frac{\bar{g}^2\lambda_p}{2}\int_{\omega,\epsilon\epsilon'} F^{\star}(\omega,\epsilon)\,D_{\mathrm{n}}(\epsilon-\epsilon')F(\omega,\epsilon').} \tag{9.6}$$

See appendix E for details on the derivation. In the above expression we have defined the following fermion-fermion bubble

$$\Pi(\omega,\epsilon) = G_{\mathrm{n}}\Big(\frac{\omega}{2} - \epsilon\Big)G_{\mathrm{n}}\Big(\frac{\omega}{2} + \epsilon\Big). \tag{9.7}$$

To make contact with the previous chapters we consider the $\omega = 0$ saddle point-equation, $F(\epsilon) = \Pi(\epsilon)\frac{\bar{g}^2\lambda_p}{2}\int_{\epsilon'} F(\epsilon')D_{\mathrm{n}}(\epsilon-\epsilon')$. Re-introducing the anomalous self energy $F(\epsilon) = \Pi(\epsilon)\Phi(\epsilon)$ we obtain precisely the sourceless linearized Eliashberg gap-equation (8.6).

Our next goal is to manipulate the above action and to derive those of a holographic scalar field. With Eq.(8.35) we have mapped the Eliashberg gap-equation to the equation for a scalar field in AdS_2. The key idea is to consider the analogue of Eq.(8.35) with $y = (1-\gamma)/2$ for the field F:

$$\tilde{\psi}(\omega,z) = c_F z^{\frac{\gamma-1}{2}} F(\omega, c_z z^{-1}), \tag{9.8}$$

where c_z and c_F are two constants that will be essential to correctly perform the matching to holography and are specified in Eq.(E.28) of appendix E. The derivation is rather technical and the interested reader can find all the details in appendix E.2. The main outcome relies in the following expression

$$\boxed{\frac{S^{(\mathrm{sc})}}{N} = \int_{z,t}\Big(|\partial_z\tilde{\psi}|^2 - |\partial_t\tilde{\psi}|^2 + \frac{m^2}{z^2}|\tilde{\psi}|^2\Big).} \tag{9.9}$$

This is the action of a free massive scalar field in Lorentian de-Sitter space in 2 dimensions (dS_2) with metric $ds^2_{\mathrm{dS}_2} = \frac{dt^2-dz^2}{z^2}$, and mass $m^2 = \frac{1}{b_\gamma}\Big(\frac{2\pi C_\gamma}{\lambda_p} - a_\gamma\Big) - \frac{1}{4}$. The parameters a_γ and b_γ are given in Eq.(E.22) of appendix E.2 and C_γ follows from the fact that we had to employ the quantum critical SYK form for the normal state propagators Eq.(6.20) to derive the above result.

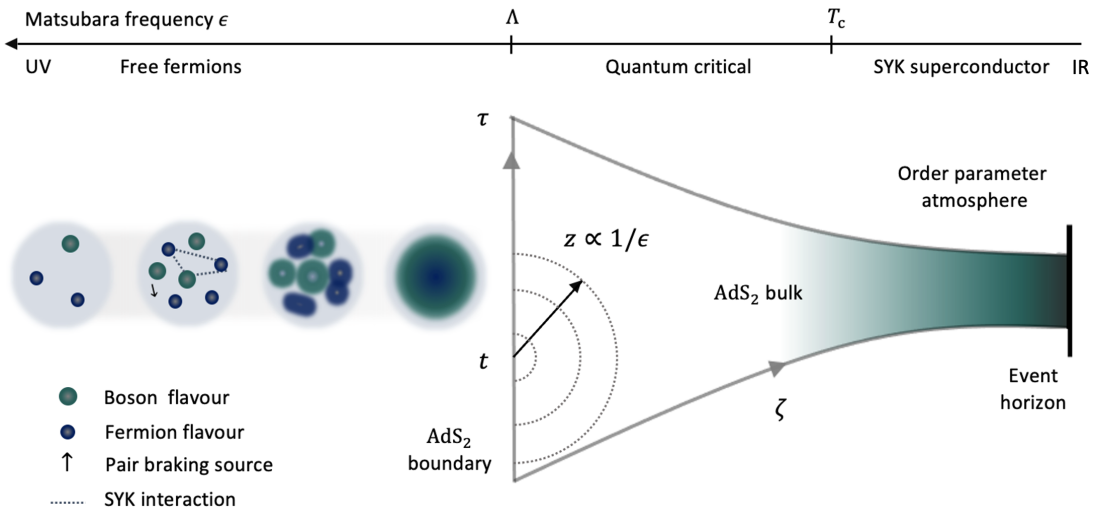

Figure 9.1: The emergence of the dual holographic theory from the SYK superconductor. Below the UV scale Λ, a strongly coupled quantum-critical fluid forms out of interacting fermions and bosons. Below this scale the fluctuating order parameter becomes a scalar field with emergent AdS_2 gravity and forms an atmosphere around a black hole event horizon. The frequency ω of the relative time $\tau_1 - \tau_2$ and the absolute time $t = (\tau_1 + \tau_2)/2$ of SYK pairing fields $F(\tau_1, \tau_2) = \frac{1}{N}\sum_{i=1}^{N} c_{i\uparrow}(\tau_1)\, c_{i\downarrow}(\tau_2)$ determine the set of geodesic half circles that span the anti-de-Sitter space (τ, ζ) on the gravity side. Figure and caption adapted from Ref. [20].

Let us momentarily ignore the temporal part. As reviewed in the first chapters of this thesis Sec. 1.2.1, the instability holographycally sets in at $m^2 = m_{\mathrm{BF}}^2 = -1/4$. This means

$$1 = \frac{\lambda_p}{2\pi C_\gamma} a_\gamma = \frac{\lambda_p}{2\pi C_\gamma} r_{\xi=0}, \tag{9.10}$$

where we made use of the integral r_ξ Eq.(E.19). This correctly reproduces the condition that comes from Eq.(8.10) after setting $\nu = 0$.

In order to flip the minus sign in front of the time-derivative term of Eq.(9.9) and consequently obtain an action in anti-de-Sitter background, the map Eq.(9.8) needs to be further generalized. To this end, we introduce a circular Radon transformation as a map of functions from Euclidean AdS_2 to Lorentzian dS_2:

$$\tilde{\psi}(y) = \int_\gamma ds\, \psi(x(s)). \tag{9.11}$$

Here $\tilde{\psi}$ corresponds to an integration over a geodesic $\gamma(y)$ in AdS_2, parametrized by coordinates $y = (t, z)$ of dS_2, whereas $x = (\tau, \zeta)$ denotes those in AdS_2. The key property of Eq.(9.11) is the sign-flipping in the Laplace operator

$$\Box_{dS_2}\tilde{\psi} = -\widetilde{\Box_{AdS_2}\psi}, \tag{9.12}$$

where $\Box_{\mathrm{dS}_2} = z^2(\partial_t^2 - \partial_z^2)$ and $\Box_{\mathrm{AdS}_2} = \zeta^2(\partial_\tau^2 + \partial_\zeta^2)$. As carefully reviewed in appendix F, this also flips the sign of the time-gradient yielding

$$\frac{S^{(\mathrm{sc})}}{N} = \int_{\zeta,\tau} \left(|\partial_\zeta \psi|^2 + |\partial_\tau \psi|^2 + \frac{m^2}{\zeta^2} |\tilde{\psi}|^2 \right). \tag{9.13}$$

This is the action of a massive scalar field in AdS_2 background. As we have seen above, the condition for superconducting instability of Eliashberg theory correctly maps into the holographic one $m^2 = m_{\mathrm{BF}}^2$. See Fig.9.1 for a sketch of the mapping to holography of the SYK-Eliashberg theory. In the following we extend such a mapping to finite temperature and chemical potential.

9.2 Beyond $\mu = T = 0$

So far, we carried out the analysis in the strict $\mu = T = 0$ limit. In this section we generalize our mapping to encode finite temperature and chemical potential. The main result will be the extension of Eq.(9.13) to the action of a holographic order parameter field in charged black hole background.

9.2.1 Holographic map at finite temperature

We start by working at $\mu = 0$. Below we follow the procedure sketched in Fig.9.2.
Let us consider the finite temperature analogue of the superconducting action Eq.(9.5)

$$\frac{S^{(\mathrm{sc})}}{N} = \Phi^\dagger \otimes_T G_{\mathrm{n}}^T \otimes_T \Phi \otimes_T G_{\mathrm{n}}^T - \frac{\bar{g}^2 \lambda_p}{2} (F^\dagger F) \otimes_T D_{\mathrm{n}}^T - F^\dagger \otimes_T \Phi - F \otimes_T \Phi^\dagger, \tag{9.14}$$

where G_{n}^T and D_{n}^T are the finite-temperature propagators of the normal state. These can be obtained from the zero-temperature ones by using the invariance at low energies of the saddle-point equations under time reparametrization $\tau \to \bar{\tau} = g(\tau)$. Specifically:

$$G_{\mathrm{n}}^T(\tau, \tau') = g'(\tau)^{\frac{1+\gamma}{4}} G_{\mathrm{n}}(g(\tau) - g(\tau')) g'(\tau')^{\frac{1+\gamma}{4}}, \tag{9.15a}$$

$$D_{\mathrm{n}}^T(\tau, \tau') = g'(\tau)^{\frac{1-\gamma}{2}} D_{\mathrm{n}}(g(\tau) - g(\tau')) g'(\tau')^{\frac{1-\gamma}{2}}, \tag{9.15b}$$

where $g(\tau) = \frac{\beta}{\pi} \tan(\pi\tau/\beta)$. See Sec. 2.3 for details.
The imaginary time is now limited by temperature as $-\frac{\beta}{2} < \tau < \frac{\beta}{2}$, with $\beta = 1/T$. Consequently, we generalize our previous convention on imaginary time trace with $M \otimes_T N = \int_{\beta/2}^{-\beta/2} d^2\tau M(\tau, \tau') N(\tau', \tau)$. Let us analyze the following term

$$(F^\dagger F) \otimes_T D_{\mathrm{n}}^T = \int_{-\frac{\beta}{2}}^{\frac{\beta}{2}} d^2\tau F^\star(\tau', \tau) F(\tau, \tau) D_{\mathrm{n}}^T(\tau, \tau') = (\bar{F}^\dagger \bar{F}) \otimes D_{\mathrm{n}}, \tag{9.16}$$

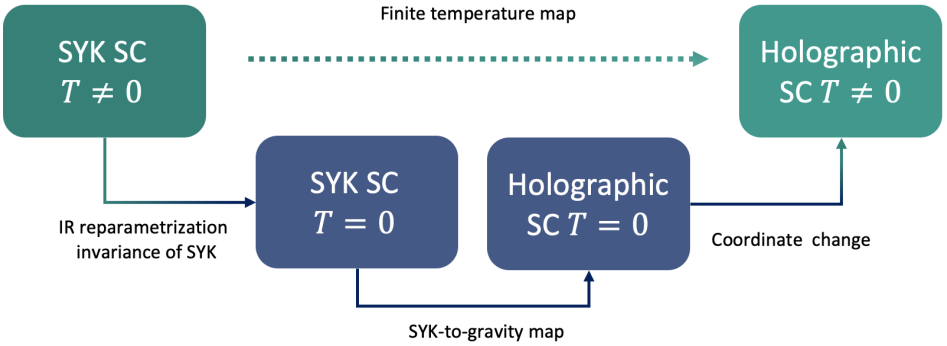

Figure 9.2: Diagram of the procedure to extend the holographic map to finite temperatures. We first relate the finite-temperature SYK propagators to the $T = 0$ ones by using the low-energy reparametrization invariance. We then utilize our known result to map the SYK action into the holographic one. We finally switch on temperature in the AdS_2 background by appropriate coordinate change.

where we have introduced $\bar{F}(\bar{\tau}, \bar{\tau}') = (1 + (\pi T)^2 \bar{\tau}^2)^{-\frac{1+\gamma}{4}} F(g^{-1}(\bar{\tau}), g^{-1}(\bar{\tau}'))(1 + (\pi T)^2 \bar{\tau}'^2)^{-\frac{1+\gamma}{4}}$. It similarly follows that

$$\begin{aligned} F^\dagger \otimes_T \Phi &= \bar{F}^\dagger \otimes \bar{\Phi}, \\ \Phi^\dagger \otimes_T G_{\mathrm{n}}^T \otimes_T \Phi \otimes_T G_{\mathrm{n}}^T &= \bar{\Phi}^\dagger \otimes G_{\mathrm{n}} \otimes \bar{\Phi} \otimes G_{\mathrm{n}}, \end{aligned} \tag{9.17}$$

with $\bar{\Phi}(\bar{\tau}, \bar{\tau}') = (1 + (\pi T)^2 \bar{\tau}^2)^{\frac{1+\gamma}{4}} \Phi(g^{-1}(\bar{\tau}), g^{-1}(\bar{\tau}'))(1 + (\pi T)^2 \bar{\tau}'^2)^{\frac{1+\gamma}{4}}$. The resulting action is then identical to the $T = 0$ one provided that we replace the superconducting degrees of freedom appropriately, i.e. $F \mapsto \bar{F}$ etc. We now apply the findings of the previous sections and introduce the gravity field according to Eq.(9.8) but this time in terms of the function $\bar{F}$ instead of F and with transformed variables $\bar{\tau}, \bar{\tau}'$ instead of τ, τ':

$$\tilde{\psi}(\bar{t}, \bar{z}) = c_F |\bar{z}|^{\frac{1-\gamma}{2}} \int_{-\infty}^{\infty} ds \bar{F}(t_+, t_-) e^{i c_z s/\bar{z}}. \tag{9.18}$$

Here $t_\pm = \bar{t} \pm \frac{s}{2}$. If we now apply the Radon transformation Eq.(9.11) to $\tilde{\psi}(\bar{t}, \bar{z})$, we get an action for a massive scalar $\psi(\bar{\tau}, \bar{\zeta})$ in $T = 0$ AdS_2 background. We finally turn temperature on again to obtain a gravity action in AdS_2-black hole background described by the following metric

$$ds^2 = \frac{1}{\zeta^2}\left(f_2(\zeta) d\tau^2 + \frac{d\zeta^2}{f_2(\zeta)}\right), \tag{9.19}$$

with blackening function $f_2(\zeta) = 1 - \zeta^2/\zeta_T^2$. Here $\zeta_T^{-1} = 2\pi T$ is the location of the even horizon that sets the temperature as outlined in Sec. 1.1.2. This scenario can be achieved through the following coordinate change $(\bar{\zeta}, \bar{\tau}) \mapsto (\zeta, \tau)$

$$\bar{\tau} = 2\zeta_T \frac{\sqrt{f_2(\zeta)} \sin\left(\tau/\zeta_T\right)}{1 + \sqrt{f_2(\zeta)} \cos\left(\tau/\zeta_T\right)}, \quad \bar{\zeta} = \frac{2\zeta}{1 + \sqrt{f_2(\zeta)} \cos\left(\tau/\zeta_T\right)}, \tag{9.20}$$

where now $0 < \tau < 1/T$ – see Refs. [55, 185] for details. This expression agrees at the boundary with the original imaginary variables of the SYK model [55]. The action of the SYK superconductor then becomes

$$\frac{S^{(\mathrm{sc})}}{N} = \int_0^{\zeta_T} d\zeta \int_{-\beta/2}^{\beta/2} d\tau \left(\frac{|\partial_\tau \psi|^2}{f_2(\zeta)} + f_2(\zeta) |\partial_\zeta \psi|^2 + \frac{m^2}{\zeta^2} |\psi|^2 \right), \tag{9.21}$$

which is precisely the holographic superconductor action at finite temperature.

9.2.2 Holographic map at finite chemical potential

In addition to the invariance under time re-parametrizations, the saddle point enjoys a $U(1)$ emergent symmetry in the infrared. In particular, the fermionic propagator at finite chemical potential can be obtained from Eq.(9.15) via

$$G_{\mathrm{n}}^{T,\mu}(\tau,\tau') \;=\; \frac{h(\tau')}{h(\tau)} G_{\mathrm{n}}^{T}(\tau,\tau'), \tag{9.22}$$

where G_{n}^{T} corresponds to the case at particle-hole symmetry. See Sec. 2.3 for details. Here h is an arbitrary function representing $U(1)$ transformations. Here we focus on

$$h(\tau) = e^{-2\pi q \mathcal{E} T \tau}, \tag{9.23}$$

where q is the fermionic charge, and $\mathcal{E}$ is the spectral asymmetry – see Refs. [55, 71, 185] and Sec. 2.3. Notice that $h(\tau)$ becomes a genuine $U(1)$ transformation once we return to real times $\tau = -it$. Normal-state propagators depend on time difference. Therefore, setting $\tau' = 0$ gives

$$G_{\mathrm{n}}^{T,\mu}(\tau) = e^{2\pi q \mathcal{E} T \tau} G_{\mathrm{n}}^{T}(\tau). \tag{9.24}$$

As function of the Matsubara frequencies, this implies

$$G_{\mathrm{n}}^{T,\mu}(\omega_n) = \int_0^\beta d\tau G_{\mathrm{n}}^{T,\mu}(\tau) e^{i\omega_n \tau} = G_{\mathrm{n}}^{T}(\omega_n - i2\pi q \mathcal{E} T). \tag{9.25}$$

As a consequence, the $T, \mu \neq 0$ analogue of the particle-particle bubble Eq.(9.7) reads $\Pi^{T,\mu}(\omega_m, \epsilon_n) = \Pi^{T}(\omega_m - i4\pi q \mathcal{E} T, \epsilon_n)$. On the real axis this corresponds to

$$\Pi_{\mathbb{R}}^{T,\mu}(\omega, \epsilon) = \Pi^{T}(\omega + 4\pi q \mathcal{E} T, \epsilon), \tag{9.26}$$

where we have performed the analytic continuations $i\omega_m \mapsto \omega + i0^+$ and $i\epsilon_n \mapsto \epsilon + i0^+$. We thus have learned that, in order to switch-on a finite chemical potential, it is sufficient to shift the absolute frequency by

$$\omega \mapsto \omega + 4\pi q \mathcal{E} T. \tag{9.27}$$

This finding parallels the holographic results of Ref. [47]. Consider a scalar particle with charge $q^\star$ in AdS_2 with a gauge-field

$$A_t = \frac{E}{\zeta}\left(1 - \frac{\zeta}{\zeta_T}\right). \tag{9.28}$$

Within the gauge $A_\zeta = 0$, this corresponds to a boundary electric field E. See also Sec. 2.1 for details. In addition, from Eq.(2.11), it follows that the particle-propagator can be obtained from the neutral one by shifting the frequency via

$$\omega \to \omega + 2\pi q^* ET. \tag{9.29}$$

Comparing this with Eq.(9.27), we can conclude that the boundary electric field E is determined by the spectral asymmetry $\mathcal{E}$ of the SYK model with effective charge $q^\star = 2q$ of the Cooper pair.

9.3 Summary

In this chapter we have manipulated the SYK action introduced in Chap. 8, and developed an effective theory around the BKT quantum critical point. We have demonstrated that it is given by the action of a holographic superconductor in AdS_2. There is a one-to-one correspondence between the parameters of the microscopic theory and those of gravity. In Sec. 9.2 we have extended such a map to finite temperature and density. Superconducting degrees of freedom of the SYK model behave like a charge $2q$ matter field with mass m on the AdS_2 background. The finite temperature theory is equivalent to a change of coordinates that corresponds to a black hole with event horizon given by the Hawking temperature. Deviations of the density from half filling give rise to a boundary electric field $\mathcal{E}$. The competition between suppressed pairing due to the absence of quasi-particles and the enhanced, singular pairing interaction is merely a balance of two contributions to the mass m.

Superconducting action

$$\frac{S^{(\mathrm{sc})}}{N} = \int_{\omega,\epsilon} \frac{F^{\star}\left(\omega,\epsilon\right) F\left(\omega,\epsilon\right)}{\Pi(\omega,\epsilon)} - \frac{\bar{g}^2\lambda_p}{2} \int_{\omega,\epsilon\epsilon'} F^{\star}\left(\omega,\epsilon\right) D_{\mathrm{n}}(\epsilon-\epsilon') F(\omega,\epsilon')$$

Fermion-fermion bubble

$$\Pi(\omega,\epsilon) = G_{\mathrm{n}}\Big(\frac{\omega}{2}-\epsilon\Big) G_{\mathrm{n}}\Big(\frac{\omega}{2}+\epsilon\Big)$$

Eliashberg-to-holography map

$$\tilde{\psi}(\omega,z) = c_F z^{\frac{\gamma-1}{2}} F(\omega, c_z z^{-1})$$

Mass squared relation

$$m^2 \;=\; \frac{1}{b_\gamma}\left(\frac{2\pi C_\gamma}{\lambda_p} - a_\gamma\right) - \frac{1}{4}$$

Radon-transform

$$\tilde{\psi}(z,t) = 2z \int_{t-z}^{t+z} d\tau \int_0^\infty \frac{dz}{\zeta} \delta\left(z^2 - (\tau-t)^2 - \zeta^2\right) \psi(\zeta,\tau)$$

Recap Box – Holographic mapping

New Entries of the Holographic Dictionary

Field-theory side	Gravity side
Frequency ϵ of time lag $\tau_1 - \tau_2$	Holographic dimension ζ
Absolute time $(\tau_1+\tau_2)/2$	Time (Euclidean) τ
Anomalous propagator F	Order parameter field ψ
Fermion bubble $\Pi_{\mathrm{n}}(\omega,\epsilon)$	$\partial_\tau\psi$, mass contrib. $m^2_{(1)} > 0$
Pairing interaction $D_{\mathrm{n}}(\epsilon)$	$\partial_\zeta\psi$, mass contrib. $m^2_{(2)} < 0$
Cooper pair charge $2q$	condensate charge $q_\star$
Spectral asymmetry $\mathcal{E}$	AdS_2 electric field E

10 Chapter 10
Dynamical pairing susceptibility

Note however the different normalization needed to match the static limit $\omega \to 0$, i.e. $\mathcal{G}(T, \omega \to 0) = \mathcal{G}(T)$.

Explicitly, the susceptibility Eq.(**??**) is given by

$$\chi(\omega, T) \quad = \gamma^2 \quad \chi_c \frac{\frac{1}{(\gamma+2\nu)^2}\left(\frac{T}{\Lambda}\right)^{-\nu} F_{-\nu,q^\star}(T/\omega) - \frac{1}{(\gamma-2\nu)^2}\left(\frac{T}{\Lambda}\right)^{\nu} F_{\nu,q^\star}(T/\omega)}{\left(\frac{T}{\Lambda}\right)^{-\nu} F_{-\nu,q^\star}(T/\omega) + \left(\frac{T}{\Lambda}\right)^{\nu} F_{\nu,q^\star}(T/\omega)},$$

where we have introduced the auxiliary function $F_{\nu,q^\star}(T/\omega) = (\gamma - 2\nu)^2 \Gamma(\frac{1}{2} - \nu + iq^\star)\Gamma(\frac{1}{2} + \nu + iq^\star - \frac{i\omega}{2\pi T})$. For small ν it holds that

$$\frac{F_{\nu,q^\star}(T/\omega)}{\gamma^2 \Gamma\left(iq^\star + \frac{1}{2}\right)\Gamma\left(iq^\star + \frac{1}{2} - \frac{i\omega}{2\pi T}\right)} \approx e^{(\theta(\omega/T) - 4/\gamma)\nu} + O(\nu^2), \tag{10.1}$$

with $\theta(\omega/T) = \psi^{(0)}\left(iq^\star + \frac{1}{2} - \frac{i\omega}{2\pi T}\right) - \psi^{(0)}\left(iq^\star + \frac{1}{2}\right)$ and $\psi^{(0)}$ is the digamma function. With this expression at hand we can re-write the susceptibility as

$$\chi(\omega, T) = \chi_c \frac{\sinh\left[\nu \log\left(\frac{T}{\Lambda} e^{\theta(\omega/T)}\right)\right]}{\sinh\left[\nu \log\left(\frac{T}{\Lambda} e^{\theta(\omega/T) - \frac{4}{\gamma}}\right)\right]}. \tag{10.2}$$

The above expression is plotted in Fig.10.1 as function of the distance from the critical point ν and of frequency ω. Qualitatively, we notice an almost flat behavior close to $\nu = 0$. Below we derive the explicit expression for real and imaginary part at low temperature and at neutrality. At the low temperatures ($T \ll \omega$) it holds that $\theta(\omega) \approx -\psi^{(0)}\left(\frac{1}{2} + iq^\star\right) + \log\left(\frac{\omega}{2\pi T}\right) - \frac{i\pi}{2}$, where we have used the expansion $\psi^{(0)}(\alpha - ix) \approx \log x - \frac{i\pi}{2}$ valid for $x \to \infty$ and $\alpha \in \mathbb{C}$. As a result, the $T = 0$ susceptibility reads

$$\chi(\omega, T = 0) = \chi_c \frac{\sinh\left[\nu \log\left(\frac{-i\omega}{2\pi\Lambda} e^{\theta_0}\right)\right]}{\sinh\left[\nu \log\left(\frac{-i\omega}{2\pi\Lambda} e^{\theta_0 - 4/\gamma}\right)\right]}, \tag{10.3}$$

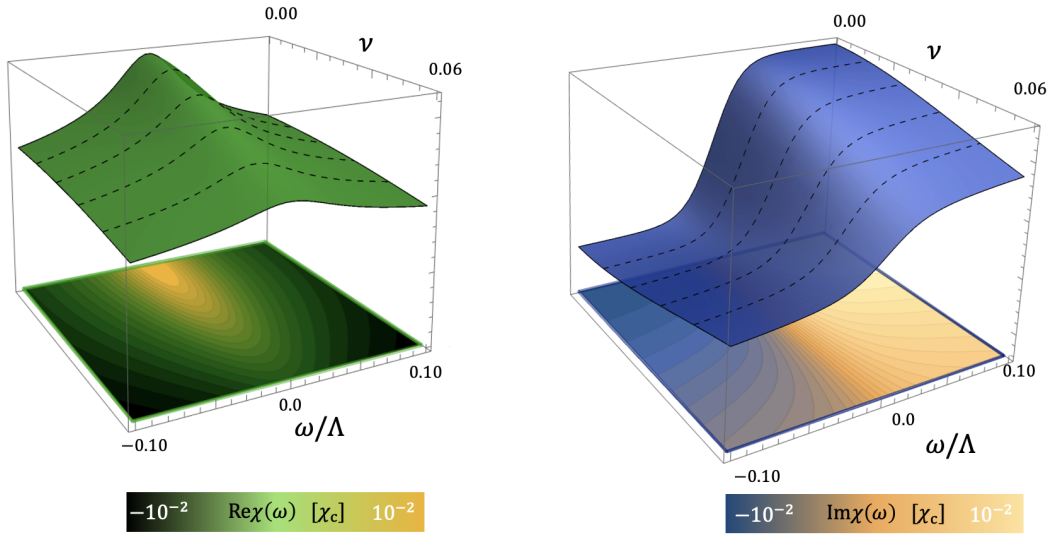

Figure 10.1: 3D plot of the real and imaginary part of the pairing susceptibility versus distance from the critical point ν and absolute frequency ω and at charge neutrality. Temperature is $T/\Lambda = 10^{-2}$ and anomalous dimension is $\gamma = 0.01$ ($\Delta = 0.2525$).

where we have defined $\theta_0 \equiv -\psi^{(0)}\left(\frac{1}{2} + iq^\star\right)$. Notice that in the condensed phase $\nu = i\sqrt{-u}$ is imaginary, and the denominator becomes a sin and gives a geometric series of poles in the upper-half complex frequency-plane at $\omega^{(n)} = 2\pi i\Lambda e^{-\frac{n\pi}{\sqrt{-u}}+\theta_0} \approx 2\pi i\Lambda e^{-\frac{n\pi}{\sqrt{-u}}}$ in accord with Refs. [59, 60].
Close to $\nu = 0$ we have

$$\frac{\mathrm{Im}\chi_{\nu=0}(\omega)}{\chi_c} = \frac{8\pi\gamma}{\pi^2\gamma^2 + (\gamma Y(\omega) - 8)^2}, \quad \frac{\mathrm{Re}\chi_{\nu=0}(\omega)}{\chi_c} = \frac{8(\gamma Y(\omega) - 8)}{\pi^2\gamma^2 + (\gamma Y(\omega) - 8)^2} + 1, \tag{10.4}$$

where $Y(\omega) = 2\log(2\omega/\Lambda\pi) + 2\gamma$. At lowest frequencies the imaginary part hence decays as $1/\log^2(\omega/\Lambda)$ while the real one as $1/\log(\omega/\Lambda)$. In Fig.10.2 we plot slices at constant ν. At zero temperature, both the imaginary and real parts are discontinuous as signaled by the ω-derivative. From Eq.(10.3), we know that at lowest frequencies and close to the critical point this is given by $\partial_\omega\chi \approx -\frac{16\chi_c\nu^2}{\gamma}\frac{\Lambda}{\omega}$. Notice that at $\nu = 0$ it vanishes for all frequencies, in accordance with the finiteness of χ at the quantum phase transition. As shown in Fig.10.2, the singular behavior is smoothened by finite temperature.

As we can observe in e.g. Fig.10.2, the charge neutral case exhibits a spectral symmetry. It is hence interesting to consider deviations from half filling. Even though the Cooper pair condensate does not have to respect any symmetry, this is often the case as dynamics is mostly governed by particle-hole excitations which are globally charge-neutral objects. In Fig.10.3 we plot the dynamic susceptibility for different values of the condensate charge. Deviations from half filling

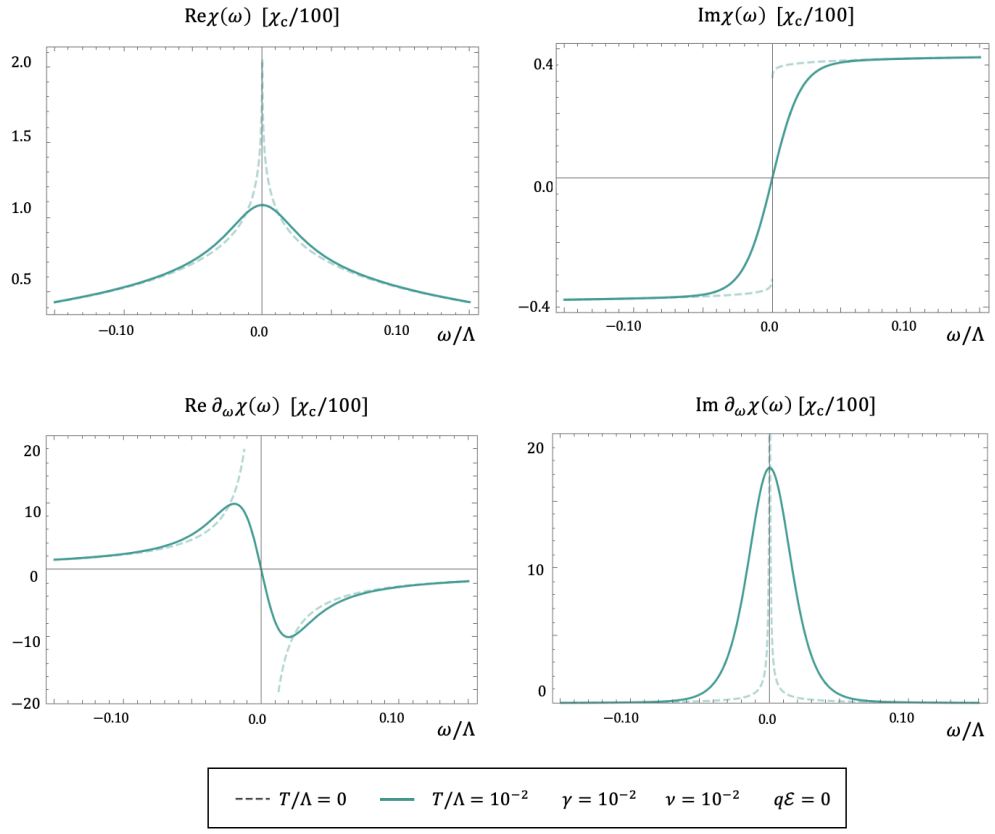

Figure 10.2: Real and imaginary part of the dynamic susceptibility (upper row) and their ω-derivatives (lower row) at different values of temperature and at charge neutrality. The anomalous dimension is $\gamma = 0.01$ ($\Delta = 0.2525$), the distance from the critical point is $\nu = 0.01$.

destroy the spectral symmetry, in contrast with the conventional BCS behavior

Finally, as can be seen in Fig.10.4, the slope of the imaginary part diverges as we get closer to T_c from above. At low frequencies, the susceptibility is well approximated by the function

$$\chi(\omega) = \frac{A_0}{\tau^{-1} - i\text{sign}(\omega)|\omega|} \rightarrow \text{Im}\chi(\omega) = A_0 \frac{\text{sign}(\omega)|\omega|}{\tau^{-2} + |\omega|^2}. \tag{10.5}$$

Here τ is a typical time-scale that describes order parameter relaxation. It holds that $\tau = \partial_\omega \chi''(\omega = 0)$. As shown in the inner panel of Fig. 10.4, τ^{-1} vanishes linearly as function of the reduced temperature $T - T_c$. As we approach the phase transition, the system need more time to come back to the equilibrium configuration after a small perturbation. This phenomenon is known as *critical slowing down* – see e.g. Ref. [211].

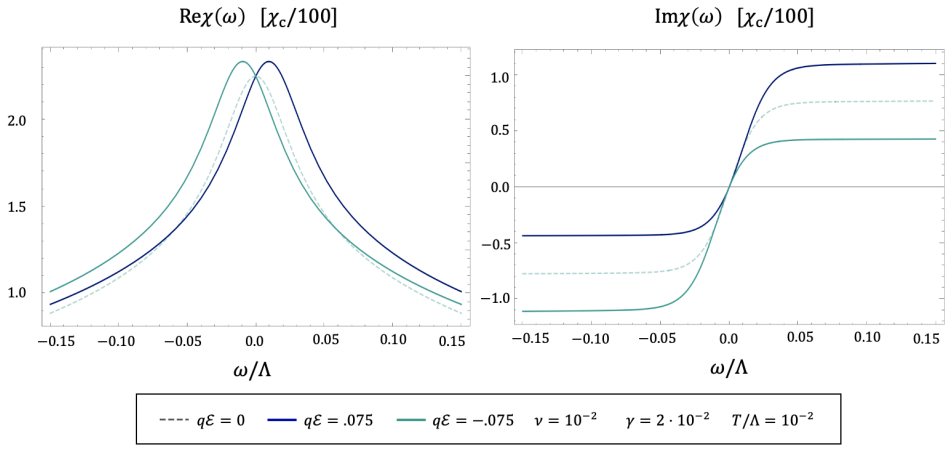

Figure 10.3: Real and imaginary part of the dynamic susceptibility away from charge neutrality. The anomalous dimension is $\gamma = 0.02$ ($\Delta = 0.2525$), the distance from the critical point is $\nu = 0.01$, temperature is $T/\Lambda = 10^{-2}$. The figure in the left panel is re-adapted from Ref. [20].

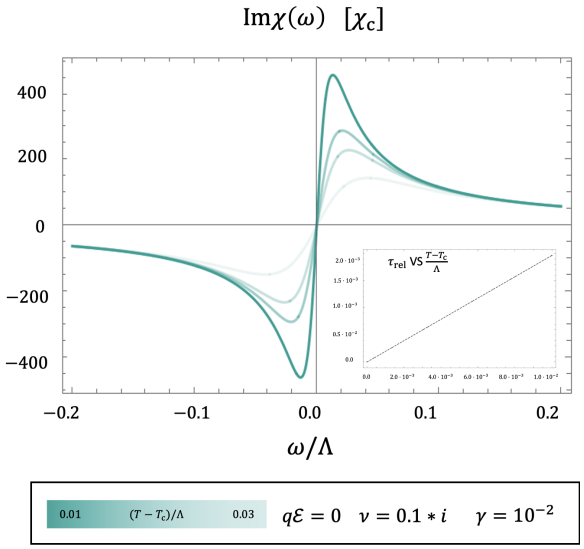

Figure 10.4: Main panel: imaginary part of the dynamical pairing susceptibility at neutrality for different values of temperature, $\gamma = 0.01$, $\nu = 0.1i$, $q\mathcal{E} = 0$. As $T \to T_c$ the slope diverges. Inset: inverse relaxation time as function of reduced temperature $(T - T_c)/\Lambda$. As the transition is approached, τ^{-1} vanishes linearly signaling critical slowing down.

10.1 Summary

In this chapter we have exploited the map derived in Chap. 9 to compute the dynamical pairing response of the Yukawa-SYK model. In the vicinity of the quantum critical point, both the real and imaginary part of the paring susceptibility have an almost flat behavior. Deviations from neutrality destroy the symmetry with respect to inversion of the absolute frequency. Finally, close to the transition temperature $T_{\rm c}$, the system exhibits a dynamical critical slowing down.

Dynamical pairing susceptibility

$$\chi(\omega,T)=\chi_{\rm c}\frac{b_{+}+b_{-}\mathcal{G}(T,\omega)\Lambda^{-2\nu}}{a_{+}+a_{-}\mathcal{G}(T,\omega)\Lambda^{-2\nu}}$$

$\chi_{\rm c}=2c_g^2c_g^2(1+\tan^2\theta)\Lambda^{\gamma}/\pi\gamma$, $a_{\pm}=b_{\pm}(1\pm 2\nu/\gamma)^2$, $b_{\pm}=1\mp 2\nu/\gamma$.

Order-parameter field propagator in AdS_2-black hole

$$\mathcal{G}(T,\omega)=T^{2\nu}\frac{2\nu-\gamma}{2\nu+\gamma}\frac{\Gamma\left(iq^{\star}-\nu+\frac{1}{2}\right)\Gamma\left(iq^{\star}+\nu+\frac{1}{2}-\frac{i\omega}{2\pi T}\right)}{\Gamma\left(iq^{\star}+\nu+\frac{1}{2}\right)\Gamma\left(iq^{\star}-\nu+\frac{1}{2}-\frac{i\omega}{2\pi T}\right)}$$

Recap Box – Dynamical pairing susceptibility of SYK from holography

Summary and Outlook

In the first part of this thesis, we have introduced the fundamentals of the AdS/CFT correspondence. We have highlighted the aspects of the holographic dictionary relevant for the applications to the phenomena of condensed matter physics addressed in this thesis. In particular, holography provides methods for computing retarded correlation functions of theories at strong coupling. This aspect led us to apply such methods to calculate transport coefficients in quantum critical systems with an emergent rotational symmetry breaking in the IR. This analysis constitutes Part II of this thesis.
Moreover, in Part I we focused on charged black holes at low temperatures. The universal low-energy theory of such spacetimes turns out to be identical to those of the Majorana SYK model. In both cases, the effective action is controlled by a Schwarzian derivative which is a signal that in both the theories the same mechanism of conformal symmetry breaking is taking place. This aspect led us to deepen this tied similarity between AdS_2 and SYK in Part III of this thesis.
Below we summarize our conclusions and outlooks for Parts II and III separately.

Quantum critical transport in anisotropic systems

In Part II we have developed a scaling theory for anisotropic, strongly coupled systems near a Lifshitz point. We have reported on the violation of universal lower bounds appearing in strongly-coupled systems due to rotational symmetry breaking. Explicit examples are merging Dirac or Weyl points or Lifshitz points near the superconductor-insulator quantum phase transition. Moreover, we have focused on particle-hole symmetric theories at charge neutrality in two spatial dimensions.

The calculations are performed using scaling arguments and by employing the duality between quantum field theories and gravitational theories in asymptotically AdS spacetimes. We have analyzed the behavior of several observables after a spacetime dilatation, emphasizing that the scale dimensionless ones must approach a constant value for low temperatures. We have shown that both the shear-viscosity to entropy-density ratio and the charge-diffusivity bounds can be generalized for anisotropic systems. As a result of the scaling analysis, some elements of the η/s-tensor have a nonzero scaling dimension while the charge diffusivity still exhibits the scaling of the rotational invariant case. However, we can construct a scale-dimensionless quantity by multiplying the former ratio by a specific combination of electric conductivities. This finding is consistent with the hydrodynamic predictions of Ref. [19]. This is significant because a well-defined lower bound serves as an indicator of strong coupling behavior in anisotropic systems.

The holographic analysis is performed in an Einstein-Maxwell-dilaton model with a massless scalar field. Through this last field, it is possible to break certain symmetries of the system. In particular, we have chosen an axion, a massless field linear in the spatial coordinates of

the boundary. The fundamental point of this ansatz lies in the fact that on the one hand an anisotropy of the metric tensor is induced as desired, on the other hand the dependence on the coordinates is not transmitted to the holographic fields. Consequently, the equations governing the gravitational background remain ordinary differential equations. However, this aspect does not apply to the boundary, which instead is affected by the breaking of translations. This is caused by the fact that the axion induces sources there that explicitly depend on the coordinates. As a consequence, certain elements of the shear viscosity tensor are not well-defined hydrodynamic transport coefficients as momentum is no longer a conserved quantity. In Ref. [212], isotropy is broken by one of the spatial components of the gauge field. In this setup, translations are unbroken and viscosities are still well-defined hydrodynamic transport coefficients. It would be interesting to further investigate such systems.

Within the Einstein-Maxwell-dilaton model considered, translational symmetry is broken along the y direction by a massless scalar in the bulk with a profile linear in y. Thus, the x-component of the momentum is still conserved and $T_{\alpha x}$ continues to be the current of a conserved quantity. Therefore, the viscosity tensor elements $\eta_{\alpha x \beta x}$ maintain their meaning as hydrodynamic transport coefficients. The different scaling of the x and y directions is encoded in the exponent ϕ. Since we can find solutions of the field equations that yield either $\phi < 1$ or $\phi > 1$, we can always construct an anisotropic geometry that violates the isotropic viscosity bound for at least one tensor element, while fulfilling the generalized bound derived with scaling arguments in Eq.(3.6) and in Ref. [19].

As translational invariance is broken, we have also analyzed the shear viscosity in momentum dissipative backgrounds, in both the high and low temperature regime. In the direction where translations are broken, momentum relaxes at a rate $1/\tau_{\rm mr}$. In a holographic system with slow momentum relaxation $1/\tau_{\rm mr} \ll \Lambda$, where Λ is a UV cutoff, there is a range of intermediate times $1/\tau_{\rm mr} \lesssim t \ll \Lambda$ where momentum is approximately conserved. In this regime, the viscosity can be defined from the shear Kubo formula, yet is still found to violate the viscosity-to-entropy-density-ratio bound. Alternatively, it is likely that the diffusivity of transverse momentum is a better quantity to bound: the results of Ref. [133] show that it obeys a bound of the kind Eq.(3.2), with the speed of light as the characteristic velocity.

The KSS bound is known to be violated by terms containing more than two derivatives of the metric (see e.g. Ref.[213] for a review), which capture finite 't Hooft coupling corrections. A possible extension of this work would be to consider the effects of higher derivative terms involving the massless scalars, along the lines of Ref. [214]. Moreover, particle-hole symmetry breaking could be taken into account as well. In any case, a specific higher derivative model has been considered in this thesis to discuss thermodynamic stable phases.

Differently from the other quantities, the diffusivity is not solely given by data at the horizon and is expressed through an integral over the radial direction. Although we do not have the full expression of bulk fields, we have derived a near horizon formula for the compressibility, and could relate the diffusion constant to the horizon data in a simple fashion. On the other hand we have calculated the butterfly velocities by moving to the Kruskal system of coordinates and using a generalization of the shock-wave technique. We have computed the proportionality factor between the diffusivity to the square butterfly velocity ratio and the inverse temperature, finding that it can be expressed in terms of the critical exponents z, ϕ, and θ. In conclusion, the

holographic analysis is consistent with the predictions of the scaling analysis and confirms that the structure of diffusivity bound is not affected by rotational symmetry breaking.

Superconductivity without quasi-particles

In Part III we have studied unconventional superconductivity in systems where the normal state is a non-Fermi liquid. Explicit examples are systems where pairing is caused by nematic quantum critical fluctuations or color magnetic interaction in high-density quark matter.

To this end, we have reviewed the 0+1 dimensional Yukawa-SYK model, i.e. an extension of the SYK model (see introductory chapters), which involves a large number of fermionic and bosonic modes. The appeal of this system lies in the fact that it is solvable on the one hand, and displays low-energy non-Fermi liquid properties on the other. Moreover, such a model is unstable towards superconductivity also in a regime where the normal state is quantum critical. Hence, this is a good candidate toy model to describe the above mentioned quantum critical systems.

For a more realistic description, we have embedded the SYK dot into a higher dimensional lattice. We have analyzed the response of the system to an external electromagnetic field. In particular we have determined the analytic expression for the low-energy electric conductivity and for the superconducting phase stiffness. In order to determine the behavior of such a thermodynamic quantity, a numerical analysis of the saddle point equations has to be employed. In addition, we have commented on the critical temperature for the superconducting phase transition of this model both as function of the SYK coupling and for different values of the hopping parameter, which has the effect of decreasing T_c.

In the remaining chapters of Part III, we have investigated the connection between SYK and holography. The phenomenon of quantum critical superconductivity can generally be tackled through two very different formalisms: Eliashberg theory and holographic superconductivity. On the one hand the Eliashberg formalism has the advantage of encoding retardation effects which turn out to be important in the description of quantum critical superconductors. On the other hand, holography allows us to rephrase superconductivity in the geometric language, which often provides simple analytic expressions.

The equations that govern the Yukawa-SYK model are the Eliasherg equations of superconductivity. Remarkably, at criticality they fall in the class of those proposed for finite-dimensional compressive quantum-critical systems, where pairing is due e.g. to critical gauge-field, nematic fluctuations, and massless gluons in high-density quark matter. Thus, we argue our analysis goes beyond the specifics of the SYK model and is directly relevant to a much broader class of physical systems.

In the introductory chapters we have seen how SYK models have clear similarities with the holographic description. As a consequence, SYK represents a good territory to compare the two formalisms. In particular, we have determined the pairing susceptibility χ of the 0+1 dimensional model, and constructed the phase diagram of the system. This is characterized by a quantum critical point with exponential suppression of the transition temperature. The pairing susceptibility is finite at this QCP, and the milder quantum phase transition is signaled by the singular behavior of the derivatives of χ. Remarkably, this behavior has also been observed in holographic works – see e.g. Ref. [60]. These aspects led us to deepen this tied similarity between

AdS_2 and SYK. Starting from the SYK action, we developed the effective theory around such a critical point and demonstrated that it is equivalent to the holographic superconductor. There is a one-to-one correspondence between the parameters of the microscopic theory and those of gravity. Finding examples where the holographic conjecture holds exactly is important. The gravity dual of e.g. $\mathcal{N} = 4$ super Yang-Mills and the Majorana SYK model can be essentially guessed by conformal symmetry arguments. In our case, the holographic map is valid in a more concrete system with superconductivity, and hence with a lower degree of symmetry.
Specifically, the low-energy theory of the SYK Hamiltonian can be formulated in terms of the action

$$S = S_{\text{gravity}} + S_{\text{sc}} + S_J.$$

Here S_{gravity} is the much discussed AdS gravity in $1 + 1$ dimensions which eventually gives rise to the Schwarzian theory, describing the SYK normal state. Hence the non-Fermi liquid normal state provides the gravitational background. Superconducting degrees of freedom of the SYK model then behave like a charge $2q$ matter field ψ on the AdS_2 background with:

$$S_{\text{sc}} = N \int d^2x \sqrt{g} \left(D_a \psi^* D^a \psi + m^2 \left|\psi\right|^2 \right),$$

where $D_a = \partial_a - i2qA_a$. The finite temperature theory is equivalent to a change of coordinates that corresponds to a black hole with event horizon given by the Hawking temperature. Deviations of the density from half filling give rise to a boundary electric field given by the spectral asymmetry $\mathcal{E}$ of SYK. The competition between suppressed pairing due to the absence of quasiparticles and the enhanced, singular pairing interaction is merely a balance of two contributions to the mass m and leads to a quantum critical point of the BKT variety. The Euler-Lagrange equation of the gravitational theory maps directly onto the Eliashberg equation intensely studied in the context of quantum critical metals. We have therefore attained an explicit and complete AdS-field theory correspondence. Our derivation of holographic superconductivity from a microscopic Hamiltonian allows for a deeper and more concrete understanding of the holographic principle.

The frequency-dependent response of the system is not easy to analyze with Eliashberg theory since a dynamical source generally spoils time translation invariance. We have used our map and exploited the power of holography to determine the dynamical pairing susceptibility of the model. In order to gain insights into the superconducting state, it would be necessary to include the back-reaction of the order parameter field onto the gravitational background.
Our approach should be the natural starting point to study superconducting fluctuations beyond the Eliashberg limit, nonlinear effects beyond the Gaussian level, for systems as diverse as magnetic and nematic quantum critical points, or critical spin liquids, and the thermodynamic contributions from the order parameter condensation. In the holographic language those effects correspond to quantum gravity corrections and gravitational back reactions, respectively.

Appendix A

The effective action for reparametrizations of the Majorana SYK model

In this appendix we derive the action for fluctuations around the saddle Eq.(2.47) of the main text. Let us start from the disorder averaged action which we rewrite here for simplicity

$$\frac{S_{\text{eff}}}{N} = -\frac{1}{2}\log\det(\partial_\tau - \Sigma) + \frac{1}{2}\int d^2\tau\Big[\Sigma(\tau_1,\tau_2)\ G(\tau_1,\tau_2) - \frac{j^2}{q}G(\tau_1,\tau_2)^q\Big]. \tag{A.1}$$

We perform a near saddle-point analysis by using

$$G(\tau_1,\tau_2) = G_{\text{s}}(\tau_1,\tau_2) + \delta G(\tau_1,\tau_2), \quad \Sigma(\tau_1,\tau_2) = \Sigma_{\text{s}}(\tau_1,\tau_2) + \delta\Sigma(\tau_1,\tau_2). \tag{A.2}$$

It is useful to parametrize the fluctuations as

$$\delta G(\tau_1,\tau_2) = |G(\tau_1,\tau_2)|^\alpha g(\tau_1,\tau_2), \quad \delta\Sigma(\tau_1,\tau_2) = |G(\tau_1,\tau_2)|^{-\alpha}\sigma(\tau_1,\tau_2), \tag{A.3}$$

with $\alpha = (2-q)/2$ and g and σ are small quantities.
We expand Eq.(A.1) to second order in the fluctuations, as linear terms vanish in the vicinity of the saddle. We also neglect constant terms as we are only interested in fluctuations.
We start with the first term in Eq.(A.1)

$$\begin{aligned}\log\det[\partial_\tau - (\Sigma_{\text{s}} + \delta\Sigma)] &\overset{G_{\text{s}}=(\partial_\tau-\Sigma_{\text{s}})^{-1}}{=} \operatorname{Tr}\log\Big(G_{\text{s}}^{-1} - \delta\Sigma\Big)\\ &\approx -\frac{1}{2}\operatorname{Tr}(G_{\text{s}}\delta\Sigma G_{\text{s}}\delta\Sigma) = -\frac{1}{2}G_{\text{s}}\otimes\delta\Sigma\otimes G_{\text{s}}\otimes\delta\Sigma,\end{aligned} \tag{A.4}$$

where we have used the matrix notation $M\otimes N = \int d^2\tau M(\tau,\tau')N(\tau',\tau)$.
Let us introduce the following four-points functions

$$K(\tau_1,\tau_2;\tau_3.\tau_4) = -j^2(q-1)G(\tau_{13})G(\tau_{24})G(\tau_{34})^{q-2}, \tag{A.5a}$$

$$\tilde{K} = |G(\tau_{12})|^{\frac{q-2}{2}} K(\tau_1, \tau_2; \tau_3.\tau_4)|G(\tau_{34})|^{\frac{2-q}{2}}. \tag{A.5b}$$

It follow that

$$\mathrm{Tr}(G_{\mathrm{s}}\delta\Sigma G_{\mathrm{s}}\delta\Sigma) = -\frac{1}{j^2(q-1)}\,\sigma\otimes\tilde{K}_{\mathrm{s}}\otimes\sigma.$$

where the kernel has been evaluated on the saddle G_{s}. The second term of Eq.(A.1) is given by

$$\int d^2\tau\Sigma(\tau_1,\tau_2)G(\tau_1,\tau_2) \approx \int d^2\tau\sigma(\tau_1,\tau_2)g(\tau_1,\tau_2) = \sigma\otimes g. \tag{A.6}$$

The third term of Eq.(A.1) is given by

$$\begin{aligned}\frac{j^2}{2q}\int d^2\tau\, G^q(\tau_1,\tau_2) &\approx \frac{j^2}{2q}\int d^2\tau G^q_{\mathrm{s}}(\tau_1,\tau_2)\left[1+G^{-1}_{\mathrm{s}}(\tau_1,\tau_2)\delta G(\tau_1,\tau_2)+\binom{q}{2}[G^{-1}_{\mathrm{s}}(\tau_1,\tau_2)\delta G_{\mathrm{s}}(\tau_1,\tau_2)]^2\right]\\ &\to \frac{j^2}{4}(q-1)\int d^2\tau g^2(\tau_1,\tau_2) = \frac{j^2}{4}(q-1)\,g\otimes g.\end{aligned} \tag{A.7}$$

Putting all together we obtain the following expression for the effective action

$$\frac{S_{\mathrm{eff}}}{N} = -\frac{\sigma\otimes\tilde{K}_{\mathrm{s}}\otimes\sigma}{4j^2(q-1)} + \frac{\sigma\otimes g}{2} - \frac{(q-1)\,g\otimes g}{4}. \tag{A.8}$$

Performing the Gaussian integral over σ and adsorbing the prefactors in the path-integral measure yield

$$\boxed{\frac{S_{\mathrm{eff}}}{N} = \frac{j^2(q-1)}{4}\,g\otimes(\tilde{K}_{\mathrm{s}}-1)\otimes g.} \tag{A.9}$$

Zero modes We now focus on the IR limit where the saddle point of the effective action is given by the conformal correlator $G_{\mathrm{s}} = G_{\mathrm{c}}$ as in Eq.(2.39). For simplicity we work at zero temperature but the results are general [68]. For the sake of the discussion we re-quote the IR-Schwinger-Dyson equation

$$(G\Sigma)(\tau,\tau'') = \delta(\tau-\tau''), \tag{A.10a}$$

$$\Sigma(\tau,\tau'') = j^2[G(\tau,\tau'')]^{q-1}. \tag{A.10b}$$

Plugging the fluctuation form Eq.(A.2) into the above equations we get $G_{\mathrm{c}}\delta\Sigma_{\mathrm{c}} + \delta G_{\mathrm{c}}\Sigma_{\mathrm{c}} = 0$. Multiplying from the right times G_{c} and using Eq.(A.10a) yields $G_{\mathrm{c}}\delta\Sigma_{\mathrm{c}}G_{\mathrm{c}} - \delta G_{\mathrm{c}} = 0$. The Σ-fluctuation can be easily expressed in terms of the G-one by means of Eq.(A.10b) $\delta\Sigma_c = j^2(q-1)G_{\mathrm{c}}^{q-2}\,\delta G_{\mathrm{c}}$, and we get

$$\delta G_{\mathrm{c}} - j^2(q-1)\,G_{\mathrm{c}}G_{\mathrm{c}}^{q-2}\delta G_{\mathrm{c}}G_{\mathrm{c}} = 0. \tag{A.11}$$

Now we massage this expression, keeping in mind that G_{c} is odd in time

$$\begin{aligned}(G_{\mathrm{c}}G_{\mathrm{c}}^{q-2}\delta G_{\mathrm{c}}G_{\mathrm{c}})(\tau_1,\tau_4) &= \int d^4\tau\, G_{\mathrm{c}}(\tau_1,\tau_2)G_{\mathrm{c}}^{q-2}(\tau_2,\tau_3)[-G_{\mathrm{c}}(\tau_4,\tau_3)]\delta G_{\mathrm{c}}(\tau_2,\tau_3)\\ &\overset{(A.5a)}{=} \frac{1}{j^2(q-1)}\int d^4\tau K_{\mathrm{c}}(\tau_1,\tau_2;\tau_3,\tau_4)\delta G_{\mathrm{c}}(\tau_2,\tau_3).\end{aligned} \tag{A.12}$$

From this we find

$$(\mathbb{1} - K_{\mathrm{c}})\delta G_{\mathrm{c}} = 0. \tag{A.13}$$

Therefore, reparametrizations of the conformal correlator are eigenvectors of the kernel (A.5a) with eigenvalue 1.
The above expression can be further expressed in terms of the symmetric kernel (A.5b)

$$\boxed{(\mathbb{1} - \tilde{K}_{\mathrm{c}})g_{\mathrm{c}} = 0,} \tag{A.14}$$

with $g_{\mathrm{c}} = |G_{\mathrm{c}}|^{\frac{q-2}{2}}\delta G_{\mathrm{c}}$. Since Eq.(A.9) can be written as $g\otimes(\tilde{K}_{\mathrm{s}}^{-1} - \mathbb{1})\otimes g$ and is therefore zero on g_{c}, we conclude that, normalized reparametrizations of the conformal correlator are zero modes of the effective action Eq.(A.9).

In the following we determine the explicit expression of such zero modes. Moreover, we work at finite temperature and adopt the angular variable $\theta = 2\pi T\tau$. Thanks to conformal invariance, the set of solutions to the saddle point equations can be generated through time-reparametrization via Eqs.(2.38). To determine the form of the fluctuation around the conformal saddle we consider infinitesimal maps $f(\theta) = \theta + \epsilon(\theta)$, with $\epsilon(\theta) \ll \theta$. We have

$$G(\theta_1, \theta_2) = [1 + (\Delta(\epsilon(\theta_1) + \epsilon(\theta_2)) + \epsilon(\theta_1)\partial_{\theta_1} + \epsilon(\theta_2)\partial_{\theta_2})]G_{\mathrm{c}}(\theta_1, \theta_2),$$

with G_{c} given by the finite-T conformal correlator Eq.(2.40). Using the notation of Eq.(A.2) we identify

$$\delta_\epsilon G_{\mathrm{c}} = [\Delta(\epsilon(\theta_1) + \epsilon(\theta_2)) + \epsilon(\theta_1)\partial_{\theta_1} + \epsilon(\theta_2)\partial_{\theta_2}]G_{\mathrm{c}}. \tag{A.15}$$

Equating the derivatives yields

$$(\epsilon(\theta_1)\partial_{\theta_1} + \epsilon(\theta_2)\partial_{\theta_2})G_{\mathrm{c}} = (\epsilon(\theta_1) - \epsilon(\theta_2))\left(\Delta\tan^{-1}(\theta_{12}/2) + \frac{\delta(\theta_{12})}{\mathrm{sgn}(\theta_{12})}\right)G_{\mathrm{c}}.$$

The second term in the parenthesis can be neglected due to the δ-function. It is convenient to switch to Fourier space via $\epsilon(\theta) = \frac{1}{2\pi}\sum_n e^{-i\theta n}\epsilon_n$. Eq.(A.15) then becomes

$$\left.\frac{\delta_\epsilon G_{\mathrm{c}}}{G_{\mathrm{c}}}\right|_{\mathrm{mode}\, n} = \frac{\Delta i}{\pi} f_n(\theta_{12}) e^{in\frac{\theta_1+\theta_2}{2}}\epsilon_n, \tag{A.16}$$

with $f_n(\theta) = \sin(n\theta/2)\cot(\theta/2) - n\cos(n\theta/2)$ and $\int_0^{2\pi} d\theta \left(f_n(\theta)\csc(\theta/2)\right)^2 = \frac{2\pi}{3}|n|(n^2-1)$. The nth Fourier mode of the normalized fluctuation Eq.(A.3) is given by

$$g_{\mathrm{c},n}(\theta_1, \theta_2) = \frac{i\Delta b^{\frac{q}{2}}}{\pi}\frac{\pi}{\beta}\left(\frac{f_n(\theta_{12})}{|\sin\left(\frac{\theta_{12}}{2}\right)|}\right)e^{in\frac{\theta_1+\theta_2}{2}}\epsilon_n. \tag{A.17}$$

Non-conformal corrections

In Eq.(A.14) we have seen that reparametrizations of the conformal correlator are eigenvectors of the symmetric kernel with eigenvalue 1. Going beyond the IR limit ($\beta\mathcal{J} \gg 1$) shifts the eigenvalue of $\tilde{K}$ as

$$\tilde{K}_{\mathrm{s}} g_{\mathrm{c},n} = \Big(1 - \alpha_\epsilon \frac{|n|}{\beta\mathcal{J}} + ...\Big) g_{\mathrm{c},n}, \tag{A.18}$$

where the dots denote higher orders in $(\beta\mathcal{J})^{-1}$ – see Ref. [68] for details. The coefficient α_ϵ can only be obtained numerically or analytically in a large-q expansion [68, 71].
The effective action Eq.(A.9) then becomes

$$\frac{S_{\mathrm{eff}}}{N} = \frac{\alpha_S'}{\beta\mathcal{J}} n^2(n^2-1)|\epsilon_n|^2, \tag{A.19}$$

with $\alpha_S' = \alpha_\epsilon \frac{b^q}{q^2\beta^2} 2\frac{(2\pi)^2}{3}$. Transforming back to the θ-coordinate we have $\sum_n n^2(n^2-1)|\epsilon_n|^2 = 2\pi \int_0^{2\pi} d\theta \left[|\partial_\theta^2 \epsilon(\theta)|^2 - |\partial_\theta \epsilon(\theta)|^2\right]$. Restoring the τ-coordinate we finally get

$$\boxed{\frac{S_{\mathrm{eff}}[\epsilon]}{N} = \frac{\alpha_{\mathrm{S}}}{\mathcal{J}} \int_0^\beta d\tau \frac{1}{2}\left[|\epsilon''|^2 - \left(\frac{2\pi}{\beta}\right)^2 |\epsilon'|^2\right].} \tag{A.20}$$

with $\alpha_{\mathrm{S}} = \frac{\alpha_\epsilon}{6\alpha_0 q^2}$.

Appendix B

Explicit solutions to the field equations of the EMD-axion(s) model

In this appendix we discuss the solutions to the equations of motion introduced in Sec. 4.1. We analyze the case where axions are irrelevant or marginally relevant deformations of the IR endpoint [90]. In the former case, the deformation decays in the interior, whereas the latter is insensitive to the flow. They should not be confused with the deformations of the UV CFT fixed point (dual to the asymptotically AdS_4 boundary conditions), even though there is of course a mapping between the IR and the UV that can be worked out by explicitly solving the RG flow. See e.g. Ref. [151] for an explicit example.
Using the equations of motion, we reduce the number of free parameters in the action Eq.(4.17) and in the ansatz Eq.(4.16). Before proceeding, we observe that the model Eq.(4.1) is invariant under a concomitant flip in the sign of δ, λ_I, ξ and Φ, so we restrict our analysis to the $\delta > 0$ case.
Notice finally that the effective potential Eq.(4.10) is given by

$$\frac{V_{\text{eff}}(r)}{\sqrt{-g}} = \frac{1}{2}\sum_I a_I^2 r^{2\Lambda_I - \theta} - V_0 r^{2\delta\kappa}, \tag{B.1}$$

where $\Lambda_1 = \kappa\lambda_x + \phi$ and $\Lambda_2 = \kappa\lambda_y + 1$.

B.1 Single axion model

In this section we analyze a geometry where momentum is conserved along one of the spatial directions, say the β-direction. This corresponds to the case $p = 1$ where only one axion is involved. The axion is a marginal deformation of the IR fixed point if the a_I-term in the effective dilaton potential Eq.(B.1) does not induce any radial dependence, while it is irrelevant if it can be neglected in comparison to the others. In the latter case we determine the $a_I = 0$ solution and afterwards we solve the EOMs order by order, as we will soon discuss. In the following we investigate two classes of $p = 1$ solutions, depending on whether the axion depends on x or y.

Single marginal axion – $\psi = a_x x$

In the marginal case we set $2\Lambda_x = 2\kappa\delta + \theta$. Considering the dilaton EOM and the following combinations of Einstein equations (up to a global factor) $\mathcal{E}^{rr} + \mathcal{E}^{yy}$, $\mathcal{E}^{rr} + \mathcal{E}^{xx}$, $\mathcal{E}^{tt} - \mathcal{E}^{rr}$, $\mathcal{E}^{rr}$ respectively, we have:

$$\begin{aligned}
&4\kappa^2 + 2z(\theta - \phi - 1) + 2\phi^2 + 2 - \theta^2 = 0,\\
&\tilde{L}^2\left(a_x^2 - 2V_0\right) + 2(z + \phi - \theta)(z + \phi + 1 - \theta) = 0,\\
&\tilde{L}^2 V_0 - (z + 1 - \theta)(z + \phi + 1 - \theta) = 0\\
&\tilde{L}^2\left(\phi\, a_x^2 - \theta\, V_0\right) - 4\kappa^2(z + \phi + 1 - \theta) = 0,\\
&\tilde{L}^2\left(a_x^2 - 2V_0\right) + 3\theta^2 - 4\theta(\phi + 1) - 4\kappa^2 + 4z(\phi + 1 - \theta) + 4\phi = 0,
\end{aligned} \tag{B.2}$$

where we also required $\theta + 2\delta\kappa = 0$ in order to obtain algebraic relations. The solution is given by:

$$\begin{aligned}
&z = 1, \quad 2\kappa\delta = -\theta, \quad \kappa\lambda_x = -\phi,\\
&4\kappa^2 = \theta(\theta - 2) - 2\phi(\phi - 1),\\
&\tilde{L}^2 = (\theta - 2)(\theta - \phi - 2)/V_0,\\
&a_x^2 = \frac{2V_0(\phi - 1)}{\theta - 2}.
\end{aligned} \tag{B.3}$$

Since $z = 1$, Lorentz symmetry is preserved. Requiring positivity of the squared quantities and the specific heat, we obtain the following set of consistency conditions:

$$\begin{aligned}
&(\theta - 2)(\phi - 1) > 0, \quad (\theta - 2)(\theta - 2 - \phi) > 0,\\
&(\theta - 2)\theta - 2(\phi - 1)\phi > 0, \quad (\phi + 1 - \theta) > 0.
\end{aligned} \tag{B.4}$$

In order for the holographic renormalization procedure to be well defined, the null energy condition (NEC) $T^{\text{tot}}_{\mu\nu} v^\mu v^\nu \geq 0$ has to be fulfilled [24]. In the present context, this is the case for any given null vector v^μ. The above inequalities imply $\delta_0 = 1 + \phi + z - \theta > 0$, therefore the temperature is a relevant deformation only if the boundary lies at $r = 0$. Furthermore, the IR-line element is required to vanish at $T = 0$, hence $\theta < 2$ and $\theta < 2\phi$. Globally we have

$$\phi < 1, \quad 2(\phi - 1)\phi < (\theta - 2)\theta, \quad \theta < 2\phi. \tag{B.5}$$

Single marginal axion – $\psi = a_y y$

In analogy to the previous section we now determine the solution with one marginal axion along y. Also in this case we set $2\Lambda_y = 2\kappa\delta + \theta$ and $\theta + 2\delta\kappa = 0$

$$\begin{aligned}
&z = \phi, \quad 2\kappa\delta = -\theta, \quad \kappa\lambda_y = -1,\\
&4\kappa^2 = \theta^2 - 2\theta\phi + 2\phi - 2,\\
&\tilde{L}^2 = (\theta - 2\phi - 1)(\theta - 2\phi)/V_0,\\
&a_y^2 = \frac{2V_0(1 - \phi)}{\theta - 2\phi}.
\end{aligned} \tag{B.6}$$

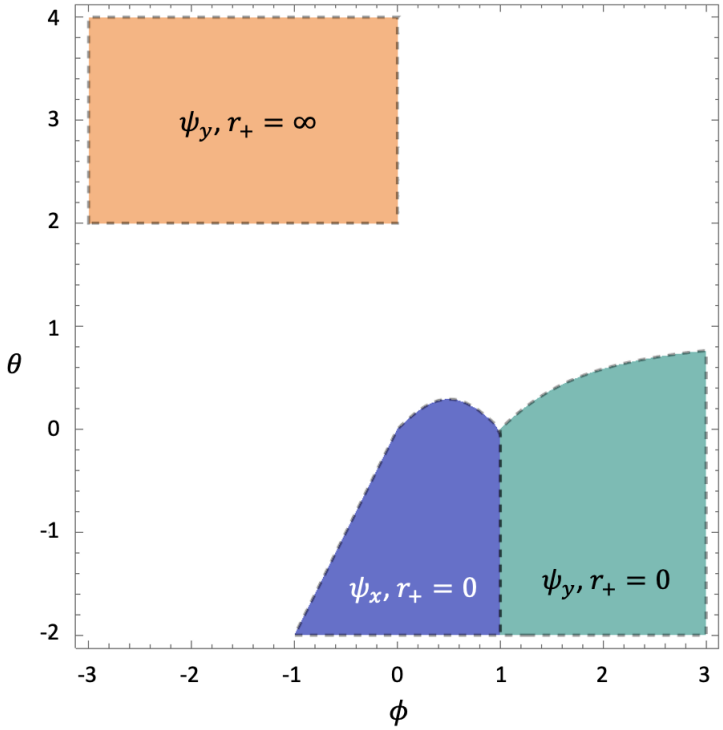

Figure B.1: Graphic representation of conditions Eq. (B.5) (blue), (B.7a) (orange) (B.7b) (teal) in the (ϕ, θ)-plane. The colored areas represent the parameter space where anisotropic scaling solutions exist. Figure adapted from Ref. [18].

The consistency conditions are

$$\theta < 2, \quad \theta^2 + 2\phi > 2\theta\phi + 2, \quad \phi > 1, \tag{B.7a}$$

$$\theta > 2, \quad \theta^2 + 2\phi > 2\theta\phi + 2, \quad \theta\phi < \phi^2 + \phi. \tag{B.7b}$$

In the former case the boundary is located at $r = \infty$ while in the latter at $r = 0$.

Single irrelevant axion

Now we wish to investigate the $p = 1$ case, where the axion induces irrelevant deformations of the IR endpoint. The axion is $\psi = ax_\alpha$, where α is fixed and equals to one of the boundary coordinates.
We first determine the solution when $a = 0$ and then consider perturbations of the form:

$$\Psi = \Psi_{a=0}\left(1 + c_\Psi a^2 r^{2\Delta_a}\right). \tag{B.8}$$

Here Ψ stands for the metric elements or the dilaton field, and c_Φ are numerical coefficients that follow from the $\mathcal{O}(a^2)$ fields equations. Such corrections are expressed in terms of a^2 as the axion enters quadratically the field equations. Moreover, such irrelevant perturbations must

grows towards the boundary of the IR region, hence Δ_a should be positive (negative) if the IR is located at $r = 0$ ($r = \infty$). The leading solution is given by

$$\begin{aligned} &z = \phi = 1, \\ &4\kappa^2 = \theta(\theta - 2), \\ &\tilde{L}^2 = (\theta - 2)(\theta - 3)/V_0, \end{aligned} \tag{B.9}$$

provided that $\theta + 2\delta\kappa = 0$. Moreover we obtain:

$$c_{g_{rr}} = \frac{\delta\left((\delta - 2\lambda_\alpha)^2 - 3\right) - 2\lambda_\alpha}{2\delta V_0\left(\delta^2 - 2\delta\lambda_\alpha + 1\right)}, \tag{B.10a}$$

$$c_{g_{tt}} = c_{g_{\overline{\alpha\alpha}}} = \frac{\lambda_\alpha}{2\delta V_0\left(-\delta^2 + \delta\lambda_\alpha + 1\right)}, \tag{B.10b}$$

$$c_\Phi = \frac{\lambda_\alpha}{2V_0\left(\delta^2 - \delta\lambda_\alpha - 1\right)}, \tag{B.10c}$$

$$c_{g_{\alpha\alpha}} = -\frac{\delta\left(-2\delta^2 + \delta\lambda_\alpha - 2\lambda_\alpha^2 + 6\right) + \lambda_\alpha}{2\delta V_0\left(\delta^2 - 2\delta\lambda_\alpha + 1\right)\left(\delta^2 - \delta\lambda_\alpha - 1\right)}. \tag{B.10d}$$

The IR scale dimension of the perturbation is given by

$$2\Delta_a = 2 + \frac{\kappa\lambda}{2}, \tag{B.11}$$

in accord with Ref. [90]. The consistency conditions read

$$\theta < 0, \quad \Delta \lesseqgtr 0, \tag{B.12}$$

where the last inequality depends on the location of the IR.

B.2 Double (marginally) relevant axions

Let us consider the case $p = 2$ where both the axions ψ_x and ψ_y are taken into account. Details on the $p = 2$ mixed case can be found in Ref. [90, 122]. In this case we set $2\Lambda_I = 2\kappa\delta + \theta$ and $\theta + 2\delta\kappa = 0$ to get algebraic equations. In the $p = 2$ case we find

$$\begin{aligned} &2\kappa\delta = -\theta, \quad \kappa\lambda_x = -\phi, \quad \kappa\lambda_y = -1, \\ &4\kappa^2 = \theta(\theta - 2z) - 2\phi(\phi - 2z) - 2(1 - z), \\ &\tilde{L}^2 = (\theta - 2z)(\theta - \phi - z - 1)/V_0, \\ &a_x^2 = \frac{2V_0(\phi - z)}{\theta - 2z}, \quad a_y^2 = \frac{2V_0(1 - z)}{\theta - 2z}, \end{aligned} \tag{B.13}$$

which reproduces Eq.(B.3) in the $a_y = 0$ case and (B.6) for $a_x = 0$.

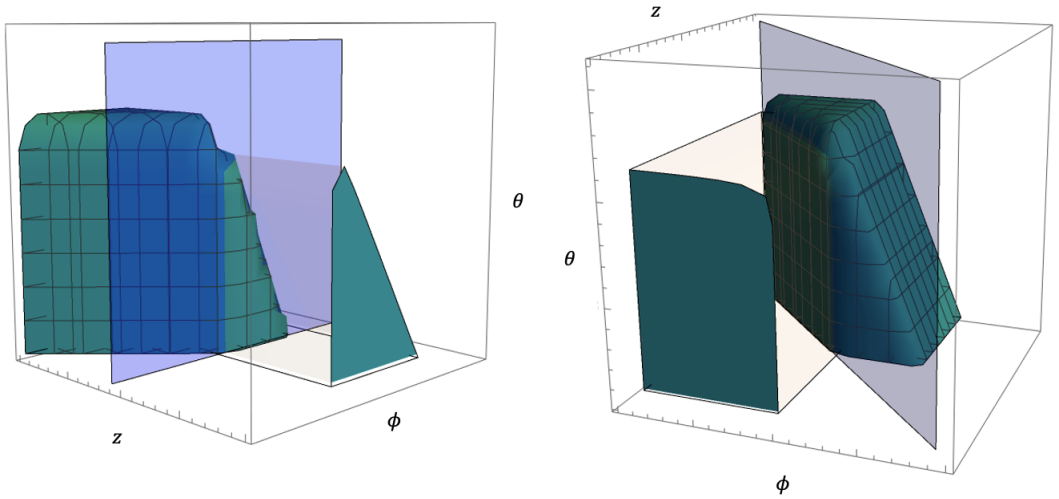

Figure B.2: Parameter space for the double marginal axions solution. The intersection with the plane $z = 1$ coincides with (B.4), while the one with $z = \phi$ yields the domain of the solution with $a_x = 0$. In the above plots $-10 < \phi < 10, -9.8 < \theta < 6, -10 < z < 10$. Figure re-adapted from Ref. [18].

The consistency conditions are

$$\begin{aligned}
&(\theta - 2z)(\phi - z) > 0, \quad (\theta - 2z)(1 - z) > 0, \\
&(\theta - 2z)(\theta - \phi - z - 1) > 0, \\
&\theta(\theta - 2z) - 2\phi(\phi - 2z) - 2(1 - z) > 0, \\
&z\,(\phi + 1 - \theta) \lesseqgtr 0 \\
&\theta \lesseqgtr 2z,\ \theta \lesseqgtr 2,\ \theta \lesseqgtr 2\phi,
\end{aligned} \tag{B.14}$$

where the last inequalities depend on whether we put the boundary at infinity or zero.

Appendix C

Effective action of the Yukawa-SYK model

C.1 Single dot effective action

In this appendix we repeat the strategy outlined in Sec. 2.3.2 to derive the effective action of the Yukawa-SYK model Eq.(6.1). The disorder-averaged partition function reads

$$\overline{Z^m} = \int \mathcal{D}\psi e^{-\sum_a S_0[\psi_a]} \left(\int dg_{ij,k} \varrho(g_{ijk}) e^{-\sum_a S_{\rm int}[\psi_a]} \right), \tag{C.1}$$

where $a = 1...m$ labels the replica and $\psi = \{c_{i\sigma a}, c^\dagger_{i\sigma a}, \phi_{ka}\}$ is a shorthand for the fields of the model. Here ϱ represents PDF for the coupling constants introduced in table 6.1 .
In Eq.(C.1) we have split the action into free and interacting contribution $S = S_0 + S_{\rm int}$, with:

$$S_0 = \sum_{i\sigma a} \int d\tau c^\dagger_{i\sigma a}(\tau)(\partial_\tau - \mu) c_{i\sigma a}(\tau) + \frac{1}{2} \sum_{ia} \int d\tau \phi_{ia}(\tau)(-\partial_\tau^2 + m_0)\phi_{ia}(\tau), \tag{C.2a}$$

$$S_{\rm int} = \sum_{a\sigma;ijk} \int_\tau \left[g_{ij,k} + g^\star_{ji,k} \right] c^\dagger_{i\sigma a}(\tau) c_{j\sigma a}(\tau) \phi_{ka}(\tau). \tag{C.2b}$$

In the following we work out the contribution to the partition function Eq.(C.1) induced by $S_{\rm int}$. Let us focus on the following integral

$$\mathcal{J}_g = \int dg_{ij,k} \varrho(g_{ijk}) \exp\left(- \sum_{a\sigma;ijk} \int d\tau \left[g_{ij,k} + g^\star_{ji,k} \right] c^\dagger_{i\sigma a}(\tau) c_{j\sigma a}(\tau) \phi_{ka}(\tau) \right). \tag{C.3}$$

Let us introduce the composite operator $O_{ijk} = \sum_{\sigma a} \int d\tau c^\dagger_{i\sigma a}(\tau) c_{j\sigma a}(\tau) \phi_{ka}(\tau)$ and the multi-index $I = (i, j, k)$. The above expression can then be re-written as

$$\mathcal{J}_g = \int d[g_I g^\star_I] \varrho(g_I) e^{-(g_I O_I + g^*_I O^\dagger_I)}. \tag{C.4}$$

To perform the Gaussian integral we split the coupling into real and imaginary part $g_I = g'_I + ig''_I$ and get

$$\begin{aligned}\mathcal{J}_g &= \int d[g'_I] e^{-g'_I(\overline{g'_I g'_J})^{-1} g'_J} e^{-(O_I+O_I^\dagger)g'_I} \times \int d[g''_I] e^{-g''_I(\overline{g''_I g''_I})^{-1} g''_I} e^{-i(O_I-O_I^\dagger)g''_I} \\ &= e^{\frac{1}{2}(O_I+O_I^\dagger)\overline{g'_I g'_J}(O_J+O_J^\dagger)} e^{-\frac{1}{2}(O_I-O_I^\dagger)\overline{g''_I g''_J}(O_J-O_J^\dagger)}. \end{aligned} \tag{C.5}$$

Below we work within the Gaussian orthogonal ensemble (first column of Tab.6.1). As we will see, this approach yields an effective action whose normal state properties can be derived by setting all the superconducting contributions to zero. We have:

$$\mathcal{J}_g = \exp\left[\frac{\bar{g}^2}{4N^2}(O_{ijk}+O_{ijk}^\dagger)\delta_{kk'}\left(\delta_{ii'}\delta_{jj'}+\delta_{ij'}\delta_{ji'}\right)(O_{i'j'k'}+O_{i'j'k'}^\dagger)\right] = \exp\left[\frac{\bar{g}^2}{2N^2}(O_{ijk}+O_{ijk}^\dagger)^2\right]. \tag{C.6}$$

This gives

$$\begin{aligned} S_{\text{int}}^{\text{eff}} &= -\frac{\bar{g}^2}{2N^2}\sum_{ijk}\int d^2\tau \sum_{\sigma\sigma',ab}\Big(c^\dagger_{j\sigma a}(\tau)c^\dagger_{j\sigma' b}(\tau')\, c_{i\sigma' b}(\tau')c_{i\sigma a}(\tau) \\ &\qquad -c^\dagger_{j\sigma a}(\tau)c_{j\sigma' b}(\tau')\, c^\dagger_{i\sigma' b}(\tau')c_{i\sigma a}(\tau)\Big)\phi_{ka}(\tau)\phi_{kb}(\tau'). \end{aligned} \tag{C.7}$$

Putting all together, we obtain the following total action:

$$\begin{aligned} S_{\text{tot}} &= \sum_{i\sigma a}\int d\tau c^\dagger_{i\sigma a}(\tau)(\partial_\tau-\mu)c_{i\sigma a}(\tau) + \frac{1}{2}\sum_{ia}\int d\tau\phi_{ia}(\tau)(-\partial_\tau^2+m_0)\phi_{ia}(\tau) \\ &- \frac{\bar{g}^2}{2N}\sum_{ijk}\int d^2\tau\sum_{\sigma\sigma',ab}\Big(c^\dagger_{j\sigma a}(\tau)c^\dagger_{j\sigma' b}(\tau')\, c_{i\sigma' b}(\tau')c_{i\sigma a}(\tau) \\ &\qquad -c^\dagger_{j\sigma a}(\tau)c_{j\sigma' b}(\tau')\, c^\dagger_{i\sigma' b}(\tau')c_{i\sigma a}(\tau)\Big)\phi_{ka}(\tau)\phi_{kb}(\tau'). \end{aligned} \tag{C.8}$$

We now introduce the a bunch of collective fields

$$G_{\sigma\sigma',ab}(\tau,\tau') = \frac{1}{N}\sum_i c^\dagger_{i\sigma' b}(\tau')c_{i\sigma a}(\tau), \quad F_{\sigma\sigma',ab}(\tau,\tau') = \frac{1}{N}\sum_i c_{i\sigma' b}(\tau')c_{i\sigma a}(\tau), \tag{C.9a}$$

$$D_{ab}(\tau,\tau') = \frac{1}{M}\sum_k \phi_{kb}(\tau')\phi_{ka}(\tau). \tag{C.9b}$$

We do so by means of path integral delta functions and further introduce Lagrange-multipliers degrees of freedom

$$1 = \int_{[G]}\prod_{\substack{ab\tau\tau'\\ \sigma\sigma'}}\delta\left(NG_{ba,\sigma\sigma'}(\tau',\tau) - \sum_i c^\dagger_{i\sigma a}(\tau)c_{i\sigma' b}(\tau')\right) \tag{C.10}$$

$$= \int_{[G,\Sigma]} e^{\left(NG_{ba,\sigma'\sigma}(\tau',\tau)-\sum_i c^\dagger_{i\sigma a x}(\tau)\, c_{i\sigma' b}(\tau')\right)\Sigma_{ab,\sigma\sigma'}(\tau,\tau')}, \tag{C.11}$$

where $\int_{[G]} ... \equiv \int \mathcal{D}G$ etc., and repeated indices are summed. Alternatively, one can introduce such fields through a Hubbard-Stratonovich transformation – see Ref.[215] and Sec. C.2. For the other fields we have

$$1 = \int_{[F^\dagger,\Phi]} e^{\frac{1}{2}\left(NF^\dagger_{ba,\sigma'\sigma}(\tau',\tau) - \sum_i c^\dagger_{i\sigma a}(\tau)\, c^\dagger{}_{i\sigma' b}(\tau')\right)\Phi_{ab,\sigma\sigma',}(\tau,\tau')}, \tag{C.12a}$$

$$1 = \int_{[F,\Phi^\dagger]} e^{\frac{1}{2}\left(NF_{ba,\sigma'\sigma}(\tau',\tau) - \sum_i c_{i\sigma a}(\tau)\, c_{i\sigma' b}(\tau')\right)\Phi^\dagger_{ab,\sigma\sigma',}(\tau,\tau')}, \tag{C.12b}$$

$$1 = \int_{[D,\Pi]} e^{\frac{1}{2}\left(ND_{ba}(\tau',\tau) - \sum_i \phi_{ia}(\tau)\,\phi_{ib}(\tau')\right)\Pi_{ab,}(\tau,\tau')}. \tag{C.12c}$$

By definition, the self energies $\Sigma, \Phi^{(\dagger)}$ fields inherit the same symmetry properties of the conjugated field. The above transformations modify the action as:

$$\begin{aligned}
S^{\text{eff}} &= \sum_{iab\sigma\sigma'} \int d^2\tau\, c^\dagger_{i\sigma a}(\tau)\left[(\partial_\tau - \mu)\delta_{ab}\delta_{\sigma\sigma'}\delta(\tau-\tau') + \Sigma_{ab,\sigma\sigma'}(\tau,\tau')\right] c_{i\sigma' b}(\tau') \\
&+ \frac{1}{2}\sum_{iab\sigma\sigma'} \int d^2\tau [c^\dagger_{i\sigma a}(\tau)\,\Phi_{ab,\sigma\sigma'}(\tau,\tau') c^\dagger_{i\sigma' b}(\tau') + c_{i\sigma a}(\tau)\,\Phi^\dagger_{ab,\sigma\sigma'}(\tau,\tau')\, c_{i\sigma' b}(\tau')] \\
&+ \frac{1}{2}\sum_{iab} \int d^2\tau\, \phi_{iax}(\tau)[(-\partial_\tau^2 + m_0)\delta_{ab}\delta(\tau-\tau') - \Pi_{ab}(\tau,\tau')]\phi_{ib}(\tau') \\
&- N\sum_{\sigma\sigma'} \int d^2\tau G_{ba,\sigma'\sigma}(\tau',\tau)\Sigma_{ab,\sigma\sigma'}(\tau,\tau') + \frac{M}{2}\int d^2\tau D_{ba}(\tau',\tau)\Pi_{ab}(\tau,\tau') \\
&- \frac{N}{2}\sum_{\sigma\sigma'} \int d^2\tau \left(F_{ba,\sigma'\sigma}(\tau'\tau)\Phi^\dagger_{ab,\sigma\sigma'}(\tau,\tau') + F^\dagger_{ba,\sigma'\sigma}(\tau'\tau)\Phi_{ab,\sigma\sigma'}(\tau,\tau')\right) \\
&+ \frac{\bar{g}^2}{2} M \sum_{\sigma\sigma'} \int d^2\tau \left(G_{ba,\sigma\sigma'}(\tau,\tau')G_{ab,\sigma'\sigma}(\tau',\tau) - F^\dagger_{ab,\sigma\sigma'}(\tau,\tau')F_{ab,\sigma'\sigma}(\tau',\tau)\right) D_{ab}(\tau,\tau').
\end{aligned} \tag{C.13}$$

This might seem a complication. However, this action is quadratic in the fermions an can therefore be simplified through a further Gaussian integration over Grassmann numbers. Specifically, the fermionic part can be reorganized in the Nambu representation as:

$$S_{\text{ferm}} = -\frac{1}{2}\sum_{iab} \int d^2\tau\ \bar{\psi}^\dagger_{ia}(\tau)\left(\bar{G}^{-1}_{0,ab}(\tau,\tau') - \bar{\Sigma}_{ab}(\tau,\tau')\right)\bar{\psi}_{ib}(\tau'), \tag{C.14}$$

with Nambu-spinor $\bar{\psi}_{ia}(\tau) = (c_{i\uparrow a}(\tau), c_{i\downarrow a}(\tau), c^\dagger_{i\uparrow a}(\tau), c^\dagger_{i\downarrow a}(\tau))^T$. Bars denote 4×4 matrices in Nambu space:

$$\bar{G}_0^{-1}(\tau,\tau') = \begin{pmatrix} \hat{G}_0^{-1}(\tau,\tau') & 0 \\ 0 & -\hat{\bar{G}}_0^{-1}(\tau',\tau) \end{pmatrix}, \quad \bar{\Sigma}(\tau,\tau') = \begin{pmatrix} \Sigma_{\sigma,\sigma'}(\tau,\tau') & \Phi_{\sigma,\sigma'}(\tau,\tau') \\ \Phi^\dagger_{\sigma,\sigma'}(\tau,\tau') & -\Sigma_{\sigma,\sigma'}(\tau',\tau) \end{pmatrix}. \tag{C.15}$$

Hats here denote 2×2 matrices in the spin-subspace. The bare propagator is given by

$$\hat{G}_0^{-1}(\tau,\tau') = \overbrace{-(\partial_\tau - \mu)}^{[G_0^{(p)}]^{-1}} \delta(\tau-\tau')\,\hat{\sigma}_0, \quad -\hat{\bar{G}}_0^{-1}(\tau,\tau') = \overbrace{-(\partial_\tau + \mu)}^{[G_0^{(h)}]^{-1}} \delta(\tau-\tau')\,\hat{\sigma}_0, \tag{C.16}$$

with $\hat{\sigma}_0$ the identity matrix in the 2 dimensional spin sub-space.
We now perform the Grassmann integral over the Nambu-fermions ψ and the Gaussian over the bosons ϕ. Within the **replica-diagonal ansatz** $\overline{Z^m} = \bar{Z}^m$, we obtain:

$$\begin{aligned}
\frac{S^{\text{eff}}}{N} &= -\frac{1}{2}\mathrm{Tr}\log\left(\bar{G}_0^{-1} - \bar{\Sigma}\right) + \frac{M}{2N}\mathrm{Tr}\log\left(D_0^{-1} - \Pi\right) \\
&- \sum_{\sigma\sigma'}\int d^2\tau G_{\sigma'\sigma}(\tau',\tau)\Sigma_{\sigma\sigma'}(\tau,\tau') + \frac{M}{2N}\int d^2\tau D(\tau',\tau)\Pi(\tau,\tau') \\
&- \frac{1}{2}\sum_{\sigma\sigma'}\int d^2\tau\left(F_{\sigma'\sigma}(\tau'\tau)\Phi^\dagger_{\sigma\sigma'}(\tau,\tau') + F^\dagger_{\sigma'\sigma}(\tau'\tau)\Phi_{\sigma\sigma'}(\tau,\tau')\right) \\
&+ \bar{g}^2\frac{M}{2N}\sum_{\sigma\sigma'}\int d^2\tau\left(G_{\sigma\sigma'}(\tau,\tau')G_{\sigma'\sigma}(\tau',\tau) - F^\dagger_{\sigma\sigma'}(\tau,\tau')F_{\sigma'\sigma}(\tau',\tau)\right)D(\tau,\tau').
\end{aligned} \tag{C.17}$$

In addition, we we work within the **spin-singlet ansatz**

$$\begin{aligned}
G_{\sigma,\sigma'}(\tau,\tau') &= G(\tau,\tau')\hat{\sigma}_0, & \Sigma_{\sigma,\sigma'}(\tau,\tau') &= \Sigma(\tau,\tau')\hat{\sigma}_0, \\
F_{\sigma,\sigma'}(\tau,\tau') &= F(\tau,\tau')\,i\hat{\sigma}_2, & \Phi_{\sigma,\sigma'}(\tau,\tau') &= \Phi(\tau,\tau')\,i\hat{\sigma}_2, \\
F^\dagger_{\sigma,\sigma'}(\tau,\tau') &= -F^\dagger(\tau,\tau')\,i\hat{\sigma}_2, & \Phi^\dagger_{\sigma,\sigma'}(\tau,\tau') &= -\Phi^\dagger(\tau,\tau')\,i\hat{\sigma}_2,
\end{aligned} \tag{C.18}$$

with Pauli matrices $\hat{\sigma}_i$. Here the bi-local fields appearing on the left hand sides are symmetric w.r.t. swapping of time arguments. This allows to perform the sums over spin indices and, noting that $\mathrm{Trlog}(\bar{G}_0^{-1} - \bar{\Sigma}) = 2\mathrm{Trlog}(\hat{G}_0^{-1} - \hat{\Sigma})$, we finally obtain Eq.(6.2) of the main text.

C.2 Hubbard-Stratonovich approach to the SYK effective action

In this appendix we derive the effective action Eq.(C.17) of the Yukawa-SYK model through an alternative method based on the Hubbard-Stratonovich transformation [185].
Let us consider the disorder-averaged effective action Eq.(C.8):

$$\begin{aligned}
S^{\text{eff}} &= \sum_{i\sigma}\int d\tau c_i^\dagger(\tau)(\partial_\tau - \mu)c_i(\tau) + \frac{1}{2}\sum_i\int d\tau\phi_i(\tau)(-\partial_\tau^2 + m_0)\phi_i(\tau) \\
&- \frac{\bar{g}^2}{2N}\sum_{ijk}\int d^2\tau\sum_{\sigma\sigma'}\left(c^\dagger_{j\sigma}(\tau)c^\dagger_{j\sigma'}(\tau')\,c_{i\sigma'}(\tau')c_{i\sigma}(\tau) - c^\dagger_{j\sigma}(\tau)c_{j\sigma'}(\tau')\,c^\dagger_{i\sigma'}(\tau')c_{i\sigma}(\tau)\right)\phi_k(\tau)\phi_k(\tau'),
\end{aligned} \tag{C.19}$$

where, for simplicity, we have suppressed the replica indexes and set $M = N$.

Integrating out bosons

We can rewrite the action as

$$S^{\text{eff}} = \sum_{i\sigma}\int d\tau c^\dagger_{i\sigma}(\tau)(\partial_\tau-\mu)c_{i\sigma}(\tau)+\frac{1}{2}\sum_i\int d^2\tau\phi_i(\tau)\left[D_0^{-1}(\tau-\tau')-W(\tau,\tau')\right]\phi_i(\tau'),$$

with $D_0^{-1}(\tau,\tau')=(-\partial_\tau^2+m_0)\delta(\tau-\tau')$ and

$$W(\tau,\tau')=-\frac{\bar{g}^2}{2N}\sum_{\sigma\sigma'}\left[\left|\sum_i^N c^\dagger_{i\sigma}(\tau)c_{i\sigma'}(\tau')\right|^2-\left(\sum_i^N c^\dagger_{i\sigma}(\tau)c^\dagger_{i\sigma'}(\tau')\right)\left(\sum_i^N c_{i\sigma'}(\tau')c_{i\sigma}(\tau)\right)\right].$$

This is an action quadratic in the bosons and we can therefore perform the integration over ϕ:

$$\int D\phi\, e^{-\frac{1}{2}\phi(D_0^{-1}-W)\phi}=\left[\det\left(D_0^{-1}-W\right)\right]^{-N/2}=e^{-\frac{N}{2}\text{trlog}\left(D_0^{-1}-W\right)}.$$

This gives

$$S^{\text{eff}} = \sum_{i\sigma}\int d\tau c^\dagger_{i\sigma}(\tau)(\partial_\tau-\mu)c_{i\sigma}(\tau)-\frac{N}{2}\text{trlog}D_0+\frac{N}{2}\text{trlog}\left(1-D_0W\right). \tag{C.20}$$

We expand the logarithm as $\log(1-D_0W)=-\sum_{\nu=1}^\infty\frac{1}{\nu}(D_0W)^\nu$. The leading term is:

$$S^{\text{eff}} \approx \sum_{i\sigma}\int d\tau c^\dagger_{i\sigma}(\tau)(\partial_\tau-\mu)c_{i\sigma}(\tau)-\frac{N}{2}\text{trlog}D_0-\frac{N}{2}\int d^2\tau D_0(\tau'-\tau)W(\tau,\tau'). \tag{C.21}$$

Explicitly, the last term is given by

$$\begin{aligned} S_g &= \underbrace{\frac{\bar{g}^2N}{4}\sum_{\sigma\sigma'}\int d^2\tau D_0(\tau'-\tau)\left|\frac{1}{N}\sum_i^N c^\dagger_{i\sigma}(\tau)c_{i\sigma'}(\tau')\right|^2}_{S_{\text{n}}} \\ &- \underbrace{\frac{\bar{g}^2N}{4}\sum_{\sigma\sigma'}\int d^2\tau D_0(\tau'-\tau)\left(\frac{1}{N}\sum_i^N c^\dagger_{i\sigma}(\tau)c^\dagger_{i\sigma'}(\tau')\right)\left(\frac{1}{N}\sum_i^N c_{i\sigma'}(\tau')c_{i\sigma}(\tau)\right)}_{S_{\text{sc}}}. \end{aligned} \tag{C.22}$$

The goal now is to decouple the fermionic bilinears by means of a Hubbard-Stratonovich transformation. Let us start with the normal state contribution S_{n}.

Coordinate change: normal-state term

Let us consider the following term

$$S_Q=\int d^2\tau\, q(\tau-\tau')\left|\tilde{Q}_{\sigma\sigma'}(\tau,\tau')\right|^2, \tag{C.23}$$

where $\tilde{Q}$ is a bi-local field whereas q is a generic regular function. We can always add such a term to the total action since it yields a constant term after Gaussian-integration over $\tilde{Q}$, namely

$$\int \mathcal{D}[c,c^\dagger;\tilde{Q}]e^{-S-\int d^2\tau\, q(\tau-\tau')|\tilde{Q}_{\sigma\sigma'}(\tau,\tau')|^2} = \int \mathcal{D}[c,c^\dagger]e^{-S+\int d^2\tau\sqrt{\pi/q(\tau-\tau')}}.$$

We now perform a field-redefinition in the measure of the partition function according to

$$\tilde{Q}_{\sigma\sigma'}(\tau,\tau') = Q_{\sigma\sigma'}(\tau,\tau') + \frac{1}{q(\tau-\tau')}\frac{1}{N}\sum_i^N c^\dagger_{i\sigma}(\tau)c_{i\sigma'}(\tau'). \tag{C.24}$$

This yields

$$\begin{aligned} S_Q &= \int d^2\tau\; q(\tau-\tau')\left|Q_{\sigma\sigma'}(\tau,\tau')\right|^2 + 2\sum_{\sigma\sigma'}\int d^2\tau\; Q_{\sigma\sigma'}(\tau,\tau')\frac{1}{N}\sum_i^N c^\dagger_{i\sigma}(\tau)c_{i\sigma'}(\tau') \\ &+ \sum_{\sigma\sigma'}\int d^2\tau\frac{1}{q(\tau-\tau')}\left|\frac{1}{N}\sum_i^N c^\dagger_{i\sigma}(\tau)c_{i\sigma'}(\tau')\right|^2. \end{aligned} \tag{C.25}$$

Choosing $\frac{1}{q(\tau-\tau')} = -\frac{\bar{g}^2N}{4}D_0(\tau'-\tau)$, the first line of Eq.(C.22) gets removed. This gives the total action

$$\begin{aligned} S_Q + S_{\rm n} &= -\frac{4}{\bar{g}^2N}\int d^2\tau\frac{1}{D_0(\tau'-\tau)}\left|Q_{\sigma\sigma'}(\tau,\tau')\right|^2 + 2\sum_{\sigma\sigma'}\int d^2\tau\, Q_{\sigma\sigma'}(\tau,\tau')\frac{1}{N}\sum_i^N c^\dagger_{i\sigma}(\tau)c_{i\sigma'}(\tau') \\ &\overset{N\Sigma_{\sigma\sigma'}=2Q_{\sigma\sigma'}}{=} -\frac{N}{\bar{g}^2}\int d^2\tau\frac{1}{D_0(\tau'-\tau)}\left|\Sigma_{\sigma\sigma'}(\tau,\tau')\right|^2 + \sum_{\sigma\sigma'}\int d^2\tau\,\Sigma_{\sigma\sigma'}(\tau,\tau')\sum_i^N c^\dagger_{i\sigma}(\tau)c_{i\sigma'}(\tau'). \end{aligned} \tag{C.26}$$

Coordinate change: superconducting term

We now have to engineer a term like S_Q that cancels the $S_{\rm sc}$ contribution in Eq.(C.22). Let us consider:

$$S_P = \sum_{\sigma\sigma'}\int d^2\tau\; \pi(\tau-\tau')\tilde{P}_{\sigma\sigma'}(\tau,\tau')\left[\tilde{P}_{\sigma\sigma'}(\tau,\tau')\right]^\dagger, \tag{C.27}$$

and shift the new coordinate according to

$$\tilde{P}_{\sigma\sigma'}(\tau,\tau') = P_{\sigma\sigma'}(\tau,\tau') + \frac{1}{\pi(\tau-\tau')}\frac{1}{N}\sum_i^N c^\dagger_{i\sigma}(\tau)c^\dagger_{i\sigma'}(\tau'), \tag{C.28a}$$

$$\left[\tilde{P}_{\sigma\sigma'}(\tau,\tau')\right]^\dagger = \left[P_{\sigma\sigma'}(\tau,\tau')\right]^\dagger + \frac{1}{\pi(\tau-\tau')}\frac{1}{N}\sum_i^N c_{i\sigma'}(\tau')c_{i\sigma}(\tau). \tag{C.28b}$$

We get:

$$\begin{aligned} S_P &= \sum_{\sigma\sigma'}\int d^2\tau\ \pi(\tau-\tau')P_{\sigma\sigma'}(\tau,\tau')\left[P_{\sigma\sigma'}(\tau,\tau')\right]^\dagger \\ &+ \sum_{\sigma\sigma'}\int d^2\tau\left[P_{\sigma\sigma'}(\tau,\tau')\frac{1}{N}\sum_i^N c^\dagger_{i\sigma}(\tau)c^\dagger_{i\sigma'}(\tau')+\left[P_{\sigma\sigma'}(\tau,\tau')\right]^\dagger\frac{1}{N}\sum_i^N c_{i\sigma'}(\tau')c_{i\sigma}(\tau)\right] \\ &+ \sum_{\sigma\sigma'}\int d^2\tau\frac{1}{\pi(\tau-\tau')}\frac{1}{N^2}\sum_i^N c^\dagger_{i\sigma}(\tau)c^\dagger_{i\sigma'}(\tau')\sum_i^N c_{i\sigma'}(\tau')c_{i\sigma}(\tau). \end{aligned} \tag{C.29}$$

Choosing $\frac{1}{\pi(\tau-\tau')}=\frac{\bar{g}^2N}{4}D_0(\tau'-\tau)$ we finally obtain:

$$\begin{aligned} S_P+S_{\rm sc} &= \frac{4}{\bar{g}^2N}\int d^2\tau\frac{1}{D_0(\tau'-\tau)}P_{\sigma\sigma'}(\tau,\tau')\left[P_{\sigma\sigma'}(\tau,\tau')\right]^\dagger \\ &+\sum_{\sigma\sigma'}\int d^2\tau\left[P_{\sigma\sigma'}(\tau,\tau')\frac{1}{N}\sum_i^N c^\dagger_{i\sigma}(\tau)c^\dagger_{i\sigma'}(\tau')+\left[P_{\sigma\sigma'}(\tau,\tau')\right]^\dagger\frac{1}{N}\sum_i^N c_{i\sigma'}(\tau')c_{i\sigma}(\tau)\right] \\ &\overset{N\Phi_{\sigma\sigma'}=2P_{\sigma\sigma'}}{=}\frac{N}{\bar{g}^2}\int d^2\tau\frac{1}{D_0(\tau'-\tau)}\Phi_{\sigma\sigma'}(\tau,\tau')\left[\Phi_{\sigma\sigma'}(\tau,\tau')\right]^\dagger \\ &+\frac{1}{2}\sum_{\sigma\sigma'}\int d^2\tau\left[\Phi_{\sigma\sigma'}(\tau,\tau')\sum_i^N c^\dagger_{i\sigma}(\tau)c^\dagger_{i\sigma'}(\tau')+\left[\Phi_{\sigma\sigma'}(\tau,\tau')\right]^\dagger\sum_i^N c_{i\sigma'}(\tau')c_{i\sigma}(\tau)\right]. \end{aligned} \tag{C.30}$$

Putting all together we find the action

$$\begin{aligned} S^{\rm eff} &= \sum_{i\sigma}\int d\tau c^\dagger_{i\sigma}(\tau)(\partial_\tau-\mu)c_{i\sigma}(\tau)-\frac{N}{2}{\rm trlog}D_0 \\ &- \frac{N}{\bar{g}^2}\sum_{\sigma\sigma'}\int d^2\tau\frac{1}{D_0(\tau'-\tau)}\left[\left|\Sigma_{\sigma\sigma'}(\tau,\tau')\right|^2-\Phi_{\sigma\sigma'}(\tau,\tau')\left[\Phi_{\sigma\sigma'}(\tau,\tau')\right]^\dagger\right] \\ &+ \sum_{\sigma\sigma'}\int d^2\tau\,\Sigma_{\sigma\sigma'}(\tau,\tau')\sum_i^N c^\dagger_{i\sigma}(\tau)c_{i\sigma'}(\tau') \\ &+ \frac{1}{2}\sum_{\sigma\sigma'}\int d^2\tau\left[\Phi_{\sigma\sigma'}(\tau,\tau')\sum_i^N c^\dagger_{i\sigma}(\tau)c^\dagger_{i\sigma'}(\tau')+\left[\Phi_{\sigma\sigma'}(\tau,\tau')\right]^\dagger\sum_i^N c_{i\sigma'}(\tau')c_{i\sigma}(\tau)\right]. \end{aligned} \tag{C.31}$$

Through this procedure we have removed the quartic terms in the fermions of Eq.(C.22) as desired. However, to do so we had to insert new degrees of freedom Φ and Σ. Since the above action is now quadratic in the fermions we can apply the Gaussian integration over Nambu-Grassman spinors as we did in Eq.(C.14). This gives:

$$\begin{aligned} S^{\rm eff} &= -\frac{N}{2}{\rm Trlog}\left[\bar{G}_0^{-1}-\bar{\Sigma}\right]-\frac{N}{2}{\rm trlog}D_0 \\ &- \frac{N}{\bar{g}^2}\sum_{\sigma\sigma'}\int d^2\tau\frac{1}{D_0(\tau'-\tau)}\left[\left|\Sigma_{\sigma\sigma'}(\tau,\tau')\right|^2-\Phi_{\sigma\sigma'}(\tau,\tau')\left[\Phi_{\sigma\sigma'}(\tau,\tau')\right]^\dagger\right]. \end{aligned} \tag{C.32}$$

Here bars denote 4×4 matrices in Nambu space

$$\bar{G}_0^{-1}(\tau,\tau') = \begin{pmatrix} \hat{G}_0^{-1}(\tau,\tau') & 0 \\ 0 & -\hat{\bar{G}}_0^{-1}(\tau',\tau) \end{pmatrix}, \quad \bar{\Sigma}(\tau,\tau') = \begin{pmatrix} \Sigma_{\sigma,\sigma'}(\tau,\tau') & \Phi_{\sigma,\sigma'}(\tau,\tau') \\ \Phi^\dagger_{\sigma,\sigma'}(\tau,\tau') & -\Sigma_{\sigma,\sigma'}(\tau',\tau) \end{pmatrix}.$$

So far we have only included the first term in the expansion of the logarithm in Eq.(C.21). A diagrammatic analysis demonstrates that at leading order in $1/N$ higher order processes will only renormalize the bosonic propagator according to

$$D_0^{-1} \mapsto D^{-1} = D_0^{-1} - \Pi, \tag{C.33}$$

with $\Pi(\tau) = -4\bar{g}^2 \sum_{\sigma\sigma'} G_{\sigma\sigma'}(\tau) G_{\sigma'\sigma}(-\tau)$. This gives as total action:

$$\begin{aligned} \frac{S}{N} &= -\frac{1}{2}\mathrm{Tr}\log\left[\bar{G}_0^{-1} - \bar{\Sigma}\right] + \frac{1}{2}\mathrm{Trlog}\left[D_0^{-1} - \Pi\right] + \frac{1}{2}\int d^2\tau D(\tau',\tau)\Pi(\tau,\tau') \\ &- \frac{1}{\bar{g}^2}\sum_{\sigma\sigma'}\int d^2\tau \frac{1}{D(\tau',\tau)}\left[\Sigma_{\sigma\sigma'}(\tau,\tau')\Sigma_{\sigma'\sigma}(\tau',\tau) - \Phi_{\sigma\sigma'}(\tau,\tau')[\Phi_{\sigma\sigma'}(\tau,\tau')]^\dagger\right]. \end{aligned} \tag{C.34}$$

Note that varying the action with respect to Π ensures Eq.(C.33) is fulfilled. Finally, we can generate the normal and anomalous bi-local fields as consequence of the Gaussian integration over a fields $G(\tau,\tau')$ and $F(\tau,\tau')$:

$$\begin{aligned} \frac{S^{\mathrm{eff}}}{N} &= -\frac{1}{2}\mathrm{Tr}\log\left[\bar{G}_0^{-1} - \bar{\Sigma}\right] + \frac{1}{2}\mathrm{Trlog}\left[D_0^{-1} - \Pi\right] \\ &- \sum_{\sigma\sigma'}\int d^2\tau G_{\sigma'\sigma}(\tau',\tau)\Sigma_{\sigma\sigma'}(\tau,\tau') + \frac{1}{2}\int d^2\tau D(\tau',\tau)\Pi(\tau,\tau') \\ &- \frac{1}{2}\sum_{\sigma\sigma'}\int d^2\tau\left(F_{\sigma'\sigma}(\tau'\tau)\Phi^\dagger_{\sigma\sigma'}(\tau,\tau') + F^\dagger_{\sigma'\sigma}(\tau'\tau)\Phi_{\sigma\sigma'}(\tau,\tau')\right) \\ &+ \frac{\bar{g}^2}{2}\sum_{\sigma\sigma'}\int d^2\tau\left(G_{\sigma\sigma'}(\tau,\tau')G_{\sigma'\sigma}(\tau',\tau) - F^\dagger_{\sigma\sigma'}(\tau,\tau')F_{\sigma'\sigma}(\tau',\tau)\right)D(\tau,\tau'), \end{aligned} \tag{C.35}$$

which is precisely the effective action given in (C.17).

C.3 The higher dimensional Yukawa-SYK model: inter-dot effective action

In this section we derive the effective action for the generalization of the phonon-fermion dot to higher dimensions introduced in Chap. 7. Our primary goal is to derive the disorder-averaged effective action of the model Eq.(7.1). We consider the partition function of the m-replicated

system

$$\overline{Z^m} = \int \mathcal{D}\psi e^{-\sum_a S_0[\psi_a]} \Bigg[\underbrace{\left(\int dg_{ijk,x} \varrho(g_{ijk,x}) e^{-\sum_a S_{\mathrm{g}}[\psi_a]} \right)}_{\mathcal{J}_g} \underbrace{\left(\int dt_{ij,xx'} \varrho(t_{ij,xx'}) e^{-\sum_a S_{\mathrm{t}}[\psi_a]} \right)}_{\mathcal{J}_t} \Bigg], \tag{C.36}$$

where $\varrho(g)$ and $\varrho(t)$ are Gaussian PDF with properties specified in Tab. 6.1 and Eq.(7.2) The strategy is identical to that outlined in Sec. C.1 for the single dot with the additional index x, the fields have to be endowed with. Therefore, we will simply state the result for $\mathcal{J}_g$ at the end, and focus on the inter-dot contribution only.

Inter-dot effective action

The hopping-action reads:

$$S_t = \int d\tau \sum_{\substack{\langle x,x' \rangle \\ ij\sigma a}} t_{ij,xx'} c^\dagger_{j\sigma x' a}(\tau) c_{i\sigma x a}(\tau) \equiv \sum_{\substack{\langle x,x' \rangle \\ ij}} t_{ijxx'} O'_{ijxx'}, \tag{C.37}$$

with $O'_{ijxx'} = \int d\tau \sum_{\sigma,a} c^\dagger_{j\sigma x' a}(\tau) c_{i\sigma x a}(\tau)$. Here i, j are flavour indices, σ denotes spin, a replica, and x, x' are site indices which are assumed to be nearest neighbor. With the same logic of Eq.(C.5) we perform the Gaussian integral and get:

$$\begin{aligned}
\mathcal{J}_t &= \int dt_{ijxx'}\, \varrho(t_{ijxx'}) e^{-S_t} = \exp\left[\frac{t_0^2}{4N} \sum_{\substack{\langle x,x' \rangle \\ ij}} \left(O'_{ijxx'} O'_{ijxx'} + O'_{ijxx'} O'^\dagger_{ijxx'} \right) \right] \\
&= \exp\left[\frac{t_0^2}{4N} \sum_{\langle x,x' \rangle} \sum_{\sigma\sigma' ab} \int d^2\tau \left(c^\dagger_{j\sigma x' a}(\tau) c_{i\sigma x a}(\tau) c^\dagger_{j\sigma' x' b}(\tau') c_{i\sigma' x b}(\tau') + c^\dagger_{j\sigma x' a}(\tau) c_{i\sigma' x b}(\tau') c^\dagger_{i\sigma x a}(\tau) c_{j\sigma' x' b}(\tau') \right) \right].
\end{aligned}$$

We now introduce the spatial-dependent version of the bilocal fields in Eq.(6.3)

$$G_{\sigma\sigma',x}(\tau,\tau') = \frac{1}{N} \sum_i c^\dagger_{i\sigma' x}(\tau') c_{i\sigma x}(\tau), \quad F_{\sigma\sigma',x}(\tau,\tau') = \frac{1}{N} \sum_i c_{i\sigma' x}(\tau') c_{i\sigma x}(\tau), \tag{C.38a}$$

$$D_{ab,x}(\tau,\tau') = \frac{1}{N} \sum_i \phi_{ix}(\tau') \phi_{ix}(\tau). \tag{C.38b}$$

Assuming replica-diagonal fields $\overline{Z^m} = \bar{Z}^m$, the effective action then becomes

$$\frac{S_t}{N} = \frac{t_0^2}{4} \sum_{\substack{\langle x,x' \rangle \\ \sigma\sigma'}} \int d^2\tau \left(G_{\sigma'\sigma,x'}(\tau,\tau') G_{\sigma\sigma',x}(\tau',\tau) - F^\dagger_{\sigma'\sigma,x'}(\tau,\tau') F_{\sigma\sigma',x}(\tau',\tau) \right). \tag{C.39}$$

This, together with the single-dot contribution yields the effective action

$$\begin{aligned}\frac{S_g^{\text{eff}}}{N} =& -\frac{1}{2}\sum_x \operatorname{Tr}\log\left(\bar{G}_0^{-1}-\bar{\Sigma}_x\right)+\frac{1}{2}\sum_x \operatorname{Tr}\log\left(D_0^{-1}-\Pi_x\right)\\ &-\sum_{\sigma\sigma',x}\int d\tau d\tau' G_{\sigma'\sigma,x}(\tau',\tau)\Sigma_{\sigma\sigma',x}(\tau,\tau')+\frac{1}{2}\sum_x\int d\tau d\tau' D_x(\tau',\tau)\Pi_x(\tau,\tau')\\ &-\frac{1}{2}\sum_{\sigma\sigma',x}\int d\tau d\tau'\left(F_{\sigma'\sigma,x}(\tau'\tau)\Phi^\dagger_{\sigma\sigma',x}(\tau,\tau')+F^\dagger_{\sigma'\sigma,x}(\tau'\tau)\Phi_{\sigma\sigma',x}(\tau,\tau')\right)\\ &+\frac{\bar{g}^2}{2}\sum_{\sigma\sigma',x}\int d\tau d\tau'\left(G_{\sigma\sigma',x}(\tau,\tau')G_{\sigma'\sigma,x}(\tau',\tau)-F^\dagger_{\sigma\sigma',x}(\tau,\tau')F_{\sigma'\sigma,x}(\tau',\tau)\right)D_x(\tau,\tau')\\ &+\frac{t_0^2}{4}\sum_{\substack{\langle x,x'\rangle\\ \sigma\sigma'}}\int d^2\tau\left(G_{\sigma'\sigma,x'}(\tau,\tau')G_{\sigma\sigma',x}(\tau',\tau)-F^\dagger_{\sigma'\sigma,x'}(\tau,\tau')F_{\sigma\sigma',x}(\tau',\tau)\right).\end{aligned}\tag{C.40}$$

As in the previous chapter, bars denote 4×4 matrices in Nambu space – see e.g. Eq.(C.15). Working under the simplifying assumption of singlet pairing Eq.(C.18), we obtain Eq.(7.3) of the main text.

Complex hopping As an aside, we consider $t\in\mathbb{C}\to t_{ij,xx'}=t^\star_{ji,x'x}$ with Gaussian PDF having the properties.

$$\overline{t'_{ijxx'}t'_{ijyy'}}=\frac{t_0^2}{4N}\left(\delta_{ii'}\delta_{jj'}\delta_{xy}\delta_{x'y'}+\delta_{ij'}\delta_{ji'}\delta_{xy'}\delta_{x'y}\right),\tag{C.41a}$$

$$\overline{t''_{ijxx'}t''_{ijyy'}}=\frac{t_0^2}{4N}\left(\delta_{ii'}\delta_{jj'}\delta_{xy}\delta_{x'y'}-\delta_{ij'}\delta_{ji'}\delta_{xy'}\delta_{x'y}\right).\tag{C.41b}$$

We have

$$\begin{aligned}\mathcal{J}_t=\int dt_{ijxx'}\,\varrho(t_{ijxx'})e^{-S_t}&=\exp\left[\frac{t_0^2}{4N}\sum_{\substack{\langle x,x'\rangle\\ ij}}O_{ijxx'}O^\dagger_{ijxx'}\right]\\ &=\exp\left[\frac{t_0^2}{4N}\sum_{\substack{\langle x,x'\rangle\\ ij}}\left(\sum_{a\sigma}\int d\tau c^\dagger_{j\sigma x'a}(\tau)c_{i\sigma xa}(\tau)\right)\left(\sum_{b\sigma'}\int d\tau' c^\dagger_{i\sigma' xb}(\tau')c_{j\sigma' x'b}(\tau')\right)\right]\\ &=\exp\left[-\frac{t_0^2}{4}N\sum_{\langle x,x'\rangle}\sum_{\sigma\sigma' ab}\int d^2\tau\; G_{ba,\sigma' x,\sigma x'}(\tau',\tau)G_{ab,\sigma\sigma',x}(\tau,\tau')\right].\end{aligned}\tag{C.42}$$

Focusing once again on replica-diagonal solution we find

$$\frac{S_t}{N}=\frac{t_0^2}{4}\sum_{\substack{\langle x,x'\rangle\\ \sigma\sigma'}}\int d\tau d\tau' G_{\sigma'\sigma,x'}(\tau,\tau')G_{\sigma\sigma',x}(\tau',\tau),\tag{C.43}$$

Notice how the above result follow from Eq.(C.39) after setting $F = 0$. This is consistent with the physical argumentation that a complex hopping destroy time reversal symmetry of the Hamiltonian of the model with consequent disappearance of superconductivity.

C.4 Action for charge fluctuations

In this section we derive the action for charge fluctuations around the saddle point of the higher dimensional SYK model introduced in Chap. 7. For simplicity we re-quote here the term of the disorder averaged effective action which is affected by the U(1) transformations Eq.(7.10)

$$\frac{S'}{N} = -\sum_x \mathrm{Tr}\log\left(\hat{G}_0^{-1} - \hat{\Sigma}_x\right) + \frac{t_0^2}{2}\sum_{\langle x,x'\rangle}\int d^2\tau \left(G_x(\tau_1,\tau_2)G_{x'}(\tau_1,\tau_2) - F_x^\dagger(\tau_1,\tau_2)F_{x'}(\tau_2,\tau_1)\right).$$

Using the U(1) ansatz Eq.(7.10), we would get exponential pre-factors in front of the self energy matrix. To remove these factors we make a step back and consider the action before Grassmann integration over Nambu spinor, i.e. the analogue of Eq.(C.14) of the previous chapter. We have:

$$\int d^2\tau\ \hat{\psi}_x^\dagger(\tau_1)\hat{\Sigma}_x\left(\tau_1,\tau_2\right)\hat{\psi}_x(\tau_2) = \int d^2\tau_1\ \hat{\psi}_x^\dagger(\tau_1)e^{i\varphi_x(\tau_1)\hat{\sigma}_z}\hat{\Sigma}\left(\tau_1-\tau_2\right)e^{-i\varphi_x(\tau_2)\hat{\sigma}_z}\hat{\psi}_x(\tau_2),$$

where $\hat{\psi}_x^t(\tau) = (c_{i\uparrow x}(\tau), c_{i\downarrow x}^\dagger(\tau))$. We exploit the U(1)-gauge freedom enjoyed by the Nambu spinor in order to remove the exponential factor. We consider the following definition

$$\hat{\psi}_x(\tau) \quad = \quad e^{i\varphi_x(\tau)\hat{\sigma}_z}\underbrace{\begin{pmatrix}\gamma_{i\uparrow x}(\tau)\\ \gamma_{i\downarrow x}^\dagger(\tau)\end{pmatrix}}_{\hat{\gamma}_x(\tau)}. \tag{C.44}$$

The free propagator term instead reads

$$\int d^2\tau\ \hat{\psi}_x^\dagger(\tau_1)\hat{G}_0^{-1}\left(\tau_1-\tau_2\right)\hat{\psi}_x(\tau_2) \quad = \quad \int d^2\tau\ \hat{\gamma}_x^\dagger(\tau_1)e^{-i\varphi_x(\tau_1)\hat{\sigma}_z}\hat{G}_0^{-1}\left(\tau_1-\tau_2\right)e^{i\varphi_x(\tau_2)\hat{\sigma}_z}\hat{\gamma}_x(\tau_2).$$

Explicitly, we get:

$$\begin{aligned} e^{-i\varphi_x(\tau_1)\hat{\sigma}_z}\hat{G}_0^{-1}\left(\tau_1-\tau_2\right)e^{i\varphi_x(\tau_2)\hat{\sigma}_z} &= e^{-i\varphi_x(\tau_1)\hat{\sigma}_z}\begin{pmatrix}-(\partial_{\tau_1}-\mu)\delta_{\tau_1\tau_2} & 0\\ 0 & -(\partial_{\tau_1}+\mu)\delta_{\tau_1\tau_2}\end{pmatrix}e^{i\varphi_x(\tau_2)\hat{\sigma}_z}\\ &= \begin{pmatrix}-(\partial_{\tau_1}+i\dot{\varphi}_x-\mu)\delta_{\tau_1\tau_2} & 0\\ 0 & -\left(\partial_{\tau_1}-i\dot{\varphi}_x+\mu\right)\delta_{\tau_1\tau_2}\end{pmatrix}, \end{aligned}$$

where we have used the notation $\delta_{\tau_1\tau_2} = \delta(\tau_1-\tau_2)$. The gauge transformation Eq.(C.44) shifts the chemical potential as $\mu \mapsto \mu - i\dot{\varphi}_x$. Eventually, we obtain:

$$\int d^2\tau\ \hat{\psi}_x^\dagger(\tau_1)\hat{G}_0^{-1}\left(\tau_1-\tau_2\right)\hat{\psi}_x(\tau_2) \quad = \quad \int d^2\tau\ \hat{\gamma}_x^\dagger(\tau_1)\left(\hat{G}_0^{-1}\left(\tau_1-\tau_2\right) - i\partial_\tau\hat{\varphi}_x(\tau_1-\tau_2)\right)\hat{\gamma}_x(\tau_2),$$

where we have introduced $\partial_\tau \hat{\varphi}_x(\tau_1 - \tau_2) = \dot{\varphi}_x \hat{\sigma}_z \delta(\tau_1 - \tau_2)$.
Trace-log term: let us tackle the trace-log term in Eq.(7.12) first. We have:

$$\mathrm{Trlog}\left[\hat{G}_0^{-1} - i\partial_\tau \hat{\varphi}_x - \hat{\Sigma}_x\right] \quad = \quad \mathrm{Tr}\log\left[\hat{G}^{-1} - i\partial_\tau \hat{\varphi}_x\right],$$

where we employed the Dyson equation Eq.(7.5). In the next we perform a φ-expansion and equate the trace over imaginary time and Nambu sub-spaces:

$$\begin{aligned}
\mathrm{Tr}\log\left[\hat{G}^{-1} - i\partial_\tau \hat{\varphi}_x\right] &= \mathrm{Tr}\log\left(\hat{G}^{-1}\right) + \mathrm{Tr}\log\left(1 - i\hat{G}\partial_\tau \hat{\varphi}_x\right) \\
&\approx \text{const} + \frac{1}{2}\mathrm{Tr}\left[\hat{G}\partial_\tau \hat{\varphi}_x \hat{G}\partial_\tau \hat{\varphi}_x\right] \\
&\overset{\tau-\mathrm{tr}}{=} \text{const} + \frac{1}{2}\int d^4\tau\, \mathrm{Tr}_\mathrm{N}\left[\hat{G}(\tau_1 - \tau_2)\partial_\tau \hat{\varphi}(\tau_2 - \tau_3)\hat{G}(\tau_3 - \tau_4)\partial_\tau \hat{\varphi}(\tau_4 - \tau_1)\right] \\
&= \text{const} + \frac{1}{2}\int d^2\tau\, \mathrm{Tr}_\mathrm{N}\left[\hat{G}(\tau_1 - \tau_2)\hat{\sigma}_z \hat{G}(\tau_2 - \tau_1)\hat{\sigma}_z\right] \dot{\varphi}_x(\tau_1)\dot{\varphi}_x(\tau_2),
\end{aligned}$$

where we have grouped in "const" all the terms independent on φ. Using the explicit expression for the Nambu propagator Eq.(6.5), we obtain

$$\mathrm{Tr}_\mathrm{N}\left[\hat{G}(\tau_1 - \tau_2)\hat{\sigma}_z \hat{G}(\tau_2 - \tau_1)\hat{\sigma}_z\right] = 2G(\tau_1 - \tau_2)G(\tau_2 - \tau_1) - 2F(\tau_1 - \tau_2)F^\dagger(\tau_2 - \tau_1),$$

where we have used the symmetry of the anomalous propagator F under time-arguments swapping. The trace-log action is therefore given by:

$$\mathrm{Trlog}\left[\hat{G}_0^{-1} - i\partial_\tau \hat{\varphi}_x - \hat{\Sigma}_x\right] = \int d^2\tau \dot{\varphi}_x(\tau_1)\Pi_-(\tau_1 - \tau_2)\dot{\varphi}_x(\tau_2), \tag{C.45}$$

with

$$\Pi_\pm(\tau) = \Pi_G(\tau) \pm \Pi_F(\tau), \tag{C.46a}$$
$$\Pi_G(\tau) = G(\tau)G(-\tau), \tag{C.46b}$$
$$\Pi_F(\tau) = F(\tau)F^\dagger(-\tau). \tag{C.46c}$$

Hopping term: we now focus on the hopping part of the effective action Eq.(7.12)

$$\frac{S_2'}{N} = \frac{t_0^2}{2}\sum_{\langle x,x'\rangle}\int d^2\tau \left(G_x(\tau_1,\tau_2)G_{x'}(\tau_2,\tau_1) - F_x^\dagger(\tau_1,\tau_2)F_{x'}(\tau_2,\tau_1)\right). \tag{C.47}$$

It is useful to introduce the notion of gradient:

$$\varphi_x(\tau) - \varphi_{x'}(\tau) \equiv \nabla_x \varphi(\tau) a. \tag{C.48}$$

Here $a = x - x'$ is the displacement between two neighbor sites that we have taken to be the same for every sites. Moreover, the above expression is valid for small displacements only. Let

us Taylor-expand w.r.t. φ

$$\begin{aligned}\frac{2S_2'}{t_0^2 N} &= \sum_{\langle x,x'\rangle}\int d^2\tau\Big(G(\tau_1-\tau_2)G(\tau_2-\tau_1)\,e^{i(\nabla_x\varphi(\tau_1)-\nabla_x\varphi(\tau_2))a} \\ &\qquad - F^\dagger(\tau_1-\tau_2)F(\tau_2-\tau_1)\,e^{-i(\nabla_x\varphi(\tau_1)+\nabla_x\varphi(\tau_2))a}\Big) \\ &\approx -\frac{1}{2}\sum_{\langle x,x'\rangle}\int d^2\tau\Big(G(\tau_1-\tau_2)G(\tau_2-\tau_1)\left[(\nabla_x\varphi(\tau_1)a)^2-2(\nabla_x\varphi(\tau_1)a)(\nabla_x\varphi(\tau_2)a)+(\nabla_x\varphi(\tau_2)a)^2\right] \\ &\qquad - F^\dagger(\tau_1-\tau_2)F(\tau_2-\tau_1)\left[(\nabla_x\varphi(\tau_1)a)^2+2(\nabla_x\varphi(\tau_1)a)(\nabla_x\varphi(\tau_2)a)+(\nabla_x\varphi(\tau_2)a)^2\right]\Big) \\ &= -\sum_p \epsilon(p)\int d^2\tau\Big[\Pi_-(\tau_1-\tau_2)(\varphi_p(\tau_1)\varphi_{-p}(\tau_1)+\varphi_p(\tau_2)\varphi_{-p}(\tau_2))-2\Pi_+(\tau_1-\tau_2)\varphi_p(\tau_1)\varphi_{-p}(\tau_2)\Big].\end{aligned} \tag{C.49}$$

In the last step we Fourier transformed the phase field to momentum space $\varphi(\tau,x) = \sum_p \varphi_p(\tau)e^{ipx}$. In the above expression we have defined $\epsilon(p) = \frac{1}{2}\sum_{x'\text{near }x}(\vec{p}\cdot\vec{a})^2$,which in the case of isotropic Bravais lattices with unit spacing, is simply given by $\epsilon(p) = |\mathbf{p}|^2$. After some algebra we can rewrite it as

$$\frac{S_2'}{N} = -\sum_p \epsilon(p)\int d^2\tau\ \varphi_p(\tau_1)L(\tau_1-\tau_2)\varphi_{-p}(\tau_2), \tag{C.50}$$

with

$$L(\tau) = t_0^2\Big(\delta(\tau)\int_{-\beta}^{\beta} d\bar{\tau}\Pi_-(\bar{\tau}) - \Pi_+(\tau)\Big). \tag{C.51}$$

We finally switch to Matsubara frequencies using the following conventions

$$\varphi_p(\tau) = T\sum_{\epsilon_n} e^{-i\epsilon_n\tau}\varphi_{p\epsilon_n}, \tag{C.52a}$$

$$\varphi_{p\epsilon_n} = \frac{1}{2}\int d\tau e^{i\epsilon_n\tau}\varphi_p(\tau), \tag{C.52b}$$

and get the total effective action for the phase mode Eq.(7.13) of the main text. The Fourier transform of Eq.(C.51) is given by

$$\begin{aligned}L(i\epsilon_n) &= \frac{1}{2}\int_{-\beta}^{\beta} d\tau e^{i\epsilon_n\tau}L(\tau) = \frac{t_0^2}{2}\left(\int d\tau\Pi_-(\tau) - \int d\tau e^{i\epsilon_n\tau}\Pi_+(\tau)\right) \\ &= \frac{t_0^2}{2}\left(\int d\tau\Pi_G(\tau)\left(1-e^{i\epsilon_n\tau}\right) - \Pi_F(\tau)\left(1+e^{i\epsilon_n\tau}\right)\right) \\ &= \frac{t_0^2}{2}\left[\Pi_G(0)-\Pi_G(i\epsilon_n)-\Pi_F(0)-\Pi_F(i\epsilon_n)\right] \qquad \text{(C.53)} \\ &\approx -\frac{t_0^2}{2}\left(2\int d\tau\Pi_F(\tau) + i\epsilon_n\int d\tau\Pi_+(\tau)\right) + O(\epsilon_n^2). \qquad \text{(C.54)}\end{aligned}$$

From the last line it is clear that the low frequency behavior of the transport correlator $L_{\mathbb{R}\epsilon_n}$ is non-vanishing provided that $\int d\tau\Pi_F(\tau) \neq 0$.

Appendix D

The superconducting kernel

In this appendix we analyze the electromagnetic response of a conductor to external scalar and vector potentials. Our main goal is to identify a quantity suitable to test superconductivity of the extended SYK model introduced in Chap. 7.
We start from the Maxwell equations for the electric and magnetic fields:

$$\begin{aligned} \nabla \cdot \mathbf{E} &= 4\pi\rho_{\text{tot}}, \\ \nabla \times \mathbf{B} &= \frac{4\pi}{c}\mathbf{j}_{\text{tot}} + \frac{1}{c}\partial_t \mathbf{E}, \end{aligned} \tag{D.1}$$

where c is the speed of light. Here ρ_{tot} and $\mathbf{j}_{\text{tot}}$ are the total charge and current densities. It is useful to introduce the displacement field $\mathbf{D}$ and the magnetizing field $\mathbf{H}$ which are sourced by external charges and currents

$$\begin{aligned} \nabla \cdot \mathbf{D} &= 4\pi\rho_{\text{ext}}, \\ \nabla \times \mathbf{H} &= \frac{4\pi}{c}\mathbf{j}_{\text{ext}} + \frac{1}{c}\partial_t \mathbf{D}. \end{aligned} \tag{D.2}$$

These auxiliary fields are related to the total ones via constitutive relations $D_\alpha = \epsilon_{\alpha\beta}E_\beta$ and $H_\alpha = \mu^{-1}_{\alpha\beta}B_\beta$, where $\epsilon_{\alpha\beta}$ and $\mu_{\alpha\beta}$ are the dielectric and magnetic permeability tensors respectively.
The intrinsic electromagnetic response of the system is encoded into the polarization $\mathbf{P}$ and the magnetization $\mathbf{M}$, defined via $\mathbf{D} = \mathbf{E} + 4\pi\mathbf{P}$ and $\mathbf{H} = \mathbf{B} - 4\pi\mathbf{M}$. We can therefore rewrite the Maxwell equations using the induced densities only:

$$\begin{aligned} \delta\rho &\equiv \rho_{\text{tot}} - \rho_{\text{ext}} = -\nabla \cdot \mathbf{P}, \\ \delta\mathbf{j} &\equiv \mathbf{j}_{\text{tot}} - \mathbf{j}_{\text{ext}} = \partial_t \mathbf{P} + c\nabla \times \mathbf{M}. \end{aligned} \tag{D.3}$$

Using the constitutive relations, we can express the induced densities in terms of $\mathbf{E}$ and $\mathbf{B}$:

$$\delta\rho = -iq_\alpha P_\alpha = -\frac{i}{4\pi}q_\alpha(\epsilon_{\alpha\beta} - \delta_{\alpha\beta})E_\beta,$$

$$\delta j_\alpha = -i\omega P_\alpha + ic\varepsilon_{\alpha\beta\gamma}q_\beta M_\gamma \tag{D.4}$$

$$= -\frac{i}{4\pi}\omega(\epsilon_{\alpha\beta} - \delta_{\alpha\beta})E_\beta + \frac{i}{4\pi}c\,\varepsilon_{\alpha\beta\gamma}q_\beta\left(\delta_{\gamma\delta} - \mu^{-1}_{\gamma\delta}\right)B_\delta, \tag{D.5}$$

where we have performed the Fourier transformation to frequency and momentum space. The magnetic and electric fields can be then expressed in terms of potentials, i.e. $E_\alpha = -iq_\alpha\phi + i\frac{\omega}{c}A_\alpha$ and $B_\alpha = i\varepsilon_{\alpha\beta\gamma}q_\beta A_\gamma$. It is convenient to write the vector potential as

$$A_\alpha \;=\; \frac{q_\alpha}{q}A_l + A_{t,\alpha},$$

where $A_l = \frac{\mathbf{q}\cdot\mathbf{A}}{q}$ is the longitudinal component and $A_{t,\alpha} = A_\alpha - \frac{q_\alpha}{q}A_t$ are the transversal components of $\mathbf{A}$ with respect to the incident momentum $\mathbf{q}$.
We obtain:

$$\delta\rho \;=\; \frac{1-\epsilon_l}{4\pi}q^2\Big(\phi - \frac{\omega}{cq}A_l\Big), \tag{D.6}$$

$$\delta j_\alpha \;=\; \frac{1-\epsilon_t}{4\pi}\omega q_\alpha\Big(\phi - \frac{\omega}{cq}A_l\Big) - \frac{1}{4\pi}\Big((1-\epsilon_l)\frac{\omega^2}{c} - (1-\mu_t^{-1})cq^2\Big)A_{t,\alpha}, \tag{D.7}$$

where we have used the following decomposition for the dielectric and magnetic permeability tensors $\epsilon_{\alpha\beta} = \epsilon_l\frac{q_\alpha q_\beta}{|\mathbf{q}|^2} + \epsilon_t\Big(\delta_{\alpha\beta} - \frac{q_\alpha q_\beta}{|\mathbf{q}|^2}\Big)$, and $\mu^{-1}_{\alpha\beta} = \mu_l^{-1}\frac{q_\alpha q_\beta}{|\mathbf{q}|^2} + \mu_t^{-1}\Big(\delta_{\alpha\beta} - \frac{q_\alpha q_\beta}{|\mathbf{q}|^2}\Big)$. The charge response is governed by the longitudinal dielectric function ϵ_l, while the induced current consists of both longitudinal and a transverse contributions.
Written in terms of charge compressibility χ and electrodynamic kernel $\mathcal{K}$ [216], the above relations become

$$\delta\rho(\mathbf{q},\omega) \;=\; -\chi(\mathbf{q},\omega)\Big(\phi(\mathbf{q},\omega) - \frac{\omega}{cq}A_l(\mathbf{q},\omega)\Big), \tag{D.8}$$

$$\begin{aligned}\delta j_\alpha(\mathbf{q},\omega) \;&=\; \mathcal{K}_{\alpha\beta}(\mathbf{q},\omega)\Big(A_\beta(\mathbf{q},\omega) - q_\beta\frac{c}{\omega}\phi(\mathbf{q},\omega)\Big)\\ &=\; \frac{q_\alpha}{q}\mathcal{K}_l(\mathbf{q},\omega)\Big(A_l(\mathbf{q},\omega) - \frac{cq}{\omega}\phi(\mathbf{q},\omega)\Big) + \mathcal{K}_t(\mathbf{q},\omega)A_{t,\alpha}(\mathbf{q},\omega).\end{aligned} \tag{D.9}$$

Here, the combinations of the vector and scalar potentials are all gauge invariant, i.e. do not change when we substitute $A_\alpha \mapsto A_\alpha - iq_\alpha\Lambda$ and $\phi \mapsto \phi - i\frac{\omega}{c}\Lambda$, where Λ is a smooth function. The advantage of such a rewriting is that, in some cases, the response functions χ and $\mathcal{K}$ can be derived straightfowordly from the field-theoretical action – see e.g. Chap.7.
Comparing Eqs.(D.6) and (D.8) we find that $\epsilon_l = 1 + 4\pi\chi$. On the other hand, from (D.7) it follow shat $\epsilon_l = 1 + \frac{4\pi c}{\omega^2}\mathcal{K}_l$. This allows us to identify

$$\chi(\mathbf{q},\omega) = \frac{cq^2}{\omega^2}\mathcal{K}_l(\mathbf{q},\omega). \tag{D.10}$$

Since moreover the longitudinal electric conductivity is given by $\sigma_l = \frac{-i\omega}{q^2}\chi$, it holds that

$$\sigma_l(\mathbf{q},\omega) = c\frac{\mathcal{K}_l(\mathbf{q},\omega)}{i\omega}. \tag{D.11}$$

Finally, we obtain for the transverse current response:

$$\frac{1}{4\pi}\left[(1-\mu_t^{-1}(\mathbf{q},\omega))c\,q^2 - \Big(1-\epsilon_t(\mathbf{q},\omega)\Big)\frac{\omega^2}{c}\right] = \mathcal{K}_t(\mathbf{q},\omega). \tag{D.12}$$

Hence, the knowledge of $\mathcal{K}_t$ does not determine independently the transverse permeability and the transverse dielectric response. However, if we consider homogeneous processes we have

$$\epsilon_t(\mathbf{0},\omega) = 1 + \frac{4\pi c}{\omega^2}\mathcal{K}_t(\mathbf{0},\omega). \tag{D.13}$$

On the other hand, for static processes we find for the permeability

$$\mu_t^{-1}(\mathbf{q},0) = 1 - \frac{4\pi}{c}\frac{\mathcal{K}_t(\mathbf{q},0)}{q^2}. \tag{D.14}$$

This last identity helps in establishing whether the magnetic field get expelled from the interior of the system. This phenomenon occurs in type-I superconductor and in type-II below the lower critical field and is known as Meissner effect. It corresponds to a vanishing permeability $\mu_{\alpha\beta} = 0$. Hence, $\mathcal{K}_t(\mathbf{q} \to 0, 0)$ should vanish slower than q^2. Consider a static configuration ($\omega = 0$) for which $q^2 A_{t,\alpha} = \frac{4\pi}{c}(j_{\text{ext},\alpha} + \delta j_\alpha)$. From Eq.(D.7) it follows that

$$A_{t,\alpha} = \frac{4\pi}{c}\frac{j_{\text{ext},\alpha}}{q^2 - \mathcal{K}_t(\mathbf{q},0)}, \tag{D.15}$$

which yields for the magnetic field

$$\mathbf{B}(\mathbf{r}) = \frac{4\pi}{c}\int \frac{d\mathbf{q}}{(2\pi)^3}\frac{i\mathbf{q}\times\mathbf{j}_{\text{ext}}}{q^2 - \mathcal{K}_t'(\mathbf{q},0)}e^{i\mathbf{q}\cdot\mathbf{r}}. \tag{D.16}$$

The characteristic length scale of the decay of the magnetic field near the surface is therefore given by

$$\lambda^{-2} = \frac{4\pi}{c}\rho_s = -\lim_{\mathbf{q}\to 0}\mathcal{K}_t'(\mathbf{q},\omega=0) \tag{D.17}$$

where ρ_s denotes the superconducting phase stiffness.

Appendix E

Details on the derivation of the holographic action from SYK

E.1 Fourier transformation over relative and absolute times

In this section we manipulate the effective action of the Yukawa SYK Eq.(6.1) model which contains only the superconducting degrees of freedom. For simplicity we re-quote it here

$$S^{(\mathrm{sc})} \approx \widetilde{G}_{\mathrm{n}} \otimes \Phi^{\dagger} \otimes G_{\mathrm{n}} \otimes \Phi - \frac{\bar{g}^2 \lambda_p}{2} (F^{\dagger} F) \otimes D_{\mathrm{n}} - F^{\dagger} \otimes \Phi - F \otimes \Phi^{\dagger}. \tag{E.1}$$

In the following we perform Fourier transformation over absolute and relative times $\frac{\tau+\tau'}{2}$ and $\tau - \tau'$.

Let us focus on the first term. It is given by

$$\begin{aligned} S_1^{(\mathrm{sc})} &= -\int d^4\tau G_{\mathrm{n}}(\tau_2 - \tau_1)\Phi^{\star}(\tau_3, \tau_2) G_{\mathrm{n}}(\tau_3 - \tau_4)\Phi(\tau_4, \tau_1) \\ &\mapsto -\int d^4\tau G_{\mathrm{n}}(\tau_2 - \tau_1) G_{\mathrm{n}}(\tau_3 - \tau_4)\Phi^{\star}\Big(\frac{\tau_2 + \tau_3}{2}, \tau_3 - \tau_2\Big)\Phi\Big(\frac{\tau_1 + \tau_4}{2}, \tau_4 - \tau_1\Big), \end{aligned} \tag{E.2}$$

where in the last passage we have expressed the anomalous self energy in terms of the absolute and relative times through a change of variables. This is formally done by introducing a new set of fields e.g. via $\Phi(\tau, \tau') \equiv \tilde{\Phi}(\frac{\tau+\tau'}{2}, \tau - \tau')$. Since however both the fields encode the same physics, we use the same symbol to keep the notation lighter.
We now perform Matsubara transformations. In the following we denote with ω absolute frequencies and with ϵ the relative ones. We have:

$$\begin{aligned} S_1^{(\mathrm{sc})} = -\int_{\epsilon\epsilon',\omega\omega',\nu\nu'} & \Phi^{\star}(\omega, \epsilon)\, \Phi(\omega', \epsilon') G_{\mathrm{n}}(\nu) G_{\mathrm{n}}(\nu') \\ & \times \int d^4\tau e^{-i(\nu(\tau_2-\tau_1)+\nu'(\tau_3-\tau_4)-\omega\frac{\tau_2+\tau_3}{2}-\epsilon(\tau_3-\tau_2)+\omega'\frac{\tau_1+\tau_4}{2}+\epsilon'(\tau_4-\tau_1))}. \end{aligned}$$

Working-out the time-integrals yields the following constraints: $\epsilon' = \epsilon,\ \omega' = \omega,\ , \nu = \frac{\omega}{2} - \epsilon,\ \nu' = \frac{\omega}{2} + \epsilon$. This ultimately yields:

$$S_1^{(\mathrm{sc})} = -\int_{\omega\epsilon} d^2\tau\, \Phi^\star\left(\omega,\epsilon\right) \Pi(\omega,\epsilon) \Phi\left(\omega,\epsilon\right), \tag{E.3}$$

with fermion-fermion bubble

$$\Pi(\omega,\epsilon) = G_{\mathrm{n}}\Big(\frac{\omega}{2} - \epsilon\Big) G_{\mathrm{n}}\Big(\frac{\omega}{2} + \epsilon\Big). \tag{E.4}$$

Next we analyze the second term of Eq.(E.1) :

$$\begin{aligned} -\frac{2}{\bar{g}^2\lambda_p} S_2^{(\mathrm{sc})} &= (F^\dagger F) \otimes D_{\mathrm{n}} = \int d^2\tau F^*(\tau_2,\tau_1) F(\tau_1,\tau_2) D_{\mathrm{n}}(\tau_2-\tau_1) \\ &\mapsto \int d^2\tau F^\star\Big(\frac{\tau_1+\tau_2}{2}, \tau_2-\tau_1\Big) F\Big(\frac{\tau_1+\tau_2}{2}, \tau_2-\tau_1\Big) D_{\mathrm{n}}(\tau_2-\tau_1) \\ &= \int_{\omega,\epsilon\epsilon'} F^\star(\omega,\epsilon) F(\omega,\epsilon') D_{\mathrm{n}}(\epsilon-\epsilon'), \end{aligned} \tag{E.5}$$

which is non-local in ϵ-space. Finally, the third term is given by

$$\begin{aligned} -S_3^{(\mathrm{sc})} &= F^\dagger \otimes \Phi + F \otimes \Phi^\dagger \\ &= \int d^2\tau (F^*(\tau_2,\tau_1)\Phi(\tau_2,\tau_1) + (F(\tau_1,\tau_2)\Phi^\star(\tau_1,\tau_2)) \\ &\mapsto \int d^2\tau \Big[F^\star\Big(\frac{\tau_1+\tau_2}{2}, \tau_2-\tau_1\Big)\Phi\Big(\frac{\tau_1+\tau_2}{2}, \tau_2-\tau_1\Big) + F \leftrightarrow \Phi\Big] \\ &= \int_{\omega,\epsilon} \Big[F^\star\left(\omega,\epsilon\right)\Phi\left(\omega,\epsilon\right) + F\left(\omega,\epsilon\right)\Phi^\star\left(\omega,\epsilon\right)\Big]. \end{aligned} \tag{E.6}$$

Globally, we have:

$$\begin{aligned} S^{(\mathrm{sc})} = &-\int_{\omega,\epsilon} \Phi\left(\omega,\epsilon\right)\Pi(\omega,\epsilon)\Phi^\star\left(\omega,\epsilon\right) - \int_{\omega,\epsilon}\Big[F^\star\left(\omega,\epsilon\right)\Phi\left(\omega,\epsilon\right) + F\left(\omega,\epsilon\right)\Phi^\star\left(\omega,\epsilon\right)\Big] \\ &- \frac{\bar{g}^2\lambda_p}{2}\int_{\omega,\epsilon\epsilon'} F^\star\left(\omega,\epsilon\right) F(\omega,\epsilon') D_{\mathrm{n}}(\epsilon-\epsilon'). \end{aligned} \tag{E.7}$$

E.2 Derivation of the holographic action

We are now ready to perform the Gaussian integration over Φ. Let us focus on the first line and consider the partition function

$$\begin{aligned} Z &= \int \mathcal{D}[\Phi,\Phi^\star]\, e^{\int_{\omega,\epsilon}\Phi(\omega,\epsilon)\Pi(\omega,\epsilon)\Phi^\dagger(\omega,\epsilon) + \int_{\omega,\epsilon}\left[F^\star(\omega,\epsilon)\Phi(\omega,\epsilon) + F(\omega,\epsilon)\Phi^\star(\omega,\epsilon)\right]} \\ &= \prod_{\epsilon,\omega}\left(\int d\left[\Phi\left(\omega,\epsilon\right)\Phi^\star\left(\omega,\epsilon\right)\right] e^{\Phi(\omega,\epsilon)\Pi(\omega,\epsilon)\Phi^\dagger(\omega,\epsilon) + F^\star(\omega,\epsilon)\Phi(\omega,\epsilon) + F(\omega,\epsilon)\Phi^\star(\omega,\epsilon)}\right) \\ &= e^{-\int_{\omega,\epsilon}\frac{F^\star(\omega,\epsilon)F(\omega,\epsilon)}{\Pi(\omega,\epsilon)}} \end{aligned} \tag{E.8}$$

This leads to the following Gaussian-in-F action:

$$S^{(\mathrm{sc})}=\int_{\omega,\epsilon}\frac{F^{\star}\left(\omega,\epsilon\right)F\left(\omega,\epsilon\right)}{\Pi(\omega,\epsilon)}-\frac{\bar{g}^{2}\lambda_{p}}{2}\int_{\omega,\epsilon\epsilon'}F^{\star}\left(\omega,\epsilon\right)D_{\mathrm{n}}(\epsilon-\epsilon')F(\omega,\epsilon'). \tag{E.9}$$

We now manipulate the above expression by utilizing the boson and fermion propagators Eq.(8.7), which we re-quote here for simplicity $G_{\mathrm{n}}\left(\epsilon\right)=c_{g}\left(\tan\theta+i\mathrm{sign}\left(\epsilon\right)\right)\left|\epsilon\right|^{-\frac{1-\gamma}{2}}$, $D_{\mathrm{n}}\left(\epsilon\right)=c_{b}\left|\epsilon\right|^{-\gamma}$. We remind that θ parametrizes the deviation from half filling and was defined in Eq.(6.25). Starting from the fermion-fermion bubble Eq.(9.7), we perform a small ω-expansion and obtain:

$$\Pi(\omega,\epsilon) \;=\; c_{g,\theta}^{2}|\epsilon|^{\gamma-1}\left(1+\frac{1-\gamma}{8}\left(\frac{\omega}{\epsilon}\right)^{2}\right)+O(\omega^{2}), \tag{E.10}$$

where $c_{g,\theta}^{2}=c_{g}^{2}(\tan^{2}\theta+1)$. Plugging this into the action gives

$$\int_{\omega,\epsilon}\frac{F^{\star}\left(\omega,\epsilon\right)F\left(\omega,\epsilon\right)}{\Pi(\omega,\epsilon)} \;=\; c_{g,\theta}^{-2}\int_{\omega,\epsilon}F^{\star}\left(\omega,\epsilon\right)\epsilon^{1-\gamma}\left[1-\frac{1-\gamma}{8}\left(\frac{\omega}{\epsilon}\right)^{2}\right]F\left(\omega,\epsilon\right). \tag{E.11}$$

We now use the map Eq.(9.8) of the main text, which we re-quote here for simplicity

$$\tilde{\psi}(\omega,z)=c_{F}z^{\frac{\gamma-1}{2}}F(\omega,c_{z}z^{-1}). \tag{E.12}$$

Employing the identity $\int_{-\infty}^{\infty}\frac{d\epsilon}{2\pi}...=\frac{c_{z}}{\pi}\int_{0}^{\infty}\frac{dz}{z^{2}}$ we find

$$\begin{aligned}\int_{\omega,\epsilon}\frac{F^{\star}\left(\omega,\epsilon\right)F\left(\omega,\epsilon\right)}{\Pi(\omega,\epsilon)} \;&=\; \frac{c_{g,\theta}^{-2}c_{z}^{2-\gamma}}{\pi c_{F}^{2}}\int_{\omega}dz\frac{\tilde{\psi}^{\star}\left(\omega,z\right)\tilde{\psi}\left(\omega,z\right)}{z^{2}}\\ &-\; \frac{1-\gamma}{8\pi c_{F}^{2}}c_{g,\theta}^{-2}c_{z}^{-\gamma}\int_{\omega}dz\omega^{2}\tilde{\psi}^{\star}\left(\omega,z\right)\tilde{\psi}\left(\omega,z\right).\end{aligned} \tag{E.13}$$

Transforming-back to time domain yields

$$\int_{\omega,\epsilon}\frac{F^{\star}\left(\omega,\epsilon\right)F\left(\omega,\epsilon\right)}{\Pi(\omega,\epsilon)}=m_{(1)}^{2}\int_{t,z}\frac{|\tilde{\psi}^{\star}\left(t,z\right)|^{2}}{z^{2}}+A_{t}\int_{t,z}|\partial_{t}\tilde{\psi}\left(t,z\right)|^{2}, \tag{E.14}$$

with $m_{(1)}^{2}=\frac{c_{g,\theta}^{-2}c_{z}^{2-\gamma}}{\pi c_{F}^{2}}$ and $A_{t}=-\frac{1-\gamma}{8\pi c_{F}^{2}}c_{g,\theta}^{-2}c_{z}^{-\gamma}$.
Let us now focus on the non-local term in Eq.(E.9)

$$s_{\mathrm{nl}}\equiv-\frac{2}{c_{b}\bar{g}^{2}\lambda_{p}}S_{\mathrm{nl}} \;=\; \int_{\omega,\epsilon\epsilon'}\frac{F^{\star}\left(\omega,\epsilon\right)F\left(\omega,\epsilon'\right)}{|\epsilon-\epsilon'|^{\gamma}}, \tag{E.15}$$

where we have used the explicit expression for the pairing field $D_{\mathrm{n}}(\epsilon)=c_{b}|\epsilon|^{-\gamma}$. In order to diagonalize such a term we consider the following transformation

$$F(\omega,\epsilon)=\int_{-\infty}^{\infty}\frac{d\xi}{\sqrt{2\pi}}f_{\xi}(\omega)|\epsilon|^{i\xi}|\epsilon|^{-1+\gamma/2}. \tag{E.16}$$

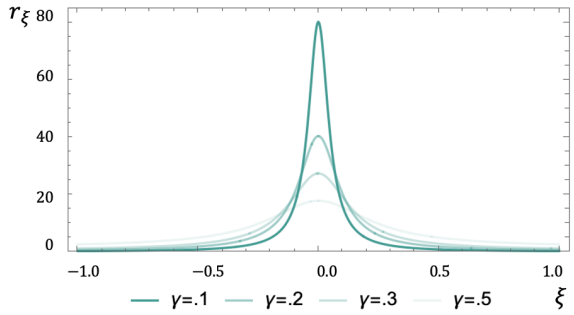

Figure E.1: Behavior of the integral $r(\xi)$ in Eq.(E.19) for several values of the γ-exponent. The bell shape around $\xi = 0$ becomes a delta-function in the $\gamma \to 0$ limit.

This is a Fourier expansion with respect to $\log \xi$, also known as Mellin transformation – see e.g. Ref.[217]. We have

$$s_{\rm nl} = \frac{1}{2\pi} \int_{\omega,\epsilon\epsilon',\xi\xi'} f^\star_{\xi'}(\omega) f_\xi(\omega) \frac{|\epsilon|^{-i\xi'} |\epsilon|^{-1+\gamma/2} |\epsilon'|^{i\xi} |\epsilon'|^{-1+\gamma/2}}{|\epsilon - \epsilon'|^\gamma}. \tag{E.17}$$

We now introduce an auxiliary variable $x = \epsilon'/\epsilon$

$$\begin{aligned} s_{\rm nl} &= \frac{1}{(2\pi)^2} \int_{\omega,\epsilon,\xi\xi'} f^\star_{\xi'}(\omega) f_\xi(\omega) \frac{|\epsilon|^{i(\xi-\xi')}}{|\epsilon|} \int_x \frac{|x|^{i\xi}}{|1-x|^\gamma |x|^{1-\gamma/2}} \\ &= \frac{1}{4\pi^3} \int_{\omega,\xi\xi'} r_\xi f^\star_{\xi'}(\omega) f_\xi(\omega) \int d(\log\epsilon) e^{i(\xi-\xi')(\log\epsilon)} \\ &= \frac{1}{2\pi^2} \int_{\omega,\xi} r_\xi f^\star_\xi(\omega) f_\xi(\omega). \end{aligned} \tag{E.18}$$

Here

$$r_\xi = \int_x \frac{|x|^{i\xi}}{|1-x|^\gamma |x|^{1-\gamma/2}}, \tag{E.19}$$

and is bell-shaped around $\xi = 0$ and becomes a Dirac delta for small γ –see Fig.E.1. In conclusion, the non-local contribution to the action is given by:

$$S_{\rm nl} = -\frac{c_b \bar{g}^2 \lambda_p}{4\pi^2} \int_{\omega,\xi} r_\xi f^\star_\xi(\omega) f_\xi(\omega). \tag{E.20}$$

The leading contribution to the partition function comes from the maximum value of $S_{\rm nl}$ which is around $\xi = 0$. This allows to perform the expansion $r_\xi \approx a_\gamma - b_\gamma \xi^2$ and gives

$$S_{\rm nl} \approx -\frac{c_b \bar{g}^2 \lambda_p}{4\pi^2} \int_{\omega,\xi} (a_\gamma - b_\gamma \xi^2) f^\star_\xi(\omega) f_\xi(\omega), \tag{E.21}$$

with

$$a_\gamma = \frac{\pi^2 \csc^2\left(\frac{\pi\gamma}{4}\right)\sec\left(\frac{\pi\gamma}{2}\right)}{2\Gamma\left(1-\frac{\gamma}{2}\right)^2\Gamma(\gamma)}, \tag{E.22a}$$

$$b_\gamma = \frac{\pi^2\left(\pi^2 - 4\sin^2\left(\frac{\pi\gamma}{4}\right)\psi^{(1)}\left(1-\frac{\gamma}{2}\right)\right)}{8\Gamma\left(1-\frac{\gamma}{2}\right)^2\Gamma(\gamma)\sin^4\left(\frac{\pi\gamma}{4}\right)\cos\left(\frac{\pi\gamma}{2}\right)}, \tag{E.22b}$$

where $\psi^{(1)}$ is the Poly-Gamma function.
To apply the map Eq.(E.12) we need the Mellin-decomposition of the field $\tilde{\psi}$ and of its derivative:

$$\begin{aligned}\tilde{\psi}(\omega,z) &= c_F c_z^{\frac{\gamma}{2}-1}\int_\xi \sqrt{\frac{z}{2\pi}} f_\xi(\omega)\left|\frac{z}{c_z}\right|^{-i\xi},\\ \partial_z\tilde{\psi}(\omega,z) &= c_F c_z^{\frac{\gamma}{2}-1}\int \frac{d\xi}{\sqrt{2\pi z}}\left(\frac{1}{2}-i\xi\right) f_\xi(\omega)\left|\frac{z}{c_z}\right|^{-i\xi}.\end{aligned} \tag{E.23}$$

It then follows that:

$$\int_z |\partial_z\tilde{\psi}(\omega,z)|^2 = c_F^2 c^{\gamma-2}\int_\xi\left(\frac{1}{4}+\xi^2\right) f_\xi^\star(\omega) f_\xi(\omega), \tag{E.24}$$

$$\int_z \frac{|\tilde{\psi}(\omega,z)|^2}{z^2} = c_F^2 c_z^{\gamma-2}\int_\xi f_\xi^\star(\omega) f_\xi(\omega). \tag{E.25}$$

The non-local action then becomes

$$S_{\rm nl} = m_{(2)}^2 \int_{z\omega}\frac{|\tilde{\psi}(\omega,z)|^2}{z^2} + A_z\int_{z\omega}|\partial_z\tilde{\psi}(\omega,z)|^2, \tag{E.26}$$

with $m_{(2)}^2 = -\frac{c_b\bar{g}^2\lambda_p b_\gamma}{4\pi^2 c_F^2 c_z^{\gamma-2}}\left(\frac{a_\gamma}{b_\gamma}+\frac{1}{4}\right)$ and $A_z = \frac{c_b\bar{g}^2\lambda_p b_\gamma}{4\pi^2 c_F^2 c_z^{\gamma-2}}$. To complete our derivation we transform-back to time domain and get as total action

$$\boxed{S^{\rm sc} = \int_{z,t}\left(A_t|\partial_t\tilde{\psi}|^2 + A_z|\partial_z\tilde{\psi}|^2 + \frac{m^2}{z^2}|\tilde{\psi}|^2\right),} \tag{E.27}$$

with $m^2 = m_{(1)}^2 + m_{(2)}^2 = \frac{c_z^2}{\pi c_F^2 c_{g,\theta}^2 c_z^\gamma}\left[1 - \frac{\lambda_p b_\gamma}{2\pi C_\gamma}\left(\frac{a_\gamma}{b_\gamma}+\frac{1}{4}\right)\right]$.
In the following we fix the free parameters c_z and c_F of the map Eq.(E.12). The choice $A_z/A_t = 1$ would give the action for a massive scalar field in AdS_2 background. However, the constant c_z resulting from this condition would be complex yielding an ill-defined coordinate change in Eq.(E.12). If instead we require $A_z/A_t = -1$ we obtain

$$c_F^2 = \frac{b_\gamma\lambda_p}{2\pi^2 C_\gamma c_{g,\theta}^2 c_z^\gamma}c_z^2, \quad c_z^2 = \frac{(1-\gamma)C_\gamma\pi}{4b_\gamma\lambda_p}, \tag{E.28}$$

which are real since $0<\gamma<1$. We then obtain Eq.(9.9) of the main text.

Appendix F

Radon transformation

In this appendix we elaborate on the Radon transformation introduced in Eq.(9.11) in the main text. We will draw our conclusions by applying the results of Ref. [218], where the Radon transformation has been carefully analyzed.

F.1 Eigenfunctions of the Laplacian operator

In this section we give details on the eigenfunctions of the Laplacian operator both in Euclidean AdS_2 and Lorentzian dS_2 signatures.
Eigenfunctions and eigenvalues of the E-AdS_2 Laplacian: consider the eigenvalue equation

$$\Box_{\mathrm{AdS}_2}\psi_\lambda = \mu\psi_\lambda, \tag{F.1}$$

where $\Box_{\mathrm{AdS}_2} = \zeta^2(\partial_\tau^2 + \partial_\zeta^2)$ and $\lambda = (p, \omega)$. Separation of variables $\psi_\lambda(\tau, \zeta) = h(\tau)f(\zeta)$ leads to $f(\tau) = e^{i\omega\tau}$ and

$$\partial_z^2 h(\zeta) = \left(\frac{\mu}{\zeta^2} + \omega^2\right)h(z), \tag{F.2}$$

which is the Bessel equation. The solution is therefore given by

$$\psi_{p,\omega}(\tau, \zeta) = a_p e^{i\omega\tau}\sqrt{\zeta}K_{ip}(|\omega|\zeta), \tag{F.3}$$

where $a_p = \sqrt{p\sinh(\pi p)/\pi^3}$, K_{ip} are modified Bessel functions, and $p = -i\nu > 0$. Moreover, the eigenvalue is given by $\mu = -(p^2 + 1/4)$. Such eigenfunctions are orthonormal:

$$\int_{-\infty}^{\infty} d\tau \int_0^\infty \frac{d\zeta}{\zeta^2}\psi^\star_{p,\omega}(\tau, \zeta)\psi_{p',\omega'}(\tau, \zeta) = \delta(p - p')\delta(\omega - \omega'). \tag{F.4}$$

Eigenfunctions and eigenvalues of the L-dS_2 Laplacian: we now apply the same strategy to the Lorentzian dS_2 case. The eigenvalues problem $\Box_{\mathrm{dS}_2}\tilde{\psi}_\lambda = \tilde{\mu}\tilde{\psi}_\lambda$, with $\Box_{\mathrm{dS}_2} = z^2(\partial_t^2 - \partial_z^2)$, is solved by

$$\tilde{\psi}_{p,\omega}(t, z) = b_p e^{-i\omega t}\sqrt{z}Z_{ip}(|\omega|z), \tag{F.5}$$

with $b_p = \sqrt{p/(4\pi\sinh(\pi p))}$ and $\tilde{\mu} = p^2 + 1/4$. Here $Z_\nu(x) = J_\nu(x) + \frac{\tan(\pi\nu/2)+1}{\tan(\pi\nu/2)-1} J_{-\nu}(x)$ with $J_\nu(x)$ Bessel functions of the first kind. The orthonormality condition reads

$$\int_{-\infty}^{\infty} dt \int_0^{\infty} \frac{dz}{z^2} \tilde{\psi}^\star_{p,\omega}(t,z)\tilde{\psi}_{p',\omega'}(t,z) = \delta(p-p')\delta(\omega-\omega'). \tag{F.6}$$

In a coordinate-independent form, the orthogonality conditions can be written as

$$\int d^2x \sqrt{g_{\mathrm{AdS}_2}} \psi^\star_\lambda(x)\psi_{\lambda'}(x) = \delta_{\lambda\lambda'}, \tag{F.7a}$$

$$\int d^2y \sqrt{-g_{\mathrm{dS}_2}} \tilde{\psi}^\star_\lambda(y)\tilde{\psi}_{\lambda'}(y) = \delta_{\lambda\lambda'}. \tag{F.7b}$$

F.2 Normal mode expansion of the actions

In this section we show the equivalence of the following actions

$$S_{\mathrm{AdS}_2} = \int_x \sqrt{g_{\mathrm{AdS}_2}} \psi^\star(x) \left[m^2 - \Box_{\mathrm{AdS}_2}\right] \psi(x), \tag{F.8a}$$

$$S_{\mathrm{dS}_2} = \int_y \sqrt{-g_{\mathrm{dS}_2}} \tilde{\psi}^\star(y) \left[m^2 + \Box_{\mathrm{dS}_2}\right] \tilde{\psi}(y), \tag{F.8b}$$

which are respectively Euclidean-AdS_2 and Lorentzian-dS_2, while $g_{\mathrm{AdS}_2}, g_{\mathrm{dS}_2}$ are the associated metric determinants. Let us perform an expansion in terms of eigenfunctions of the Laplacian operators:

$$\psi(x) = \sum_\lambda a_\lambda \psi_\lambda(x), \quad \tilde{\psi}(y) = \sum_\lambda \tilde{a}_\lambda \tilde{\psi}_\lambda(y), \tag{F.9}$$

where $\Box_{\mathrm{AdS}_2}\psi_\lambda = \mu_\lambda\psi_\lambda$, $\Box_{\mathrm{dS}_2}\tilde{\psi}_\lambda = \tilde{\mu}_\lambda\tilde{\psi}_\lambda$ and λ is a generic quantum number we specify shortly. $\{\psi_\lambda\}$ and $\{\tilde{\psi}_\lambda\}$ are orthonormal sets of functions

$$\int d^2x \sqrt{g_{\mathrm{AdS}_2}} \psi^\star_\lambda(x)\psi_{\lambda'}(x) = \delta_{\lambda\lambda'}, \tag{F.10a}$$

$$\int d^2y \sqrt{-g_{\mathrm{dS}_2}} \tilde{\psi}^\star_\lambda(y)\tilde{\psi}_{\lambda'}(y) = \delta_{\lambda\lambda'}, \tag{F.10b}$$

Notice that Eq.(9.12) for one eigenfunction leads to $\mathcal{R}[\Box_{\mathrm{AdS}_2}\psi_\lambda] = \mu_\lambda \mathcal{R}\psi_\lambda$, and

$$\Box_{\mathrm{dS}_2} \underbrace{\mathcal{R}\psi_\lambda}_{\tilde{\psi}_\lambda} = -\mu_\lambda \underbrace{\mathcal{R}\psi_\lambda}_{\tilde{\psi}_\lambda}. \tag{F.11}$$

It then follows follows that the Radon transformation of the eigenfunctions are themselves eigenfunctions with eigenvalue of opposite sign, i.e. $\tilde{\mu}_\lambda = -\mu_\lambda$. Plugging these expressions into the actions yields

$$\begin{aligned} S_{\mathrm{AdS}_2} &= \sum_{\lambda\lambda'} \int_x a^\star_\lambda a_{\lambda'} \sqrt{g_{\mathrm{AdS}_2}} \psi^\star_\lambda(x) \left[m^2 - \Box_{\mathrm{AdS}_2}\right] \psi_\lambda(x) \\ &= \sum_\lambda |a_\lambda|^2 \left[m^2 - \mu_\lambda\right]. \end{aligned} \tag{F.12}$$

Analogously, the dS_2 action reads

$$\begin{aligned} S_{\mathrm{dS}_2} &= \sum_{\lambda\lambda'} \tilde{a}^\star_\lambda \tilde{a}_{\lambda'} \int_y \sqrt{-g_{\mathrm{dS}_2}} \tilde{\psi}^\star_\lambda(y) \left[\Box_{\mathrm{dS}_2} + m^2\right] \tilde{\psi}_{\lambda'}(y) \\ &= \sum_\lambda |\tilde{a}_\lambda|^2 \left[m^2 - \mu_\lambda\right], \end{aligned} \tag{F.13}$$

where we have used $\tilde{\mu}_\lambda = -\mu_\lambda$. In Eq.(3.20) of Ref.[218] it was shown that $\mathcal{R}[\psi_\lambda](z,t) = L_\lambda \tilde{\psi}_\lambda(z,t)$, with so-called leg factor $L_p = -2i\sqrt{\pi}\Gamma\left(\frac{1}{4} + i\frac{p}{2}\right)/\Gamma\left(\frac{3}{4} + i\frac{p}{2}\right)$. Here we have used the momentum-frequency representation of the eigenfunctions $\lambda = (p,\omega)$. Such a relation leads to the following constraint between expansion coefficients $\tilde{a}_{p\omega} = L_p a_{p\omega}$, and hence

$$S_{\mathrm{dS}_2} = \int_{\omega p} \left(m^2 + p^2 + \frac{1}{4}\right) |L_p|^2 |a_{p\omega}|^2. \tag{F.14}$$

At small p holds $|L_p| = \frac{4\pi\Gamma^2(1/4)}{\Gamma^2(3/4)}(1 - 4c_{\mathrm{G}}p^2)$, where $c_{\mathrm{G}} = \sum_{n=0}^\infty \frac{(-1)^n}{(2n+1)^2} \approx 0,915966$ is Catalan's constant. It then follows

$$S_{\mathrm{dS}_2}[m, \mathcal{R}\psi] = c_S S_{\mathrm{AdS}_2}[m', \psi], \tag{F.15}$$

with overall coefficient $c_S = 4\pi\Gamma^2(1/4)\left[1 - 4c_{\mathrm{G}}(m^2 + 1/4)\right]$ and

$$m'^2 = \frac{m^2 + 1/4}{1 - 4c_{\mathrm{G}}(m^2 + 1/4)} - \frac{1}{4}.$$

Thus, near the BF-bound $m'^2 \approx m^2$ and the two actions are, up to a numerical constant the same.

F.3 Radon transform in the frequency domain

In this section we analyze the Radon transformation in frequency space. To do so, we first write Eq.(9.11) explicitly, by noting that a geodesic in AdS_2 is given by semicircles $z^2 = \zeta^2 + (\tau - t)^2$ of radius z and centered around $(\zeta, \tau) = (0, t)$. Then it follows that

$$\tilde{\psi}(z,t) = 2z \int_{t-z}^{t+z} d\tau \int_0^\infty \frac{dz}{\zeta} \delta\left(z^2 - (\tau - t)^2 - \zeta^2\right) \psi(\zeta, \tau), \tag{F.16}$$

where we have used the notation $\mathcal{R}[\psi] = \tilde{\psi}$. Fourier transforming with respect to times yields

$$\begin{aligned} \tilde{\psi}(z,\omega) &= \int_{-\infty}^\infty dt e^{i\omega t} \tilde{\psi}(z,t) \\ &= 2z \int_{-\infty}^\infty d\tau \int_0^\infty \frac{d\zeta}{\zeta} \psi(\zeta,\tau) \underbrace{\int_{\tau-z}^{\tau+z} dt\, e^{i\omega t} \delta\left(z^2 - (\tau - t)^2 - \zeta^2\right)}_{\mathcal{J}_\delta}, \end{aligned} \tag{F.17}$$

where we have transferred integration limits from the τ to the t-integral.

We now shift $t \mapsto t - \tau$ and get $\mathcal{J}_\delta = e^{i\omega\tau} \int_{-z}^{z} dt\, e^{i\omega t} \delta(z^2 - t^2 - \zeta^2)$. Since z and ζ are both positive and t is real, the condition $t^2 = z^2 - \zeta^2$ has solution only if $0 < \zeta < z$. Therefore:

$$\mathcal{J}_\delta(z, \zeta, \tau) \quad = \quad e^{i\omega\tau} \theta(z - \zeta) \int_{-\infty}^{\infty} dt \cos(\omega t) \delta\left(t^2 - z^2 + \zeta^2\right) \theta(z^2 - t^2), \tag{F.18}$$

where we have used the Heaviside function to properly extend the integration limits.
Working-out the delta function gives $\delta(t^2 - (z^2 - \zeta^2)) = (\delta(t + t_0) - \delta(t - t_0))/2t_0$ with $t_0 = \sqrt{z^2 - \zeta^2}$. Consequently:

$$\mathcal{J}_\delta(z, \zeta, \tau) \quad = \quad e^{i\omega\tau} \theta(z - \zeta) \frac{\cos(\omega\sqrt{z^2 - \zeta^2})}{\sqrt{z^2 - \zeta^2}}. \tag{F.19}$$

Plugging this into the initial expression gives

$$\tilde{\psi}(z, \omega) \quad = \quad 2z \int_0^z \frac{d\zeta}{\zeta} \psi(\zeta, \omega) \frac{\cos(\omega\sqrt{z^2 - \zeta^2})}{\sqrt{z^2 - \zeta^2}}, \tag{F.20}$$

where $\psi(\zeta, \omega) = \int_\tau \psi(\zeta, \tau) e^{i\omega\tau}$. We thus have found that the Radon transformation is local in ω but non-local in the radial coordinates.

F.4 Pairing response after Radon transformation

In the previous section we have established that the Radon transformation Eq.(9.11) correctly maps the problem Eq.(9.9) into an Euclidean AdS_2 action. We now want to check how such a map affects the pairing response. To do so, we consider the following action

$$S_{J,\mathrm{dS}_2} = -\int d^2y \sqrt{-g_{\mathrm{dS}_2}} \left(J(y)\tilde{\psi}^\star(y) + \text{h.c.}\right). \tag{F.21}$$

In Chap. 8 we have seen that the SYK superconductor leads to a source term $J(z,t) = \frac{c_z}{c_F} z^{\frac{1-\gamma}{2}} J_0(t)$, where $J_0(t)$ couples to $\sum_i c^\dagger_{i\downarrow}(t) c^\dagger_{i\uparrow}(t)$. Fourier transforming with respect to times yields

$$S_{J,\mathrm{dS}_2} - \frac{c_z}{c_F} \int \frac{d\omega dz}{z^2} \left(J_0(\omega) z^{\frac{1-\gamma}{2}} \tilde{\psi}^\star(z, \omega) + \text{h.c.}\right). \tag{F.22}$$

Applying the Radon transformation in frequency space Eq.(F.20) we obtain

$$S_{J,\mathrm{dS}_2} = S_{J,\mathrm{AdS}_2} = -\frac{c_z}{c_F} \int \frac{d\omega d\zeta}{\zeta^2} \left(J_{\mathrm{AdS}_2}(\zeta, \omega) \psi^\star(\zeta, \omega) + \text{h.c.}\right), \tag{F.23}$$

where

$$J_{\mathrm{AdS}_2}(\zeta, \omega) \quad \equiv \quad 2J_0(\omega)\zeta \int_\zeta^\infty \frac{d\zeta}{z^{\frac{1+\gamma}{2}}} \frac{\cos\left(\omega\sqrt{z^2 - \zeta^2}\right)}{\sqrt{z^2 - \zeta^2}}. \tag{F.24}$$

At small ω we obtain

$$J_{\mathrm{AdS}_2}(\zeta,\omega) \approx J_0(\omega)\zeta^{\frac{1-\gamma}{2}}\left[\frac{\sqrt{\pi}\Gamma\left(\frac{1+\gamma}{4}\right)}{\Gamma\left(\frac{3+\gamma}{4}\right)} + |\omega\zeta|^{\frac{1+\gamma}{2}}\Gamma\Big(-\frac{1+\gamma}{2}\Big)\cos\Big(\frac{\pi}{4}(1+\gamma)\Big)\right]. \tag{F.25}$$

Hence, for $\omega < z^{-1}$we have essentially the same response as without the Radon transform.

F.4.1 Static susceptibility

In Sec.8.2 we have found that the static pairing susceptibility of the Yukawa-SYK model is given by

$$\chi \;=\; \gamma^2\chi_{\mathrm{c}}\frac{\Lambda^{2\nu}-T^{2\nu}}{(\gamma+2\nu)^2\Lambda^{2\nu}-(\gamma-2\nu)^2T^{2\nu}}. \tag{F.26}$$

Our goal is now to understand how this changes upon a Radon transformation. To do so, we first have to see how the pairing susceptibility formally originates from the field $\tilde{\psi}$. In Sec.8.3.1, we have seen that the $\omega = 0$ solution of the gap equation is $\tilde{\psi}\,(0,z) = \tilde{A}z^{\frac{1}{2}-\nu} + \tilde{B}z^{\frac{1}{2}+\nu}$. $\tilde{A}$ and $\tilde{B}$ are determined by the boundary condition translated for $\tilde{\psi}(\omega,\zeta)$:

$$\begin{aligned}\frac{\tilde{\psi}'(z_T)}{\psi(z_T)} &= \frac{1-\gamma}{2z_T},\\ \tilde{\psi}'(z_\Lambda) &= \frac{1+\gamma}{2z_\Lambda}\tilde{\psi}(z_\Lambda) - \gamma\, c_0' J_0 {z_\Lambda}^{-\frac{\gamma+1}{2}},\end{aligned} \tag{F.27}$$

with $c_0' = \frac{c_F c_{g,\theta}^2}{c_z^{1-\gamma}}$. Reminding that $\tilde{\psi}(\omega,\zeta) = c_F\zeta^{\frac{\gamma-1}{2}}F(\omega, c_z\zeta^{-1})$, the static susceptibility Eq.(8.30) is given by

$$\chi \;=\; \frac{c_z}{2\pi c_F}\int_{c_z/\Lambda}^{c_z/T} dz\, z^{-\frac{\gamma+3}{2}}\,\frac{d\psi(z)}{dJ_0}\bigg|_{J=0}, \tag{F.28}$$

that correctly reproduces the result Eq.(F.26). We already showed that the source field $J_0 \mapsto J_{0,\mathrm{AdS}_2} = J_0(\omega)\zeta^{\frac{1-\gamma}{2}}\sqrt{\pi}\Gamma\left(\frac{1+\gamma}{4}\right)/\Gamma\left(\frac{3+\gamma}{4}\right)$ when we consider the theory in AdS_2. This will renormalize the denominator of the above expression. To see how the numerator changes, we have to explicitly perform the Radon transformation of $\tilde{\psi}$. Let us consider the $\omega = 0$ version of the Radon transform Eq.(F.20)

$$\tilde{\psi}(z) = 2\int_0^1 \frac{dx}{x}\frac{\psi(zx)}{\sqrt{1-x^2}}. \tag{F.29}$$

It holds for $\psi(\zeta) = \zeta^{\frac{1}{2}\pm\nu}$ that for $-\frac{1}{2} < \mathrm{Re}\nu < \frac{1}{2}$ follows

$$\tilde{\psi}(z) = 2z^{\frac{1}{2}\pm\nu}\int_0^1 \frac{dx}{x}\frac{x^{\frac{1}{2}\pm\nu}}{\sqrt{1-x^2}} = 4\sqrt{\pi}\frac{\Gamma\left(\frac{1}{2}\pm\nu\right)}{\Gamma\left(1\pm\nu\right)}z^{\frac{1}{2}\pm\nu}. \tag{F.30}$$

Thus, assuming $\psi(\zeta) = A\zeta^{\frac{1}{2}-\nu} + B\zeta^{\frac{1}{2}+\nu}$ yields:

$$\tilde{A} = 4\sqrt{\pi}\frac{\Gamma\left(\frac{1}{2}-\nu\right)}{\Gamma\left(\frac{1}{2}-\nu\right)}A, \quad \tilde{B} = 4\sqrt{\pi}\frac{\Gamma\left(\frac{1}{2}+\nu\right)}{\Gamma\left(\frac{1}{2}+\nu\right)}B. \tag{F.31}$$

Following Eq.(F.28), the analogue in this case is

$$\chi_{\text{Radon}} = \frac{c_z}{2\pi c_F}\frac{\Gamma\left(\frac{3+\gamma}{4}\right)}{\sqrt{\pi}\Gamma\left(\frac{1+\gamma}{4}\right)}\int_{c/\Lambda}^{c/T} d\zeta\, \zeta^{-\frac{\gamma+3}{2}}\left.\frac{d\psi(\zeta)}{dJ_0}\right|_{J=0} \overset{\nu\ll 1}{\approx} \frac{\Gamma\left(\frac{\gamma+3}{4}\right)}{4\pi^{3/2}\Gamma\left(\frac{\gamma+1}{4}\right)}\chi. \tag{F.32}$$

The static susceptibilities coincide at small ν up to a numerical coefficient of order 10^{-1}.

Bibliography

[1]P. Drude, "Zur Elektronentheorie der Metalle," Annalen der Physik **306**, 566–613 (1900).

[2]A. A. Abrikosov, *Introduction to the Theory of Normal Metals, Solid State Physics Series* (Solid State Physics Series (Academic Press, 1972)).

[3]H. K. Onnes, "The resistance of pure mercury at helium temperatures," Commun. Phys. Lab. Univ. Leiden, vol. 12, 1911, p. 120.

[4]H. London and F. London, "The electromagnetic equations of the supraconductor," Proceedings of the Royal Society of London. Series A - Mathematical and Physical Sciences **149**, 71–88 (1935).

[5]J. Bardeen, L. N. Cooper, and J. R. Schrieffer, "Microscopic Theory of Superconductivity," Phys. Rev. **106**, 162–164 (1957).

[6]J. Schmalian, "Failed theories of superconductivity," Modern Physics Letters B **24**, 2679–2691 (2010).

[7]M. Gurvitch and A. T. Fiory, "Resistivity of $La_{1.825}Sr_{0.175}CuO_4$ and $YBa_2Cu_3O_7$ to 1100 K: Absence of saturation and its implications," Phys. Rev. Lett. **59**, 1337–1340 (1987).

[8]S. Martin, A. T. Fiory, R. M. Fleming, L. F. Schneemeyer, and J. V. Waszczak, "Temperature Dependence of the Resistivity Tensor in Superconducting $Bi_2Sr_{2.2}Ca_{0.8}$ Cu_2O_8 Crystals," Phys. Rev. Lett. **60**, 2194–2197 (1988).

[9]A. Tyler and A. Mackenzie, "Hall effect of single layer, tetragonal $Tl_2Ba_2CuO_{6+\delta}$ near optimal doping," Physica C: Superconductivity **282-287**, 1185–1186 (1997).

[10]J. Erdmenger, "Introduction to Gauge/Gravity Duality (TASI Lectures 2017)," 1–37 (2018).

[11]J. Maldacena, "The Large-N Limit of Superconformal Field Theories and Supergravity," International Journal of Theoretical Physics **38**, 10.1023/A:1026654312961 (1999).

[12]K. S. Thorne, R. H. Price, and D. A. MacDonald, *Black holes: The membrane paradigm* (1986).

[13]N. Iqbal and H. Liu, "Universality of the hydrodynamic limit in AdS/CFT and the membrane paradigm," Physical Review D - Particles, Fields, Gravitation and Cosmology **79**, 1–15 (2009).

[14]S. A. Hartnoll, "Theory of universal incoherent metallic transport," Nature Physics **11**, 54 EP – (2014).

[15]M. Blake, "Universal Charge Diffusion and the Butterfly Effect in Holographic Theories," Physical Review Letters **117**, 1–6 (2016).

[16]M. Blake, "Universal diffusion in incoherent black holes," Physical Review D **94**, 1–9 (2016).

[17]L. Susskind and J. Lindesay, *An Introduction to Black Holes, Information and the String Theory Revolution: The Holographic Universe* (World Scientific, 2005).

[18]G. A. Inkof, J. M. C. Küppers, J. M. Link, B. Goutéraux, and J. Schmalian, "Quantum critical scaling and holographic bound for transport coefficients near Lifshitz points," **2020**, 10.1007/jhep11(2020)088 (2020).

[19]J. M. Link, B. N. Narozhny, E. I. Kiselev, and J. Schmalian, "Out-of-Bounds Hydrodynamics in Anisotropic Dirac Fluids," Phys. Rev. Lett. **120**, 196801 (2018).

[20]G.-A. Inkof, K. Schalm, and J. Schmalian, "Quantum critical Eliashberg theory, the Sachdev-Ye-Kitaev superconductor and their holographic duals," npj Quantum Materials **7**, 10.1038/s41535-022-00460-8 (2022).

[21]I. Esterlis and J. Schmalian, "Cooper pairing of incoherent electrons: An electron-phonon version of the Sachdev-Ye-Kitaev model," Physical Review B **100**, 1–26 (2019).

[22]D. Hauck, M. J. Klug, I. Esterlis, and J. Schmalian, "Eliashberg equations for an electron–phonon version of the Sachdev–Ye–Kitaev model: Pair breaking in non-Fermi liquid superconductors," Annals of Physics **417**, Eliashberg theory at 60: Strong-coupling superconductivity and beyond, 168120 (2020).

[23]J. Erdmenger and M. Ammon, *Gauge / Gravity Duality: Foundations and Applications* (2015).

[24]S. A. Hartnoll, A. Lucas, and S. Sachdev, "Holographic quantum matter," 1–178 (2016).

[25]J. Zaanen, Y. Liu, Y.-W. Sun, and K. Schalm, *Holographic Duality in Condensed Matter Physics* (2015).

[26]A. Amoretti, *Condensed Matter Applications of AdS/CFT* (2017).

[27]M. Baggioli, "A Practical Mini-Course on Applied Holography," 10.1007/978-3-030-35184-7 (2019).

[28]S. A. Hartnoll, "Lectures on holographic methods for condensed matter physics," Classical and Quantum Gravity **26**, 10.1088/0264-9381/26/22/224002 (2009).

[29]J. McGreevy, "Holographic duality with a view toward many-body physics," Advances in High Energy Physics **2010**, 10.1155/2010/723105 (2010).

[30]E. Witten, "Anti de Sitter space and holography," Advances in Theoretical and Mathematical Physics **2**, 253–291 (1998).

[31]S. Gubser, I. Klebanov, and A. Polyakov, "Gauge theory correlators from non-critical string theory," Physics Letters B **428**, 105 –114 (1998).

[32]S. Carroll and Addison-Wesley, *Spacetime and Geometry: An Introduction to General Relativity* (Addison Wesley, 2004).

[33]S. W. Hawking, "Black hole explosions?" Nature **248**, 30–31 (1974).

[34]J. D. Bekenstein, "Black Holes and Entropy," Phys. Rev. D **7**, 2333–2346 (1973).

[35]J. De Boer, E. Verlinde, and H. Verlinde, "On the holographic renormalization group," Journal of High Energy Physics **4**, 1–15 (2000).

[36]S. De Haro, K. Skenderis, and S. N. Solodukhin, "Holographic reconstruction of spacetime and renormalization in the AdS/CFT correspondence," Communications in Mathematical Physics **217**, 595–622 (2001).

[37]K. Skenderis, "Lecture notes on holographic renormalization," Classical and Quantum Gravity **19**, 5849–5876 (2002).

[38]T. Faulkner, N. Iqbal, H. Liu, J. McGreevy, and D. Vegh, "Holographic non-Fermi liquid fixed points," 10.1098/rsta.2010.0354 (2011).

[39]P. Breitenlohner and D. Z. Freedman, "Positive energy in anti-de Sitter backgrounds and gauged extended supergravity," Physics Letters B **115**, 197–201 (1982).

[40]D. T. Son and A. O. Starinets, "Minkowski-space correlators in AdS/CFT correspondence: recipe and applications," Journal of High Energy Physics **2002**, 042–042 (2002).

[41]V. Balasubramanian, P. Kraus, and A. Lawrence, "Bulk versus boundary dynamics in anti–de Sitter spacetime," Phys. Rev. D **59**, 046003 (1999).

[42]E. Witten, "Multi-Trace Operators, Boundary Conditions, And AdS/CFT Correspondence," (2001).

[43]W. Mück, "An improved correspondence formula for AdS/CFT with multi-trace operators," Physics Letters, Section B: Nuclear, Elementary Particle and High-Energy Physics **531**, 301–304 (2002).

[44]R. Wald, *General Relativity* (University of Chicago Press, 1984).

[45]S. S. Gubser, "Breaking an Abelian gauge symmetry near a black hole horizon," Physical Review D - Particles, Fields, Gravitation and Cosmology **78**, 10.1103/PhysRevD.78.065034 (2008).

[46]B Pioline and J Troost, "Schwinger pair production in AdS2," Journal of High Energy Physics **2005**, 043–043 (2005).

[47]T. Faulkner, H. Liu, J. McGreevy, and D. Vegh, "Emergent quantum criticality, Fermi surfaces, and AdS_2," Physical Review D - Particles, Fields, Gravitation and Cosmology **83**, 1–34 (2011).

[48]S. A. Hartnoll, C. P. Herzog, and G. T. Horowitz, "Building an AdS/CFT superconductor," 10.1103/PhysRevLett.101.031601 (2008).

[49]S. A. Hartnoll, C. P. Herzog, and G. T. Horowitz, "Holographic superconductors," Journal of High Energy Physics **2008**, 015–015 (2008).

[50]G. T. Horowitz, "Introduction to holographic superconductors," Lecture Notes in Physics **828**, 313–347 (2011).

[51]C. P. Herzog, "Lectures on holographic superfluidity and superconductivity," Journal of Physics A: Mathematical and Theoretical **42**, 23–31 (2009).

[52]S. S. Gubser and A. Nellore, "Low-temperature behavior of the Abelian Higgs model in anti-de Sitter space," JHEP **04**, 008 (2009).

[53]F. Denef and S. A. Hartnoll, "Landscape of superconducting membranes," Phys. Rev. D **79**, 126008 (2009).

[54]T. Albash and C. V. Johnson, "A holographic superconductor in an external magnetic field," Journal of High Energy Physics **2008**, 121–121 (2008).

[55]S. Sachdev, "Universal low temperature theory of charged black holes with AdS_2 horizons," Journal of Mathematical Physics **60**, 0–23 (2019).

[56]U. Moitra, S. P. Trivedi, and V. Vishal, "Extremal and near-extremal black holes and near-CFT1," Journal of High Energy Physics **2019**, 10.1007/JHEP07(2019)055 (2019).

[57]P. Nayak, A. Shukla, R. M. Soni, S. P. Trivedi, and V. Vishal, "On the dynamics of near-extremal black holes," Journal of High Energy Physics **2018**, 10.1007/JHEP09(2018)048 (2018).

[58]N. Iqbal, H. Liu, and M. Mezei, "Semi-local quantum liquids," **2012**, 10.1007/jhep04(2012)086 (2012).

[59]N. Iqbal, H. Liu, and M. Mezei, "Lectures on holographic non-Fermi liquids and quantum phase transitions," 10.1142/9789814350525_0013 (2011).

[60]N. Iqbal, H. Liu, and M. Mezei, "Quantum phase transitions in semilocal quantum liquids," Phys. Rev. D **91**, 025024 (2015).

[61]A. Almheiri and J. Polchinski, "Models of AdS_2 backreaction and holography," Journal of High Energy Physics **2015**, 1–19 (2015).

[62]J. Maldacena, D. Stanford, and Z. Yang, "Conformal symmetry and its breaking in two-dimensional nearly anti-de Sitter space," Progress of Theoretical and Experimental Physics **2016**, 10.1093/ptep/ptw124 (2016).

[63]G. Sárosi, "AdS_2 holography and the SYK model," Proceedings of Science **323** (2017).

[64]S. Sachdev and J. Ye, "Gapless spin-fluid ground state in a random quantum Heisenberg magnet," Phys. Rev. Lett. **70**, 3339–3342 (1993).

[65]A. Kitaev, "A simple model of quantum holography," Talk 1 (2015).

[66]A. Kitaev, "A simple model of quantum holography," Talk 2 (2015).

[67]D. Chowdhury, A. Georges, O. Parcollet, and S. Sachdev, *Sachdev-Ye-Kitaev Models and Beyond: A Window into Non-Fermi Liquids*, 2021.

[68]J. Maldacena and D. Stanford, "Remarks on the Sachdev-Ye-Kitaev model," Physical Review D, 10.1103/PhysRevD.94.106002 (2016).

[69]I. Aref'eva, M. Khramtsov, M. Tikhanovskaya, and I. Volovich, "Replica-nondiagonal solutions in the SYK model," Journal of High Energy Physics **2019**, 10.1007/jhep07(2019)113 (2019).

[70]J. Maldacena, S. H. Shenker, and D. Stanford, "A bound on chaos," Journal of High Energy Physics **2016**, 106 (2016).

[71]R. A. Davison, W. Fu, A. Georges, Y. Gu, K. Jensen, and S. Sachdev, "Thermoelectric transport in disordered metals without quasiparticles: The Sachdev-Ye-Kitaev models and holography," Physical Review B **95**, 36–38 (2017).

[72]P. K. Kovtun, D. T. Son, and A. O. Starinets, "Viscosity in strongly interacting quantum field theories from black hole physics," Physical Review Letters **94**, 23–26 (2005).

[73]T. Schäfer, "Fluid Dynamics and Viscosity in Strongly Correlated Fluids," Annual Review of Nuclear and Particle Science **64**, 125–148 (2014).

[74]J. Thomas, "Is an Ultra-Cold Strongly Interacting Fermi Gas a Perfect Fluid?" Nuclear Physics A **830**, 665c –672c (2009).

[75]M. Müller, J. Schmalian, and L. Fritz, "Graphene: A Nearly Perfect Fluid," Phys. Rev. Lett. **103**, 025301 (2009).

[76]A. F. Ioffe and A. R. Regel, "Non-crystalline, amorphous and liquid electronic semiconductors," Prog. Semicond. **26**, 237–291 (1960).

[77]N. F. Mott, "Conduction in non-crystalline systems IX. the minimum metallic conductivity," The Philosophical Magazine: A Journal of Theoretical Experimental and Applied Physics **26**, 1015–1026 (1972).

[78]M. Gurvitch, "Ioffe-Regel criterion and resistivity of metals," Phys. Rev. B **24**, 7404–7407 (1981).

[79]V. J. Emery and S. A. Kivelson, "Superconductivity in Bad Metals," Phys. Rev. Lett. **74**, 3253–3256 (1995).

[80]N. E. Hussey, K. Takenaka, and H. Takagi, "Universality of the Mott–Ioffe–Regel limit in metals," Philosophical Magazine **84**, 2847–2864 (2004).

[81]J. Zaanen, "Why the temperature is high," Nature **430**, 512–513 (2004).

[82]S. Sachdev and B. Keimer, "Quantum criticality," Physics Today **64**, 29–35 (2011).

[83]S. H. Shenker and D. Stanford, "Black holes and the butterfly effect," Journal of High Energy Physics **2014**, 67 (2014).

[84]S. H. Shenker and D. Stanford, "Stringy effects in scrambling," Journal of High Energy Physics **2015**, 10.1007/JHEP05(2015)132 (2015).

[85]D. A. Roberts, D. Stanford, and L. Susskind, "Localized shocks," Journal of High Energy Physics **2015**, 51 (2015).

[86]D. A. Roberts and B. Swingle, "Lieb-Robinson Bound and the Butterfly Effect in Quantum Field Theories," Phys. Rev. Lett. **117**, 6 (2016).

[87]M. Blake, R. A. Davison, and S. Sachdev, "Thermal diffusivity and chaos in metals without quasiparticles," Phys. Rev. **D96**, 106008 (2017).

[88]M. J. Klug, M. S. Scheurer, and J. Schmalian, "Hierarchy of information scrambling, thermalization, and hydrodynamic flow in graphene," Phys. Rev. B **98**, 10.1103/PhysRevB.98.045102 (2018).

[89]R. A. Davison, S. A. Gentle, and B. Goutéraux, "Slow relaxation and diffusion in holographic quantum critical phases," (2018).

[90]R. A. Davison, S. A. Gentle, and B. Goutéraux, "Impact of irrelevant deformations on thermodynamics and transport in holographic quantum critical states," (2018).

[91]S. Grozdanov, K. Schalm, and V. Scopelliti, "Black hole scrambling from hydrodynamics," 10.1103/PhysRevLett.120.231601 (2017).

[92]T. Hartman, S. A. Hartnoll, and R. Mahajan, "An upper bound on transport," 10.1103/PhysRevLett.119.141601 (2017).

[93]R. A. Davison and B. Goutéraux, "Momentum dissipation and effective theories of coherent and incoherent transport," Journal of High Energy Physics **2015**, 10.1007/JHEP01(2015)039 (2015).

[94]S. Grozdanov, A. Lucas, and N. Poovuttikul, "Holography and hydrodynamics with weakly broken symmetries," Phys. Rev. **D99**, 086012 (2019).

[95]C. Q. Cook and A. Lucas, "Electron hydrodynamics with a polygonal Fermi surface," (2019).

[96]E. M. Lifshitz, "On the theory of phase transformations of the second order. I. Changes of the elementary cell of a crystal in phase transitions of the second order.," J. Phys. (Moscow) **6**, 61–74 (1942).

[97]I. E. Dzyaloshinski, "Theory of Helicoidal Structures in Antiferromagnets. I. Nonmetals," Zh. Eksp. Teor. Fiz. **46**, 1420 (1964).

[98]S. Goshen, D. Mukamel, and S. Shtrikman, "Non-crystalline, amorphous and liquid electronic semiconductors," Int. J. Magn. **6**, 221 (1974).

[99]R. M. Hornreich, M. Luban, and S. Shtrikman, "Critical Behavior at the Onset of $\vec{k}$-Space Instability on the λ Line," Phys. Rev. Lett. **35**, 1678–1681 (1975).

[100]H. W. Diehl and M. Shpot, "Critical behavior at m-axial Lifshitz points: Field-theory analysis and ϵ-expansion results," Phys. Rev. B **62**, 12338–12349 (2000).

[101]M. Shpot and H. Diehl, "Two-loop renormalization-group analysis of critical behavior at m-axial Lifshitz points," Nuclear Physics B **612**, 340 –372 (2001).

[102]M. A. Shpot, Y. M. Pis'mak, and H. W. Diehl, "Large-n expansion form-axial Lifshitz points," Journal of Physics: Condensed Matter **17**, S1947–S1972 (2005).

[103]M. A. Shpot, H. W. Diehl, and Y. M. Pis'mak, "Compatibility of 1/n and epsilon expansions for critical exponents at m-axial Lifshitz points," 10.1088/1751-8113/41/13/135003 (2008).

[104]A. Rebhan and D. Steineder, "Violation of the Holographic Viscosity Bound in a Strongly Coupled Anisotropic Plasma," Phys. Rev. Lett. **108**, 021601 (2012).

[105]S. Jain, N. Kundu, K. Sen, A. Sinha, and S. P. Trivedi, "A strongly coupled anisotropic fluid from dilaton driven holography," Journal of High Energy Physics **2015**, 1–76 (2015).

[106]X.-H. Ge, Y. Ling, C. Niu, and S.-J. Sin, "Thermoelectric conductivities, shear viscosity, and stability in an anisotropic linear axion model," Phys. Rev. **D92**, 106005 (2015).

[107]X.-H. Ge, S.-J. Sin, and S.-F. Wu, "Universality of DC Electrical Conductivity from Holography," 10.1016/j.physletb.2017.01.056 (2015).

[108]M. Baggioli, B. Padhi, P. W. Phillips, and C. Setty, "Conjecture on the Butterfly Velocity across a Quantum Phase Transition," 10.1007/JHEP07(2018)049 (2018).

[109]K. A. Mamo, "Holographic RG flow of the shear viscosity to entropy density ratio in strongly coupled anisotropic plasma," 10.1007/JHEP10(2012)070 (2012).

[110]D. Giataganas, "Observables in Strongly Coupled Anisotropic Theories," (2013).

[111]D. Giataganas, U. Gürsoy, and J. F. Pedraza, "Strongly Coupled Anisotropic Gauge Theories and Holography," Physical Review Letters **121**, 10.1103/PhysRevLett.121.121601 (2018).

[112]H. Isobe, B.-J. Yang, A. Chubukov, J. Schmalian, and N. Nagaosa, "Emergent Non-Fermi-Liquid at the Quantum Critical Point of a Topological Phase Transition in Two Dimensions," Phys. Rev. Lett. **116**, 076803 (2016).

[113]A. Kobayashi, Y. Suzumura, F. Piéchon, and G. Montambaux, "Emergence of Dirac electron pair in the charge-ordered state of the organic conductor α-(BEDT-TTF)$_2$I$_3$," Phys. Rev. B **84**, 075450 (2011).

[114]V. Pardo and W. E. Pickett, "Half-Metallic Semi-Dirac-Point Generated by Quantum Confinement in TiO_2/VO_2 Nanostructures," Phys. Rev. Lett. **102**, 166803 (2009).

[115]S. Banerjee, R. R. P. Singh, V. Pardo, and W. E. Pickett, "Tight-Binding Modeling and Low-Energy Behavior of the Semi-Dirac Point," Phys. Rev. Lett. **103**, 016402 (2009).

[116]C. Fang and L. Fu, "New classes of three-dimensional topological crystalline insulators: Nonsymmorphic and magnetic," Phys. Rev. B **91**, 161105 (2015).

[117]S.-M. Huang, S.-Y. Xu, I. Belopolski, C.-C. Lee, G. Chang, T.-R. Chang, B. Wang, N. Alidoust, G. Bian, M. Neupane, D. Sanchez, H. Zheng, H.-T. Jeng, A. Bansil, T. Neupert, H. Lin, and M. Z. Hasan, "A new type of Weyl semimetal with quadratic double Weyl fermions in SrSi2," Proceedings of the National Academy of Sciences **113**, 1180–1185 (2016).

[118]B. Goutéraux, "Charge transport in holography with momentum dissipation," JHEP **04**, 181 (2014).

[119]S. A. Hartnoll and A. Karch, "Scaling theory of the cuprate strange metals," Phys. Rev. **B91**, 155126 (2015).

[120]J. M. Link, D. E. Sheehy, B. N. Narozhny, and J. Schmalian, "Elastic response of the electron fluid in intrinsic graphene: The collisionless regime," Phys. Rev. B **98**, 195103 (2018).

[121]A. Donos and J. P. Gauntlett, "Lifshitz solutions of D=10 and D=11 supergravity," Journal of High Energy Physics **2010**, 10.1007/jhep12(2010)002 (2010).

[122]H. S. Jeong, Y. Ahn, D. Ahn, C. Niu, W. J. Li, and K. Y. Kim, "Thermal diffusivity and butterfly velocity in anisotropic Q-lattice models," Journal of High Energy Physics **2018**, 10.1007/JHEP01(2018)140 (2018).

[123]A. Donos and J. P. Gauntlett, "Novel metals and insulators from holography," JHEP **06**, 007 (2014).

[124]D. Mateos and D. Trancanelli, "The anisotropic N=4 super Yang-Mills plasma and its instabilities," Phys. Rev. Lett. **107**, 101601 (2011).

[125]D. Mateos and D. Trancanelli, "Thermodynamics and Instabilities of a Strongly Coupled Anisotropic Plasma," JHEP **07**, 054 (2011).

[126]A. Donos and J. P. Gauntlett, "Holographic Q-lattices," Journal of High Energy Physics **2014**, 10.1007/JHEP04(2014)040 (2014).

[127]D. Giataganas, "Probing strongly coupled anisotropic plasma," 10.1007/JHEP07(2012)031 (2012).

[128]M. Baggioli, K.-Y. Kim, L. Li, and W.-J. Li, "Holographic axion model: A simple gravitational tool for quantum matter," Science China Physics, Mechanics & Astronomy **64**, 10.1007/s11433-021-1681-8 (2021).

[129]K. Landsteiner, Y. Liu, and Y. W. Sun, "Odd Viscosity in the Quantum Critical Region of a Holographic Weyl Semimetal," Physical Review Letters **117**, 10.1103/PhysRevLett.117.081604 (2016).

[130]T. Andrade and B. Withers, "A simple holographic model of momentum relaxation," Journal of High Energy Physics **2014**, 10.1007/JHEP05(2014)101 (2014).

[131]S. A. Hartnoll, D. M. Ramirez, and J. E. Santos, "Entropy production, viscosity bounds and bumpy black holes," Journal of High Energy Physics **2016**, 10.1007/JHEP03(2016)170 (2016).

[132]L. Alberte, M. Baggioli, and O. Pujolas, "Viscosity bound violation in holographic solids and the viscoelastic response," JHEP **07**, 074 (2016).

[133]T. Ciobanu and D. M. Ramirez, "Shear hydrodynamics, momentum relaxation, and the KSS bound," (2017).

[134]P. Burikham and N. Poovuttikul, "Shear viscosity in holography and effective theory of transport without translational symmetry," Physical Review D **94**, 1–25 (2016).

[135]Y. Ling, Z. Xian, and Z. Zhou, "Holographic shear viscosity in hyperscaling violating theories without translational invariance," Journal of High Energy Physics **2016**, 10.1007/JHEP11(2016)007 (2016).

[136]Y. Ling, Z. Xian, and Z. Zhou, "Power Law of Shear Viscosity in Einstein-Maxwell-Dilaton-Axion model," Chin. Phys. **C41**, 023104 (2017).

[137]X.-H. Ge, "Notes on shear viscosity bound violation in anisotropic models," (2015).

[138]A. Amoretti, D. Areán, B. Goutéraux, and D. Musso, "Effective holographic theory of charge density waves," Physical Review D **97**, 1–18 (2018).

[139]A. Amoretti, D. Areán, B. Goutéraux, and D. Musso, "dc Resistivity of Quantum Critical, Charge Density Wave States from Gauge-Gravity Duality," Phys. Rev. Lett. **120**, 171603 (2018).

[140]A. Amoretti, D. Areán, B. Goutéraux, and D. Musso, "Diffusion and universal relaxation of holographic phonons," (2019).

[141]A. Donos and J. P. Gauntlett, "Thermoelectric DC conductivities from black hole horizons," Journal of High Energy Physics **2014**, 10.1007/JHEP11(2014)081 (2014).

[142]G. T. Horowitz, J. E. Santos, and D. Tong, "Optical conductivity with holographic lattices," Journal of High Energy Physics **2012**, 10.1007/JHEP07(2012)168 (2012).

[143]B. Goutéraux, "Charge transport in holography with momentum dissipation," Journal of High Energy Physics **2014**, 10.1007/JHEP04(2014)181 (2014).

[144]A. Amoretti, M. Baggioli, N. Magnoli, and D. Musso, "Chasing the cuprates with dilatonic dyons," Journal of High Energy Physics **2016**, 10.1007/JHEP06(2016)113 (2016).

[145]A. Donos and J. P. Gauntlett, "On the thermodynamics of periodic AdS black branes," Journal of High Energy Physics **2013**, 10.1007/JHEP10(2013)038 (2013).

[146]A. Amoretti, D. Areán, R. Argurio, D. Musso, and L. A. Zayas, "A holographic perspective on phonons and pseudo-phonons," Journal of High Energy Physics **2017**, 10.1007/JHEP05(2017)051 (2017).

[147]J. Casalderrey-Solana, N. I. Gushterov, and B. Meiring, "Resurgence and hydrodynamic attractors in Gauss-Bonnet holography," Journal of High Energy Physics **2018**, 10.1007/JHEP04(2018)042 (2018).

[148]M. Baggioli, B. Goutéraux, E. Kiritsis, and W. J. Li, "Higher derivative corrections to incoherent metallic transport in holography," Journal of High Energy Physics **2017**, 10.1007/JHEP03(2017)170 (2017).

[149]S. Jain, R. Samanta, and S. P. Trivedi, "The shear viscosity in anisotropic phases," Journal of High Energy Physics **2015**, 10.1007/JHEP10(2015)028 (2015).

[150]A. Lucas and S. Sachdev, "Memory matrix theory of magnetotransport in strange metals," Physical Review B - Condensed Matter and Materials Physics **91**, 1–20 (2015).

[151]Y. Ling, Z. Xian, and Z. Zhou, "Holographic shear viscosity in hyperscaling violating theories without translational invariance," Journal of High Energy Physics **2016**, 10.1007/JHEP11(2016)007 (2016).

[152]Y. Ling, Z. Xian, and Z. Zhou, "Power law of shear viscosity in Einstein-Maxwell-Dilaton-Axion model," Chinese Physics C **41**, 10 (2017).

[153]M. Baggioli and W.-J. Li, "Universal Bounds on Transport in Holographic Systems with Broken Translations," SciPost Phys. **9**, 7 (2020).

[154]M. M. Caldarelli, A. Christodoulou, I. Papadimitriou, and K. Skenderis, "Phases of planar AdS black holes with axionic charge," Journal of High Energy Physics **2017**, 10.1007/JHEP04(2017)001 (2017).

[155]Y. Ling, P. Liu, and J.-P. Wu, "Holographic Butterfly Effect at Quantum Critical Points," 10.1007/JHEP10(2017)025 (2016).

[156]W.-H. Huang, "Holographic Butterfly Velocities in Brane Geometry and Einstein-Gauss-Bonnet Gravity with Matters," 10.1103/PhysRevD.97.066020 (2017).

[157]V. Jahnke, "Delocalizing Entanglement of Anisotropic Black Branes," 10.1007/JHEP01(2018)102 (2017).

[158]V. Jahnke, "Recent developments in the holographic description of quantum chaos," (2018).

[159]M. Mezei, "On entanglement spreading from holography," 10.1007/JHEP05(2017)064 (2016).

[160]A. A. Patel, M. J. Lawler, and E.-A. Kim, "Coherent Superconductivity with a Large Gap Ratio from Incoherent Metals," Phys. Rev. Lett. **121**, 187001 (2018).

[161]D. Chowdhury and E. Berg, "Intrinsic superconducting instabilities of a solvable model for an incoherent metal," Physical Review Research **2**, 013301, 013301 (2020).

[162]E. Lantagne-Hurtubise, V. Pathak, S. Sahoo, and M. Franz, "Superconducting instabilities in a spinful Sachdev-Ye-Kitaev model," Phys. Rev. B **104**, L020509 (2021).

[163]H. Wang, A. L. Chudnovskiy, A. Gorsky, and A. Kamenev, "SYK Superconductivity: Quantum Kuramoto and Generalized Richardson Models," 1–19 (2020).

[164]Y. Wang and A. V. Chubukov, "Quantum phase transition in the Yukawa-SYK model," Phys. Rev. Research **2**, 033084 (2020).

[165]Y. Wang, "Solvable Strong-Coupling Quantum-Dot Model with a Non-Fermi-Liquid Pairing Transition," Phys. Rev. Lett. **124**, 017002 (2020).

[166]A. Abanov, A. V Chubukov, and A. M Finkel'stein, "Coherent vs.incoherent pairing in 2D systems near magnetic instability," **54**, 488–494 (2001).

[167]A. Abanov, A. V. Chubukov, and J. Schmalian, "Quantum-critical superconductivity in underdoped cuprates," Europhysics Letters (EPL) **55**, 369–375 (2001).

[168]A. V. Chubukov and J. Schmalian, "Superconductivity due to massless boson exchange in the strong-coupling limit," **72**, 10.1103/physrevb.72.174520 (2005).

[169]J.-H. She, B. J. Overbosch, Y.-W. Sun, Y. Liu, K. E. Schalm, J. A. Mydosh, and J. Zaanen, "Observing the origin of superconductivity in quantum critical metals," Phys. Rev. B **84**, 144527 (2011).

[170]R. Roussev and A. J. Millis, "Quantum critical effects on transition temperature of magnetically mediatedp-wave superconductivity," **63**, 10.1103/physrevb.63.140504 (2001).

[171]M. A. Metlitski, D. F. Mross, S. Sachdev, and T. Senthil, "Cooper pairing in non-Fermi liquids," **91**, 10.1103/physrevb.91.115111 (2015).

[172]S. Raghu, G. Torroba, and H. Wang, "Metallic quantum critical points with finite BCS couplings," **92**, 10.1103/physrevb.92.205104 (2015).

[173]D. T. Son, "Superconductivity by long-range color magnetic interaction in high-density quark matter," **59**, 10.1103/physrevd.59.094019 (1999).

[174]M. Mehta, *Random matrices* (Elsevier, Cambridge, 2004).

[175]G. M. Eliashberg, "Interactions between electrons and lat- tice vibrations in a superconductor," Sov. Phys. JETP **11** (1960).

[176]G. M. Eliashberg, "Temperature Green's functions for elec- trons in a superconductor.," Sov. Phys. JETP **12** (1961).

[177]G. A. C. Ummarino, *Chapter 13 - Eliashberg Theory*, Vol. 3 (2013).

[178]F. Marsiglio and J. P. Carbotte, "Electron - Phonon Superconductivity," (2001).

[179]F. Marsiglio, "Eliashberg theory: A short review," **417**, 168102 (2020).

[180]D. Chowdhury and E. Berg, "The unreasonable effectiveness of Eliashberg theory for pairing of non-Fermi liquids," Annals of Physics **417**, 168125 (2020).

[181]P. Anderson, "Theory of dirty superconductors," Journal of Physics and Chemistry of Solids **11**, 26–30 (1959).

[182]J. M. Luttinger, "Fermi Surface and Some Simple Equilibrium Properties of a System of Interacting Fermions," Phys. Rev. **119**, 1153–1163 (1960).

[183]A. Georges, O. Parcollet, and S. Sachdev, "Quantum fluctuations of a nearly critical Heisenberg spin glass," Phys. Rev. B **63**, 134406 (2001).

[184]Y. Gu, A. Kitaev, S. Sachdev, and G. Tarnopolsky, "Notes on the complex Sachdev-Ye-Kitaev model," Journal of High Energy Physics **2020**, 157 (2020).

[185]S. Sachdev, "Bekenstein-hawking entropy and strange metals," Physical Review X **5**, 1–13 (2015).

[186]Y. Gu, X.-L. Qi, and D. Stanford, "Local criticality, diffusion and chaos in generalized Sachdev-Ye-Kitaev models," Journal of High Energy Physics **2017**, 125 (2017).

[187]M. Berkooz, P. Narayan, M. Rozali, and J. Simón, "Higher dimensional generalizations of the SYK model," **2017**, 10.1007/jhep01(2017)138 (2017).

[188]X. Y. Song, C. M. Jian, and L. Balents, "Strongly Correlated Metal Built from Sachdev-Ye-Kitaev Models," Physical Review Letters **119**, 1–18 (2017).

[189]F. Salvati and A. Tagliacozzo, "Superconducting critical temperature in the extended diffusive Sachdev-Ye-Kitaev model," Phys. Rev. Research **3**, 033117 (2021).

[190]P. Zhang, "Dispersive Sachdev-Ye-Kitaev model: Band structure and quantum chaos," Physical Review B **96**, 1–9 (2017).

[191]D. Chowdhury, Y. Werman, E. Berg, and T. Senthil, "Translationally Invariant Non-Fermi-Liquid Metals with Critical Fermi Surfaces: Solvable Models," Phys. Rev. X **8**, 031024 (2018).

[192]D. Valentinis, G. A. Inkof, and J. Schmalian, (2022).

[193]R. Peierls, "Zur Theorie des Diamagnetismus von Leitungselektronen," **80**, 763–791 (1933).

[194]A. M. Goldman, "The Order Parameter Susceptibility and Collective Modes of Superconductors," **19**, 317–330 (2006).

[195]N. E. Bonesteel, I. A. McDonald, and C. Nayak, "Gauge Fields and Pairing in Double-Layer Composite Fermion Metals," **77**, 3009–3012 (1996).

[196]A. Abanov and A. V. Chubukov, "Interplay between superconductivity and non-Fermi liquid at a quantum critical point in a metal. I. The γ model and its phase diagram at $T = 0$: The case $0 < \gamma < 1$," Phys. Rev. B **102**, 024524 (2020).

[197]Y.-M. Wu, A. Abanov, Y. Wang, and A. V. Chubukov, "Interplay between superconductivity and non-Fermi liquid at a quantum critical point in a metal. II. The γ model at a finite T for $0 < \gamma < 1$," Phys. Rev. B **102**, 024525 (2020).

[198]Y.-M. Wu, A. Abanov, and A. V. Chubukov, "Interplay between superconductivity and non-Fermi liquid behavior at a quantum critical point in a metal. III. The γ model and its phase diagram across $\gamma = 1$," Phys. Rev. B **102**, 094516 (2020).

[199]Y.-M. Wu, S.-S. Zhang, A. Abanov, and A. V. Chubukov, "Interplay between superconductivity and non-Fermi liquid at a quantum critical point in a metal. IV. The γ model and its phase diagram at $1 < \gamma < 2$," Phys. Rev. B **103**, 024522 (2021).

[200]Y.-M. Wu, S.-S. Zhang, A. Abanov, and A. V. Chubukov, "Interplay between superconductivity and non-Fermi liquid behavior at a quantum-critical point in a metal. V. The γ model and its phase diagram: The case $\gamma = 2$," Phys. Rev. B **103**, 184508 (2021).

[201]S.-S. Zhang, Y.-M. Wu, A. Abanov, and A. V. Chubukov, "Interplay between superconductivity and non-Fermi liquid at a quantum-critical point in a metal. VI. The γ model and its phase diagram at $2 < \gamma < 3$," (2021).

[202]V. L. Berezinskiĭ, "Destruction of Long-range Order in One-dimensional and Two-dimensional Systems having a Continuous Symmetry Group I. Classical Systems," Soviet Journal of Experimental and Theoretical Physics **32**, 493 (1971).

[203]J. M. Kosterlitz and D. J. Thouless, "Ordering, metastability and phase transitions in two-dimensional systems," **6**, 1181–1203 (1973).

[204]J. M. Kosterlitz, "The critical properties of the two-dimensional xy model," **7**, 1046–1060 (1974).

[205]D. B. Kaplan, J.-W. Lee, D. T. Son, and M. A. Stephanov, "Conformality lost," Phys. Rev. D **80**, 125005 (2009).

[206]K. Jensen, A. Karch, D. T. Son, and E. G. Thompson, "Holographic Berezinskii-Kosterlitz-Thouless Transitions," **105**, 10.1103/physrevlett.105.041601 (2010).

[207]P. Gegenwart, Q. Si, and F. Steglich, "Quantum criticality in heavy-fermion metals," **4**, 186–197 (2008).

[208]H. v. Löhneysen, A. Rosch, M. Vojta, and P. Wölfle, "Fermi-liquid instabilities at magnetic quantum phase transitions," **79**, 1015–1075 (2007).

[209]T. Senthil, A. Vishwanath, L. Balents, S. Sachdev, and M. P. A. Fisher, "Deconfined Quantum Critical Points," **303**, 1490–1494 (2004).

[210]Q. Si, S. Rabello, K. Ingersent, and J. L. Smith, "Locally critical quantum phase transitions in strongly correlated metals," **413**, 804–808 (2001).

[211]M. Scheffer, J. Bascompte, W. A. Brock, V. Brovkin, S. R. Carpenter, V. Dakos, H. Held, E. H. van Nes, M. Rietkerk, and G. Sugihara, "Early-warning signals for critical transitions," **461**, 53–59 (2009).

[212]K. Landsteiner, Y. Liu, and Y.-W. Sun, "Odd viscosity in the quantum critical region of a holographic Weyl semimetal," 10.1103/PhysRevLett.117.081604 (2016).

[213]S. Cremonini, "The Shear Viscosity to Entropy Ratio: A Status Report," Mod. Phys. Lett. **B25**, 1867–1888 (2011).

[214]M. Baggioli, B. Goutéraux, E. Kiritsis, and W. J. Li, "Higher derivative corrections to incoherent metallic transport in holography," Journal of High Energy Physics **2017**, 10.1007/JHEP03(2017)170 (2017).

[215]S. Sachdev, "Bekenstein-Hawking Entropy and Strange Metals," Phys. Rev. X **5**, 041025 (2015).

[216]H. Stolz, *Supraleitung*, Reihe Wissenschaft (Akademie-Verlag, 1979).

[217]G. Arfken, H. Weber, and F. Harris, *Mathematical Methods for Physicists: A Comprehensive Guide* (Elsevier Science, 2013).

[218]S. R. Das, A. Ghosh, A. Jevicki, and K. Suzuki, "Space-Time in the SYK Model," JHEP **07**, 184 (2018).

Acronyms and conventions

AdS: **A**nti-**d**e **S**itter
BF: **B**reitenlohner-**F**reedman
CFT: **C**onformal **F**ield **T**heory
CMT: **C**ondensed **M**atter **T**heory
EMD: **E**instein **M**axwell **D**ilaton
EOM: **E**quations **O**f **M**otion
ESB: **E**xplicit **S**ymmetry **B**reaking
FL: **F**ermi **L**iquid
GKPW: **G**ubser **K**lebanov **P**olyakov **W**itten
MFT: **M**ean **F**ield **T**heory
NFL: **N**on **F**ermi **L**iquid
PDF: **P**robability **D**istribution **F**unction
QCD: **Q**uantum **C**hromo**d**ynamics
QCP: **Q**uantum **C**ritical **P**oint
QFT: **Q**uantum **F**ield **T**heory
QGP: **Q**uark **G**luon **P**lasma
RN: **R**eissner-**N**ordström
SCT: **S**pecial **C**onformal **T**ransformations
SSB: **S**pontaneous **S**ymmetry **B**reaking
SYK: **S**achdev **Y**e **K**itaev
VEV: **V**acuum **E**xpectation **V**alue

Acronyms (1)

General relativity

External-covariant derivative:

$$dT = \nabla_\mu T^\rho{}_\sigma = \partial_\mu T^\rho{}_\sigma + \Gamma^\rho_{\mu\lambda} T^\lambda{}_\sigma - \Gamma^\lambda_{\mu\sigma} T^\rho{}_\lambda$$

Lie derivative:

$$\mathcal{L}_V T^\mu{}_\nu = V^\lambda \nabla_\lambda T^\mu{}_\nu - \nabla_\lambda V^\mu T^\lambda{}_\nu + \nabla_\nu V_\lambda T^\mu{}_\lambda$$

Christoffel symbols:

$$\Gamma^\rho_{\mu\nu} = \frac{1}{2} g^{\rho\lambda} (\partial_\mu g_{\lambda\nu} + \partial_\nu g_{\mu\lambda} - \partial_\lambda g_{\mu\nu})$$

Riemann tensor:

$$\mathcal{R}^\sigma{}_{\mu\rho\nu} = \partial_\rho \Gamma^\sigma_{\mu\nu} + \Gamma^\lambda_{\mu\nu} \Gamma^\sigma_{\rho\lambda} - \partial_\nu \Gamma^\sigma_{\mu\rho} - \Gamma^\lambda_{\mu\rho} \Gamma^\sigma_{\nu\lambda}$$

Ricci tensor:

$$\mathcal{R}_{\mu\nu} = R^\lambda{}_{\mu\lambda\nu}$$

Ricci scalar:

$$\mathcal{R} = g^{\mu\nu} R_{\mu\nu}$$

Einstein tensor:

$$\mathcal{E}_{\mu\nu} = \mathcal{R}_{\mu\nu} - \frac{1}{2} \mathcal{R} g_{\mu\nu}$$

Bianchi identities:

$$\nabla_\lambda \mathcal{R}_{\rho\sigma\mu\nu} + \nabla_\sigma \mathcal{R}_{\lambda\rho\mu\nu} + \nabla_\rho \mathcal{R}_{\sigma\lambda\mu\nu} = 0$$

Frequency integrals

$$\int_\omega (...) = \int_{-\Lambda_{\text{low}}}^{\Lambda_{\text{up}}} \frac{d\omega}{2\pi} (...)$$

Generic integrals

$$\int_X (...) = \int dX (..)$$

Low T Matsubara sums

$$T \sum_{\omega_n} (...) = \int d\omega (...)$$

Conventions (2)

Acknowledgments

I got into this institute with the need to grow from both a personal and scientific point of view, with a basic level of English (as is typical of Italians) and knowing only *ja* and *außergewöhnlich* as German words. Today I feel more adult and capable of doing science than in previous years (I hope the committee will agree). Now I can follow a Netflix episode in English without getting lost at the second sentence 'cause I'm trying to get the first one, and, most important of all, I have argued a few times with my neighbor in German for the garbage cans. (She won, for now).
Therefore, I need to thank who made this possible in the first place: my doctoral supervisor Prof. Jörg Schmalian. Thank you for initially welcoming me here as a visiting student and later letting me be a Ph.D. student. Thank you for always having the ability to talk to me without making me feel stupid. Thank you for allowing me to expand my scientific knowledge in our endless meetings. Thank you for letting me periodically break and mend my comfort zone. Thank you for the conferences in Israel, for the encouragement and the possibilities even in moments of intense frustration. Thank you, lastly, for the freedom I needed so much.
Thanks to the project *Porta la Laurea in Azienda* of the University of Genoa, as well, for supporting my initial stay in Karlsruhe.
Special thanks to Prof. Koenraad Schalm for co-refereeing this thesis, his infinite availability, and for allowing me to visit the Lorentz Institute.
I would like to give a special thanks to Blasie Goutéraux, for his patience, professionalism, and availability. Moreover, thanks for allowing me to visit the CPHT two times.
A special thanks to Davide Valentinis, for joining my office *col San Daniele*, for the discussions (on science and beyond), and for the support (scientific and beyond) in these years. Thanks to him and Vanessa Gall for proofreading this work.
Thanks to Prof. Nicodemo Magnoli, Andrea Amoretti, Julia Link, Joachim Küppers, and Daniel Hauck for the insightful scientific discussions. I am also grateful to all current and former members of TKM, and especially to my office mates Janina, Gu and Vanessa (again). Special thanks to Sonja König for always helping me with German bureaucracy. I would also like to thank the Karlsruhe House of Young Scientists for supporting me during these years in learning German (thanks to you I was able to argue with my neighbor).
I cannot forget to thank my family and my dear ones for all the unconditional support in these very intense academic years.

Gian